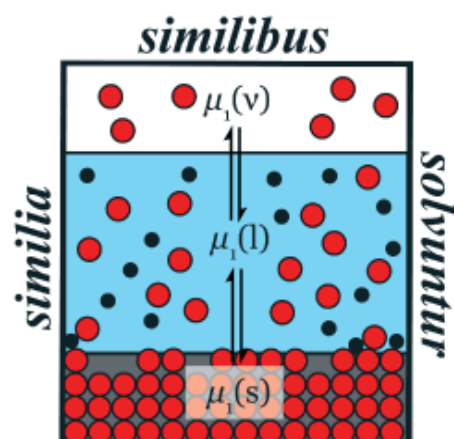


ISSP 2012



15th ISSP, Xining, 2012

Qinghai Institute of Salt Lakes, China
July 23th - 27th, 2012



Abstract Volume

Preface

The International Symposium on Solubility Phenomena and Related Equilibrium Data (ISSP) conference series, which is organized by the IUPAC Subcommittee on Solubility and Equilibrium Data (SSED), has been held in even years 14 times at various locations around the world:

1984	1 st	ISSP, London, Ontario, Canada
1986	2 nd	ISSP, Newark, New Jersey, USA
1988	3 rd	ISSP, Guildford, UK
1990	4 th	ISSP, Troy, NY, USA
1992	5 th	ISSP, Moscow, Russia
1994	6 th	ISSP, Buenos Aires, Argentina
1996	7 th	ISSP, Leoben, Austria
1998	8 th	ISSP, Niigata, Japan
2000	9 th	ISSP, Hammamet, Tunisia
2002	10 th	ISSP, Varna, Bulgaria
2004	11 th	ISSP, Aveiro, Portugal
2006	12 th	ISSP, Freiberg, Germany
2008	13 th	ISSP, Dublin, Ireland
2010	14 th	ISSP, Leoben, Austria

The Qinghai Institute of Salt Lakes (QISL), Chinese Academy of Sciences, is honoured to undertake the organization of the 15th ISSP under the auspices of SSED and IUPAC. At this conference five areas will be emphasized: 1) Many participants will contribute presentations in honour of Prof. Heinz Gamsjäger's 80th birthday, in appreciation of his outstanding contribution in steering and carrying out the production and critical evaluation of solubility data, his services as former Secretary and Chair of SSED and his significant involvement in the organization of the ISSP conference series. 2) Understanding solubility phenomena in multi-component systems will highlight the importance of thermodynamic models and will show their distinctive role in correlation, prediction and critical evaluation of solubilities and phase diagrams. 3) The kinetics of solubility phenomena are of special engineering significance. Topics to be discussed include metastable phase diagrams, transformation of solid phases in equilibrium with aqueous solutions, mobilization of key elements in resource extraction and environmental evolution, and drug-release retardants and enhancers. 4) Solubility features of ionic liquids and molten salts will be reported. 5) Fundamental effects of solute-solvent interactions on solubility phenomena in electrolyte and non-electrolyte solutions will also be presented, including solution structure, component activities and liquid-liquid equilibria.

Parallel to the Symposium, a workshop entitled "Solubility and Other Equilibria in Salt Brines" will be held. Topics covered will include solubility determination, phase diagram simulation and prediction, solution structure and solid phase transformations in relation to salt lake brines. This workshop will help to facilitate the completion of phase diagrams of hundreds of salt brine systems needed in resource extraction from salt lakes and related chemical engineering design.

The local organizing institute of QISL has been engaged in resource extraction from salt lake brines for almost 50 years, since its establishment in 1965. Solubility phenomena run through the whole process of salt lake chemical engineering. The 15th ISSP will make a special contribution towards understanding solubility phenomena in salt lake brines in China and all over the world. We wish all participants have an inspirational conference and spend a pleasant summer in Xining.

Organizing Committee
Xining, July 2012

INTERNATIONAL SCIENTIFIC AND ORGANIZING COMMITTEE

Heinz Gamsjäger (Chair, Austria)

Christov Balarew (Bulgaria)

Peter Fogg (UK)

Wolfgang Hummel (Switzerland)

John W. Lorimer (Canada)

Yizhak Marcus (Israel)

Mark Salomon (USA)

Kiyoshi Sawada (Japan)

Hongwei Sun (China)

Alexander Toikka (Russia)

Wolfgang Voigt (Germany)

Peter A. Williams (Australia)

Conference Editor: Earle Waghorne (Ireland)

Jitka Eysseltová (Czech)

Marcelle Gaune-Escard (France)

Petros G. Koutsoukos (Greece)

Clara Magalhães (Portugal)

Leslie D. Pettit (UK)

David G. Shaw (USA)

Staffan Sjöberg (Sweden)

Reginald Tomkins (USA)

Vladimir Valyashko (Russia)

Hans Wanner (Switzerland)

Junlin Yang (China)

LOCAL ORGANIZING COMMITTEE

Xiaogang Dang, QISL, CAS

Yanming Hu, QISL, CAS

Yan Jing, QISL, CAS

Wu Li, QISL, CAS

Zhijian Wu, QISL, CAS

Yuan Zhou, QISL, CAS

Chunhui Fang, QISL, CAS

Youliang Jia, QISL, CAS

Fafu Li, QISL, CAS

Chensong Wang, QISL, CAS

Yan Yao, QISL, CAS

Conference CHAIR

Haizhou Ma

Conference Co-CHAIR

Dewen Zeng

dewen_zeng@hotmail.com

Phone:+86 13618496806

Conference SECRETARY

Haijun Han

haijunhan@126.com

Qinghai Institute of Salt Lakes

Chinese Academy of Sciences

Xinning Road 18,

810008 Xining,

P.R. China

Fax: +86-(0)971- 6306002

CONTENT

A. PLENARY LECTURES

SOLUBILITY PHENOMENA IN SCIENCE AND EDUCATION - EXPERIMENTS, THERMODYNAMIC ANALYSES AND THEORETICAL ASPECTS <i>Gamsjäger H.</i>	1
SOLID-SOLUTE PHASE EQUILIBRIA IN AQUEOUS SOLUTION – FUNDAMENTALS AND APPLICATION <i>Königsberger E.</i>	2
THE HIGHS AND LOWS (AND IN-BETWEENS) OF SOLUBILITY MEASUREMENTS OF ELECTROLYTES <i>Hefter G.</i>	3
MODELLING OF THE SOLUBILITY OF INORGANIC COMPOUNDS IN MULTICOMPONENT PROCESS SOLUTIONS OVER WIDE TEMPERATURE RANGES <i>Papangelakis V.</i>	4
SOLUBILITY PHENOMENA STUDY CONCERNING BRINES IN CHINA <i>Song P.S. and Zeng D.</i>	5
SOLID PHASE EQUILIBRIA IN IONIC LIQUIDS – CRYSTALLIZATION PHENOMENA <i>König A., Keil P. and Kick M.</i>	7
PHASE BEHAVIOR AND INTERMOLECULAR INTERACTION OF GREEN SOLVENT SYSTEMS <i>Han B.X.</i>	8

B. INVITED LECTURES

SOLID SOLUTIONS OF LAYERED OXIDES WITH RARE EARTH ELEMENTS <i>Zvereva I.</i>	9
SOLUBILITY PHENOMENA RELATED TO CO ₂ CAPTURE AND STORAGE <i>De Visscher A.</i>	10
INVESTIGATION OF RADIONUCLIDE SOLUBILITY AND SPECIATION IN CONCENTRATED SALT BRINE SOLUTIONS <i>Altmaier M.</i>	11
MODELING MIXED SOLVENT ELECTROLYTE SYSTEMS: PHASE BEHAVIOR, CHEMICAL EQUILIBRIA, AND TRANSPORT PROPERTIES <i>Wang P., Kosinski Jerzy J., Anderko A.</i>	12

C. ORAL PRESENTATION

SOLUBILITY CHANGE OF THE TERNARY SYSTEM KCl-NH ₄ Cl-H ₂ O FROM 15 °C TO 65 °C <i>Chen J.X., Li R.J. and Zhang H.C.</i>	13
--	----

STABLE AND METASTABLE PHASE EQUILIBRIUM PHENOMENA IN SALT-WATER SYSTEMS <i>Deng T.L., Wang S.Q., Guo Y.F., Yu X.P. and Gao D.L.</i>	14
SOLUBILITY OF RARE EARTH FLUORIDES IN AQUEOUS SYSTEMS <i>Gumiński C. and Zeng D.</i>	15
SOLUBILITIES OF POORLY WATER-SOLUBLE DRUGS AND ENHANCEMENT OF THEIR SOLUBILITIES BY ADDING CO-SOLVENTS <i>Matsuda H.</i>	16
A STUDY ON SOLUBILITY ENHANCEMENT OF POORLY WATER SOLUBLE DRUG OXCARBAZEPINE USING DIFFERENT SOLUBILIZATION TECHNIQUES <i>Kulkarni A., Toshniwal S. and Naik J.</i>	17
METASTABLE PHASE EQUILIBRIA OF RUBIDIUM CONTAINING SYSTEM AT MULTI-TEMPERATURE <i>Yu X.D., Zeng Y., Li J.J., Jiang D.B. and Yin Q.H.</i>	19
CONDITIONAL SALT-FORMING REGIONS OF SEAWATER TYPE SOLUTION IN THE NONEQUILIBRIUM STATE OF ISOTHERMAL BOILING EVAPORATION <i>Zhou H., Gao F., Bao Y., Huangfu L., Zhang C. and Bai X.</i>	20
ULTRASOUND CHANGE SOLID-LIQUID EQUILIBRIUM? <i>Yang X.G., Dong H.X., Lv Y., Tang J.Y., Yue G.J. and Liu W.X.</i>	21
THERMODYNAMIC MODELING OF THE SOLUBILITY OF ALKALI AND EARTH ALKALI BORATES <i>Thomsen K.</i>	22
THE PREDICTION OF MINERAL SOLUBILITIES IN NATURAL WATERS: THE K-Mg-Rb-Cs-Cl-H ₂ O SYSTEM AT 298K <i>Nie Z., Song P.S., Bu L.Z., Wang Y.S. and Zheng M.P.</i>	23
THE EFFECT OF CONCENTRATION OF SODIUM OF SODIUM CARBONATE ON SCHEELITE DIGESTION <i>Zhao Z., Liao Y., Tu S., Liu X. and Li H.</i>	24
THE INFLUENCE OF MINERAL PHASES ON TRACE ELEMENTS DISPERSION BY LEACHATES FROM SULFIDE CONTAINING TAILINGS FROM SÃO DOMINGOS MINE, PORTUGAL. POT EXPERIMENTS <i>Magalhães M.C.F., Santos E.S., Abreu M.M. and Macías F.</i>	25
ABSORPTION EQUILIBRIA OF (SO ₂ +NO ₂ +NaClO ₂ +NaOH) SYSTEM <i>Mondal M.K.</i>	26
SOLUBILITY OF METAL OXIDES AND HYDROXIDES IN ALKALINE SOLUTIONS. <i>Königsberger L.C., Königsberger E., Heftler G. and May P.M.</i>	27
SOLUBILITY CALCULATIONS FOR THE OCEANIC SALT SYSTEM USING THE THEREDA – NEW DEVELOPMENTS <i>Voigt W.</i>	28

THERMODYNAMIC PROPERTIES OF LiCl(aq) AND CALCULATION OF SOLUBILITIES IN THE Li ⁺ -Na ⁺ -Mg ²⁺ -Cl ⁻ -SO ₄ ²⁻ -H ₂ O SYSTEM <i>Steiger M.</i>	29
SOLUBILITIES OF BASIC MAGNESIUM SALT HYDRATES AT DIFFERENT TEMPERATURES <i>Oestreich M., Freyer D. and Voigt W.</i>	30
THERMODYNAMIC PROPERTIES OF MIXTURES CONTAINING IONIC LIQUIDS BASED ON BIS[(TRIFLUOROMETHYL)SULFONYL]IMIDE FOR APPLICATION IN HOMOGENEOUS CATALYSIS <i>Machanová K., Bendová M., Jacquemin J., Troncoso J. and Wagner Z.</i>	31
PHASE EQUILIBRIA IN RbBr-LaBr ₃ BY THERMODYNAMIC MODELLING <i>Gong W.P., Zhang L. and Gaune-Escard M.</i>	32
THE HYDRATE WATER CONTENT OF BASSANITE – DEPENDENCE ON WATER ACTIVITY <i>Freyer D.</i>	33
CRYSTALLIZATION PATHS IN CaO-Al ₂ O ₃ -SiO ₂ SYSTEM <i>Lutsyk V.I. and Zelenaya A.E.</i>	34
A NOVEL QSPR METHOD FOR ESTIMATION OF HANSEN SOLUBILITY PARAMETERS USING COSMO-RS SIGMA MOMENTS <i>Járvás G. and Dallos A.</i>	35
SOLUBILITY, CRITICAL STATES AND THERMODYNAMIC PECULIARITIES OF MULTICOMPONENT REACTIVE LIQUID – LIQUID SYSTEMS <i>Toikka A.</i>	36
SOLUBILITY OF THREE-PRIMARY-COLORS DISPERSE DYES AND THEIR BLENDS IN SUPERCRITICAL CARBON DIOXIDE <i>Tamura K., Tanaka K. and Hiraki D.</i>	37
SOLUBILITY AND SOLVOPHOBICITY PHENOMENA IN SELF-ASSOCIATED SOLVENTS <i>Sedov I.A and Solomonov B.N.</i>	38
PARTITIONING OF ORGANIC ACIDS INTO THE SOLVENTS WITH IONIC LIQUIDS AND THEIR RHEOLOGY <i>Schlosser Š., Marták J. and Blahušiak M.</i>	39
PHASE BEHAVIOR OF AQUEOUS MIXTURES OF TETRAHYDROFURAN WITH BIOLOGICAL BUFFER HEPES <i>Taha M. and Lee M.J.</i>	40
EXPERIMENTAL AND MOLECULAR DYNAMICS SIMULATION STUDIES ON THE SOLUBILITY OF AMINO ACIDS IN AQUEOUS ELECTROLYTE SOLUTIONS <i>Tomé L.I.N., Pinho S.P., Jorge M., Gomes J.R.B. and Coutinho J.A.P.</i>	41
THE FATE OF THE WATER-SOLUBLE COMPONENTS OF SOME OIL PRODUCTS: THE SOLUBILITY LIMITS AND DISSOLUTION/EVAPORATION EQUILIBRIUMS	

<i>Winkler I., Sapronova A. and Rogozynskiy M.</i>	42
PREDICABILITY OF SETCHENOV COEFFICIENTS IN FLUOROCARBON-ALCOHOL-NaOH SYSTEMS WITH THE GROUP CONTRIBUTION METHOD <i>Ago K. and Nishiumi H.</i>	43
WHAT IS SOLVENT BASICITY? <i>Waghorne W.E.</i>	44
SOLUBILITY MEASUREMENTS FOR DETERMINATION OF EQUILIBRIUM CONSTANTS IN AQUEOUS SOLUTION <i>Furia E., Napoli A., Sindona G. and Tagarelli A.</i>	45
TOWARD A MOLECULAR MODEL FOR AQUEOUS SOLUTIONS OF NONPOLAR FLUIDS <i>Jirsák J., Škvor J. and Nezbeda I.</i>	46
SOLUBILITY OF BIOACTIVE COMPONENTS OF MANGO GINGER (CURCUMA AMADA ROXB) IN SUPERCRITICAL CARBON DIOXIDE <i>Krishna Murthy T.P. and Manohar B.</i>	47
D: POSTERS	
SOLID - LIQUID EQUILIBRIA FOR THE TERNARY Na ₂ B ₄ O ₇ - NaBr - H ₂ O SYSTEM AT 323 K <i>Sang S.H., Sun M.L., Cui R.Z. and Li T.</i>	48
SOLID-LIQUID EQUILIBRIUM OF KOH-K ₃ VO ₄ -H ₂ O SYSTEM AT (40 AND 80) °C <i>Yang N., Wang S.N., Du H., Zheng S.L. and Zhang Y.</i>	49
STUDY ON THE EQUILIBRIUM IN THE QUINARY SYSTEM Li ⁺ , Mg ²⁺ //Cl ⁻ , SO ₄ ²⁻ , B ₆ O ₁₀ ²⁻ -H ₂ O AT 25 °C <i>Sun B. and Song P.S.</i>	50
THE PHASE EQUILIBRIUM BEHAVIORS OF THE AQUEOUS SYSTEMS MAGNESIUM BORATE AT MULTI-TEMPERATURES <i>Ge H.W., Deng T.L. and Yao Y.</i>	51
THE PROGRESS OF POTENTIAL-pH DIAGRAMS FOR V-H ₂ O SYSTEM <i>Zhao X. and Zeng Y.</i>	52
THE SOLUBILITY OF CETYLTRIMETHYLAMMONIUM BROMIDE IN METHANOL-WATER MIXED SOLVENT MEDIA <i>Bhattarai A.</i>	53
SUBSOLIDUS BINARY PHASE DIAGRAM OF THE PEROVSK TYPE LAYER MATERIALS [n-CnH _{2n+1} N(CH ₃) ₃] ₂ ZnCl ₄ (n=16, 18) <i>Ren B.Y. and Wu K.Z.</i>	54
BINARY AND TERNARY PHASE EQUILIBRIA FOR C18 BIODIESEL IN SUPERCRITICAL METHANOL <i>Fang T., Shimoyama Y., Iwai Y. and Goto M.</i>	55

CORRELATING AND PREDICTING THE SOLUBILITIES OF SOLID N-ALKANES AND POLYCYCLIC AROMATIC HYDROCARBONS IN SUPERCRITICAL CARBON DIOXIDE USING THE COMPRESSED GAS MODEL AND THE REFERENCE SOLUBILITIES <i>Li H.R., Li S.F. and Shen B.Q.</i>	56
TEMPERATURE VARIATION CHEMICAL MODEL FOR CHLORIDE–BROMIDE INTERACTION PARAMETERS AND EQUILIBRIUM SOLUBILITIES IN THE AQUEOUS SYSTEM OF MAGNESIUM CHLORIDE AND MAGNESIUM BROMIDE <i>Meng L.Z., Li D., Guo Y.F. and Deng T.L.</i>	57
PREDICTION OF VAPOR PRESSURE DATA FOR MULTI-COMPONENT SYSTEMS CONTAINING IMIDAZOLIUM-BASED PHOSPHATE IONIC LIQUID BASED ON THE GROUP CONTRIBUTION <i>Wang J.F. and Li Z.B.</i>	58
POSSIBILITY OF THE QUATERNARY SYSTEM $\text{KCl-NH}_4\text{Cl-CaCl}_2\text{-H}_2\text{O}$ AS POTENTIAL PHASE MATERIAL — PREDICTION AND EXPERIMENTAL VERIFICATION <i>Dong O.Y., Zeng D., Han H. J. and Yin X.</i>	59
THERMODYNAMIC UNDERSTANDING ON THE LIQUID-SOLID EQUILIBRIUM OF THE TERNARY SYSTEM $\text{CaCl}_2\text{-SrCl}_2\text{-H}_2\text{O}$ <i>Guo L., Zeng D. and Yao Y.</i>	60
PHASE DIAGRAM SIMULATION OF THE SYSTEMS $\text{ACl+MgCl}_2\text{+H}_2\text{O}$ (A = Na, K) AND THEIR APPLICATION IN PURIFICATION OF CHEMICAL REAGENTS <i>Li D., Zeng D., Zhou H. and Dong O.Y.</i>	61
PHASE DIAGRAM PREDICTION OF THE SYSTEM $\text{NaNO}_3\text{-LiNO}_3\text{-KNO}_3\text{-H}_2\text{O}$ AS ROOM TEMPERATURE PHASE CHANGE MATERIALS <i>Yin X., Chen Q. and Zeng D.</i>	62
SOLUBILITY PREDICTION OF THE QUATERNARY SYSTEM $\text{CaSO}_4\text{-MgSO}_4\text{-H}_2\text{SO}_4\text{-H}_2\text{O}$ AT TEMPERATURES FROM 298.15 TO 363.15 K <i>Wang W. and Zeng D.</i>	63
QUANTITATIVE ANALYSIS OF MULTI-COMPONENT ACID-BASE TITRATION AND SELECTIVE RECOVERY OF METALS FROM ACIDIC MINE DRAINAGE WATERS <i>Räsänen L., Blomberg P., Mäki T. and Koukkari P.</i>	64
SOLUBILITY DIAGRAMS OF $\text{Na}_2\text{SO}_4\text{-Rb}_2\text{SO}_4\text{-MgSO}_4\text{-H}_2\text{O}$, $\text{Na}_2\text{SO}_4\text{-Cs}_2\text{SO}_4\text{-MgSO}_4\text{-H}_2\text{O}$ AND $\text{K}_2\text{SO}_4\text{-Cs}_2\text{SO}_4\text{-MgSO}_4\text{-H}_2\text{O}$ AT 298.15 K <i>Hu B.</i>	65
SOLUBILITY PHASE DIAGRAM OF THE SYSTEM $\text{Li}^+, \text{Mg}^{2+} // \text{Cl}^-, \text{SO}_4^{2-}\text{-H}_2\text{O}$ AT 298.15 K ---- EXPERIMENTAL REDETERMINATION AND MODEL SIMULATION <i>Li H., Zeng D., Yao Y., Yin X. and Li D.</i>	66
SOLUBILITY OF GYPSUM AND INSOLUBLE ANHYDRITE IN THE TERNARY SYSTEM $\text{CaSO}_4\text{+H}_2\text{SO}_4\text{+H}_2\text{O}$ <i>Wang W. and Zeng D.</i>	67

PHASE DIAGRAM OF THE SYSTEM $\text{MgCl}_2\text{-LiCl-NH}_4\text{Cl-H}_2\text{O}$ AT 298.15 K <i>Yang H.T., Zeng D., Yin X. and Liang T.Y.</i>	68
SOLUBILITY OF BASIC ZINC SULFATE IN THE SYSTEM $\text{ZnSO}_4\text{-H}_2\text{O}$ <i>Yin X., Zeng D. and Wu Y.</i>	69
SOLUBILITY PHASE DIAGRAM OF THE SYSTEM $\text{Li}_2\text{SO}_4\text{-K}_2\text{SO}_4\text{-MgSO}_4\text{-H}_2\text{O}$ <i>Zhou H., Zeng D., Han H., Dong O., Li D. and Yao Y.</i>	70
MEASUREMENT AND CORRELATION OF LIQUID-LIQUID EQUILIBRIUM DATA FOR IONIC LIQUID-BASED AQUEOUS TWO-PHASE SYSTEM OF $[\text{C}_8\text{mim}]\text{Br-Cs}_2\text{CO}_3\text{-H}_2\text{O}$ <i>Yin G.W., Li S.N., Zhai Q.G., Jiang Y.C. and Hu M.C.</i>	71
SOLUBILITY DATA OF LITHIUM SULFATE IN BINARY AND HIGHER SYSTEMS: COMPILATION AND CRITICAL EVALUATION <i>Schmitt J. and Voig W.</i>	72
TOPOLOGICAL RULES TO CHECK THE POLYHEDRATION OF RECIPROCAL SALT SYSTEMS A, B, C X, Y (A, B X, Y, Z) <i>Lutsyk V.I. and Vorobjeva V.P.</i>	73
TIE-LINE METHODS TO SEARCH QUATERNARY EUTECTIC COMPOSITION <i>Lutsyk V.I. and Zyryanov A.M.</i>	74
METASTABLE PHASE EQUILIBRIA OF THE QUINARY SYSTEM ($\text{Li}^+, \text{Na}^+, \text{Mg}^{2+} // \text{Cl}^-, \text{SO}_4^{2-}\text{-H}_2\text{O}$) AT 273.15 K <i>Wang S.Q., Guo Y.F., Gao D.L. and Deng T.L.</i>	75
STABLE AND METASTABLE PHASE EQUILIBRIA OF THE TERNARY AQUEOUS SYSTEM OF SODIUM SULFATE AND LITHIUM SULFATE <i>Guo Y.F., Han H.J., Wang Q., Wang S.Q. and Deng T.L.</i>	76
METASTABLE PHASE EQUILIBRIA FOR THE TERNARY AQUEOUS SYSTEM SODIUM CHLORIDE AND SODIUM SULFATE <i>Shen D.L., Guo Y.F., Wang S.Q. and Deng T.L.</i>	77
METASTABLE PHASE EQUILIBRIA OF THE QUATERNARY AQUEOUS SYSTEM ($\text{Li}^+, \text{Mg}^{2+} // \text{Cl}^-, \text{SO}_4^{2-}\text{-H}_2\text{O}$) AT 348.15 K <i>Wang Q., Guo Y.F., Wang S.Q., Yu X.P. and Deng T.L.</i>	78
STUDY OF THE SOLUBILITY AND METASTABLE ZONE WIDTH OF BORAX DECAHYDRATE IN LITHIUM SULFATE SOLUTION <i>Peng J.Y., Dong Y.P., Li L.L., Meng Q.F. and Li W.</i>	79
PRELIMINARY STUDY ON CONCENTRATED OIL FIELD BRINE UNDER FRIGID CONDITIONS <i>Yang H.J., Chai X.L., Xiao S.Y., Li W. and Li B.</i>	80
LIQUID-SOLID METASTABLE EQUILIBRIA IN SYSTEM $\text{Na}^+, \text{K}^+ // \text{Cl}^-, \text{SO}_4^{2-}, \text{NO}_3^- \text{-H}_2\text{O}$ AT 298 K <i>Huang X.L., Zhou T., Li H., Liu N. and Feng T.</i>	81

THERMODYNAMICS OF MAGNESIUM CARBONATE PHASES IN DILUTE TO CONCENTRATED MAGNESIUM CHLORIDE SOLUTIONS AT 25 °C <i>Bube C., Altmaier M., Metz V., Schild D., Kienzler B. and Neck V.</i>	82
DISSOLUTION OF ZINNWALDITE AND MOBILIZATION OF LITHIUM <i>Hertam A. and Voigt W.</i>	83
STUDIES OF PHASE BEHAVIORS AND THERMODYNAMICS FOR SYSTEMS $MgB_4O_7 + H_2O$ AND $MgSO_4 + MgB_4O_7 + H_2O$ AT 298.15 K <i>Ge H.W., Yao Y., Deng T.L., Guo L.J. and Li D.</i>	84
CHARACTERISTICS OF THE PHOSPHONIC ACID DTPMP AND THEIR SALTS <i>Winkler A. and Voigt W.</i>	85
EQUILIBRIUM CALCULATIONS OF SO_2 ABSORPTION FOR THERMAL POWER PLANT STACK GASES <i>Mondal M.K.</i>	86
HIGHLY WATER SOLUBLE COMPOUND METOPROLOL: STUDY USING DRUG RELEASE RETARDANTS <i>Kulkarni A., Toshniwal S. and Naik J.</i>	87
SPECIES DISTRIBUTION AND PHYSICOCHEMICAL PROPERTIES IN AQUEOUS MAGNESIUM BORATE SOLUTIONS AT 298.15 K <i>Chen Q.L., Fang C.H., Deng T.L., Fang Y., Zhou Y.Q., Zhu F.Y. and Ge H.W.</i>	89
POLYBORATE SPECIATION IN AQUEOUS LITHIUM PENTABORATE SOLUTION AT 323.15K <i>Ge H.W., Fang C.H., Deng T.L., Fang Y., Zhou Y.Q. and Zhu F.Y.</i>	90
CHEMICAL SPECIES DISTRIBUTION AND PHYSICOCHEMICAL PROPERTIES IN AQUEOUS LITHIUM TETRABORATE SOLUTION AT THE METASTABLE STATE <i>Xu S., Deng T.L., Fang Y., Fang C.H., Zhou Y.Q., Zhu F.Y. and Tao S.</i>	91
STRUCTURE OF AQUEOUS ALKALINE SODIUM BOROHYDRIDE SOLUTIONS <i>Tao S., Fang Y., Fang C.H., Zhou Y.Q., Zhu F.Y., Xu S. and Chen Q.L.</i>	92
AQUO- $B(OH)_4^-$ CLUSTERS IN SOLUTION: A DFT AND VIBRATIONAL SPECTRUM STUDY <i>Zhou Y.Q., Fang C.H., Fang Y., Zhu F.Y., Ge H.W. and Chen Q.L.</i>	93
STRUCTURE OF AQUEOUS POTASSIUM TETRABORATE SOLUTIONS BY X-RAY SCATTERING <i>Zhu F.Y., Fang C.H., Fang Y., Zhou Y.Q., Xu S. and Tao S.</i>	94
ACTIVITY COEFFICIENT OF $CsCl$ IN AQUEOUS MIXTURES WITH HIGH DIELECTRIC CONSTANT SYSTEM: N-METHYLFORMAMIDE + WATER BY POTENTIOMETRIC MEASUREMENTS AT 298.15 K <i>Lu J., Li S.N., Zhai Q.G., Jiang Y.C. and Hu M.C.</i>	95
ACTIVITY COEFFICIENTS OF $CsNO_3$ IN ALCOHOL-WATER MIXED SOLVENT FROM POTENTIOMETRIC METHOD <i>Tang J., Li S.N., Zhai Q.G., Jiang Y.C. and Hu M.C.</i>	96

PARTIAL MOLAR VOLUMES OF AMINO ACIDS IN AQUEOUS SOLUTIONS
CONTAINING AMMONIUM SULFATE

Martins M.A., Mota P.C., Ferreira O., Hnědkovský L., Pinho S.P. and Cibulka I. 97

SOLUBILITIES, DENSITIES AND REFRACTIVE INDICES FOR THE TERNARY
SYSTEMS ETHYLENE GLYCOL + MBr (M = K, Rb, Cs) + H₂O AT 288.15 K

Li Y.J., Li S.N., Zhai Q.G., Jiang Y.C. and Hu M.C. 98

THERMODYNAMIC PROPERTIES OF CsF IN WATER + L-ALANINE SYSTEM

Ma L., Li Sh.N., Zhai Q.G., Jiang Y.C., Hu M.C. 99

List of Participants (alphabetically by name) 100

List of Participants (alphabetically by countries/regions) 107

A: PLENARY LECTURE

SOLUBILITY PHENOMENA IN SCIENCE AND EDUCATION - EXPERIMENTS, THERMODYNAMIC ANALYSES AND THEORETICAL ASPECTS

Gamsjäger H.

Lehrstuhl für Physikalische Chemie, Montanuniversität Leoben, A-8700 Leoben, Austria

Solubility equilibria between solid salts, salt hydrates and water play an important role in fundamental and applied branches of chemistry. The continuous interest in this field is reflected by the 15th International Symposium on Solubility Phenomena as well as by the ongoing IUPAC-NIST Solubility Data Series (SDS), which by now comprises one hundred volumes.

Three examples concerning solubility phenomena of ionic solids in aqueous solutions will be described in detail.

- 1) Sparingly and easily soluble, simple molybdates.
- 2) Sparingly soluble ionic solids and solid-solutions with basic anions.
- 3) Hydrolysis of inert hexa-aqua-M(III) ions, where M is Ir, Rh or Cr.

In each case experimental specialities will be discussed, an outline of thermodynamic analyses will be given, theoretical aspects will be emphasized, and where appropriate educational suggestions will be made.

Solubility equilibria are described, discussed and depicted by two-dimensional phase diagrams. The common basis of these phase diagrams are Gibbs-Duhem equations with only three variable potentials, e.g. p , T , μ_i , whereas all the others are held constant. For binary systems temperature vs. mole fraction diagrams summarize and deal concisely with their thermodynamic properties. Plotting osmotic coefficient multiplied by total molality $\varphi \cdot \Sigma m$ vs. mole fraction x of the solid and dissolved compounds, respectively, plays an analogous role for ternary solid-solution aqueous-solution systems [1,2]. In case sparingly soluble solid-solutions are investigated at constant ionic strength of a supporting electrolyte $\varphi \cdot \Sigma m - x$ and Lippmann diagrams are equivalent, the latter became a popular tool to visualize solid-solution aqueous-solution equilibria [3].

References

- [1] Königsberger E., Gamsjäger H., Graphical representation of solid solute phase equilibria in aqueous solution, *Ber. Bunsenges. Phys. Chem.*, **95**, (1991) 734–737.
- [2] Königsberger E., Gamsjäger H., Comment: solid-solution aqueous solution equilibria: thermodynamic theory and representation, *Am. J. Sci.*, **292**, (1992) 199–214.
- [3] Bruno J., Bosbach D., Kulik D., Navrotsky A., Chemical thermodynamics of solid solutions of interest in radioactive waste management. a state of the art report, 1st Ed, *Nuclear Energy Agency Data Bank OECD, Ed.*, Chemical Thermodynamics, OECD Publications, **10**, (2007) 266.

A: PLENARY LECTURE

SOLID-SOLUTE PHASE EQUILIBRIA IN AQUEOUS SOLUTION – FUNDAMENTALS AND APPLICATION

Königsberger E.

School of Chemical and Mathematical Sciences, Murdoch University, Murdoch, WA 6150,
Australia,
e-mail: E.Koenigsberger@murdoch.edu.au

This presentation in honour of Professor Heinz Gamsjäger on his 80th birthday will highlight his seminal contributions to our understanding of solubility phenomena in aqueous media. These include the development of apparatus for accurate solubility measurements, particularly of solid solutions, and theoretical methods to extract thermodynamic quantities from these experimental data. Recent applications to systems of industrial, geochemical and medical interest will be discussed.

A: PLENARY LECTURE

THE HIGHS AND LOWS (AND IN-BETWEENS) OF SOLUBILITY MEASUREMENTS OF ELECTROLYTES

Hefter G.

Chemistry Department, Murdoch University, Murdoch WA 6150, Australia

Solubility determinations probably represent the oldest quantitative measurements in chemistry. The principles involved in such measurements have been understood for a very long time and have become part of the common fabric of physical chemistry. Often even very old solubility measurements compare well with modern determinations and yet, as can be seen in the critically-evaluated compilations of the IUPAC-NIST *Solubility Data Series*, agreement amongst independent measurements is frequently poor, even for simple systems. Clearly, there are more pitfalls and difficulties than are apparent in such measurements. This is especially true when measuring the solubilities of electrolytes because the solute-solute-solvent interactions occurring are much stronger than for non-electrolytes. This talk will highlight some of the practical problems encountered recently in the author's laboratories in trying to quantify the solubilities in water of some simple electrolytes, whose solubilities range from very low (PbSO_4) to very high (LiTf , lithium trifluoromethanesulfonate).

A: PLENARY LECTURE

MODELLING OF THE SOLUBILITY OF INORGANIC COMPOUNDS IN MULTICOMPONENT PROCESS SOLUTIONS OVER WIDE TEMPERATURE RANGES

Papangelakis V.G.

University of Toronto, Dept. of Chemical Engineering and Applied Chemistry, 200 College Street, Toronto, ON, Canada M5S 3E5

Solubility measurements of inorganic compounds in aqueous solutions are used to evaluate the performance of equilibrium chemical models. They are also used to develop databases of model-specific parameters that allow chemical modeling of solution speciation and solubility under conditions outside the range of parameterization. For this approach to be particularly useful for multicomponent systems, only models that obey the additivity rule can be used; otherwise a prohibitively large volume of experimental data is required. Such multicomponent systems are encountered, for example, in the metals and minerals process industry. Hydrometallurgical processing involves the selective extraction of metals from natural and recycled resources by using aqueous solutions. To minimize chemical plant size, the solutions are often close to saturation resulting in the formation of equilibrium or metastable phases. To achieve dissolution selectivity for certain metals over iron and other impurities, as well as high productivity rates, solutions at temperatures as high as 270 °C are often employed. As a consequence, control of solution chemistry, minimum reagent consumption, quality and nature of precipitating phases including chemical fouling phenomena require chemical models with good prediction ability to assist in the chemical plant design and operation phases. Such a model is the Mixed Solvent Electrolyte (MSE) as provided by OLI Systems in specialized software packages. The model makes standard property extrapolations with temperature using the HKF model, and excess free energy calculations based on Pitzer, Middle Range and UNIQUAC models. Examples from the use of the MSE model in two cases of industrial relevance are presented.

The first example involves an experimental and theoretical investigation of calcium sulphate solubility in process solutions containing H₂SO₄, NiSO₄, MgSO₄, and Al₂(SO₄)₃ at 25-95 °C and 150-250 °C. The solubility values at high temperatures are much lower than those at temperatures below 100 °C as gypsum (CaSO₄·2H₂O_(s)) transforms to CaSO_{4(s)} anhydrous. This means that recycled process solutions, saturated with CaSO₄ at low temperatures, can reject calcium and form scale inside autoclaves and heaters resulting in lower thermal efficiencies and reactor fouling. A new database for the MSE model was developed to predict the solid and aqueous phase equilibria of calcium sulphate in the systems studied. The model predictions were in very good agreement with experimental data not used in the parameterization in the temperature range studied.

The second example is from the nickel production industry and deals with sulphuric acid addition and control in an autoclave reactor at 250 °C. It involves the performance evaluation of a ceramic high temperature pH probe. The sensor was calibrated independently and its ability to read pH consistently was evaluated based on calculations of pH using the MSE model, previously tuned on solubility measurements of MgSO₄, and Al₂(SO₄)₃ in H₂SO₄. Again, very good agreement between the measured and calculated pH values was obtained. Insights into the reason why high Mg-containing ores require excess acid, i.e., over and above the stoichiometric requirement to dissolve Mg, to achieve similar Ni dissolution rates with low Mg-containing ores, were obtained.

A: PLENARY LECTURE

SOLUBILITY PHENOMENA STUDY CONCERNING BRINES IN CHINA

Song P.S. and Zeng D.

Institute of Salt Lakes, Academia Sinica, 810008, Xining, Qinghai, China
songpsh@isl.ac.cn; dewen_zeng@hotmail.com

Because of great importance of solubility phenomena in theoretical and engineering practice, solubility phenomena study has been an active field in China. The extensive review about the study work is given in the present paper. Aqueous systems of salts, existing naturally and produced in plants are most often treated with. Especially, abundant salt resources occur over China. Most salt lakes on the Qinghai-Xizang (Tibet) Plateau are famous for high concentration of lithium and boron in their brines. Exploitation and comprehensive utilization of such kind of salt resources promote solubility phenomena studies on salt-water systems.

1. Studies for aqueous carbonate systems with Li or borate

Because of introduction of Li and borate ions into the carbonate system, great different solubility phenomena and construction of the phase diagram appear. Chinese chemists have studied solid-liquid phase equilibrium for the following quinary systems: Li,K//Cl,B₄O₇,CO₃-H₂O (25 °C), Li,Na//Cl,B₄O₇,CO₃-H₂O (25 °C), Li,Na,K//B₄O₇,CO₃-H₂O (15 °C), Li,Na,K//Cl,CO₃-H₂O (25 °C), Li//Cl,SO₄,B₄O₇,CO₃-H₂O (25 °C) etc. and their quaternary and ternary subsystems. The above studies are useful for recovery of Li₂CO₃ from brine of salt lakes in Xizang, e.g. Zabuye Salt Lake whose brine has the second high concentration of Li 1.0~1.2g/L on the world.

2. Studies for aqueous systems of sulfate and chloride with Li and borate

Chinese chemists have also worked on solubility phenomena for many aqueous sulfate and chloride systems. For example quinary systems Li,K,Mg//Cl,SO₄-H₂O (25 °C), Li,Na,K,Mg//SO₄-H₂O (25 °C), Li,Mg//Cl,SO₄, B₆O₁₀-H₂O (25 °C), Li,Na,K//Cl,B₄O₇-H₂O (25 °C), Li,Na,K//SO₄,B₄O₇-H₂O (0 °C), Na,K,Mg//SO₄,B₄O₇-H₂O (15 °C) were studied on solubility phenomena and phase diagram. All the research work has obviously resource characteristics of China. Because of lack of information about solubility phenomena for Li-compounds in chemical literatures, the studies widen knowledge of lithium chemistry. In the Li,Na,K,Mg//Cl,SO₄-H₂O (25 °C) system lithium exists as solid phase of much soluble salts: LiCl·H₂O, Li₂SO₄·H₂O, and its double salts: LiCl·MgCl₂·7H₂O (Li-Carnallite), Li₂SO₄·3Na₂SO₄·12H₂O (Db1), Li₂SO₄·Na₂SO₄ (Db2), 2Li₂SO₄·Na₂SO₄·K₂SO₄ (Db3), Li₂SO₄·K₂SO₄ (Db4) in classical sea-water system with the component lithium ion. The research results show that component lithium may be precipitated as double salt of Li-sulfate during the evaporation of Li-brine.

3. Studies for metastable equilibrium and non-equilibrium solubility

As is generally known that solubility phenomena in the metastable equilibrium state may be more important for many practical processes. For example, much more sea salt are harvested from solar pond of sea water due to the presence of the metastable equilibrium without precipitation of bloedite (Na₂SO₄·MgSO₄·4H₂O). Chinese chemists have done a lot of work on metastable equilibrium solubility. For the classical sea water quinary system Na,K,Mg//Cl,SO₄-H₂O, metastable equilibrium solubility and entirely phase diagram at 15, 25, and 35 °C have completely studied by Dr. Jin et al. And they found that the phase assemblage and space volume of some solid phases are quite different from stable equilibrium solubilities. Crystallization volume of Schonite (K₂SO₄·MgSO₄·6H₂O) at 25 °C is the biggest in the temperature range of 15~35 °C. Quinary systems Na,K//Cl,SO₄,CO₃-H₂O (25 °C), Li,Na,K//B₄O₇,CO₃-H₂O (15 °C), Li,Na//SO₄,B₄O₇,CO₃-H₂O (15 °C), Li,K//SO₄,B₄O₇,

A: PLENARY LECTURE

$\text{CO}_3\text{-H}_2\text{O}$ (15 °C) and many quaternary systems were also studied, and have obvious importance for industrial applications. Another research work have done on the non-equilibrium state solubility during boiling evaporation process of the system $\text{Na,Mg//Cl,SO}_4\text{-H}_2\text{O}$ and its subsystems. The work show some interesting results and authors proposed concepts of primary, extended, overlay salt-forming regions to characterize difference of solubility phenomena from that in stable and metastable equilibria.

4. Studies for processing technology of other natural mineral resources

In order to utilize some mineral resources of China, e.g. ludwigite(syngenetic magnetite-ascharite), natural nitrate containing magnesium, natural soda, underground brines, solubility phenomena studied for corresponding systems were carried out. Systems $\text{Na,K,Mg//Cl,SO}_4,\text{NO}_3\text{-H}_2\text{O}$ (25 °C), $\text{Na,Mg//Cl,SO}_4,\text{NO}_3\text{-H}_2\text{O}$ (25 °C), $\text{Na,K//Cl,NO}_3\text{-H}_2\text{O}$ (25, 50 °C), $\text{Na,K,Mg//Cl,NO}_3\text{-H}_2\text{O}$ (25 °C), $\text{K,Mg//Cl,NO}_3\text{-H}_2\text{O}$ (25 °C), $\text{K,Mg//SO}_4,\text{NO}_3\text{-H}_2\text{O}$ (25 °C), and $\text{Na,K,Mg//NO}_3\text{-H}_2\text{O}$ (25 °C) were studied. $\text{Mg//SO}_4,\text{Cl-H}_2\text{BO}_3\text{-H}_2\text{O}$ (25, 100 °C), $\text{Mg//SO}_4,\text{NO}_3\text{-H}_2\text{BO}_3\text{-H}_2\text{O}$ (25,100 °C), $\text{Na//Cl,SO}_4\text{-H}_2\text{BO}_3\text{-H}_2\text{O}$ (25, 100 °C), $\text{Na,K//Cl,SO}_4\text{-H}_3\text{BO}_3\text{-H}_2\text{O}$ (25°C), $\text{Na,Mg//Cl-H}_2\text{BO}_3\text{-H}_2\text{O}$ (25, 100 °C) etc. were studied for borate system. Some good work were finished on solubility phenomena for the quinary systems $\text{Na,K,NH}_4\text{//Cl,SO}_4\text{-H}_2\text{O}$ (100 °C), $\text{Na//Cl,SO}_4,\text{CO}_3,\text{HCO}_3\text{-H}_2\text{O}$ (150 °C), $\text{Na//Cl,SO}_4,\text{OH,CO}_3\text{-H}_2\text{O}$ (150 °C), and their quaternary systems $\text{Na//Cl,SO}_4,\text{OH-H}_2\text{O}$ (150°C), $\text{Na//Cl,OH,CO}_3\text{-H}_2\text{O}$ (150 °C), $\text{Na//Cl,SO}_4,\text{OH-H}_2\text{O}$ (150 °C), $\text{Na//Cl,SO}_4,\text{CO}_3\text{-H}_2\text{O}$ (150 °C). And some research work on aqueous strontium salt systems has done for the particular Sr-rich underground brine. Chinese chemists have also done many works on solubility phenomena for other cases including that in phase transformation, molten salt hydrates as phase change materials, and studies on salt-water systems with organic component.

A: PLENARY LECTURE

SOLID PHASE EQUILIBRIA IN IONIC LIQUIDS – CRYSTALLIZATION PHENOMENA

König A., Keil P. and Kick M.

Chair of Separation Science and Technology, Friedrich-Alexander-University Erlangen,
D-91058 Erlangen, Germany
e-mail: axel.koenig@cbi.uni-erlangen.de

Ionic Liquids are molten salts with melting points below 100 °C where numerous are even liquid below room-temperature. The large liquidus range is caused by steric bulky organic cations with a high intramolecular mobility. Commonly used cations are alkylimidazolium, alkyropyridinium, tetraalkylammonium or tetraalkylphosphonium in combination with various anions e.g. halides, fluorinated imides, alkylsulfates, organic acids or amino acids. For many applications it is a crucial point in respect to process stability and safety that the working fluid mixture remains in liquid state. Detailed knowledge about the phases and crystallization behaviour is hence indispensable to choose operation points with clear distance to the regions where solidification occurs. For Ionic Liquids the determination of these regions is often tricky because the formation of a solid phase may last days or even longer due to the low melting points and the mobility of the alkyl chains. Additionally, crystallization often occurs not on cooling down but upon heating from the glassy state.

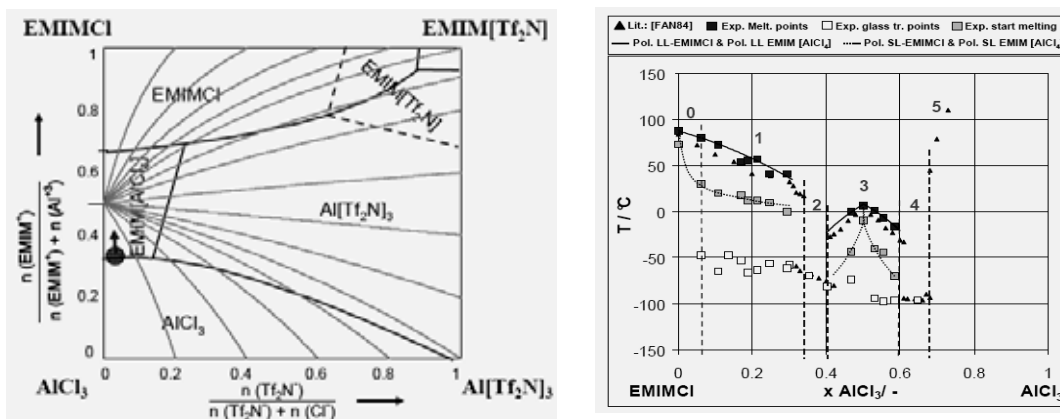


Fig. 1. Jänicke's plot phase diagram of the reciprocal system EMIM Tf₂N–AlCl₃ with hypothetical crystallization pathways (left) and subsystem EMIM Cl–AlCl₃ with compound formation EMIM[AlCl₄] (right) [3].

The presentation gives an overview on the determination of solid-liquid equilibria of slowly crystallizing mixtures containing Ionic Liquids, salts and solvents by dynamic and isothermal methods. Regions in these phase diagrams where no crystallization phenomena are observed are discussed in respect to the molecular interactions. Details are given on the solid-liquid phase behaviour in reciprocal systems containing Ionic Liquids. Moreover, the long term behaviour of "non-crystallizing" mixtures at different temperature levels is presented. The combination of experimental data obtained by different methods combined with a thermodynamic modelling gives a brighter picture of the phase behaviour and allows also an extrapolation of possible liquid-solid transition temperatures into the regions where no experimental data points can be found.

References

- [1] König A., Stepanski M. et al., *Chem. Eng. Res. Des.*, **86**, (2008) 775-780.
- [2] Sola J.L., König A., *Chem. Eng. Technol.*, **33**, (2010) 1979–1988.
- [3] Sola J.L., Keil P., König A., *Chem. Eng. Technol.* **2010**, 33 (5) 821-826.
- [4] Keil P., König A., *Thermochim. Acta*, **524**, (2011) 202-204.

A: PLENARY LECTURE

PHASE BEHAVIOR AND INTERMOLECULAR INTERACTION OF GREEN SOLVENT SYSTEMS

Han B.X.

Institute of Chemistry, Chinese Academy of Sciences, Beijing 100190, China.
E-mail: Hanbx@iccas.ac.cn

Scientists and engineers have paid much attention to clean or environmentally more acceptable solvents, such as supercritical fluid (SCFs) and ionic liquids (ILs). In recent years, we carried out a series of researches on the chemical thermodynamics of green solvents systems and their applications in chemical reactions and material science, including mainly: 1) phase behavior and intermolecular molecular interaction in complex supercritical fluids (SCFs), IL, supercritical (SC) CO₂/IL and SC CO₂/PEG systems; 2) effect of phase behavior and intermolecular interaction on the properties of chemical reactions in SC CO₂, ILs and CO₂/ILs; 3) the phase behavior of surfactant systems and creation of the green microemulsions related with SC CO₂ and ILs. In this presentation, we will discuss some of our recent work [1-12].

Acknowledgements: We thank National Natural Science Foundation of China (20903109, 21073207, 21133009, 21021003) for the financial support.

References

- [1] Li J.S., Zhang J.L., Zhao Y.J., Han B.X., Yang G.Y. High-internal-ionic liquid-phase emulsions, *Chem. Commun.*, **48**, (2012) 994–996.
- [2] Yang D.Z., Hou M.Q., Ning H., Liu Y.H., Han B.X., *J. Supercrit. Fluids*, (2012), *in press*.
- [3] Zhang J.L., Han B.X., Li J.S., Zhao Y.J., Yang G.Y., Carbon dioxide-in-ionic liquid microemulsions, *Angew. Chem. Int. Ed.*, **50**, (2011) 9911–9915.
- [4] Zhang J.L., Li J.S., Zhao Y.J., Han B.X., Hou M.Q., Yang G.Y., Separation of surfactant and organic solvent by CO₂, *Chem. Commun.*, **50**, (2011) 5816–5818.
- [5] Zhang J.L., Han B.X., Zhao Y.J., Li J.S., Hou M.Q. Yang G.Y., CO₂ capture by hydrocarbon surfactant liquids, *Chem. Commun.*, **47**, (2011) 1033–1035.
- [6] Zhang J.L., Han B.X., Zhao Y.J., Li J.S., Yang G.Y., Switching micellization of pluronics in water by CO₂, *Chem. Eur. J.*, **17**, (2011) 4266–4272.
- [7] Zhao Y.J., Zhang J.L., Wang Q., Li J.S., Water-in-oil-in-water double nanoemulsion induced by CO₂, *Phys. Chem. Chem. Phys.*, **13**, (2011) 684–689.
- [8] Li W., Zhang J.L., Zhao Y.J., Hou M.Q., Han B.X., Yu C.L., Ye J.P., Switching micelle-to-vesicle transition reversibly by compressed CO₂, *Chem. Eur. J.*, **16**, (2010) 1296–1305.
- [9] Song J.Y., Hou M.Q., Liu G., Zhang J.L., Han B.X., Yang G.Y., Effect of phase behavior on the ethenolysis of ethyl oleate in compressed CO₂, *J. Phys. Chem. B*, **113**, (2009) 2810–2814.
- [10] Zhang J.L., Han B.X., Zhang C.X., Li W., Feng X.Y., Nanoemulsions induced by compressed gases, *Angew. Chem. Int. Ed.*, **47**, (2008) 3012–3015.
- [11] Zhang J.L., Han B.X., Li W., Zhao Y.J., Hou M.Q., *Angew. Chem. Int. Ed.*, **47**, (2008) 10119–10123.
- [12] Liu J.H., Cheng S.Q., Zhang J.L., Feng X.Y., Fu X.Q., Han B.X., Reverse micelles in carbon dioxide with ionic liquid domains, *Angew. Chem. Int. Ed.*, **46**, (2007) 3313–3315.

B: INVITED LECTURE

SOLID SOLUTIONS OF LAYERED OXIDES WITH RARE EARTH ELEMENTS

Zvereva I.

Department of Chemical Thermodynamics and Kinetics, Faculty of Chemistry,
Saint-Petersburg State University, Universitetskiy prospect 26, Peterhof, Saint-Petersburg,
198504, Russia, e-mail: irina.zvereva@spbu.ru

Layered perovskite-type oxides with rare earth elements and their solid solutions are considered as compounds perspective for functional materials. In this respect, data on solid-solid and solid-liquid equilibrium, process of formation, thermal and chemical stability of layered oxides and their solid solutions are of importance for the synthesis and application of functional materials.

Layered oxides containing rare-earth and alkaline-earth (or alkaline) elements exhibit a set of physical properties (electrical and magnetic) and chemical properties (catalytic, photocatalytic, high reactivity and application in synthesis as precursors). Such wide range of properties results from rich and variable cationic content and different type of layered structure (thickness of perovskite layers and nature of interlayer space between them).

Report presents review on the study of different types of solid solutions of oxides with rare earth elements resulting from:

- isovalent and heterovalent substitution of rare-earth cations,
- isovalent and heterovalent substitution in perovskite layers,
- protonation of alkaline containing oxides in aqueous medium.

Particularities of isovalent and heterovalent substitution of rare-earth cations are demonstrated by solid solutions $(\text{Ln}_{1-x}\text{Ln}'_x)_2\text{SrM}_2\text{O}_7$ and $\text{Ln}_{2-x}\text{Sr}_{1+x}\text{M}_2\text{O}_7$ (M – Al or 3-d metal). Phase equilibrium in pseudo-binary subsystems of quaternary system $\text{La}_2\text{O}_3 - \text{Ln}_2\text{O}_3 - \text{SrO} - \text{Al}_2\text{O}_3$ (Ln = Nd, Ho) and determination of the temperature and concentration limits of phase stability will be present. The main aims of the research are an investigation of the difference in process of the formation of solid solutions and a study of processes of their melting. The experimental data were obtained by heating-quenching method, X-ray phase analysis, visual thermal analysis and DTA. The comparison of thermal characteristics of the process of phase formation in the row of perovskite-like compounds $\text{Ln}_2\text{SrAl}_2\text{O}_7$ (Ln = La – Ho) and solid solutions $(\text{Ln}_{1-x}\text{Ln}'_x)_2\text{SrAl}_2\text{O}_7$ has been performed taking into account the distribution of Ln and Sr cations over two structural positions. Difference in structure-chemical mechanism of the formation of oxides results in the peculiarities of phase formation of solid solutions – transformation of the composition of solid solution during the time of synthesis and the transition of the formation mechanism of layered type solid solutions along the all concentration range. The differences in a character of the melting and of the stability of components have a prominent influence on particularities of phase diagrams in systems under investigation.

Solid solutions with heterovalent substitution of rare-earth cations will be considered for $\text{Ln}_{2-x}\text{Sr}_{1+x}\text{M}_2\text{O}_7$ (M = Cr, Fe) in respect of mixed valent state of transitional 3-d metal, stability of structure, electronic properties.

Protonated solid solutions of full cationic ordered layered oxides obtained in aqueous medium as $(\text{A}, \text{H})\text{LnTiO}_4$, $(\text{A}, \text{H})_2\text{Ln}_2\text{Ti}_3\text{O}_{10}$, $(\text{A}, \text{H})\text{LnTa}_2\text{O}_7$, A = Li – Cs will be considered in view of their catalytic properties in photoinduced process of water splitting

Acknowledgements: This research was supported by Russian Foundation for Basic Research (grant 12-03-00761).

B: INVITED LECTURE

SOLUBILITY PHENOMENA RELATED TO CO₂ CAPTURE AND STORAGE

De Visscher A.

Department of Chemical and Petroleum Engineering, and Centre for Environmental Engineering Research and Education (CEERE), University of Calgary, Calgary, Alberta, Canada,
e-mail: adevissc@ucalgary.ca

The solubility of CO₂ in various systems is of utmost importance in the issue of global climate change. Dissolution of CO₂ in the ocean is one of the main removal mechanisms of CO₂ from the atmosphere. The capture of CO₂ from waste gases, an approach currently contemplated to reduce CO₂ emissions into the atmosphere, is based on the solubility of CO₂ in scrubbing liquids. Storage of CO₂ in underground aquifers is based on the solubility of CO₂ in these aquifers, and the interactions with the mineral matrix.

Volume 95 of the IUPAC-NIST Solubility Data Series [1,2], which deals with the solubility of alkaline earth carbonates, including the ubiquitous CaCO₃ (limestone) in simple aqueous systems, can inform future researchers on the capture and storage of CO₂, because the solubility of CO₂ and the solubility of alkaline earth carbonates are interrelated.

In this presentation, some issues with the proper estimation of the solubility of CO₂ in water and carbonate systems are discussed. Estimations of the solubility enhancing effect of limestone on the solubility of CO₂, both in ambient conditions and in carbon storage conditions, are presented. Thermodynamic calculations show that the current practice of CO₂ capture consumes much more energy than thermodynamically required. Simple solubility studies are presented to indicate how the energy efficiency of such processes can be improved.

References

- [1] De Visscher A., Vanderdeelen J., Königsberger E., Churgalov B.R., Ichikuni M., Tsurumi M., IUPAC-NIST solubility data series. 95. alkaline earth carbonates in aqueous systems. part 1. introduction, Be and Mg, *J. Phys. Chem. Ref. Data*, **41**, (2012) 013105-1–013105-67.
- [2] De Visscher A., Vanderdeelen J., IUPAC-NIST solubility data series. 95. alkaline earth carbonates in aqueous systems. part 2. Ca, *J. Phys. Chem. Ref. Data*, **41**, (2012) 023105-1–023105-137.

B: INVITED LECTURE

INVESTIGATION OF RADIONUCLIDE SOLUBILITY AND SPECIATION IN CONCENTRATED SALT BRINE SOLUTIONS

Altmaier M.

Institute for Nuclear Waste Disposal (INE), Karlsruhe Institute of Technology,
PO Box 3640, 76021 Karlsruhe, Germany,
e-mail: marcus.altmaier@kit.edu

Long-term disposal of nuclear waste in deep underground repositories is the safest option to separate the potentially highly hazardous radionuclides from the environment. On an international scale three different host rock formations (crystalline, clay, rock salt) are currently considered. Repositories for nuclear waste disposal in rock salt, as discussed in Germany (Gorleben) and being realized in the USA (WIPP) are constructed in an exceptionally dry and geologically stable surrounding. In the unlikely case of water intrusion, concentrated salt brine solutions (NaCl, MgCl₂ or CaCl₂) that may mobilize the radionuclides can be generated. For such scenarios, the specific solution chemistry controlling actinide behavior under extremely high ionic strength conditions must be known.

Based on solubility studies and thermodynamic calculations, upper limit radionuclide concentrations are derived for source term estimations as basis for simulations of radionuclide transport and risk assessment. Obviously it is highly important to understand and quantify the main factors controlling radionuclide solubility, i.e. solubility limiting solid phases, aqueous actinide complexation reactions, sorption retention effects and ion-interaction processes. Actinide solubility and speciation strongly depends on geochemical boundary conditions (pH, E_h, I) and information on brine chemistry, redox control by iron phases or mechanisms controlling the free carbonate concentration in solution is providing direct input for predicting actinide behavior. Actinide chemistry in brine systems is a particular case and cannot simply be extrapolated from well investigated low ionic strength systems as chemical processes in concentrated salt solutions significantly differ from dilute aqueous solutions and typical groundwater conditions. Dissolved actinide species in salt brines face a unique environment of various ions strongly interacting and competing for water. Ion interaction processes can lead to stabilization or destabilization of actinide species thus strongly influencing the chemical behavior and overall solubility phenomena. As a consequence, dedicated research efforts focusing on high ionic strength conditions are necessary.

As typical examples for the general conceptual and experimental approach, new investigations on actinide brine chemistry at KIT-INE are presented, focusing on neptunium chemistry in dilute to concentrated NaCl and CaCl₂ solutions. Neptunium is a long-lived alpha emitting radionuclide and constitutes one of the main elements relevant in nuclear waste disposal. In order to derive a detailed understanding of neptunium speciation at the molecular level as basis for advanced chemical process understanding and model development, advanced spectroscopic tools are used to support conventional solubility studies. The work is focusing on the penta- and hexavalent neptunium oxidation states. Np(V) and Np(VI) are relevant for environmental and oxidizing conditions and frequently used chemical analogs for Pu(V) and Pu(VI) chemistry. The presented studies include (i) identification of Np(V) solubility limiting solid phases in aqueous NaCl solutions of different ionic strengths, (ii) detailed investigation of Np(V) speciation and solubility in alkaline CaCl₂ solutions indicating formation of hitherto unknown ternary Ca-Np(V)-OH complexes, and (iii) thermodynamic investigation of Np(VI) solubility and speciation in alkaline NaCl solutions compared to related U(VI) and Pu(VI) systems.

B: INVITED LECTURE

MODELING MIXED SOLVENT ELECTROLYTE SYSTEMS: PHASE BEHAVIOR, CHEMICAL EQUILIBRIA, AND TRANSPORT PROPERTIES

Wang P., Kosinski Jerzy J. and Anderko A.

OLI Systems, Inc., 108 American Road, Morris Plains, NJ 07950, U.S.A.,
pwang@olisystems.com

Modeling electrolyte systems under conditions pertinent to laboratory and industrial applications is important to facilitate an effective prediction of their chemical and phase behavior. Development of electrolyte models that cover wide ranges of chemical composition (aqueous and mixed-solvent, dilute and concentrated solutions), conditions (from ambient temperature and pressure to supercritical conditions) and physical phenomena (phase equilibria, chemical speciation, transport of species to a reacting interface, etc.) is a research subject of paramount significance. Systems with strong chemical speciation (i.e. hydrolysis, ion-association, complexation, acid-base equilibria) and complex phase behavior (e.g. formation of multiple hydrated salts or double salts, presence of eutectic points, and/or presence of two liquid phases) can present a great challenge in modeling their thermodynamic and thermophysical properties.

In the present work, we apply a comprehensive thermodynamic model, referred to as the Mixed-Solvent Electrolyte (MSE) model,[1-3] to calculate phase equilibria, speciation, and other thermodynamic properties of selected systems that are of interest in the chemistry of salt lake and natural waters. In particular, solubilities and chemical speciation in various boron-containing systems (i.e. boric acid, sodium borates, lithium borates, and sodium borohydride) are analyzed as they represent an important class of systems for these applications. The MSE model has been developed to be equally valid for classical aqueous systems, those with more than one distinct solvent and mixtures in which a given component may continuously vary from being a solute to being a solvent (e.g. in acid-water mixtures). Such examples will also be given for other complex chemical systems to demonstrate the applicability of the MSE model for simultaneously representing vapor-liquid, liquid-liquid, and solid-liquid equilibria and for predicting the effects of chemical speciation, temperature, and concentrations of selected molecular solvents on phase equilibria. For a given chemical system, the speciation results predicted by the thermodynamic model have been used to calculate transport properties (self-diffusivity, viscosity, electrical and thermal conductivities) for multicomponent solutions using separate models with the same range of applicability.[4-7] A good accuracy of the calculated transport properties, especially the electrical conductivity, demonstrates the model's capability of accurately predicting both phase equilibria and chemical behavior in electrolyte systems.

References

- [1] Wang, P., Anderko, A., Young, R. D., *Fluid Phase Equilibria*, **203**, (2002) 141-176.
- [2] Wang, P., Anderko, A., Springer, R. D., Young, R. D., *Journal of Molecular Liquids*, **125**, (2006) 37-44.
- [3] Kosinski, J.J., Wang, P., Springer, R. D., Anderko, A., *Fluid Phase Equilibria*, **256**, (2007) 34-41.
- [4] Wang, P., Anderko, A., *Ind. Eng. Chem. Res.*, **42**, (2003) 3495-3504.
- [5] Wang, P., Anderko, A., Young, R. D., *Fluid Phase Equilibria*, **226**, (2004) 71-82.
- [6] Wang, P., Anderko, A., Young, R. D., *Ind. Eng. Chem. Res.*, **43**, (2004) 8083-8092.
- [7] Wang, P., Anderko, A., *Ind. Eng. Chem. Res.*, **47**, (2008) 5698-5709.

C: ORAL PRESENTATION

SOLUBILITY CHANGE OF THE TERNARY SYSTEM KCl-NH₄Cl-H₂O FROM 15 °C TO 65 °C

Chen^{1,2} J.X., Li² R.J. and Zhang² H.C.

¹Engineering Research Center of Seawater Utilization Technology, Ministry of Education, Tianjin, 300130, China

²School of Chemical Engineering, Hebei University of Technology, Tianjin, 300130, China
e-mail: chjx2000@gmail.com

The phase equilibrium profile of the K⁺, NH₄⁺//Cl⁻-H₂O ternary system from 15 °C to 65 °C were determined using the wet-residue method. The salts' solubilities in the KCl + NH₄Cl + H₂O system at $T=(15\text{ °C to }65\text{ °C})$ were also compared with published data [1,2], some are good agreement between the experimental and literature values. Their solubilities are increased with the elevatory temperature. Two-dimensional phase diagrams are widely used to describe, discuss and depict phase equilibrium in chemical, materials and process technology. The common basis of these phase diagrams are Gibbs-Duhem equations with only three variable generalized forces (potentials) e.g. p , T , μ_i , whereas the others are held constant. The phase areas in the equilibrium diagrams of 25 °C, 65 °C were compared. The unsaturated zone at 65 °C is larger than those at 25 °C. The two co-saturation point compositions are different. While the KCl content is almost unchanged, the NH₄Cl content at these three saturated points varies remarkably. They have similar phase regions, namely pure NH₄Cl, KCl. NH₄Cl and KCl dominant solid solution crystallization area respectively, and these two kinds of solid solutions co-crystallization area, and unsaturated zone.

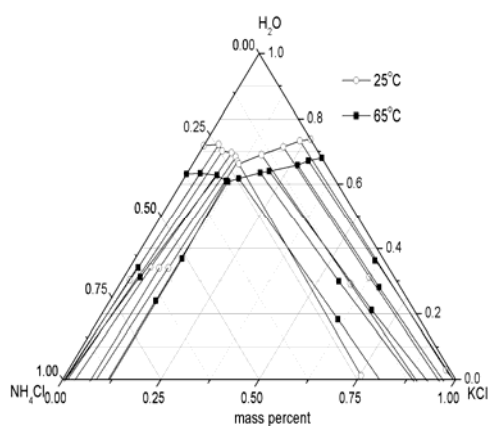


Fig.1. Solubility diagram of the ternary system KCl-NH₄Cl-H₂O at 25 °C and 65 °C.

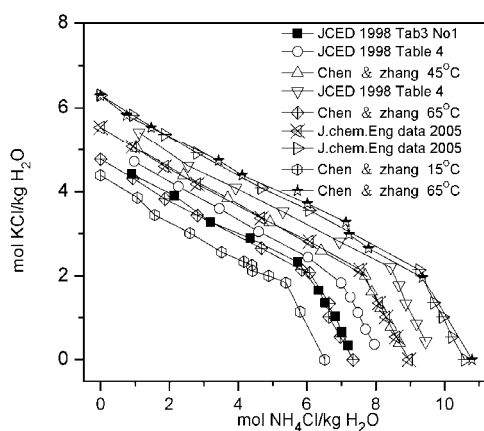


Fig.2. Solubility of the ternary system KCl-NH₄Cl-H₂O at 15 °C to 65 °C.

Acknowledgements: The supports by the Natural Science Fund of Hebei Province (No.B2010000042), Tianjin Natural Science Fund (No.10JCYBJC04300), support Program for Hundred Excellent Innovation Talents from the Universities of Hebei Province (No.CPRC013), China is gratefully acknowledged.

References

- [1] Farelo F., Fernandes C., Avelino A., Solubilities for six ternary systems: NaCl + NH₄Cl + H₂O, KCl + NH₄Cl + H₂O, NaCl + LiCl + H₂O, KCl + LiCl + H₂O, NaCl + AlCl₃ + H₂O, and KCl + AlCl₃ + H₂O at $T=(298\text{ to }333)\text{ K}$, *J. Chem. Eng. Data*, **50**, (2005) 1470–1477.
- [2] Zhang L., Gui Q., Lu X., Wang Y., Shi J., Lu B.C.Y., Measurement of solid-liquid equilibria by a flow-cloud-point method. *J. Chem. Eng. Data*, **43**, (1998) 32–37.

C: ORAL PRESENTATION

STABLE AND METASTABLE PHASE EQUILIBRIUM PHENOMENA IN SALT-WATER SYSTEMS

Deng^{1,2} T.L., Wang¹ S.Q., Guo¹ Y.F., Yu² X.P. and Gao¹ D.L.

¹Tianjin Key Laboratory of Marine Resources and Chemistry, College of Marine Science and Engineering, Tianjin University of Science and Technology Tianjin, 300457, P. R. China
e-mail: tldeng@tust.edu.cn

²ACS Key Laboratory of Salt Lake Resources and Chemistry, Qinghai Institute of Salt Lakes, Chinese Academy of Sciences, Xining, 810008, P. R. China, e-mail: tldeng@isl.ac.cn

Salt lakes are widely distributed in the world, and Salt lakes in China are mainly located in the area of the Qinghai-Xizang (Tibet) Plateau, and the Autonomous Regions of Xinjiang and Inner Mongolia. The composition of salt lake brines can be summarized to the complex salt-water multi-component system (Li-Na-K-Ca-Mg-H-Cl-SO₄-B₄O₇-OH-HCO₃-CO₃-H₂O) [1]. However, the phenomena of super-saturation of brines containing magnesium sulphate and borate are often found both in natural salt lakes and solar ponds around the world [2]. In order to separate and utilize the mixture salts effectively by salt-field engineering or solar ponds in Qaidam Basin, Qinghai province, our studies on the phase equilibria of salt-water systems are mainly focused on the metastable phase equilibria and phase diagrams at present years [3-9].

In this paper, the stable and metastable phase equilibria of the multi-component aqueous systems containing lithium, sodium, potassium, magnesium, chloride, sulphate, and borate ions at (263.15~348.15) K were investigated using the methods of isothermal dissolution and isothermal evaporation. On the basis of Pitzer and its extend model, the stable and metastable predictive solubilities and the phase diagrams were demonstrated. Compared with stable phase equilibria for the same system at the same temperature, some new knowledge and novel crystallization behaviours of hydrates and double salts in the metastable phase equilibrium systems were achieved. Finally, a briefly summary of our group work at present years was also introduced in the paper.

Acknowledgments: Financial support from the State Key Program of NNSFC (20836009), the NNSFC (21106103), the “A Hundred Talents Program” of CAS (0560051057), the Specialized Research Fund for the Doctoral Program of Chinese Higher Education (20101208110003 and 20111208120003), and The Key Pillar Program in the Tianjin Municipal S&T (11ZCKFGX2800) and Senior Professor Program for TUST (20100405) is acknowledged.

References

- [1] Zheng M.P., Xiang J., Wei X.J., Zheng Y., Saline lakes on the Qinghai-Xizang (Tibet) Plateau, Beijing: *Beijing Science and Technology Press*, (1989).
- [2] Deng T.L., Advance in crystallization processes: stable and metastable phase equilibria in the salt-water systems, In: *Yitzhak Mastai ed., Croatia: InTech Publisher*, (2012).
- [3] Liu Y.H., Deng T.L., Song P.S., *J. Chem. Eng. Data*, **56** (2011) 1139–1147.
- [4] Gao J., Deng T.L., *J. Chem. Eng. Data*, **56** (2011) 1452–1458.
- [5] Gao J., Deng T.L., *J. Chem. Eng. Data*, **56** (2011) 1847–1851.
- [6] Meng L.Z., Deng T.L., *Russ. J. Inorg. Chem.*, **56** (2011) 1–4.
- [7] Meng L.Z., Yu X.P., Li D. et al., *J. Chem. Eng. Data*, **56** (2011) 4627–4632.
- [8] Meng L.Z., Yin H.J., Guo Y.F., *J. Chem. Eng. Data*, **56** (2011) 3585–3588.
- [9] Meng L.Z., Li D., Guo Y.F. et al., *J. Chem. Eng. Data*, **56** (2011) 5060–5065.

C: ORAL PRESENTATION

SOLUBILITY OF RARE EARTH FLUORIDES IN AQUEOUS SYSTEMS

Gumiński¹ C. and Zeng² D.

Partly based on achievements of the late Tomasz Mioduski

¹Department of Chemistry, University of Warsaw, Pasteura 1, 02093 Warszawa, Poland
e-mail: cegie@chem.uw.edu.pl

²College of Chemistry and Chemical Engineering, Central South University, 410083
Changsha, P.R. China
e-mail: dewen_zeng@hotmail.com

IUPAC project of collection, compilation and critical evaluation of solubility data of fluorides of Sc, Y, La and all Ln's in water and aqueous systems containing various acids, salts or organic co-solvents as the third (or fourth) added component is under final preparation. By similarity to the chlorides [1] and iodides [2] recently published, some regularities of the solubility values (smoothly increasing with the atomic number of Ln) for fluorides should be also observed. Unfortunately, the corresponding results collected are very scattered (for some systems even several orders of magnitude) as well as the precise and accurate solubility data have been quite seldom determined what complicates their evaluation.

Assuming a smooth changes of the solubilities versus the atomic number of Ln, one may predict solubility of PmF₃ ($\sim 6 \cdot 10^{-6}$ mol·dm⁻³ at 298 K) which is experimentally undeterminable.

It was observed in the case of the binary LaF₃-H₂O system, which was most frequently investigated, that LaF₃ solubility considerably depended on form the equilibrium solid and increased at room temperature in the order: single crystal, poly-crystal, slightly hydrated (LaF₃·0.5H₂O) and highly hydrated (LaF₃·4H₂O) solute. The dehydration process of the latter occurred at 310-350 K and was completed at 600-750 K. Solubility of the hydrated forms increased with temperature whereas solubility of the non-hydrated forms decreased with temperature. A solubility equation may be only formulated for the non-hydrated form of LnF₃ because the corresponding solubility data were more reliable. Influence of ionic strength and pH on the solubility was observed but the effects were rather moderate. An addition of organic solvent to water made always a significant decrease of the solubility.

Some general features of the ternary systems were also observed. A presence of anions, which form stable complexes with Ln³⁺, made increase of the apparent solubility. Well soluble fluorides brought true enough common ions F⁻ and should decrease the solubility LnF₃ but due to the more effective complexation of Ln³⁺ by F⁻ an increase of the apparent solubility was observed. Likewise some cations, which form stable complexes with F⁻, made increase of the LnF₃ solubility. Similar influence was observed by addition of strong acids, however, at very high contents of strong acids the solubilities decreased. Influence of HF added made moderate effects on LnF₃ solubilities. In alkaline solutions a co-precipitation of LnF₃·Ln(OH)₃ was found because both components expressed similar solubilities.

References

- [1] T. Mioduski, C. Gumiński, and D. Zeng, *J. Phys. Chem. Ref. Data*, **37**, (2008) 1765–1853; **38**, (2009) 441-562; **38**, (2009) 925-1011.
[2] T. Mioduski, C. Gumiński, and D. Zeng, *J. Phys. Chem. Ref. Data*, **41**, (2012) 013104-1–013104-94.

C: ORAL PRESENTATION

SOLUBILITIES OF POORLY WATER-SOLUBLE DRUGS AND ENHANCEMENT OF THEIR SOLUBILITIES BY ADDING CO-SOLVENTS

Matsuda H.

Department of Materials and Applied Chemistry, Nihon University, Japan
e-mail: matsuda.hiroyuki@nihon-u.ac.jp

Drug candidates with strong pharmacological activity are increasingly being developed using combinatorial chemistry (CC) and high-throughput screening (HTS). As a result of these screening methods, the number of drugs with decreased water solubilities has increased because of higher molecular weights and more complicated chemical structures. The water solubilities of pharmaceutical compounds and the enhancement of their solubilities by adding co-solvents are therefore important parameters in the pharmaceutical process. Accurate solubility data are therefore necessary not only in the pharmaceutical process but also in the development of more accurate prediction models.

Our group has investigated the water solubilities of several pharmaceutical compounds such as salicylic acid, famotidine, naringin, and etodolac, and the enhancement of their solubilities by adding co-solvents [1-2]. Ethanol, polyethylene glycol (PEG), lauryl sulfate (SLS), and several cyclodextrins (CDs) have been applied as a co-solvent, and the enhancement of the solubilities of the pharmaceutical compounds has been discussed.

Figure 1 shows the experimental results of the solubilities of famotidine at 298.15 K in mixed solvents: water + ethanol, water + PEG 400. In the mixed solvents containing liquid co-solvent, the solubilities were measured over the solute-free mole fraction of the co-solvents [3]. The experimental values in the ethanol + water mixture were maximum at a liquid composition of ethanol $x_2 = 0.4811$. The experimental values in the water + PEG 400 mixture increased with increasing amounts of co-solvent. Fig. 1 also shows the experimental solubility

data of famotidine in water + β -CD mixed solvent. The solubilities increased with increasing mole fraction of the co-solvent. The maximum mole fraction solubilities in co-solvents β -CD, PEG 1000, and SLS, were 0.79×10^{-3} , and this value was 13.2 times the mole fraction solubility in pure water: 0.06×10^{-3} .

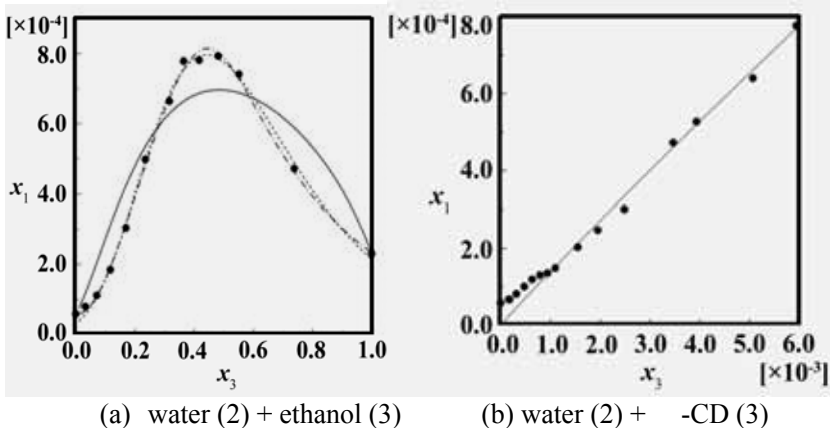


Fig. 1. Experimental solubilities of famotidine (1) in binary mixtures water (2) + co-solvent (3) at 298.15 K.

References

- [1] Matsuda H., Kaburagi K., Matsumoto S., Kurihara K., Tochigi K., Tomono K., Solubilities of salicylic acid in pure solvents and binary mixtures containing co-Solvent, *J. Chem. Eng. Data*, **54**, (2009) 480–484.
- [2] Matsuda H., Matsumoto S., Kaburagi K., Kurihara K., Tochigi K., Tomono K., Determination and correlation of solubilities of famotidine in water + co-solvent mixed solvents, *Fluid Phase Equilib.*, **302**, (2011) 116–123.

C: ORAL PRESENTATION

A STUDY ON SOLUBILITY ENHANCEMENT OF POORLY WATER SOLUBLE DRUG OXCARBAZEPINE USING DIFFERENT SOLUBILIZATION TECHNIQUES

Kulkarni¹ A., Toshniwal² S., and Naik³ J.

¹Department of Chemical Technology, Dr. Babasaheb Ambedkar Marathwada University, Aurangabad, (M.S.), India
e-mail: anakulw@gmail.com

²Vidarbha Institute of Pharmacy, Washim, (M.S.), India. e-mail: toshniwal_ss@yahoo.com

³Department of Chemical Technology, North Maharashtra University, Jalgaon, (M.S.), India
e-mail: jitunaik@gmail.com

Poorly soluble compounds represent an estimated 60% of compounds in pharmaceutical discovery, development and many major marketed drugs in pharmaceutical industry. It is important to measure and predict solubility and permeability accurately at an early stage, and interpret these data to help assess the potential for the development of the candidates. This requires developing an effective strategy to select the most appropriate tools to examine and improve solubility in each phase of development, optimization of solid-state approaches to enhance solubility including the use of polymorphs, co-crystals, and amorphous solids. All of these would affect the dissolution rates and bioavailability that require to be studied with solubilization technology.

Regardless of the stage of the final formulation as tablet, capsules, suspensions etc., the active pharmaceutical ingredient (API) must be released from the drug delivery system and as the first step, should be dissolved in an aqueous environment; this will then be followed possibly by one or more transfers across non aqueous barriers.

The presented study was focused using Oxcarbazepine as a model drug which is commonly used in epilepsy and dose requirement can be very high based on patient condition. Various approaches have been developed and evaluated to overcome the aqueous solubility problem of model drug. The approaches include micronization, use of hydrophilic excipients, use of different solubilizers, inclusion of compounds, meltable binders and amorphous solid dispersion preparation. The solubility of Oxcarbazepine was compared with different technology in pH 6.8 physiological pH buffer medium. The resultant solubility enhanced formulation was formulated into drug product and evaluated for improvement in the drug release profile. Refer to table 1 for details on various approaches evaluated during solubility enhancement.

The different mechanism of solubility enhancement can help pharmaceutical industry to choose suitable technology to improve solubility of compounds and provide benefit for patient to reduce the dose requirement.

Acknowledgements: Author would like to acknowledge M/s Wockhardt Ltd. India for drug sample. M/s Navketan Pharma, India for providing the opportunity for research. Author acknowledges Dr. Deepak Hegde, Vice President and Mrs. Sushma K. Scientist at WuXi AppTec, Shanghai, China for valuable suggestions and support for the research work.

References

- [1] Yang D., Kulkarni R., Behme R. and Kotiyan P., Effect of the melt granulation technique on the dissolution characteristics of griseofulvin. *Int. J. Pharm.*, **329**, (2007) 72–80.
- [2] Amidon G., Lennernas H., Shah V., Crison J., A theoretical basis for a biopharmaceutics drug classification: the correlation of in vitro drug product dissolution and in vivo bioavailability. *Pharm. Res.*, **12**, (1995) 413–420.
- [3] Lipinski C., Drug- like properties and the causes of poor solubility and poor permeability, *J. Pharmacol.*

C: ORAL PRESENTATION

Toxicol. Methods, **44**, (2000) 235–249.

Table 1: Solubility enhancement technology evaluation:

Sample code	Sample /Solubility evaluation type	Excipient concentration	Solubility of Oxcarbazepine (mg/ml)
Control samples			
A	Oxcarbazepine (unmicronized) in purified water.	Unmicronized without any excipient.	0.310 mg/ml
B	Oxcarbazepine (unmicronized) in pH 6.8 phosphate buffer	Unmicronized without any excipient.	0.400 mg/ml
Micronization			
C	Micronization using air jet mill size D90) in pH 6.8 phosphate buffer	Micronized without any excipient.	0.512 mg/ml
Use of hydrophilic or hydrophobic excipient			
D	Lactose monohydrate (Hydrophilic excipient)	10 % of lactose with micronized active	0.537 mg/ml
E	Microcrystalline cellulose (Hydrophobic excipient)	10 % of microcrystalline cellulose with micronized active	0.360 mg/ml
Solubilizer/surfactant effect			
F	Cremophore RH40	1% Cremophore	0.302 mg/ml
G	Sodium lauryl sulfate	3 % Sodium lauryl sulfate	4.010 mg/ml
H	Docusate Sodium	3% Docusate Sodium	5.121 mg/ml
Melt granulation binder (Melt dispersion)			
I	PEG 400	2 % PEG 400	0.601 mg/ml
J	PEG 6000	2 % PEG 6000	0.781 mg/ml
K	PEG 10000	2 % PEG 10000	0.867 mg/ml
Complexation / Inclusion complex			
L	Hydroxy propyl beta cyclodextrin	5% of HPBCD	1.316 mg/ml
M	Hydroxy propyl beta cyclodextrin (HPBCD) and Povidone K 30	5% of HPBCD and 2 % of Povidone K 30	1.823 mg/ml
Spray dried amorphous solid dispersion			
N	Hydroxy propyl methyl cellulose	3 %	3.109 mg/ml
O	Povidone K 30	3 %	2.607 mg/ml
P	Hydroxy propyl methyl cellulose and Sodium lauryl sulfate	3 % HPMC and 5% SLS	6.971 mg/ml

Note: All samples were prepared in same way. The concentration analysis was performed using UV visible spectrophotometer analyzed at 256nm wavelength.

C: ORAL PRESENTATION

METASTABLE PHASE EQUILIBRIA OF RUBIDIUM CONTAINING SYSTEM AT MULTI-TEMPERATURE

Yu¹ X.D., Zeng^{1,2*} Y., Li¹ J.J., Jiang¹ D.B. and Yin¹ Q.H.

¹College of Materials and Chemistry & Chemical Engineering, Chengdu University of Technology, Chengdu, 610059, P.R. China

²Mineral Resources Chemistry Key Laboratory of Sichuan Higher Education Institutions, Chengdu, 610059, P. R. China, e-mail: zengyster@gmail.com

Pingluoba underground brine, located in the west of Sichuan basin, with distinguishing features of deep buried depth (over 4500 m), high temperature (about 393 K), and high salinity (over 420 g/L). It is reported that the brine contains 210.08 g·L⁻¹ chloride ion, 53.27 g·L⁻¹ potassium, 8.99×10^{-2} g·L⁻¹ lithium ion, 3.75×10^{-2} g·L⁻¹ rubidium ion. After the brine exploited, sodium chloride is supersaturated and can be precipitated easily; borate can be separated using acid method and extraction method; although the magnesium content in the original brine is not high, in the exploiting process, magnesium continue to be enriched in the brine; thus, the main component of the brine can be simplified as a quinary system $\text{Li}^+ + \text{K}^+ + \text{Rb}^+ + \text{Mg}^{2+} + \text{Cl}^- + \text{H}_2\text{O}$. In this complex system, a solid solution [(K,Rb)Cl] can be easily formed between rubidium and potassium in chloride solution. To exploit the rubidium from the brine, mineral equilibrium studies on the rubidium containing system are essential.

Up to now, some papers described phase equilibria aiming at the rubidium containing system have been reported. The quaternary system $\text{K}^+, \text{Rb}^+, \text{Mg}^{2+} // \text{Cl}^- - \text{H}_2\text{O}$ at 293 K, 298 K and 373 K had been studied by Feit [1], however the author only gave partial experimental data. Nario [2] and Gao [3] investigated the phase equilibrium of the rubidium containing system in mixed solvent. D'Ans [4] studied the phase equilibrium of $\text{K}^+, \text{Rb}^+ // \text{Cl}^- - \text{H}_2\text{O}$ at 298 K. Overall, the relevant phase relations of the rubidium containing system are lacking, which affect the comprehensive utilization of rubidium in the brine. Accordingly, the metastable phase equilibria in the rubidium containing system at multi-temperature are necessary. To make certain the crystallization form and crystallization area of the solid solution [(K, Rb)Cl] change with temperature, the metastable phase equilibria of ternary system $\text{K}^+, \text{Rb}^+ // \text{Cl}^- - \text{H}_2\text{O}$ at 298 K, 323 K, 348 K investigated by our research group. Results showed that there are three crystallization areas corresponding to [(K, Rb)Cl], KCl, and RbCl in the metastable phase diagram. The crystallization zone of solid solution [(K, Rb)Cl] almost occupies the entire phase region and decreases with the increase of temperature.

Acknowledgements: Project supported by the State 863 Projects (2012AA061704), NNSFC(41173071) and the Doctoral Foundation of Ministry of Education of China (20115122110001).

References

- [1] Feit W., Kubierschky K., Extraction rubidium and cesium from carnallite. *Chem. Ztg.*, **16**, (1892) 335–336.
- [2] Nario Yui., Yoichi K., Equilibrium Compositions of 1-Butanol – Water – MCl (M=Li, Na, K, Rb, Cs and NH_4^+), *Nippon Kagaku Zasshi.*, **87**, (1966) 1138–1143.
- [3] Zhang J., Gao S.Y., Xia S.P., Yao Y., Study of thermodynamic properties of quaternary mixture $\text{Rb}_2\text{SO}_4 + \text{RbCl} + \text{CH}_3\text{OH} + \text{H}_2\text{O}$ by EMF measurement at 298.15 K, *Fluid Phase Equilib.*, **226**, (2004) 307–312.
- [4] D'Ans J., Busch F Z., The quaternary system $\text{KCl} - \text{RbCl} - (\text{CsCl}) - \text{MgCl}_2 - \text{H}_2\text{O}$ at 25°C, *Anorg. Allg. Chem.*, **232**, (1937) 337–368.

C: ORAL PRESENTATION

CONDITIONAL SALT-FORMING REGIONS OF SEAWATER TYPE SOLUTION IN THE NONEQUILIBRIUM STATE OF ISOTHERMAL BOILING EVAPORATION

Zhou* H., Gao F., Bao Y., Huangfu L., Zhang C. and Bai X.

Tianjin Key Laboratory of Marine Resources and Chemistry, College of Marine Science and Engineering, Tianjin University of Science and Technology, Tianjin TEDA, 300457, P.R. China

e-mail: zhouhuan@tust.edu.cn

Industry evaporation processes are often operated at the compulsive nonequilibrium state at boiling temperature with high evaporation intensity; meanwhile, the metastable phenomena for a complex salt-water system as seawater are still typical in this case. The salts forming regions in this condition are thus more complex and not always following the solubility diagram. However, the data of the metastable equilibria are lacking in high temperature, and the stability of metastable equilibria in industry process attracts special attention. Therefore, to know more about the behaviours of salt-forming region departing from the equilibrium phase area, the experiments of determining salt-forming region of $\text{Na}^+, \text{Mg}^{2+} // \text{Cl}^-, \text{SO}_4^{2-} - \text{H}_2\text{O}$ system, $\text{K}^+, \text{Mg}^{2+} // \text{Cl}^-, \text{SO}_4^{2-} - \text{H}_2\text{O}$ system, $\text{Na}^+, \text{Mg}^{2+} // \text{SO}_4^{2-} - \text{H}_2\text{O}$ system, and $\text{K}^+, \text{Mg}^{2+} // \text{SO}_4^{2-} - \text{H}_2\text{O}$ system were carried out by the isothermal boiling evaporation method. The salt-forming regions were determined where one-salt stable regions and a complex conditional region are existed. The conditional region were not existed in the solubility diagram or metastable diagram but accounts for a large area in the nonequilibrium state, where the salts precipitating may be one or another or together which depend more on the non-thermodynamic conditions, such as crystal seed, evaporation intensity, mechanical effects etc, it would be extremely valuable to the industry process design and control.

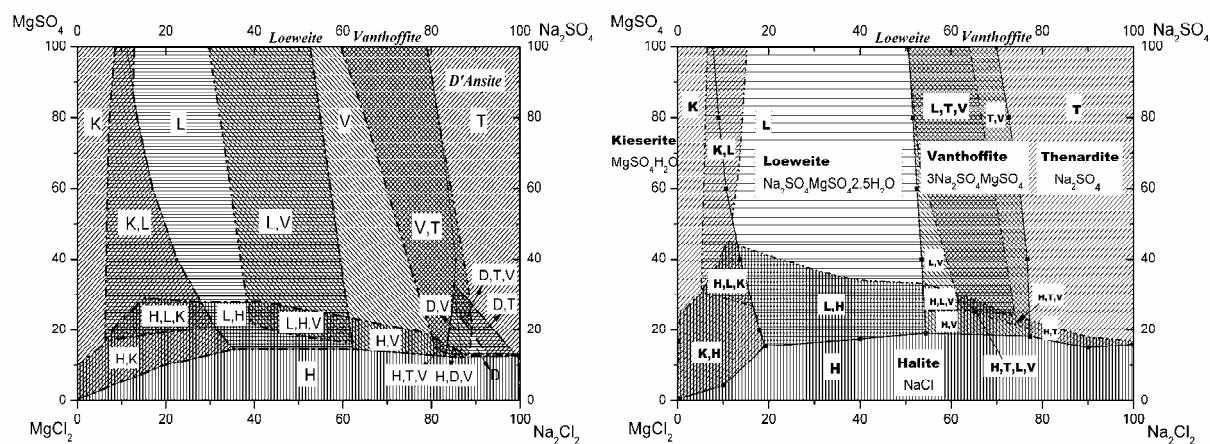


Fig. 1 and 2. Isothermal phase diagram include one-salt stable regions and a complex conditional region of $\text{Na}^+, \text{Mg}^{2+} // \text{Cl}^-, \text{SO}_4^{2-} - \text{H}_2\text{O}$ system at 348.15 K (Figure 1) and 373.15 K (Figure 2). —■— Solubility data at 348.15 K. —•— Border for conditional salt-forming regions. K, L, V, T, H denote the single salt region for Kieserite, Loewite, Vanthoffite, Thenardite and Halite. K+L, H+T, L+H, H+K denote the region may be one or another one, or together forming region. L+T+V, H+L+K, H+T+L+V denote the region may be one or two or three salts could be formed in different condition.

C: ORAL PRESENTATION

ULTRASOUND CHANGE SOLID-LIQUID EQUILIBRIUM?

Yang¹ X.G., Dong¹ H.X., Lv¹ Y., Tang¹ J.Y., Yue² G.J. and Liu³ W.X.

¹College of Materials Science and Chemical Engineering, Harbin Engineering University, Harbin 150001, China. e-mail: yxg1122@163.com; hongxingd6@yahoo.com.cn

²COFCO Biochemical Energy Co. Ltd, Beijing, 100005, China. e-mail: yuegj@cofco.com

³COFCO Biochemical Energy Co. Ltd, Zhaodong, 151100, China. e-mail: liuwx@cofco.com

This work reports that ultrasound changes solid-liquid equilibrium of glycyrrhizic acid (GA) leached from glycyrrhiza uralensis in water and it almost does not change the equilibrium of sodium chloride dissolved in water. To investigate the cause, a scanning electron microscope is used to observe the solid structure before ultrasound treatment and after that. It is found that ultrasound is able to change the structure of glycyrrhiza uralensis. So a new equilibrium is built and the equilibrium concentration of GA is influenced. But, ultrasound can not change the structure of sodium chloride and the equilibrium keeps almost unchanged. So whether the equilibrium is changed by ultrasound depends on whether the solid structure is done. And the mechanism that ultrasound affects the structure will be studied in the future.

C: ORAL PRESENTATION

THERMODYNAMIC MODELING OF THE SOLUBILITY OF ALKALI AND EARTH ALKALI BORATES

Thomsen K.

CERE, Department of Chemical and Biochemical Engineering, Technical University of Denmark, 2800, Kongens Lyngby, Denmark,
e-mail: kth@kt.dtu.dk

Solutions with borates have complex solubility behaviour. Boron appears in precipitates and in aqueous solutions in many forms such as H_3BO_3 , B_5O_8^- , $\text{B}_{10}\text{O}_{17}^{4-}$, $\text{B}_{18}\text{O}_{29}^{4-}$, $\text{B}_4\text{O}_7^{2-}$, and BO_2^- . Solubility of borates in solutions containing lithium, sodium, potassium, magnesium, and calcium salts was modelled, using the Extended UNIQUAC thermodynamic model for electrolytes [1]. $\text{H}_3\text{BO}_3(\text{s})$ forms at pH less than around 6. Salts containing the ions B_5O_8^- , $\text{B}_{10}\text{O}_{17}^{4-}$, and $\text{B}_{18}\text{O}_{29}^{4-}$, precipitate in the pH range from around 6 to 8. Tetraborates are salts containing the ion $\text{B}_4\text{O}_7^{2-}$. Tetraborates are reported to precipitate at pH from around 7 and up to 13. Metaborates contain the ion BO_2^- and precipitate at pH 13 and higher.

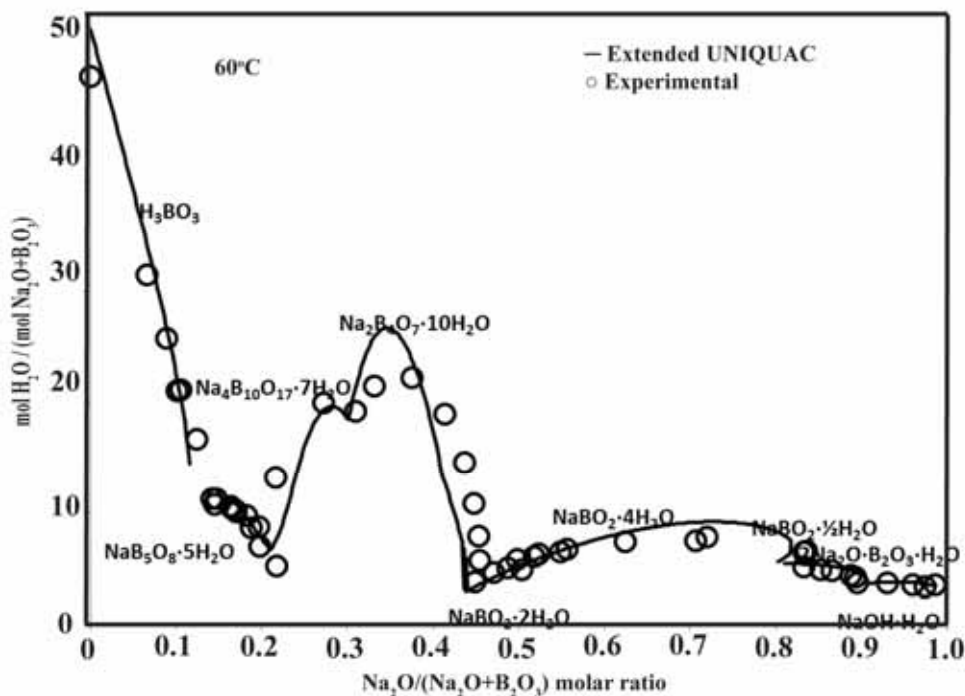


Fig. 1. Solubility in the system: $\text{B}_2\text{O}_3\text{-Na}_2\text{O-H}_2\text{O}$ at 60 °C. Experimental data are marked with circles. Solubility lines are calculated with the Extended UNIQUAC model [1]. The ordinate is mol water per mol oxides. High values therefore mean low solubility. The abscissa axis stretches from B_2O_3 to Na_2O .

References

[1] Thomsen K., Modeling Electrolyte Solutions with the extended universal quasichemical (UNIQUAC) model, *Pure Appl. Chem.*, 77, (2005) 531-542.

C: ORAL PRESENTATION

THE PREDICTION OF MINERAL SOLUBILITIES IN NATURAL WATERS: THE K-Mg-Rb-Cs-Cl-H₂O SYSTEM AT 298 K

Nie^{1,2} Z., Song^{2,3} P.S., Bu^{1,2} L.Z., Wang^{1,2} Y.S. and Zheng^{1,2} M.P

¹Institute of Mineral Resources, Chinese Academy of Geological Sciences, Beijing, China, 100037, e-mail: niezhen518@163.com;

²Key Laboratory of Saline Lake Resources and Environment, Ministry of Land and Resources, Beijing, China, 100037;

³Institute of Salt Lakes, Chinese Academy of Sciences, Xining, Qinghai, China, 810008

In Sichuan basin, China, there are huge reserves of underground brine resources. The brine of Pingluoba structure contains not only extraordinarily large amount of potassium but also high concentration of B, Cs and Rb. This paper introduces some solubility prediction research of the K, Mg, Rb, Cs//Cl-H₂O system at 298 K.

Some single salt parameters such as MgCl₂, KCl and a few mixing parameters were found from literature for Pitzer model. As for salt RbCl and CsCl, their parameters are unavailable up to near saturation. These were fitted by using the thermodynamic data and solubility data. Moreover, the mixing parameters $\theta(K,Cs)$ and $\Psi(K, Cs, Cl)$ were obtained from fitting the osmotic data of Kirginchev etc.. After the species have been parameterized, the Pitzer models were established for the quinary system and its quaternary, ternary subsystems. Then the solubility data were calculated with satisfactory results. With the prediction data, some phase diagrams as Figure 1 and 2 were drawn for the quinary system and its subsystems.

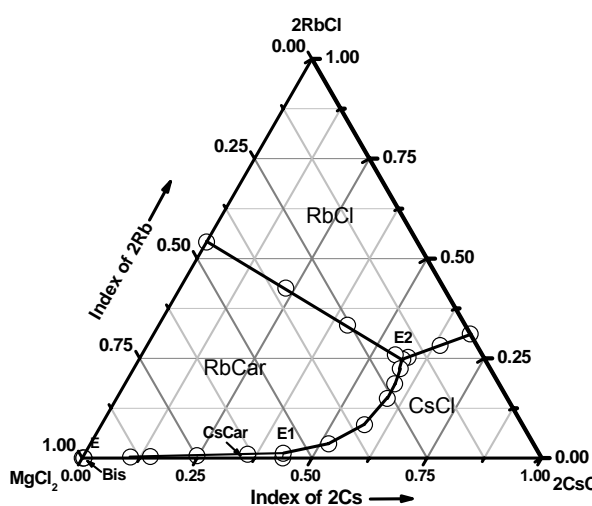


Fig. 1. Phase diagram of the system RbCl-MgCl₂-CsCl-H₂O at 298 K.

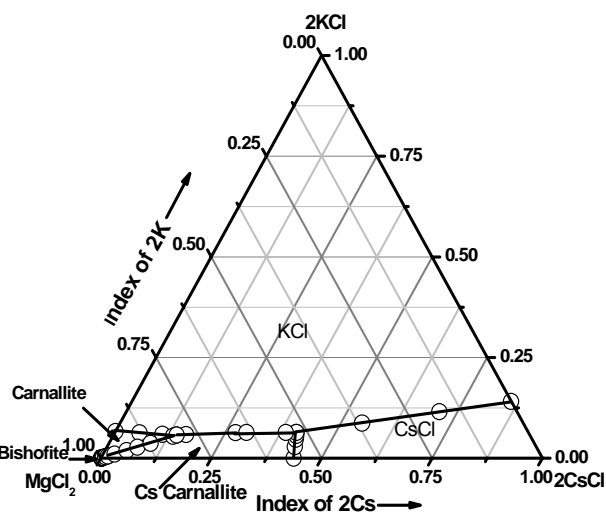


Fig. 2. Phase diagram of the system KCl-MgCl₂-CsCl-H₂O at 298 K.

C: ORAL PRESENTATION

THE EFFECT OF CONCENTRATION OF SODIUM OF SODIUM CARBONATE ON SCHEELITE DIGESTION

Zhao Z., Liao Y., Tu S., Liu X. and Li H.

School of Metallurgical Science and Engineering, Central South University, Changsha 410083, Hunan, China, e-mail: zhaozw@csu.edu.cn

After the pioneering works of Hamilton and Masleniskii, Na_2CO_3 had been used as the leaching agent to digest scheelite. It was observed that the exorbitant concentration of Na_2CO_3 (230 g/L) can deteriorate the leaching rate of scheelite. Then further investigations were carried out, and different reasons for this phenomenon were put forward [1]. The most popular explanation is that Na_2CO_3 reacted with CaCO_3 to produce double salts, so the leaching agent was consumed, while these double salts were hard to produce and easy to decompose according to other research. In this article, the pseudo-ternary-system phase diagram method is used for studying the effect of concentration of Na_2CO_3 on scheelite digestion at 75 °C and 225 °C respectively [2]. It shows that under the condition of over high initial concentration of Na_2CO_3 , the sodium tungstate generated by digesting scheelite will lead to “salting out effect”, which make the leaching agent Na_2CO_3 crystallize from the solution; thereby it will go against the leaching of scheelite.

References

- [1] Martins J.P., Martins F., Soda ash leaching of scheelite concentrations: the effect of high concentration of sodium carbonate, *Hydrometallurgy*, **46**, (1997) 191–203.
- [2] Zhao Z., Li H., Thermodynamics for leaching of scheelite— pseudo-ternary-system phase diagram and its application, *Metall. Mater. Trans. B*, **39B**, (2008) 519–523.

C: ORAL PRESENTATION

THE INFLUENCE OF MINERAL PHASES ON TRACE ELEMENTS DISPERSION BY LEACHATES FROM SULFIDE CONTAINING TAILINGS FROM SÃO DOMINGOS MINE, PORTUGAL. POT EXPERIMENTS.

Magalhães¹ M.C.F., Santos^{2,3} E.S., Abreu² M.M. and Macías⁴ F.

¹Departamento de Química and CICECO, Universidade de Aveiro, P-3810-193 Aveiro, Portugal

e-mail: mclara@ua.pt

²Unidade de Investigação de Química Ambiental (UIQA), Instituto Superior de Agronomia, TU Lisbon, Tapada da Ajuda, P-1349-017 Lisboa, Portugal, e-mail: manuelaabreu@isa.utl.pt

³Centro de Investigação em Ciências do Ambiente e Empresariais (CICAE), Instituto Superior Dom Afonso III, Convento Espírito Santo, P-8100-641 Loulé, Portugal

e-mail: erika.santos@inuaf-studia.pt

⁴Departamento de Edafología y Química Agrícola, Facultad de Biología, Universidad de Santiago de Compostela, *Campus* Universitario Sur, E-15782 Santiago de Compostela, Spain

e-mail: felipe.macias.vazquez@usc.es

The mining activity in the pyrite containing ore bodies produces usually, wastes generating acid drainage, the called acid mine drainage (AMD), with serious environmental impact. The AMD has frequently pH < 1.5 and can promote trace elements dispersion on the adjacent areas decreasing the local biodiversity (vegetation and other organisms). Greenhouse pot experiments, containing wastes from São Domingos mine, Portugal, were conducted in order to study, during one year, the behaviour of the systems water + mining wastes, and water + mining wastes + amendment mixture (solid wastes from agriculture (plant remains+strawberry substrate and rockwool used to strawberry crop) and from liquor distillation of *Ceratonia siliqua* L. fruits and *Arbutus unedo* L. fruits, and limestone rock wastes with particle size < 2 mm).

To study the time evolution of the leachates, aqueous samples were collected from the bottom of the pots, after one, four, seven and thirteen months of incubation, and were analyzed for electrical conductivity, pH and total concentrations of As, Al, Ca, Cu, Fe, K, Mg, Mn, Pb, Zn, sulfate and phosphates. The crystal phases that grow as efflorescence on the top of the solid materials contained in the pots, as well as the possible crystal evolution in the core of the systems were analyzed by X-ray diffraction. After thirteen months of incubation there were no significant differences in the leachates composition from both systems that showed a significant decrease in the concentrations of As, Al, Cu, Fe, Pb, Zn and sulfate when compared to the values measured in the first month. The amendments addition led to differences in the solid phases formed, after thirteen months of incubation, in efflorescent salts and in core materials from non-amended and amended systems. In efflorescent salts were found very soluble aluminium sulfates together with alunite-jarosite group solid phases for amended systems (pH ≈ 2.1), and copiapite group solid phases for non-amended systems (pH ≈ 1.6). The presence of various solid phases with lower solubility as berlinite, scorodite, philipsbornite and beudantite, principally in core materials, explained the low trace elements concentrations in the acid leachates. These solid phases are only stable in acid medium, being the minerals presented in the efflorescences very soluble and only possible to crystallize in dry conditions. In wet conditions they do not crystallize and the mobilization of the constituent elements will be again dispersed in the environment.

The stability conditions of some of the solid phases will be analysed as well as their environmental implications.

C: ORAL PRESENTATION

ABSORPTION EQUILIBRIA OF (SO₂+NO₂+NaClO₂+NaOH) SYSTEM

Mondal M.K.

Department of Chemical Engineering and Technology, Institute of Technology, Banaras Hindu University, Varanasi 221005, Uttar Pradesh, India
email: mkmondal.che@itbhu.ac.in; mkmondal13@yahoo.com

Simultaneous absorption of SO₂ and NO₂ was carried out in a blend of NaClO₂ and NaOH at SO₂ concentrations from (500 to 1500) ppm, NO₂ concentrations from (200 to 1000) ppm, and temperatures in the range of (305 to 321) K. The concentrations of NaClO₂ solution were varied from (0.005 to 0.01) M along with fixed 0.001 M NaOH concentration. The absorption equilibria was experimented and executed by the saturation method [1] using a laboratory scale semi-batch agitated vessel. The experimental runs were carried out at atmospheric pressure. Both SO₂ and NO₂ removal efficiencies decreased with time and finally attained zero removal efficiency showing that solutions become saturated or equilibrium was established.

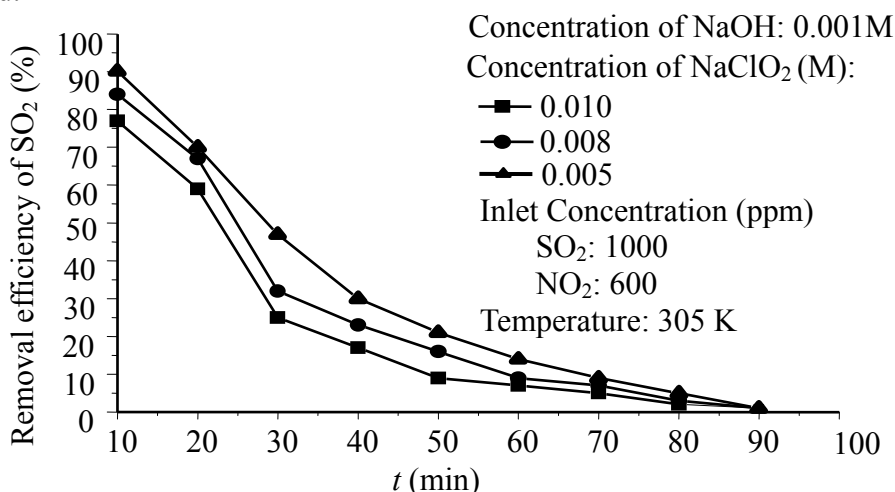


Fig. 1. Effect of various concentrations of NaClO₂ on SO₂ removal efficiency in simultaneous removal of SO₂ and NO₂.

SO₂ removal efficiency increased with decrease in NaClO₂ concentration from 0.005 to 0.01 M for fixed time of absorption (Fig. 1) because the dissolved SO₂ reacts with OH⁻ to form SO₃²⁻ [2] which is then oxidized by ClO₂⁻ to form SO₄²⁻. The formation of ClO₂⁻ is more for higher concentration of NaClO₂ which reduces the solubility of SO₂ in scrubbing solution. The NO₂ removal efficiency for simultaneous removal of SO₂ and NO₂ showed same trend as that of SO₂ for various concentrations of NaClO₂. ClO₂⁻ formation is more which consumes more OH⁻ ions rather in the formation of SO₄²⁻ and NO₃⁻ ions which actually reduces the solubility of both SO₂ and NO₂ in the system. Optimum operating conditions for maximum NO₂ and SO₂ removal efficiencies were observed as NaClO₂ concentration of 0.005 M, NaOH concentration of 0.001 M and 305 K temperature.

References

- [1] Mondal M.K., Solubility of carbon dioxide in an aqueous blend of diethanolamine and piperazine, *J. Chem. Eng. Data*, **54**, (2009) 2381–2385.
- [2] Jin D.S., Deshwal B.R., Park Y.S., Lee H.K., A simultaneous removal of SO₂ and NO by wet scrubbing using aqueous chlorine dioxide solution, *J. Hazard. Mater.*, **B135**, (2006) 412–417.

C: ORAL PRESENTATION

SOLUBILITY OF METAL OXIDES AND HYDROXIDES IN ALKALINE SOLUTIONS

Königsberger L.C., Königsberger E., Hefter G. and May P.M.

School of Chemical and Mathematical Sciences, Murdoch University, Murdoch, WA 6150,
Australia,

e-mail: L.Koenigsberger@murdoch.edu.au

E.Koenigsberger@murdoch.edu.au

G.Hefter@murdoch.edu.au

P.May@murdoch.edu.au

Reliable solubility data for oxides and hydroxides of heavy metals in alkaline solutions are relevant to a number of industrial and geochemical processes, including the production of high-purity alumina in the Bayer process, the formation of ores from geothermal solutions at high pH, hydrometallurgical leaching processes for the extraction of metal values from ores and plant residues, and the storage and processing of certain types of radioactive waste.

Recent results obtained for various systems will be reported, including experimental and modelling aspects. A new facility for the storage, handling and processing of solubility data will be outlined.

C: ORAL PRESENTATION

SOLUBILITY CALCULATIONS FOR THE OCEANIC SALT SYSTEM USING THE THEREDA – NEW DEVELOPMENTS

Voigt W.

Department of Inorganic Chemistry; TU Bergakademie Freiberg, 09596 Freiberg, Germany,
e-mail: wolfgang.voigt@chemie.tu-freiberg.de

THEREDA is a project dedicated to a **THE**rmodynamic **RE**ference **DA**tabase. The main objective is to establish a comprehensive and internally consistent thermodynamic reference database for the geochemical modeling of near-field and far-field processes occurring in the different rock formations currently under discussion in Germany to host a repository for radioactive waste. The project commenced in 2006 and is organized and conducted by the leading research institutes in the field of radioactive and (chemo)toxic waste disposal in Germany (GRS Braunschweig, INE Karlsruhe, Helmholtz-Zentrum Dresden-Rossendorf, AF-Consult Switzerland AG and TU Bergakademie Freiberg), where every institution contributes for particular chemical parts of the database. Thus for a quite large range of substance classes as the oceanic salt components, silicates, cement phases, heavy metal as well as actinide compounds consistent sets of standard formation data and ionic interaction coefficients are established and made available through the internet (www.thereda.de) for users world-wide.

Integration of new data sets is performed following strict quality rules supported by suited software and checked by bench-mark calculations from all participating groups. Since ionic interactions are described on the basis of the Pitzer's equations, solubility calculations in complex systems can be performed from dilute to concentrated solutions. In order to avoid typing errors and to simplify data transfer to the user data can be retrieved as files directly readable for the geochemical codes PHREEQC, EQ3/6, Geochemists Workbench and for the ChemApp - FACTSAGE family.

With the last release solubility calculations are possible for the hexary oceanic salt system Na^+ , K^+ , Mg^{2+} , Ca^{2+} , Cl^- , SO_4^{2-} completed by the corresponding acids and bases (HCl , H_2SO_4 , NaOH , KOH , $\text{Mg}(\text{OH})_2$, $\text{Ca}(\text{OH})_2$) in a temperature range between 0 °C to approx.. 110 °C, in certain cases up to 200 °C.

Examples of the description quality of solubility data will be given. Next steps of developments concern the inclusion of CO_2 up to pressures of 300 bars and the solubility of carbonates of alkaline and alkaline earth metals. First results will be presented and problems with the handling of pressure dependencies by the various codes will be discussed. Extension of the database to these systems and pressures will open it for applications in the field of geothermal energy and CO_2 sequestration in deep geological formations.

C: ORAL PRESENTATION

THERMODYNAMIC PROPERTIES OF LiCl(aq) AND CALCULATION OF SOLUBILITIES IN THE $\text{Li}^+\text{-Na}^+\text{-Mg}^{2+}\text{-Cl}^-\text{-SO}_4^{2-}\text{-H}_2\text{O}$ SYSTEM

Steiger M.

Department of Chemistry, University of Hamburg, Germany
email: steiger@chemie.uni-hamburg.de

Lithium chloride is an important constituent in natural brines from salt lakes in South America and China. These brines are major resources to meet the increasing demand in lithium, e.g. for the production of rechargeable batteries. The recovery of lithium compounds from natural brines requires solubility diagrams of mixed electrolyte solutions, hence, the ability to predict solubility equilibria in these brines.

The prediction of solubilities in mixed solutions requires an electrolyte solution model such as the ion interaction (Pitzer) model for the calculation of activities in concentrated solutions. The present work is part of a study aiming at the prediction of solubilities in mixed electrolyte systems, e.g. the $\text{Li}^+\text{-Na}^+\text{-Mg}^{2+}\text{-Cl}^-\text{-SO}_4^{2-}$ system. However, the calculation of thermodynamic properties in aqueous solutions containing LiCl and the prediction of phase equilibria is challenging due to the extremely high concentrations in saturated solutions. In fact, existing accurate equations for the thermodynamic properties of LiCl(aq) that are based on the conventional ion interaction equations are either limited to molalities $<6 \text{ mol}\cdot\text{kg}^{-1}$ or, they make use of more complicated equations.

In the present work we present an extended Pitzer ion interaction model that can be used to represent the thermodynamic properties of LiCl(aq) to high concentrations. The model is also used to reproduce the solubilities in the binary LiCl–H₂O system from 172 K to about 450 K including the crystalline phases LiCl·*n*H₂O with *n* = 0,1,2,3,5 (see Fig. 1a). We also present an ion interaction model for Li₂SO₄(aq) and show first results of the prediction of solubilities in the quinary $\text{Li}^+\text{-Na}^+\text{-Mg}^{2+}\text{-Cl}^-\text{-SO}_4^{2-}$ system at various temperatures. For example, Fig. 1b depicts solubilities of MgSO₄·7H₂O and Li₂SO₄·H₂O in aqueous LiCl–MgSO₄ mixed solutions.

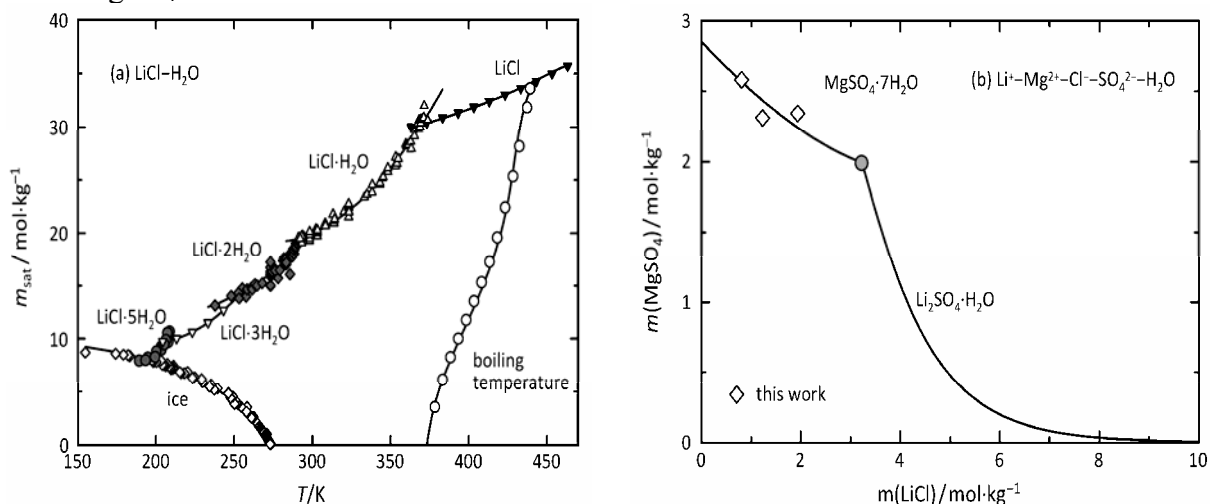


Fig. 1. (a) Freezing temperatures, boiling temperatures and solubilities in the LiCl–H₂O system; symbols represent literature data, curves calculated with the present model. (b) Solubilities of MgSO₄·7H₂O and Li₂SO₄·H₂O in LiCl–MgSO₄ mixed solutions at 293 K; white diamonds represent experimental solubilities of MgSO₄·7H₂O.

C: ORAL PRESENTATION

SOLUBILITIES OF BASIC MAGNESIUM SALT HYDRATES AT DIFFERENT TEMPERATURES

Oestreich M., Freyer D. and Voigt W.

Institut für Anorganische Chemie, TU Bergakademie Freiberg, D-09599 Freiberg,
Deutschland,
e-mail: melanie.oestreich@chemie.tu-freiberg.de

Basic magnesium salt hydrates are formed when caustic magnesium oxide reacts with concentrated solutions of magnesium salts. In case of MgCl_2 the mixtures solidify as a cement named after the discover Sorel cement [1]. Besides its application as floating floor MgO -based concrete represents one of the most promising building materials in salt mines.

To ensure long-term stability against salt solutions containing Na^+ , K^+ , Mg^{2+} , Ca^{2+} , Cl^- and SO_4^{2-} the solubility diagrams with the respective crystallization branches of the basic salts $x \text{Mg}(\text{OH})_2 \cdot y \text{MgA} \cdot z \text{H}_2\text{O}$ ($A = \text{Cl}^-$, SO_4^{2-}) have to be known at the temperatures of interest.

Solubility data and structural characteristics of occurring basic salt in the subsystem MgO - MgCl_2 - H_2O have been published at 25 °C and 120 °C by us recently [2]. Here we present our latest results for this system at 40 °C, 60 °C, 80 °C and 100 °C. In the corresponding sulphate system we present our new solubility data at temperatures between 25 °C and 120 °C. The experimental details and the protracted establishment of equilibrium state for the different phases will be discussed.

References

- [1] Sorel S., Sur un nouveau ciment magnésien, *C. R. Acad. Sci.*, **65**, (1867) 102–104.
- [2] Dinnebier R.E., Freyer D., Bette S., Oestreich M., $9 \text{Mg}(\text{OH})_2 \cdot \text{MgCl}_2 \cdot 4\text{H}_2\text{O}$, a high temperature phase of the magnesia binder system, *Inorg. Chem.*, **49**, (2010) 9770–9776.

C: ORAL PRESENTATION

THERMODYNAMIC PROPERTIES OF MIXTURES CONTAINING IONIC LIQUIDS BASED ON BIS[(TRIFLUOROMETHYL)SULFONYL]IMIDE FOR APPLICATION IN HOMOGENEOUS CATALYSIS

Machanová¹ K., Bendová¹ M., Jacquemin² J., Troncoso³ J. and Wagner¹ Z.

¹E.Hala Laboratory of Thermodynamics, Institute of Chemical Process Fundamentals, AS CR, v.v.i., Rozvojova 135, 16002 Prague 6, Czech Republic, e-mail: machanova@icpf.cas.cz

²QUILL Research Centre, Queen's University of Belfast, David Keir Building, Stranmillis Road, Belfast BT9 5AG Northern Ireland, UK, e-mail: johan.jacquemin@qub.ac.uk

³Dpto. Física Aplicada, Facultad de Ciencias de Ourense, Universidade de Vigo, As Lagoas s/n, 32004 Ourense, Spain, e-mail: jacobotc@uvigo.es

Over the last two decades ionic liquids have started to play an important role in the world of chemistry. Owing to their unique properties scientists predicted a brilliant future for them. The influence of ionic liquids has spread to many areas, such as electrochemistry, classical synthesis, and automotive or pharmaceutical industry, the latter involving homogeneous catalysis.

Homogeneous catalysis is highly effective, nevertheless, separation of products poses a serious problem. Herein, we present a set of ionic liquids providing asymmetric enantioselective hydrogenation, which are readily separable from the reaction mixture due to their hydrophobicity. Moreover, a precious catalytic complex Ru-BINAP can be immobilized by the ionic liquids for recyclation and further reuse.

The new set of ionic liquids prepared in laboratory comprises n-alkyl-triethylammonium bis[(trifluoromethyl)sulfonyl]imides (abbrev. [NR222][Tf2N]) with alkyl chain lengths R = 6, 7, 8, 10, 12 and 14 [1].

We have started a comprehensive characterization of the set not only by means of pure-liquid properties but also by properties in mixtures with methanol and/or water. We have obtained the rheological behaviour and thermodynamic properties of pure ionic liquids as densities, viscosities, refractive indices, heat capacity etc. Moreover, thanks to the collaboration with Spanish University of Vigo, selected excess quantities in mixtures with methanol were determined. Last but not least, solubilities were measured by two verified methods, a cloud-point method and volumetric method [2], in water and in a mixture with methanol and water (1:1 weight ratio).

The experimental data were correlated by the Redlich-Kister equation (excess properties) and the Flory-Huggins equation modified by De Sousa and Rebelo (LLE data). The studied properties were also predicted using the ERAS [3] and COSMO-RS [4] models.

References

- [1] Floriš T., Klusoň P., Bártek L., Pelantová H., Quaternary ammonium salts ionic liquids for immobilization of chiral Ru-BINAP complexes in asymmetric hydrogenation of ketoesters, *Appl. Catal. A.*, **366**, (2009) 160–165.
- [2] Bendová M., Wagner Z., Liquid–Liquid Equilibrium in Binary System [bmim][PF6] + 1-Butanol, *J. Chem. Eng. Data*, **51**, (2006) 2126–2131.
- [3] Garcia-Miaja G., Troncoso J., Romani L., Excess properties for binary systems ionic liquid + ethanol: Experimental results and theoretical description using the ERAS model, *Fluid Phase Equilib.*, **274**, (2008) 59–67.
- [4] Diedenhofen M., Klamt A., COSMO-RS as a tool for property prediction of IL mixtures - A review, *Fluid Phase Equilib.*, **294**, (2010) 31–38.

C: ORAL PRESENTATION

PHASE EQUILIBRIA IN RbBr–LaBr₃ BY THERMODYNAMIC MODELLING

Gong^{1,2} W.P., Zhang¹ L. and Gaune-Escard³ M.

¹Electronic science department, Huizhou University,
Huizhou 516001, Guangdong, P. R. China
Telephone: +86-752-2527271, 13825471698

e-mail address: weiping_gong@mail.csu.edu.cn, gwp@hzu.edu.cn

²State Key Laboratory of Powder Metallurgy, Central South University,
Changsha 410083, Hunan, P. R. China

³Polytech Marseille, Laboratoire IUSTI, CNRS-UMR 6595, Technopole de Chateau-Gombert,
5 rue Enrico Fermi, 13453 Marseille cedex 13, France

Lanthanide halides and their mixtures with alkali metal halides play a significant role in a number of industrial applications largely based on molten salt technologies, many still under development. Their thermodynamic and transport properties can provide basic information for process development and optimization. However these data are scarce and not easily accessible in literature. Accordingly, intensive efforts are being made at an international level both in R&D aspects and also in database development. This paper performed thermodynamic calculations on the RbBr-LaBr₃ binary system over the entire temperature and composition range. A two sub-lattice ionic solution model (Rb⁺)_P: (Br⁻, LaBr₆³⁻, LaBr₃)_Q was adopted to describe the liquid phase and the thermodynamic parameters for each phase in the RbBr-LaBr₃ system were reassessed by using available experimental information on phase diagram and thermodynamic properties. Compared with the results from literature, all of the current parameters are introduced according to the types of experimental data, and the present calculations explain the experimental data satisfactorily.

Acknowledgments: The funding for projects came from the Natural Science Foundation of China (No.51171069) and Guangdong (No. S2011010004094). The support from the Special Talents of Higher Education Office of Guangdong Province is also greatly appreciated.

C: ORAL PRESENTATION

THE HYDRATE WATER CONTENT OF BASSANITE–DEPENDENCE ON WATER ACTIVITY

Freyer D.

Institut für Anorganische Chemie, TU Bergakademie Freiberg, D-09596 Freiberg,
Deutschland,
e-mail: daniela.freyer@chemie.tu-freiberg.de

Bassanite or hemihydrate ($\text{CaSO}_4 \cdot 0.5 \text{H}_2\text{O}$) is the basic material of gypsum plaster building materials. According to the setting reaction: $\text{CaSO}_4 \cdot 0.5 \text{H}_2\text{O} + n \text{H}_2\text{O} \rightarrow \text{CaSO}_4 \cdot 2 \text{H}_2\text{O} + n-1.5 \text{H}_2\text{O}$ gypsum products are produced for a wide range of applications primarily in the building material sector such as plasters, gypsum mortars, plaster flow screeds and plasterboards as well as a setting retarder in cement manufacture. Gypsum products are also used for producing models and moulds and in the medical sector.

The world-wide production of the basic material hemihydrate is based on calcination (drying of gypsum at enhanced temperatures: production of β -hemihydrate) or autoclaving (crystallization in aqueous solutions: production of α -hemihydrate) of gypsum. In the latter case a suspension of gypsum is heated above the transformation temperature gypsum-hemihydrate (above 100 °C) according the solubility diagram $\text{CaSO}_4\text{--H}_2\text{O}$. Because the transition temperature depends on the water activity, α -hemihydrate can be formed in solutions of lower water activity, such as in salt solutions (e.g. NaCl, MgCl_2) or concentrated strong acids (e.g. HNO_3) near room temperature [1].

The stoichiometry of the hemihydrate is generally known as “ $\text{CaSO}_4 \cdot 0.5 \text{H}_2\text{O}$ ” although the existence of so-called subhydrates ($\text{CaSO}_4 \cdot x \text{H}_2\text{O}$ with $0.5 \leq x \leq 0.8$) is discussed in literature for long time on the basis of small changes in the powder diffraction pattern dependent on water vapour pressure starting at about 40% relative air humidity.

By our latest single crystal structure analysis the existence of a subhydrate ($\text{CaSO}_4 \cdot 0.625 \text{H}_2\text{O}$) [2,3] was evidenced. In this context actual investigations to the systematic formation and existence of hemihydrate and its higher hydrates (subhydrates) in presence of definite air humidity (by powder x-ray and TG/DTA) as well as in aqueous solutions with different water activities (by Raman Spectroscopy) were carried out. The results of the reversible changing hydrate water content as a function of water activity respectively the relative air humidity will be discussed.

References

- [1] Freyer D., Voigt W., Crystallization and phase stability of CaSO_4 and CaSO_4 -based salts, *Chemical Monthly*, **134**, (2003) 693–719.
- [2] Schmidt H., Paschke I., Freyer D., Voigt W., Water channel structure of bassanite at high air humidity: crystal structure of $\text{CaSO}_4 \cdot 0.625 \text{H}_2\text{O}$, *Acta Cryst.*, **B67**, (2011) 467–475.
- [3] Schmidt H., Paschke I., Freyer D., Voigt W., Water channel structure of bassanite at high air humidity: crystal structure of $\text{CaSO}_4 \cdot 0.625 \text{H}_2\text{O}$, *Acta Cryst.*, **B68**, (2012) 1.

C: ORAL PRESENTATION

CRYSTALLIZATION PATHS IN CaO–Al₂O₃–SiO₂ SYSTEM

Lutsyk^{1,2} V.I. and Zelenaya¹ A.E.

¹Institute of Physical Materials Science (Siberian Branch of RAS), Ulan-Ude, 670047, Russia

²Buryat State University, Ulan-Ude, 670000, Russia, e-mail: vluts@pres.bsnet.ru

Even in this system, that is very important for technology, there are contradictions in data. E.g., compound C₁₂A₇ has been ignored in calculation [1], but it was found as mineral [2] and was investigated as the dense ceramics [3]. It is possible to find information about the restricted number of crystallisation paths in the liquidus fields CaO (triangles CaO–C₃S–C₃A, C₃S–C₂S–C₃A, C₂S–C₃A–C₁₂A₇), C₃S, CA, C₂AS, A(Al₂O₃), A₃S₂. We used a computer model of T-x-y diagram with the mass balances to check the known crystallisation paths and to design the new ones. Twelve compounds have their own liquidus in the model: C₃S(R₁), C₃S₂, C₃A(R₆), CA₆ – incongruent, and C₂S(R₂), CS, A₃S₂, C₁₂A₇(R₇), CA, CA₂, C₂AS, CAS₂. Projecting surfaces to the composition simplex, 325 concentration fields were received: 117 two-, 163 one- and 45 zero-dimensional ones. Some fields are not the original, because they haven't their own set of phase reactions and their own set of microstructure elements.

Let's consider the mass center $G \in Q_1-Q_2-8-6$ (Figure 1a) intersecting the phase regions L+R₁, L+R₁+R₆, L+R₂+R₆, R₂+R₆+R₇, two planes of four-phase regrouping at the temperature of invariant points Q₂ and Q₃. It is characterized by the following set of phase transformations: $L^1 \rightarrow R_1^1$, $L^e \rightarrow R_1^{R_6} + R_6^{R_1}$, $L^{Q_2} + R_1 \rightarrow R_2^{Q_2} + R_6^{Q_2}$, $L^{ep} \rightarrow R_2^{R_6,ep} + R_6^{R_2,ep}$, $L^{Q_3} + R_6 \rightarrow R_2^{Q_3} + R_7^{Q_3}$ with formation of structural elements R₂^{R₁}, R₂^{Q₂}, R₆^{Q₂}, R₂^{R_{6,ep}}, R₆^{R_{2,ep}}, R₂^{Q₃}, R₇^{Q₃} (Figure 1b). The crystals R₁ are replaced by crystals R₂ at the regrouping on plane at Q₂. And so crystals R₁¹ and R₁^{R₆} are absent in microstructure set. The adjoining field Q₁-Q₂ has the same microstructure set, but differs by the absence of reaction $L^1 \rightarrow R_1^1$, since it belongs to the monovariant liquidus line.

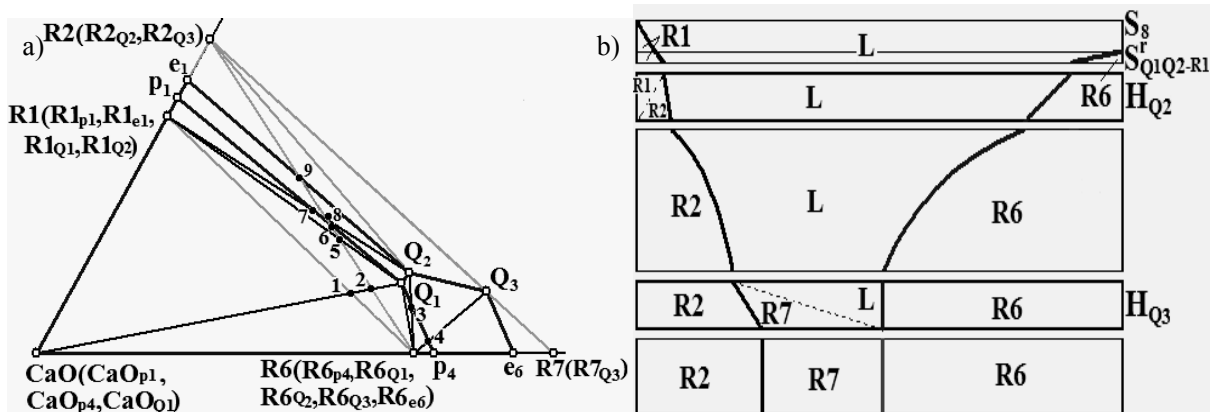


Fig. 1. $G \in (Q_1-Q_2-8-6)$ mass balance, $8=R_1Q_2 \cap R_2R_6$, $6=p_1Q_1 \cap R_2R_6$

References

- [1] Shobu K., CaTCalc: new thermodynamic equilibrium calculation software, *CALPHAD*, **33**, (2009) 279–287.
- [2] Hentschel G., Mayenit, 12CaO·7Al₂O₃ und Brownmillerit, 2CaO·(Al,Fe)₂O₃, zwei neue Minerale in den Kalksteineinschlüssen der Lava des Ettringer Bellerberges, *Neues Jahrb. Mineral, Mh.* (1964) 22–29.
- [3] Tolkacheva A.S., Shkerin S.N., Plaksin S.V. et al., Synthesis of dense ceramics of single-phase mayenite (CA₁₂AL₁₄O₃₂)O, *Rus. J. App. Chem.*, **84**, (2011) 907–911.
- [4] Lutsyk V., Zelenaya A., Savinov V., Melt solidification in the ceramic system CaO–Al₂O₃–SiO₂, *IOP Conf. Ser.: Mater. Sci. Eng.*, **18**, (2011) 1–4.

C: ORAL PRESENTATION

A NOVEL QSPR METHOD FOR ESTIMATION OF HANSEN SOLUBILITY PARAMETERS USING COSMO-RS SIGMA MOMENTS

Járvás G. and Dallos A.

Department of Chemistry, University of Pannonia, H-8200, Veszprém, Hungary,
e-mail: jarvasg@gmail.com

The three-dimensional Hansen solubility theory gives information about the relative strengths of solvents and allows determining solvents, which can be used to dissolve a specific solute. This approach has significantly upgraded the power and usefulness of the solubility parameter in the screening and selection of the appropriate solvents in industry and in laboratory applications. Although the definition of the Hansen Solubility Parameters (HSPs) is simple, their experimental determination is not always easy, especially for non-volatile compounds. Thus, several methods are published for the estimation of HSPs, i.a. Cohesive energy density methods based on the molecular structure and molecular dynamics computer simulation and group contribution methods. However, the group contribution methods require the knowledge of all chemical group contributions, which is difficult for ionic liquids or acid/base mixtures (organic salts) involving molecular association.

To eliminate the disadvantage of existing models, a novel multivariate nonlinear QSPR model has been developed based on COSMO-RS sigma-moments as molecular descriptors. The sigma-moments are obtained from high quality quantum chemical calculations using the continuum solvation model COSMO-RS and a subsequent statistical decomposition of the resulting polarization charge densities. Artificial neural network was applied to describe the correlation between three-dimensional Hansen solubility parameters and sigma-moments. The nonlinear QSPR models for HSPs were built on a training/validation data set of compounds having a broad diversity of chemical characters.

The prediction power of the correlation models for HSPs was validated on a test set of compounds with various functional groups and polarity, among them drug-like molecules, organic salts, solvents and ion-pairs.

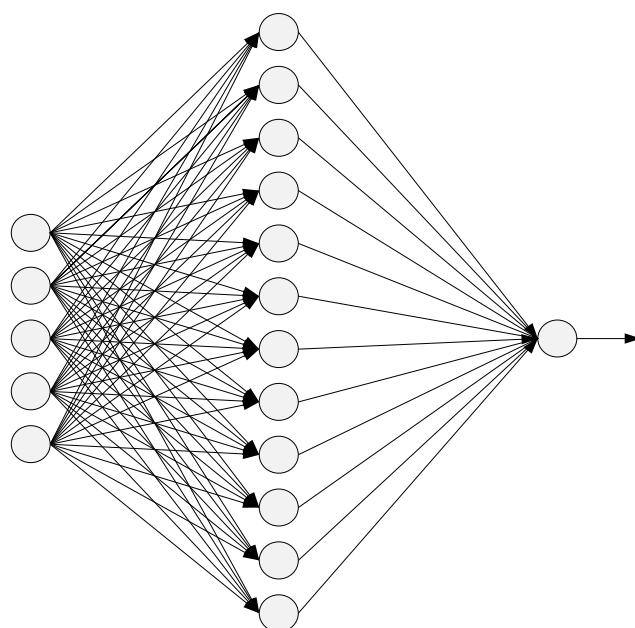


Fig. 1. Visualization of architecture of the optimized ANN using 5 σ -moments.

C: ORAL PRESENTATION

SOLUBILITY, CRITICAL STATES AND THERMODYNAMIC PECULIARITIES OF MULTICOMPONENT REACTIVE LIQUID – LIQUID SYSTEMS

Toikka A.

Department of Chemical Thermodynamics and Kinetics, Faculty of Chemistry,
Saint-Petersburg State University, Universitetskiy prospect 26, Peterhof, Saint-Petersburg,
198504, Russia, e-mail: alexander.toikka@chem.spbu.ru

Limited solubility in reactive systems may significantly influence on the run of chemical engineering processes. On the one hand the splitting of the reacting mixture leads to the unfavorable changes in reaction kinetics and hydrodynamic conditions in chemical reactor. On the other hand the reactions in heterogeneous media may be useful for the design of coupled processes “reaction + separation” such as reactive extraction. The study of reactive liquid – liquid (LL) systems is also of well-known importance for the development of basic physical-chemical theory of heterogeneous systems with chemical interactions. In this work we present the results of our recent experimental research in this area. The peculiarities of multicomponent reacting systems with immiscibility gap are considered on the base of thermodynamic approach.

The new experimental data sets on LL systems with ester synthesis reaction (*n*-propyl acetate and ethyl acetate) at few temperatures gave the opportunity to construct the polythermal critical surface of LL equilibrium in composition tetrahedron. For the system with *n*-propyl acetate synthesis reaction the lines of chemically equilibrium critical phases had been determined at 293 – 313 K. The general consideration of mutual disposition of chemical equilibrium and binodal surfaces will be presented. The topology of phase diagrams of reactive liquid-liquid equilibrium with critical points of LL equilibrium is discussed for some types of binary, ternary and quaternary systems.

The thermodynamic analysis of systems with limited solubility in the system with equilibrium and non-equilibrium chemical reactions is carried out for the case of ternary systems. In comparison with non-reactive mixtures the state diagrams of heterogeneous reacting systems include some additional singularities: stoichiometric lines, chemical equilibrium and iso-affinity curves (curves of constant affinity). The change of affinity on binodal curves is determined by the run of chemical equilibrium curve, tie-lines and stoichiometric lines dispositions in composition triangle. The thermodynamic analysis is carried out on the base of stability conditions and conditions of phase equilibrium. The special cases of extremum of the affinity at the curves of LL equilibrium and variants of disposition of chemical equilibrium curve in composition triangle of heterogeneous system are discussed.

Acknowledgements: This research was supported by Russian Foundation for Basic Research (grant 12-03-00522a). Author is also grateful to Maria Toikka, Maya Trofimova and Boris Gorovitz for fruitful discussion and help.

References

- [1] Trofimova M., Toikka M., Toikka A. Solubility, liquid-liquid equilibrium and critical states for the quaternary system acetic acid–ethanol–ethyl acetate–water at 293.15 K, *Fluid Phase Equilib.*, **313**, (2012) 46–51.
- [2] Toikka A.M., Trofimova M.A., Toikka M.A., Chemical equilibrium of esterification reaction in the AcOH–EtOH–H₂O–EtOAc system at 293.15 K, *Russ. Chem. Bull*, Issue **3**, (2012) 659–661.

C: ORAL PRESENTATION

SOLUBILITY OF THREE-PRIMARY-COLORS DISPERSE DYES AND THEIR BLENDS IN SUPERCRITICAL CARBON DIOXIDE

Tamura K., Tanaka K. and Hiraki D.

Division of Material Sciences and Material Engineering,
Graduate School of Natural Science and Technology, Kanazawa University, Kanazawa
920-1192, Japan, e-mail: tamura@t.kanazawa-u.ac.jp

In supercritical carbon dioxide (SC-CO₂) dyeing process we can save and reuse the additives and dyes more than the conventional wet dyeing process. This process has a considerable potential as an attractive alternative method from a viewpoint of environmental protection and sustainable development. To develop and assist the design of the supercritical carbon dioxide dyeing process actually, the experimental solubilities of various kinds of dyes and the blends of their dyes in SC-CO₂ and their accurate representation using a thermodynamic model are required. In this work we measured the solubilities of C.I. Disperse Blue, Yellow and Red at the pressure ranges from 10 MPa to 25 MPa and the temperatures at 323 K, 353 K and 383 K as well as those of their disperse dye mixture in SC-CO₂ at the pressures of 15 MPa and 25 MPa and the temperatures of 323 K and 393 K. The experimental results were calculated using the equations of state proposed by Peng-Robinson.

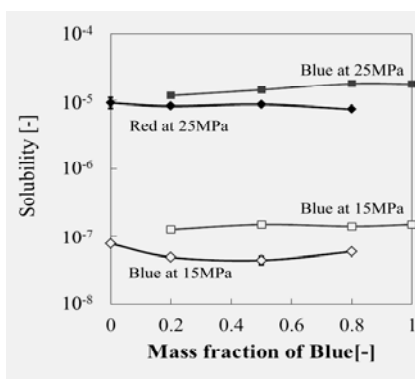


Fig. 1. Solubilities of Blue and Red mixtures in SC-CO₂ at 353 K.

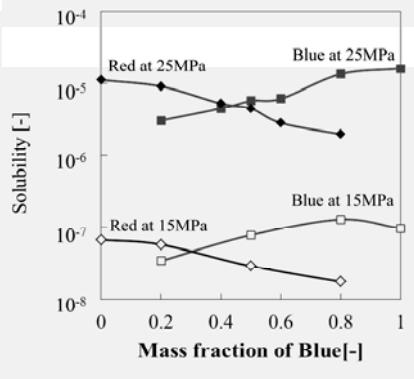


Fig. 2. Solubilities of Blue and Red mixtures in SC-CO₂ at 393 K.

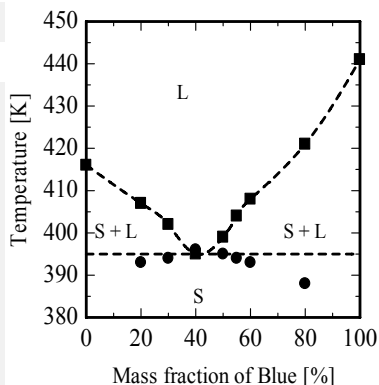


Fig. 3. Phase diagram of Blue and Red mixtures analyzed by DSC.

Figures 1 and 2 show the experimental results for the binary mixtures of C.I. Disperse Blue and Red at 15 MPa and 25 MPa as the temperature changed at 353 K to 393 K. The solubilities of the binary Blue and Red mixtures in SC-CO₂ were independent of the composition of the dye mixtures at 353 K, but depend on the mixture composition at 393 K. In 398 K the solubility of mixed dye decreased as the mass fraction became small. Figure 3 depicts the solid-liquid phase equilibria for the binary Blue and Red mixtures determined by the measurements of differential scanning calorimetry (DSC) at 0.1 MPa. As shown in Fig. 3 it exists the binary mixtures as a solid-like at below the temperature 393 K. Also the pressure increasing to 15 MPa and 25 MPa makes a possibility of the melting point depression. Accordingly the experimental results shown in Fig. 2 demonstrate the liquid phase has appeared at the temperature and pressure conditions measured in the present work. The molecular interactions between liquid-dyes in SC-CO₂ works strongly compared with those of solid-dyes in SC-CO₂. As a result, it can be concluded that the solubilities of the Blue and Red dye mixtures in SC-CO₂ were decreased considerably due to the molecular interactions of the liquid-dyes in dissolving into SC-CO₂. We will present further the experimental solubilities for Blue-Yellow and Yellow-Red dye mixtures in the conference.

C: ORAL PRESENTATION

SOLUBILITY AND SOLVOPHOBICITY PHENOMENA IN SELF-ASSOCIATED SOLVENTS

Sedov I.A and Solomonov B.N.

Department of Physical Chemistry, Kazan Federal University, Kazan, Russia,
e-mail: igor_sedov@inbox.ru

Low solubility of hydrocarbons in water is usually attributed to their hydrophobicity. In other self-associated and especially in highly structured solvents such as glycols, amides or aminoalcohols, the solubility of apolar molecules is also significantly decreased. For such systems, one can speak about the solvophobicity or the solvophobic effect [1] instead of the hydrophobicity. An interest to the solubility phenomena in highly structured solvents is due to that they are extensively used in industry and may serve as the models for some biological media. At the same time, little is known about the nature of the solvophobic effect and only not very much experimental thermodynamic data are available for the process of dissolution of hydrocarbons in the above-mentioned solvents.

We have measured the values of the gas-to-solvent and liquid-to-solvent solubilities, excess enthalpies and Gibbs energies of dissolution of several alkanes and aromatic hydrocarbons in ethylene glycol and formamide. Two experimental tools: titration calorimetry and gas chromatographic headspace analysis were used to determine the thermodynamic functions of the dissolution process. It is important to note that direct measurement of the solubility in considered systems by preparation of saturated solutions is complicated due to the solvent viscosity. A study of vapour-liquid equilibria provides a possibility to determine this quantity indirectly.

In order to describe the solvophobic effects qualitatively and quantitatively, we have analyzed the obtained and literature data using our recently suggested approach [2]. By considering the thermodynamic functions of solvation of alkanes in various self-associated and non-associated solvents, we concluded that the solvophobic effects can be identified by considering the relationships between the Gibbs energies and enthalpies of solvation of alkanes in various solvents. For a large group of non-associated solvents there is a linear correlation between the two quantities. Self-associated solvents show deviations from this line. These deviations are always positive, leading to a decrease in solubility, and can be used as a measure of the strength of the solvophobic effects. However, we show that the solvophobic effects are not the only factor determining the solubility even for alkane solutes. We analyze the contributions of various types of intermolecular interactions into the Gibbs energies of solvation and their effect on the value of solubility.

References

- [1] Ray A., Solvophobic interactions and micelle formation in structure forming nonaqueous solvents, *Nature*, **231**, (1971) 313-315.
- [2] Sedov I.A., Stolov M.A., Solomonov B.N., Solvophobic effects and relationships between the Gibbs energy and enthalpy for the solvation process, *J. Phys. Org. Chem.*, **24**, (2011) 1088-1094.

C: ORAL PRESENTATION

PARTITIONING OF ORGANIC ACIDS INTO THE SOLVENTS WITH IONIC LIQUIDS AND THEIR RHEOLOGY

Schlosser Š., Marták J. and Blahušiak M.

Institute of Chemical and Environmental Engineering, Slovak University of Technology
Radlinského 9, 812 37 Bratislava, Slovakia; e-mail: stefan.schlosser@stuba.sk

Coordinating ionic liquids (ILs), e.g. phosphonium and ammonium ILs, can be effectively used as extractants or carriers of solutes in reactive extraction or pertraction through liquid membrane. ILs can have advantageous extraction properties in separation of organics and metals. In reactive extraction of organic acids by the solvents with hydrophobic ILs besides formation of acid-IL complexes several phenomena occurred as reverse micelles formation and breaking, structuring of ILs and synergy effects between IL anion and cation. Interplay of these phenomena will be discussed. Structure of an IL anion has great influence on partitioning of the solute and also on extraction mechanism, Fig.1a. Good performance of microporous particles impregnated with IL will be presented.

Rheology of the solvents with IL is greatly influenced by an aggregation of IL, formation of reverse micelles and temperature. Addition of diluents, e. g. dodecane, and saturation with water greatly decrease viscosity of IL and improve mass-transfer in it, Fig.1b. Importance of rheology of the solvents with ILs in their formulation for separations will be discussed.

There is a tendency in selection or development of ILs for reactive extraction to take care mostly of high value of the distribution coefficient for the target solute. Unfortunately, coordinating hydrophobic ILs has usually high viscosity which slows down mass-transfer in separations. It is suggested to take care simultaneously of these aspects in the development of extractive separation. Optimisation of the solvent with ILs will be discussed on examples from extraction and pertraction of organic acids (butyric and lactic acids) by phosphonium and ammonium ILs.

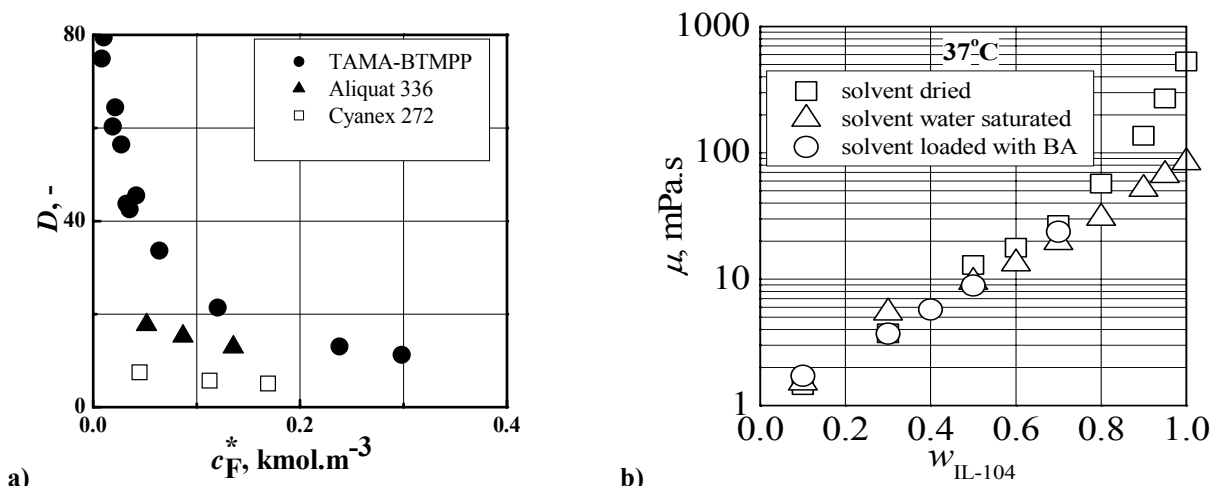


Fig. 1a. Concentration dependence of the distribution coefficient of butyric acid for ammonium IL. TAMA-BTMPP formed of Aliquat 336 cation and Cyanex 272 anion. **Fig. 1b.** Dependence of dynamic viscosity of the solvent with phosphonium IL Cyphos IL-104 in dodecane on mass fraction of IL in the solvent and influence of water saturation and acid extraction on it.

Acknowledgements: Support of the Slovak grant agency VEGA No. 1-1184-11 is acknowledged.

[1] Marták J., Schlosser Š., Vlčková S., *J. Membr. Sci.*, **318**, (2008) 298–310.

[2] Blahušiak M., Schlosser Š., Marták J., *React. Funct. Polym.*, **71**, (2011) 736–744.

[3] Marták J., Schlosser Š., Blahušiak M., *Chem. Pap.*, **65**, (2011) 608–619.

C: ORAL PRESENTATION

PHASE BEHAVIOR OF AQUEOUS MIXTURES OF TETRAHYDROFURAN WITH BIOLOGICAL BUFFER HEPES

Taha M. and Lee M.J.

Department of Chemical Engineering, National Taiwan University of Science and Technology,
43 Keelung Road, Section 4, Taipei 106-07, Taiwan,
e-mail: mtaha978@yahoo.com; e-mail: mjlee@mail.ntust.edu.tw

Liquid-liquid phase splitting was observed from the aqueous solutions of tetrahydrofuran (THF) in the presence of a biological buffer, 4-(2-hydroxyethyl) piperazine-1-ethanesulfonic acid (HEPES) at 298.2 K. Figure 1 is the phase diagram of water + THF + HEPES at ambient condition which was determined experimentally in this study. Ignoring the vapor phase, we divided the diagram into five phase regions: a homogeneous liquid phase (L); two liquid phases (2L); one solid and two liquid phases (S + 2L), one solid and one liquid phases (S + L). In order to understand why and how the buffer HEPES induced phase separation, molecular dynamics (MD) simulations were performed. The MD simulations were conducted for the aqueous mixtures with four different compositions. The reliability of the simulation results of HEPES in pure water and beyond the phase separation mixtures was justified by comparing the densities obtained from MD with the experimental values. The simulation results of HEPES in pure THF and in a composition inside the phase separation region (L) were justified qualitatively. Amazingly, all HEPES molecules entirely aggregated in pure THF. This reveals that HEPES is insoluble in pure THF, which is consistent with the experimental results. Even more amazingly, the MD simulation for the mixture with composition inside the phase separation region (2L) showed the formation of two liquid phases, as illustrated in Figure 2. The THF molecules are squeezed out from the water network into a new liquid phase. Radial distribution functions, the hydrogen-bonds, the electrostatic interactions, and the van der Waals interactions between the different species were also analyzed. A possible mechanism for the new buffering-out phase separation phenomena is postulated. This liquid-liquid phase splitting (buffering-out) effect [1] can be applied to recovery of THF from its azeotropic aqueous solutions.

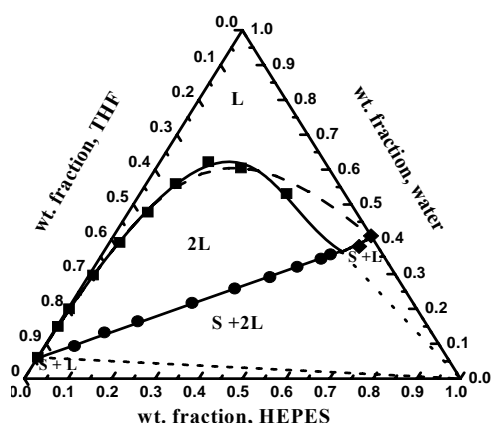


Fig. 1. Phase diagram of water+THF+HEPES at 298.2 K and atmospheric pressure

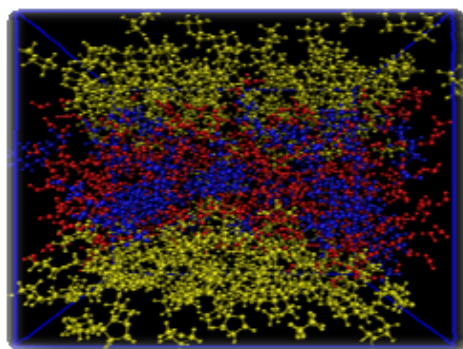


Fig. 2. Snapshots of water + THF + HEPES mixture in two-liquid phase region. (HEPES: blue; water: red; THF: yellow)

Reference

[1] Taha M., Lee M.J., Solubility and phase separation of 4-morpholine-propanesulfonic acid (MOPS), and 3-morpholino-2-hydroxypropanesulfonic acid (MOPSO) in aqueous 1,4-dioxane and ethanol solutions, *J. Chem. Thermodyn.*, **43**, (2011) 1723–1730.

C: ORAL PRESENTATION

EXPERIMENTAL AND MOLECULAR DYNAMICS SIMULATION STUDIES ON THE SOLUBILITY OF AMINO ACIDS IN AQUEOUS ELECTROLYTE SOLUTIONS

Tomé¹ L.I.N., Pinho² S.P., Jorge³ M., Gomes¹ J.R.B. and Coutinho¹ J.A.P.

¹CICECO Departamento de Química, Universidade de Aveiro, 3810-193 Aveiro, Portugal,
e-mail: jcoutinho@ua.pt

²LSRE/LCM-Laboratory of Separation and Reaction Engineering, Escola Superior de
Tecnologia e de Gestão, Instituto Politécnico de Bragança, Campus de Santa Apolónia,
5301-857, Bragança, Portugal, e-mail: spinho@ipb.pt

³LSRE/LCM-Laboratory of Separation and Reaction Engineering, Faculdade de Engenharia
da Universidade do Porto, Rua Dr. Roberto Frias s/n, 4200-465 Porto, Portugal,
e-mail: mjorge@fe.up.pt

Separation and concentration of biological compounds are current subjects of interest due to their high cost in comparison to the total manufacture cost. For that purpose electrolytes may be employed as they can affect significantly biochemicals solubilities, a feature that has been used for salt-induced precipitation of proteins. Even if amino acids are among the simplest biochemicals they present many similarities with more complex molecules and are the building blocks of proteins [1]. Despite its importance, however, the experimental information available concerning salt effect on the amino acids solubilities is still very scarce and the molecular-level mechanisms for its theoretical interpretation are far from resolved [2].

In this work, the shake-flask method was combined with density measurements to provide new experimental data for the solubility of dl-alanine, l-isoleucine and l-valine in aqueous solutions of MgCl₂ or MgSO₄, at different electrolyte molalities and 298.15 K. Both salts showed to be salting-in agents, but a more pronounced effect was observed for MgCl₂. Regarding the magnitude of the salting-in in the whole salt molality range (up to 2 molal), for the same aqueous electrolyte solution, a definite trend was not possible to establish for the three different amino acids studied.

Aiming at further understanding the molecular interactions governing the behaviour of these systems, molecular dynamics simulations were performed for aqueous solutions of alanine, valine and isoleucine in the presence of MgCl₂, MgSO₄, NH₄Cl and (NH₄)₂SO₄, at $T=298.15$ K and different concentrations. The combined analysis of the thermodynamic data and of the radial distribution functions of the various groups and moieties, as well as of their respective energy of interaction, enabled to clarify the role of the cation on the solubility effects promoted by the salts, and to provide a molecular interpretation for the experimental data based on a balance between competitive interactions established by the ions and the other species present in solution.

References

- [1] Ferreira L.A., Macedo E.A., Pinho S.P., The Effect of Ammonium Sulfate on the Solubility of Amino Acids in Water at 298.15 and 323.15 K, *J. Chem. Thermodyn.*, **41**, (2009) 193–196.
- [2] Tomé L.I.N., Jorge M., Gomes J.R.B., Coutinho, J.A.P., Towards an understanding of the aqueous solubility of amino acids in the presence of salts: A molecular dynamics simulation study, *J. Phys. Chem. B*, **114**, (2010) 16450–16459.

C: ORAL PRESENTATION

THE FATE OF THE WATER-SOLUBLE COMPONENTS OF SOME OIL PRODUCTS: THE SOLUBILITY LIMITS AND DISSOLUTION/EVAPORATION EQUILIBRIUMS

Winkler I.¹, Sapronova A.¹ and Rogozynskiy M.²

¹Department of Physical and Environmental Chemistry, Yu. Fedkovych National University of Chernivtsi, 2 Kotsybynsky St., Chernivtsi, 58012, Ukraine,
e-mail: igorw@ukrpost.ua

²Department of the Industrial Biotechnologies, Chernivtsi branch of National Technical University "KhPI", 203-A Golovna St., Chernivtsi, 58018, Ukraine,
e-mail: rmyrons@gmail.com

Approximate water-solubility limits have been determined for the gasoline/water mixtures using an original method of UV-spectrometry. It was found that some comparatively soluble oil compounds can form a true aqueous solution with limit concentration approximately 0.35 g/l (for gasoline-water mixtures) [1, 2].

Same experimental method has been engaged to determine temporal changes in concentration of the water-soluble compounds of some potential oil pollution agents of water: gasoline, diesel fuel and regular engine oil. Results of the UV-spectrometry proved that all these agents cause increase in the oil-components concentration in water followed by comparatively rapid drop in the concentration because of active evaporation of the water pollutant. However, each tested oil product exhibits a specific pattern of the pollution concentration raise/decrease and specific time to reach the maximal pollution level in water.

For example, the maximal concentration of the water-soluble components of the motor oil is reached within 15-25 min of the oil-water contacting. Then this concentration slowly decreases because of prevailing evaporation of the oil product components. This process is comparatively active during next 50-70 min then it slows down and further changes in the pollution agent concentration become much lesser.

Another tested products exhibit other temporal patterns of the concentration changes.

References

- [1] Winkler I., Investigation of the oil-products solubility in water: qualitative composition and quantitative limits of the oil-water mixtures, in: *The role of ecological chemistry in pollution research and sustainable development*. (Ed. A. M. Bahadir and G. Duca), Springer (2009) 103–108.
[2] Winkler I., Agapova N., Determination of water pollution by the oil products through UV photometry, *Env. Monit. and Assess.*, **168**, (2010) 115–119.

C: ORAL PRESENTATION

PREDICABILITY OF SETCHENOV COEFFICIENTS IN FLUOROCARBON-ALCOHOL-NaOH SYSTEMS WITH THE GROUP CONTRIBUTION METHOD

Ago¹ K. and Nishiumi² H.

¹Institute for Sustainability Research and Education, Hosei University, 2-17-1 Fujimi, Chiyoda-ku, Tokyo, Japan,

e-mail: kenichi.ago.sk@hosei.ac.jp

²Chemical Engineering Laboratory, Hosei University, 3-7-2 Kajino-cho, Koganei-city, Tokyo, Japan, e-mail: nishi@hosei.ac.jp

To prevent the ozone layer depletion, we are proposing a new dechlorination process for chlorinated fluorocarbons (CFCs or HCFCs) [1]. Starting with dissolving a fluorocarbon in an alcohol-NaOH solution, dissolved fluorocarbons reacted with alcohol-NaOH solvents. Reaction rate relates to both fluorocarbon and NaOH concentrations in a solution. However, the solubility determines the overall reaction rate, since decomposition rate of chlorinated fluorocarbons is much slower than dissolving rate in an alcohol-NaOH solution. We found that solubility of a fluorocarbon in an alcohol-NaOH solution decreased with NaOH concentration in a solution, i.e. salting effect. In a previous paper [2], we found that the solubility of fluorocarbon in an alcohol was considered with salting effect using the Setchenov coefficient. In this work, we estimated the Setchenov coefficients by the group contribution method and derived the relation between solvation number and the Setchenov coefficient. Therefore, the solvation numbers were predicted based on the model, once information of the Setchenov coefficients was obtained.

References

- [1] Nishiumi H., Sato K., (Photo)-decomposition process for compounds containing chlorine, *Trans. Mat. Res. Soc. Jpn.*, **18A**, (1994) 387–390.
- [2] Nishiumi H., Ogasawara H., Ago K., Effect of NaOH on the solubility of fluorocarbon in alcohol-NaOH systems, *Fluid Phase Equilib.*, **291**, (2010) 159–165.

C: ORAL PRESENTATION

WHAT IS SOLVENT BASICITY?

Waghorne W.E.

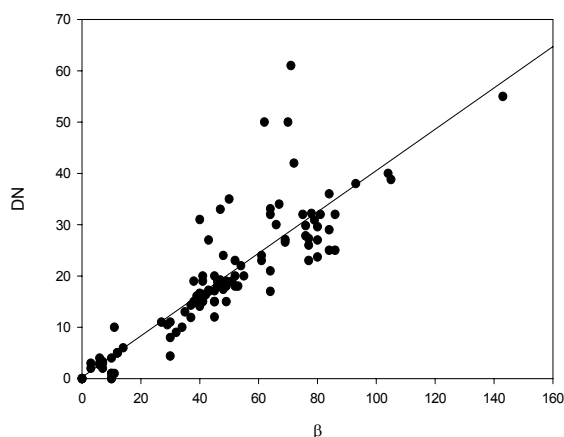
UCD School of Chemistry and Chemical Biology, University College Dublin, Belfield,
Dublin 4, Ireland, e-mail: earle.waghorne@ucd.ie

The importance of short range interactions between solute and solvent molecules is well recognized and concepts such as solvent basicity are routinely invoked to explain changes in phenomena, such as solubility, among different solvents. This is commonly quantified by multi-parameter relationships, having the general form:

$$Y = Y_0 + aA + bB + cC \dots$$

where Y represents a solvation related parameter, A , B and C represent solvent or solute properties and the corresponding coefficients a , b , and c indicate the importance of the corresponding parameters to Y for the particular process. This approach requires quantitative measures of properties such as solvent or solute basicity. Among the most direct measures Lewis basicity are Gutmann's donor numbers, Kamlet and Taft's hydrogen bond basicity and Swain et al.'s basity.

A simple comparison of these measures of basicity shows that there is only moderate agreement between them. Thus, for example, there is a relatively poor correlation between the Gutmann donor number, DN, and the Kamlet and Taft hydrogen bond basicity, β (see graph below, data from [1]).



This raises the question of why these different measures of basicity are so different and more fundamentally, what is that makes one molecule "more basic" than another.

Computational chemistry provides methods for exploring different molecular properties that can be related to basicity. Thus, for homologues, the Gutmann donor number shows excellent linearity with calculated energies of the filled frontier orbitals but these correlations, for different classes of compounds do not overlap.

In this paper we present the results of extensive calculations to provide a more quantitative description of the factors that determine experimental solvent parameters and explore the extent to which they can be predicted from such calculations.

Reference

[1] Marcus Y., The properties of organic liquids that are relevant to their use as solvating solvents, *Chem. Soc. Rev.*, **22**, (1993) 409–416.

C: ORAL PRESENTATION

SOLUBILITY MEASUREMENTS FOR DETERMINATION OF EQUILIBRIUM CONSTANTS IN AQUEOUS SOLUTION

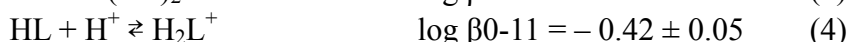
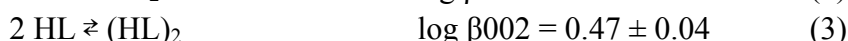
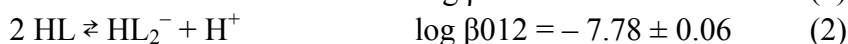
Furia E., Napoli A., Sindona G. and Tagarelli A.

Department of Chemistry, University of Calabria, Arcavacata di Rende (CS), 87036, Italy,
e-mail: e.furia@unical.it

In the last decade my research group has been interested to the systematic study of the equilibria that take place between 2-hydroxybenzoic acid (salicylic acid) and a series of biological cations. The choice rise from the fact that salicylic acid is both the simplest model for humic acids present in soil and an outstanding antirheumatic and antifungal substance.

From this point of view his derivatives, as 2-Hydroxybenzamide (HL), show the same properties; due to low solubility of this class of ligand literature data are scanty and measurements are chiefly carried out in non aqueous solvents.

To evaluate the biological property of ligands it is interesting the study of the complexing power in water. For this reason the acid-base properties of the ligands have been studied at 298.15 K and in NaClO₄ media for ionic strengths ranging from 0.5 to 3.5 mol·kg⁻¹ using emf as well as solubility measurements. For example as concerning 2-Hydroxybenzamide results relative to 1.05 mol·kg⁻¹ NaClO₄ are concisely reported here.



The uncertainties represent 3σ. Equilibria (1), (2) and (3) were obtained from potentiometric titrations with cell (G)



where RE, reference electrode, = Ag/AgCl/0.015 mol·kg⁻¹ AgClO₄, 1.035 mol·kg⁻¹ NaClO₄/1.05 mol·kg⁻¹ NaClO₄ and Test Solution = C_L mol·kg⁻¹ HL, C_A mol·kg⁻¹ HClO₄, C_B mol·kg⁻¹ NaOH, (1.05-C_A-C_B) mol·kg⁻¹ NaClO₄.

Information on equilibrium (4) has been obtained in the acidic range ([H⁺] > 0.1 mol·kg⁻¹) from solubility measurements. Starting solutions contained a NaClO₄ and HClO₄ mixture and the ionic strength was 1.05 mol·kg⁻¹ and then an excess of pure ligand was added. Test solutions were analyzed by spectrophotometric measurements in the ultraviolet region after suitable dilution with twice distilled water. The absorbance increase resulting from an increase of acid confirms the existence of equilibrium (4).

In order to extrapolate the constants at the infinite dilution reference state by Specific Interaction Theory [1,2] it is necessary to know the activity coefficients of the neutral molecules in NaClO₄ solutions (*salting-in* effect). Solutions of NaClO₄ have been equilibrated with the solid by stirring at (298.15 ± 0.1) K. After thermostatic separation through G4 glass filter and subsequent dilution, the optical absorbances of test solutions were read. The solubility was obtained by interpolation on a calibration curve.

References

- [1] Ciavatta L., The specific interaction theory in evaluating ionic equilibria, *Ann. Chim.*, **70**, (1980) 551–567.
[2] Ciavatta L., The specific interaction theory in equilibrium analysis. some empirical rules for estimating interaction coefficients of metal ion complexes, *Ann. Chim.*, **80**, (1990) 255–263.

C: ORAL PRESENTATION

TOWARD A MOLECULAR MODEL FOR AQUEOUS SOLUTIONS OF NONPOLAR FLUIDS

Jirsák^{1,2} J., Škvor¹ J. and Nezbeda^{1,2} I.

¹Faculty of Science, J. E. Purkinje University in Ústí n. L., 400 96 Ústí n. L., Czech Republic, e-mail: jan.jirsak@ujep.cz; ²Institute of Chemical Process Fundamentals, Academy of Sciences of the Czech Republic, 165 02 Prague, Czech Republic

Owing to its unique properties, water has always attracted the attention of physicists and chemists. It exhibits a number of anomalies, as both a pure liquid and a solvent. Nonpolar solutes show extremely low solubility in water, moreover, nonpolar particles tend to minimize the interface with the aqueous phase regardless of scale. The phenomenon has been named a hydrophobic effect and studied on a whole range of solutes, from noble gases over hydrocarbons to proteins.

The hydrophobic hydration is accompanied by several thermodynamic signposts, such as the temperature maximum of Henry's constant or the temperature of convergence of hydration entropy for different solute sizes. These features should be reproduced by any approach aiming at being sufficiently predictive for the mixtures of nonpolar substances with water, however, this is usually not the case of the empirical expressions commonly used in chemical engineering. In order to obtain more sophisticated and thermodynamically consistent expressions, one can consider employing the molecular theory based on a suitable model for molecular interactions. The model has to be simple enough to make a mathematical treatment possible, yet complex enough to preserve the traits necessary for a qualitatively correct description. The latter issue has not yet been satisfactorily settled, however, a number of simple molecular models have been proposed, based on different opinions on what is essential for a water-like behavior, each model qualitatively reproducing some of the desired features of pure water and aqueous solutions. [1]

In the present contribution, an associating fluid model based on so-called pseudo-hard bodies is introduced and its application to water and aqueous solutions is demonstrated. The model has already been used by the group of the present authors to reproduce, qualitatively, anomalies of pure liquid water and some properties of aqueous mixtures. [1, 2] An attempt is made to move further along this path toward a concise molecular-level understanding of hydrophobic hydration and aqueous solutions in general. In order to obtain equations of state, the thermodynamic perturbation theory is employed with pseudo-hard bodies taken as a reference system. The construction of a pseudo-hard body for water consists in the assumption that not only attractive but also repulsive forces are needed to appropriately describe the structural effects of hydrogen bonding. [1] Simulation data on mixtures of hard spherical solutes and pseudo-hard water are utilized to parameterize the reference pressure, which is then combined with attractive terms to form a molecular-based equation of state for the solution. The equation of state allows for a consistent calculation of all thermodynamic properties of the mixture. Results for selected properties relevant to hydrophobic hydration are presented and future development of the approach is outlined.

Acknowledgments: This research has been supported by the Czech Science Foundation (Grant No. P208/12/P710) and the Grant Agency of the Academy of Sciences of the Czech Republic (Grant No. IAA400720802).

References

- [1] Nezbeda I., Jirsák J., *Phys. Chem. Chem. Phys.*, **13**, (2011) 19689–19703.
[2] Rouha M., Nezbeda I., *Mol. Phys.*, **109**, (2011) 613–617.

C: ORAL PRESENTATION

SOLUBILITY OF BIOACTIVE COMPONENTS OF MANGO GINGER (CURCUMA AMADA ROXB) IN SUPERCRITICAL CARBON DIOXIDE

Krishna Murthy T.P. and Manohar B.

Dept. of Food Engg., Central Food Technological research Institute, Mysore 570020, India.

Extracts from natural plants as source material for nutraceuticals or functional foods are gaining popularity in modern days because of several advantages such as fewer adverse health side effects, better patient tolerance, relatively low price and acceptance due to a long history of use. The presentation focuses on mango ginger (*Curcuma amada roxb*) known for its exotic mango-like aroma having morphological resemblance with ginger. The spice is extensively used in the preparation of culinary items especially pickles, sauces etc, in Indian subcontinent. In Ayurveda, a traditional system of medicine in India, the plant is given importance as appetizer, alexiteric, antipyretic, aphrodisiac and laxative. Extraction of bioactive components of mango ginger using supercritical carbon dioxide extraction process was studied at pressures 100-325 MPa, temperatures 40-60 °C and various CO₂ – material ratios. Experimental solubility of total phenolics was modelled based on Peng-Robinson equation of state and a few selected empirical prediction models assuming a single pseudo-component bioactive. The talk shall also highlight some major research works carried out in the institute in the area of supercritical fluid extraction.

D: POSTER 1

SOLID - LIQUID EQUILIBRIA FOR THE TERNARY $\text{Na}_2\text{B}_4\text{O}_7$ - NaBr - H_2O SYSTEM AT 323 K

Sang^{1,2} S.H., Sun¹ M.L., Cui¹ R.Z. and Li¹ T.

¹Institute of materials and Chemistry & Chemical Engineering, Chengdu University of Technology, Chengdu 610059, China. email: sangsh@cdut.edu.cn

²Mineral Resources Chemistry Key Laboratory of Sichuan Higher Education Institutions, Chengdu 610059, China

Many salt lake brines on the Qinghai-Tibet plateau in China are well known for high concentration lithium, potassium and boron [1]. Furthermore, a huge store of underground gasfield brine was also discovered in Sichuan western basin of China. Sodium chloride, potassium, boron, bromine and sulfate are the major chemical compositions of the oilfield brine, and accompanying lithium, strontium and iodine [2]. The proved reserve of the gasfield brines is up to $2.06 \times 10^{12} \text{ m}^3$. For exploiting brine resources of the underground brines, the measurement of mineral solubilities at different temperatures is used widely [3]. This ternary system $\text{Na}_2\text{B}_4\text{O}_7$ - NaBr - H_2O is a subsystem of the underground gasfield brines.

The solid - liquid Equilibria for the ternary system $\text{Na}_2\text{B}_4\text{O}_7$ - NaBr - H_2O at 323 K were studied experimentally using the method of isothermal solution saturation. Solubilities and densities of the solution in the ternary system at 323 K were measured experimentally. On the basis of experimental data, the phase diagram of the ternary system was constructed (Figure 1). In the phase diagram, there are one invariant point E and two invariant curves E1E and E2E. E1E curve corresponds to the solubility isotherms where the solution was saturated with $\text{Na}_2\text{B}_4\text{O}_7 \cdot 10\text{H}_2\text{O}$. E2E curve corresponds to the solubility isotherms where the solution was saturated with $\text{NaBr} \cdot 2\text{H}_2\text{O}$. The invariant point E corresponds to the solution saturated with the salts $\text{NaBr} \cdot 2\text{H}_2\text{O}$ and $\text{Na}_2\text{B}_4\text{O}_7 \cdot 10\text{H}_2\text{O}$. The crystallization area $\text{Na}_2\text{B}_4\text{O}_7 \cdot 10\text{H}_2\text{O}$ (E1ED field) in the phase diagram is bigger than that of $\text{NaBr} \cdot 2\text{H}_2\text{O}$ (E2EA field). Double salts or solid solutions have not been found in the ternary system.

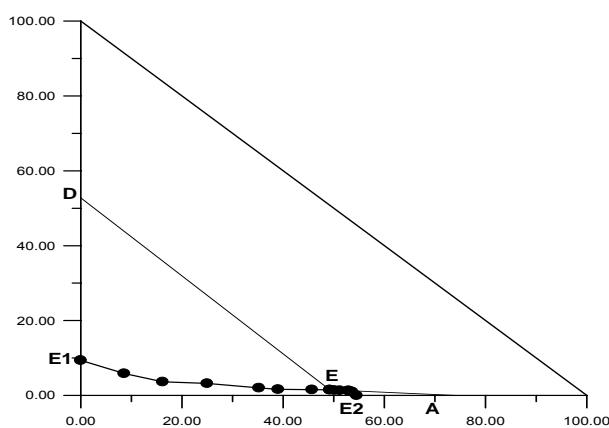


Fig. 1. Phase diagram of the ternary system $\text{Na}_2\text{B}_4\text{O}_7$ - NaBr - H_2O at 323 K.

●, Experimental data point; E1, binary system $\text{Na}_2\text{B}_4\text{O}_7$ - H_2O saturation point; E2, binary system NaBr - H_2O saturation point; A, solid phase point ($\text{NaBr} \cdot 2\text{H}_2\text{O}$); D, solid phase point ($\text{Na}_2\text{B}_4\text{O}_7 \cdot 10\text{H}_2\text{O}$); E, invariant point saturated with $\text{NaBr} \cdot 2\text{H}_2\text{O}$ and $\text{Na}_2\text{B}_4\text{O}_7 \cdot 10\text{H}_2\text{O}$.

Acknowledgements: This project was supported by the National Natural Science Foundation of China (NO. 40973047) and the Youth Science Foundation of Sichuan Province, China (08ZQ026-017).

References

- [1] Zheng X.Y., Zhang M.G., Xu Y., Li B.X., Salt lakes of china, Beijing: *Science press*, (2002).
- [2] Lin Y.T., Geochemical characteristics of gas field water in one field in west sichuan & its development evaluation. *Natural Gas Industry*, **20**, (2000) 9-14.

D: POSTER 2

SOLID-LIQUID EQUILIBRIUM OF KOH–K₃VO₄–H₂O SYSTEM AT (40 AND 80) °C

Yang^{1,2} N., Wang¹ S.N., Du¹ H., Zheng^{1,*} S.L. and Zhang¹ Y.

¹National Engineering Laboratory for Hydrometallurgical Cleaner Production Technology, Key Laboratory of Green Process and Engineering, Institute of Process Engineering, Chinese Academy of Sciences, Beijing, 100190, China

²Graduate University of the Chinese Academy of Sciences, Beijing, 100049, China
Na Yang, MS Candidate, Email: yn123466234@163.com
email: slzheng@home.ipe.ac.cn

A new cleaner hydrometallurgical process for vanadium slag has been proposed and developed to solve the low vanadium extraction efficiency, unrecyclability of chromium, serious environmental pollution problems in the traditional vanadium recovery process. The new process created by the Institute of Process Engineering, Chinese Academy of Sciences, was developed using KOH sub-molten salt and enhanced with chemical field, which enabled synchronous extraction of vanadium and chromium with high efficiency under mild reaction conditions. The conversion of vanadium is above 95% and the recovery of vanadium is raised by more than 15%, while the conversion of chromium is raised from less than 10% to above 90%, and the reaction temperature is dropped from 750 °C to 220 °C. The separation of K₃VO₄ is one of the most important operation units in the new cleaner process, but the phase diagram of KOH–K₃VO₄–H₂O system has never been studied yet. In this regard, the dissolution behaviour of K₃VO₄ in the KOH–K₃VO₄–H₂O system was investigated in this article, and the results show that the solubility of K₃VO₄ decreased from (56.87 to 8.88) % as the KOH concentration increased from (3.41 to 53.30) % at 40 °C, and the solubility of K₃VO₄ decreased from (58.43 to 18.15) % as the KOH concentration increased from (10.94 to 47.25) % at 80 °C. When the KOH concentration is above 40%, the concentration of K₃VO₄ at (80 and 40) °C shows a gradual change with an increase of KOH concentration, and then comes to a platform at 43.34% and 50.72%, reaches to 18.15% and 8.88%, respectively. There is an obvious difference in the solubility of K₃VO₄ with temperature in the whole KOH concentration range. As a goal to separate K₃VO₄ from the ternary system of KOH–K₃VO₄–H₂O with KOH concentration of about 47% at 80 °C, cooling crystallization from 80 °C to 40 °C was applied and optimized in this alkali concentration range. The solid phases were determined to be K₃VO₄·3H₂O at 40 °C and K₃VO₄·5H₂O at 80 °C by X-ray diffraction coupled with Schreinemaker's method.

D: POSTER 3

STUDY ON THE EQUILIBRIUM IN THE QUINARY SYSTEM Li^+ , $\text{Mg}^{2+}/\text{Cl}^-$, SO_4^{2-} , $\text{B}_6\text{O}_{10}^{2-}-\text{H}_2\text{O}$ AT 25 °C

Sun B. and Song P.S.

Qinghai Institute of Salt Lakes, Chinese Academy of Sciences, 810008, Xining, China

e-mail: sunb@isl.ac.cn, songpsh@isl.ac.cn

The solubilities of the quinary system Li^+ , $\text{Mg}^{2+}/\text{Cl}^-$, SO_4^{2-} , $\text{B}_6\text{O}_{10}^{2-}-\text{H}_2\text{O}$ were investigated by isothermal method at 25 °C. The part graph of the solubility in the quinary reciprocal system was obtained. Seven invariant points and ten phase solids in this quinary system at 25 °C were got. The crystal regions are respectively macallisterite ($\text{MgB}_6\text{O}_{10}\cdot 7.5\text{H}_2\text{O}$), Li-carnallite ($\text{LiCl}\cdot\text{MgCl}_2\cdot 7\text{H}_2\text{O}$), epsomite ($\text{MgSO}_4\cdot 7\text{H}_2\text{O}$), hexahydrite ($\text{MgSO}_4\cdot 6\text{H}_2\text{O}$), pentahydrite ($\text{MgSO}_4\cdot 5\text{H}_2\text{O}$), Leonhardtite ($\text{MgSO}_4\cdot 4\text{H}_2\text{O}$), bischofite ($\text{MgCl}_2\cdot 6\text{H}_2\text{O}$), lithium chlorite ($\text{LiCl}\cdot\text{H}_2\text{O}$), Lithium Sulfate ($\text{Li}_2\text{SO}_4\cdot\text{H}_2\text{O}$), and double salt of lithium and magnesium with borate ($\text{Li}_2\text{B}_6\text{O}_{10}\cdot\text{MgB}_6\text{O}_{10}\cdot 11\text{H}_2\text{O}$).

The chemical schematic for the new compound including lithium and magnesium borate is $\text{Li}_2\text{B}_6\text{O}_{10}\cdot\text{MgB}_6\text{O}_{10}\cdot 11\text{H}_2\text{O}$ according to the chemical analysis of the composition. It similar to aristarainite ($\text{Na}_2\text{MgB}_{12}\text{O}_{20}\cdot 8\text{H}_2\text{O}$) by X-ray. There is no any information about the compound in reference so far. The studies indicate that the new compound can transform into kurnakovite in pure water in a week. When bischofite did not saturated or in lower concentration of LiCl and MgCl_2 , such as the concentration of LiCl and MgCl_2 in solution corresponding to 1.34% and 6.13% which can convert into kurnakovite in two weeks.

Macallisterite ($\text{MgB}_6\text{O}_{10}\cdot 7.5\text{H}_2\text{O}$) can transform into $\text{Li}_2\text{B}_4\text{O}_7\cdot 3\text{H}_2\text{O}$ in saturated solution of $\text{LiCl}\cdot\text{H}_2\text{O}$ or $\text{Li}_2\text{SO}_4\cdot\text{H}_2\text{O}$. But it can form $\text{Li}_2\text{B}_6\text{O}_{10}\cdot\text{MgB}_6\text{O}_{10}\cdot 11\text{H}_2\text{O}$ when Lic(Li-carnallite, $\text{LiCl}\cdot\text{MgCl}_2\cdot 7\text{H}_2\text{O}$) with $\text{LiCl}\cdot\text{H}_2\text{O}$ or bischofite saturated. It can be converted into hungtsaoite till inderite in pure water and in the solution for low concentration of MgCl_2 or MgSO_4 . However, the interesting result was obtained that different with the transformation of it in pure water which macallisterite also can be converted into kurnakovite in lower concentration of LiCl with MgCl_2 .

References

- [1] Song P.S., Du X.H., Xu H.C., *Chin. Sci. Bull.*, **29**, (1985) 1072–1076.
- [2] Song P.S., Du X.H., *Chin. Sci. Bull.*, **31**, (1987) 1338–1343.
- [3] Song P.S., Du X.H., Sun B., *Chin. Sci. Bull.*, **33**, (1988) 1971–1973.
- [4] Bi W.B., Sun B., Song P.S. et al., *J. Salt Lake Res.*, **5**, (1997) 42–45.
- [5] Sun B., Song P.S., *J. Salt Lake Res.*, **7**, (1999) 16–22.
- [6] Николаев А.В., *Физико-химическое изучение природных боратов.*, 1947, Издат. АНССР, М.— Л.
- [7] D'Ans J. et al., *Kali und Steinsalz.*, **2**, (1957) 121–137.

D: POSTER 4

THE PHASE EQUILIBRIUM BEHAVIORS OF THE AQUEOUS SYSTEMS MAGNESIUM BORATE AT MULTI-TEMPERATURES

Ge¹ H.W., Deng^{1,2} T.L. and Yao¹ Y.

Qinghai Institute of Salt Lakes, Chinese Academy of Sciences, 18 Road, Xining, Qinghai 810008, PRC, E-mail: tldeng@isl.ac.cn
School of Marine Science and Engineering, Tianjin University of Science and Technology, Tianjin 300457, PRC

In this paper, the phase equilibria of the aqueous system magnesium borate at 273.15 K, 283.15 K, 293.15 K, 298.15 K, 303.15 K, 308.15 K, 313.15 K and 323.15 K were studied with the method of isothermal dissolution equilibrium method. The solubilities and physicochemical properties including pH and conductivities values of the system at eight temperatures were obtained. The solubility curve was also presented and gave a multinomial expression by the method of least square fitting. The transforming behavior of hungchaoite ($\text{MgB}_4\text{O}_7 \cdot 9\text{H}_2\text{O}$) was studied at 273.15 K, 298.15 K, 308.15 K and 323.15 K. Although there is no phase transforming for hungchaoite at 273.15 K, it was found that hungchaoite in the saturated solution of magnesium borate will transform into inderite ($\text{Mg}_2\text{B}_6\text{O}_{11} \cdot 15\text{H}_2\text{O}$) at 298.15 K, 308.15 K and 323.15 K after 10 days, in 15 hours and in 12 hours, respectively. Figure 1 shows the solubilities of magnesium borate (in the left) and the transforming behaviors of hungchaoite (in the right) at 273.15 K, 298.15 K, 308.15 K and 323.15 K, respectively.

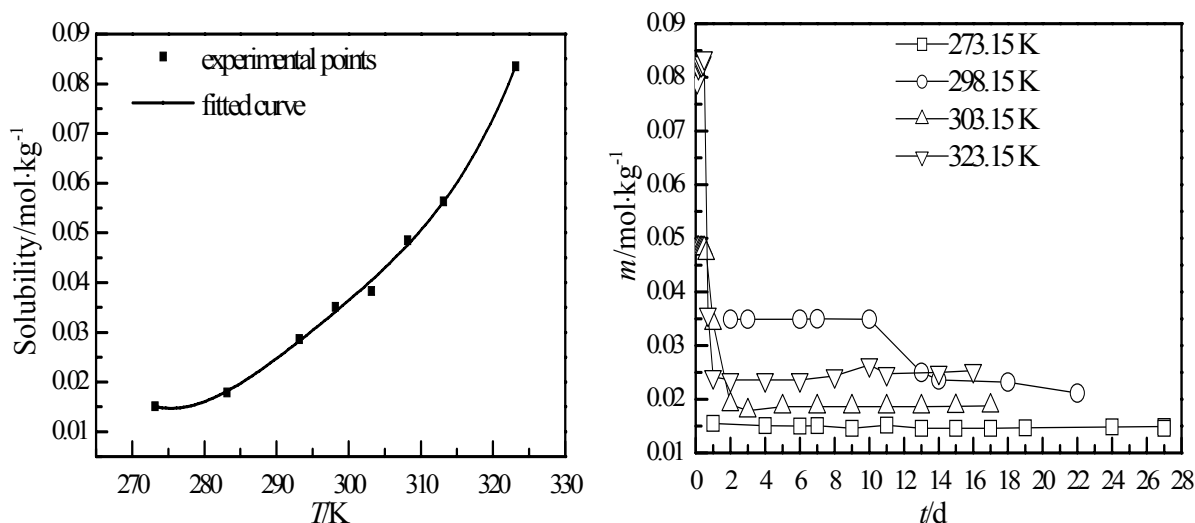


Fig. 1. The diagram of the magnesium borate solubilities and the fitting curve (in the left) and the phase transforming behaviors versus time.

Acknowledgments: Financial supported by the State Key Program of NNSFC (20836009).

References

[1] Sun B., Song P.S., Solution and phase transformation of some magnesium borates, *J. Salt Lake Res.*, 7, (1999) 16–22.

D: POSTER 5

THE PROGRESS OF POTENTIAL-pH DIAGRAMS FOR V-H₂O SYSTEM

Zhao^{1,2} X.Y. and Zeng^{1,2} Y.

¹College of Materials and Chemistry & Chemical Engineering, Chengdu University of Technology, Chengdu 610059, P. R. China

²Mineral Resources Chemistry, Key Laboratory of the Higher Education Institutions of Sichuan Province, Chengdu 610059, P. R. China
email: zengyster@gmail.com, zxycdut@hotmail.com

The potential-pH diagram was first proposed by Belgium corrosion scientist professor Pourbaix M in 1938. [1] All kinds of potential-pH diagram are thermo-dynamical tools, providing informations about the equilibrium conditions of chemical and electrochemical reactions, the possible direction of the reaction under a certain temperature and pressure conditions and the relative advantages of the region of the substances or dissolved species of the system. These diagrams are not only providing important thermodynamic data for the hydrometallurgical processes study, but also for theoretical analysis of the existing production process and improving existing production methods. There are great prospects for the potential-pH diagram development.

Vanadium is an important product which is used almost exclusively in ferrous and non-ferrous alloys due to its physical properties such as high hardness, large tensile strength, and good fatigue resistance. The core of vanadium hydrometallurgical process is to make vanadium dissolve from raw material and deposition from the solution. Vanadium species have a series of complex equalized reaction. There are different species and chemical combination state existing in solution with different Eh and pH.

Some papers have discussed the potential-pH diagrams for the V-H₂O system. Post [2], and Kelsall [3] summarized diagrams at atmospheric pressure, normal temperature, with total vanadium concentration 0.02, 0.0002 and 0.01 mol/L, respectively. Based on the principle of simultaneous equilibrium and concentration comparison, Wu [4] and Ma [5] studied the pourbaix diagrams at low vanadium concentration. According to the potential-pH diagrams drew by Zhou [6], we may know that the ranges of vanadium oxides passivation extended with increasing temperatures and increasing activities of dissolved species, and the stability region for vanadium was nearly independent of temperature, whereas it grew with increased activity, and the corrosion resistance was nearly not affected by high temperature in theory.

At present, the research about the potential-pH diagrams of the V-H₂O system has been extended to ligands, high temperature conditions, and considering the more e complex system.

References

- [1] Pourbaix M., Atlas of Electrochemical Equilibria in Aqueous Solution, Pergamon, 1963.
- [2] Post K, Robins R.G, Thermodynamic diagrams for the vanadium-water system at 298.15 K, *Electrochimica Acta*, **21**, (1976) 401–405.
- [3] Kelsall G.H., Thompson I., Francis P.A., Redox chemistry of H₂S oxidation by the British Gas Stretford process, *Journal of Applied Electrochemistry*, **23**, (1993) 417–426.
- [4] Wu J.M., Studies on predominance diagrams and pourbaix diagrams for V-S-H₂O system, Master Dissertation of Chengdu University of Technology, 2008.
- [5] Ma M., Studies on predominance diagrams and pourbaix diagrams for V-Cl-H₂O system, Master Dissertation of Chengdu University of Technology, 2009.
- [6] Zhou X.J., Wei C., Li M., Qiu S., Li X., Thermodynamics of vanadium-sulfur-water systems at 298 K, *Hydrometallurgy*, **106**, (2011) 104–112.

D: POSTER 6

THE SOLUBILITY OF CETYLTRIMETHYLAMMONIUM BROMIDE IN METHANOL–WATER MIXED SOLVENT MEDIA

Bhattarai A.

Department of Chemistry, M.M.A.M.C. (Tribhuvan University), Biratnagar, Nepal
e-mail: bkajaya@yahoo.com

The presence of alcohols in water will help in breaking down of the water structure thereby increasing the solubility of surfactant in system and hence delays the micellization process. This indicates critical micelle concentration (cmc) of Cetyltrimethylammonium Bromide (CTAB) must increase with the presence of alcohols in the water. This is the result that has been observed up to 10%, 20%, 30% and 40% of methanol in water at 308.15, 318.15 and 323.15 K. In addition to breaking down the structure of water, alcohols lower down the dielectric constant of the water thereby contributes toward the increase in cmc. This lowering of the dielectric constant of the system with alcohol percentage would also decrease the tendency of counterions to remain bound to the micellar surface and hence would contribute to decrease of the effective degree of counter-ion binding (β) for CTAB. An additional complication of alcohol-water mixtures is the possibility of the alcohol to penetrate into the micelle. It is well known that the alcohol molecules orient themselves at the micelle-solvent interface with the hydrocarbon group penetrating slightly into the micelle and the hydroxyl group remaining on the micelle-solvent interface [1, 2]. Such a penetration would lead to screening of the electrostatic repulsions between ionic head groups of the surfactant thereby promoting micellization i.e. would result in decrease in cmc and increase of β [3].

References

- [1] Emerson M.F., Holtzer A., Hydrophobic bond in micellar systems. Effects of various additives on the stability of micelles of sodium dodecyl sulfate and of n- dodecyltrimethylammonium bromide, *J. Phys. Chem.*, **71**, (1967) 3320–3330.
- [2] Miyagishi S., The effect of organic additives on the micelle formation of dodecylammonium halides in aqueous solutions, *Bull. Chem. Soc. Jap.*, **47**, (1974) 2972–2976.
- [3] Marszall L., Effect of aromatic hydrotropic agents on the cloud point of mixed ionic-nonionic surfactant solutions, *Langmuir*, **6**, (1990) 347–350.

D: POSTER 7

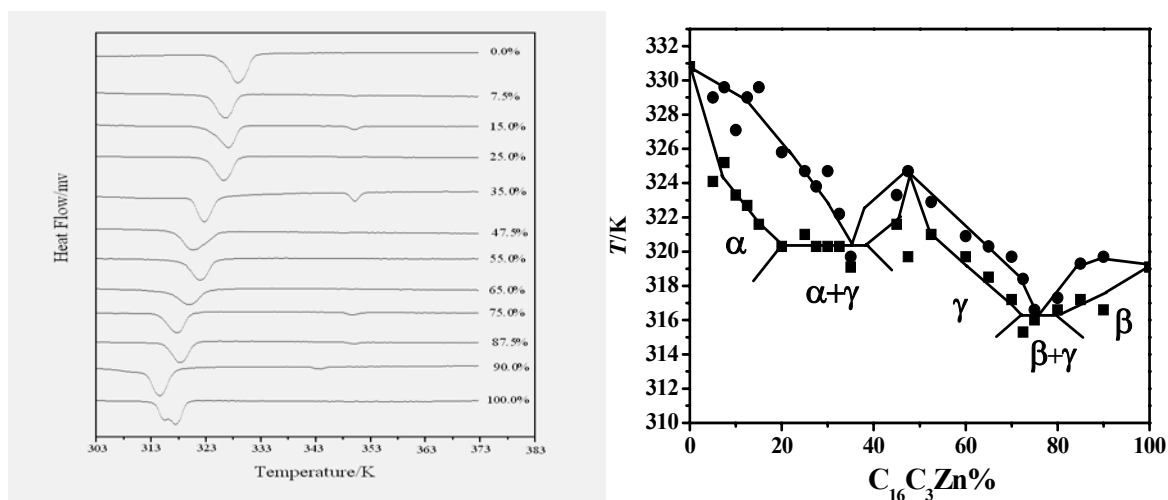
SUBSOLIDUS BINARY PHASE DIAGRAM OF THE PEROVSKITE TYPE LAYER MATERIALS $[n\text{-C}_n\text{H}_{2n+1}\text{N}(\text{CH}_3)_3]_2\text{ZnCl}_4$ ($n=16, 18$)

Ren B.Y. and Wu K.Z.

Department of Chemistry and Material Science, Hebei Normal University, Shijiazhuang 050024 China

Key Laboratory of Inorganic Nano-materials of Hebei Province, Shijiazhuang, 050024 China
e-mail: wukzh688@163.com

The perovskite type layer materials $[n\text{-C}_n\text{H}_{2n+1}\text{N}(\text{CH}_3)_3]_2\text{ZnCl}_4$ ($n=16, 18$) and a series of their mixtures were studied. The low temperature crystal structures of the pure salts are characteristic of the piling of sandwiches in which a two-dimensional macro-anion ZnCl_4^{2-} is sandwiched between two alkylammonium layers [1]. These layers become conformationally disordered in the high temperature phases. The experimental subsolidus binary phase diagram of $[n\text{-C}_{16}\text{H}_{33}\text{N}(\text{CH}_3)_3]_2\text{ZnCl}_4$ – $[n\text{-C}_{18}\text{H}_{37}\text{N}(\text{CH}_3)_3]_2\text{ZnCl}_4$ has been established over the whole composition range by Differential scanning calorimetry (DSC) and X-ray diffraction. In the phase diagram, one intermediate compound $[n\text{-C}_{16}\text{H}_{33}\text{N}(\text{CH}_3)_3][n\text{-C}_{18}\text{H}_{37}\text{N}(\text{CH}_3)_3]\text{ZnCl}_4$ at $W_{\text{C}_{16}\text{C}_3\text{Zn}}\%=47.50\%$ and two eutectoid invariants points at $W_{\text{C}_{16}\text{C}_3\text{Zn}}\%=35.00\%$ and $W_{\text{C}_{16}\text{C}_3\text{Zn}}\%=80.00\%$ were observed, two eutectoids temperatures are about 320 ± 1 K and 317 ± 1 K. There are three noticeable solid solution ranges (α , β , γ) at the left and right boundary and middle of the phase diagram.



The $\text{C}_{16}\text{C}_3\text{Zn}$ – $\text{C}_{18}\text{C}_3\text{Zn}$ binary systems were examined in the entire composition range and in a temperature range of 303 to 393 K [2]. Fig.1 shows some typical DSC curves of $\text{C}_{16}\text{C}_3\text{Zn}$ – $\text{C}_{18}\text{C}_3\text{Zn}$ binary systems with different $W_{\text{C}_{16}\text{C}_3\text{Zn}}\%$. All the $\text{C}_{16}\text{C}_3\text{Zn}$ – $\text{C}_{18}\text{C}_3\text{Zn}$ binary systems show solid–solid phase transitions in the temperature range 303–393 K. These are always reproducible after heating and cooling cycles throughout the transition points. Fig.2 was constructed according to the temperature–composition relations from the DSC and X-ray diffraction experiments.

Acknowledgments: This project was financially supported by National Natural Science Foundation of China (No.21073052), Natural Science Foundation of Hebei Province (No.B2012205034) and Science Foundation of Hebei Normal University (L2011K04).

References

- [1] Chevire F., Pallu A., Ray E., Tessier F., *J. Alloys Compd.*, **509**, (2011) 5839–5842.
- [2] Wu K.Z., Zhang J.J., *J. Therm. Anal Calorim.*, **101**, (2010) 913–917.

D: POSTER 8

BINARY AND TERNARY PHASE EQUILIBRIA FOR C18 BIODIESEL IN SUPERCRITICAL METHANOL

Fang^{1*} T., Shimoyama² Y., Iwai³ Y. and Goto⁴ M.

¹Department of Chemical Engineering, Xi'an Jiaotong University, No. 28 Xianning West Road, Xi'an 710049, China, email: taofang@mail.xjtu.edu.cn

²Department of Chemical Engineering, Tokyo Institute of Technology, Meguroku Oookayama 2-1-12, Tokyo 182-8550, Japan, email: yshimo@chemeng.titech.ac.jp

³Department of Chemical Engineering, Kyushu University, 744 Motoooka Nishi-ku, Fukuoka 819-0395, Japan, email: iwai@chem-eng.kyushu-u.ac.jp

⁴Department of Chemical Engineering, Nagoya University, Furo-cho, Chikusa-ku, Nagoya, 464-8603, Japan, email: mgoto@nuce.nagoya-u.ac.jp

Fatty acid methyl esters (FAMES) are the main compounds of biodiesel, and generally produced through the transesterification reaction between methanol and triglycerides (from animal, plant and microalgae). The research aims to establish fundamental basis for producing biofuel and tocopherols from oil byproducts with supercritical methanol. Notably, this work is the first to measure the phase equilibrium data of two systems: methanol + C18 methyl esters, methanol+C18 methyl esters + α -tocopherol (523–573 K, 2.45–11.45 MPa). Peng-Robinson equations of state were employed to correlate the measured data of the systems involving supercritical methanol. On the basis of fundamental research on phase equilibrium, a series of reactions were carried out, and some parameters were optimized.

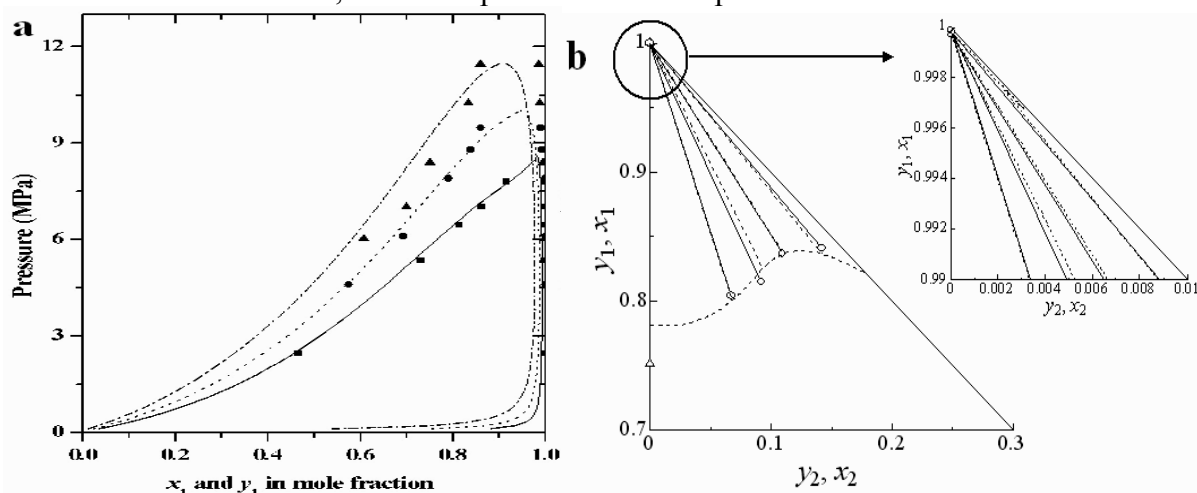


Fig. 1a. Experimental and correlated results of phase equilibria for the binary system of methanol (1) + C18 methyl esters (2) at 523(■), 548(●), 573 K(▲), respectively. [1]

Fig. 1b. Experimental and correlated results of phase equilibria for the ternary system of methanol (1) + C18 methyl esters (2) + α -tocopherol (3) system at 523 K and 6.0 MPa. [2]

References

- [1] Fang T., Shimoyama Y. et al., Phase equilibria for the mixtures of supercritical methanol + C18 methyl esters and supercritical methanol + α -tocopherol, *J. Supercrit. Fluids*, **47**, (2008) 140–146.
- [2] Fang T., Shimoyama Y. et al., Ternary phase equilibria for the mixtures of supercritical methanol + C18 methyl esters + α -tocopherol, *J. Chem. Eng. Data*, **55**, (2010) 80–84.

CORRELATING AND PREDICTING THE SOLUBILITIES OF SOLID N-ALKANES AND POLYCYCLIC AROMATIC HYDROCARBONS IN SUPERCRITICAL CARBON DIOXIDE USING THE COMPRESSED GAS MODEL AND THE REFERENCE SOLUBILITIES

Li¹ H.R., Li² S.F. and Shen¹ B.Q.

¹College of Pharmacy, Nankai University, Tianjin 300071, P. R. China
e-mail: lihongru@nankai.edu.cn, bqshen@nankai.edu.cn

²School of Chemical Engineering and Technology, Tianjin University, Tianjin 300072, P. R. China, e-mail: shfli@tju.edu.cn

The compressed gas model is widely used in solubility correlation and prediction for compounds in supercritical fluids. The challenges in using this model are the high compressibility and asymmetry of the supercritical systems and the lack of sublimation pressures of some solutes [1]. In this article, the reference solubilities were introduced into the compressed gas model to eliminate the use of sublimation pressures of solutes and reduce the applied pressure range of the equation of state and corresponding mixing rules in the compressed gas model. By using reference solubilities, the correlation and prediction capabilities of the compressed gas model are improved. The AARDs in solubility correlation for the solid *n*-alkanes and the polycyclic aromatic hydrocarbons are 22.95% and 7.12%. The reference solubilities and the linear fit of binary interaction k_{12} versus the carbon number of corresponding solid *n*-alkanes can be used to predict the solubilities of solid *n*-alkanes in supercritical CO₂ and the average AARD in prediction is 21.71%. For polycyclic aromatic hydrocarbons, the binary interaction parameter of k_{12} can be set at 0.1 and the solubility prediction results are satisfactory with an average AARD of 15.27%.

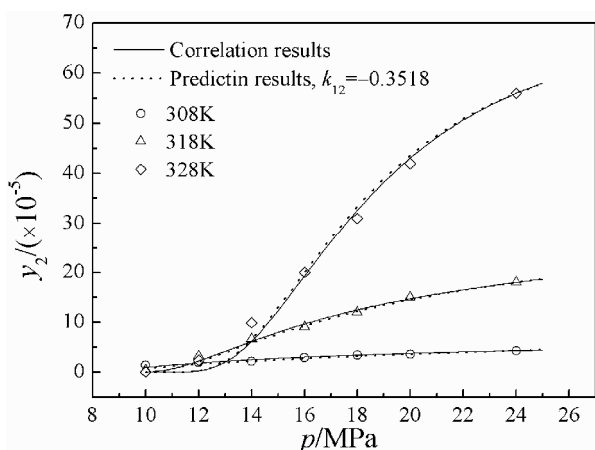


Fig. 1. Solubility correlation and prediction for *n*-dotriacontane in sc-CO₂ using compressed gas model combined with PREOS-VDW1 and reference solubilities.

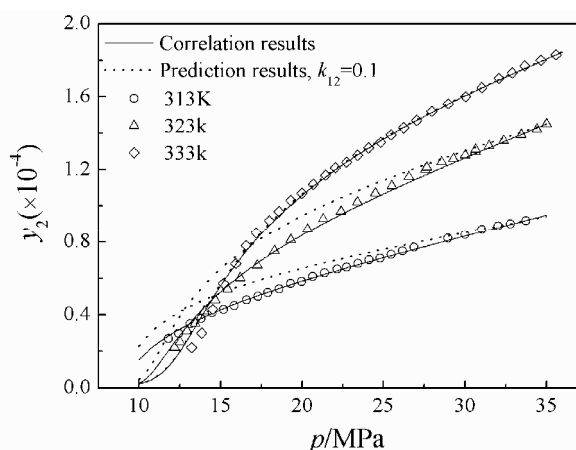


Fig. 2. Solubility correlation and prediction for anthracene in sc-CO₂ using compressed gas model combined with PREOS-VDW1 and reference solubilities.

References

- [1] Johnston K.P., Peck D.G., Modeling supercritical mixtures: how predictive is it?, *Ind. Eng. Chem. Res.*, **28**, (1989) 1115–1125.

TEMPERATURE VARIATION CHEMICAL MODEL FOR CHLORIDE–BROMIDE INTERACTION PARAMETERS AND EQUILIBRIUM SOLUBILITIES IN THE AQUEOUS SYSTEM OF MAGNESIUM CHLORIDE AND MAGNESIUM BROMIDE

Meng^{1,2} L.Z., Li¹ D., Guo² Y.F. and Deng² T.L.

¹Coll.Chem. & Chem.Eng., Linyi Univ., Linyi 276005 PRC email: menglingzong@lyu.edu.cn

²Coll. Mar. Sci. Eng., Tianjin Univ. Sci. & Technol., Tianjin 300457, PRC

Solubilities in the ternary system $\text{MgCl}_2\text{--MgBr}_2\text{--H}_2\text{O}$ at $T = (288.15\text{--}333.15)$ K were investigated, and the crystallized behaviours of solid solution $\text{Mg}(\text{Cl}, \text{Br})_2 \cdot 6\text{H}_2\text{O}$ were established. Combined our experimental results with other experimental data available in the literature [1,2] at $T = (298.15$ and $313.15)$ K, the single-salt parameters available in the literatures [3], the mixed ion-interaction parameters $\theta_{\text{Cl,Br}}$, $\psi_{\text{Mg,Cl,Br}}$ and the equilibrium constants equations of the solid solution were obtained. Based on fundamental Pitzer specific interaction equations, the solubility modelling approach achieved a very good agreement with chloride and bromide salts equilibrium solubility data. Temperature-dependent equation in the system provides reasonable mineral solubility at $T = (288.15\text{--}333.15)$ K. This model expands the solubility calculation in the systems containing solid solution by evaluating chloride-bromide mixing solution parameters. Limitations of the mixed solution models due to data insufficiencies are discussed.

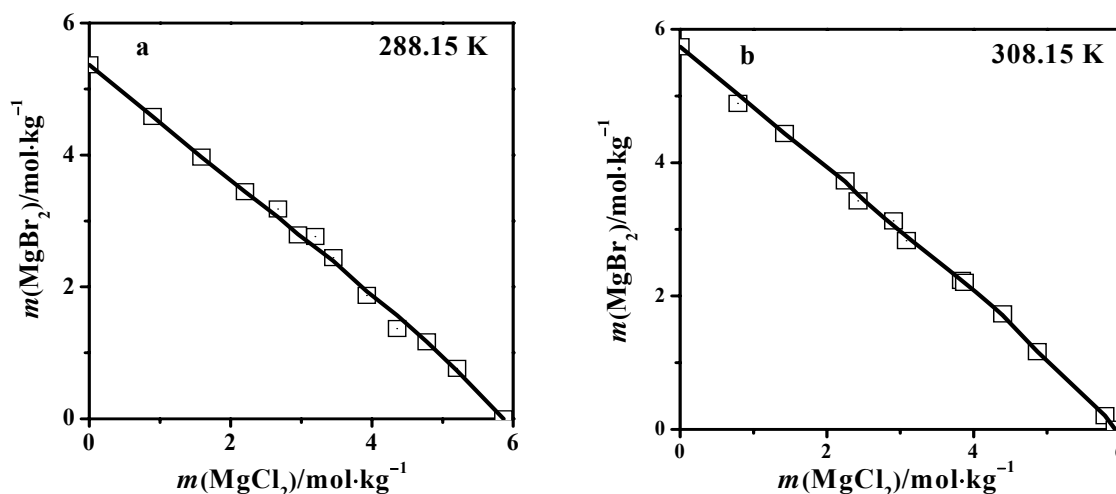


Fig. 1. Comparison of the experimental and calculated phase diagram of the stable ternary system at 288.15 K(a) and 308.15 K(b); □, experimental data; —, calculated isotherm curve.

Acknowledgments: Financial support from the State Key Program of NNSFC (Grant 20836009), the Key Pillar Program of Tianjin Municipal Science and Technology (Grant 11ZCKGX02800), the Specialized Research Fund for the Doctoral Program of Chinese Higher Education (Grant 20101208110003) and the Tianjin Key Laboratory of Marine Resources and Chemistry (Grant. 201101) is acknowledged.

References

- [1] Qiu D., Ren B.S., Phase equilibrium study of system $\text{MgCl}_2\text{--MgBr}_2\text{--H}_2\text{O}$ at 25°C , *J. Hebei Univ. Technol.*, **31**, (2002) 32–35.
- [2] Weng Y.B., Study on phase equilibria of the quinary system $\text{Na}^+, \text{K}^+, \text{Mg}^{2+} // \text{Cl}^-, \text{Br}^- \text{--H}_2\text{O}$ at 313K, *Tianjin Univ. Tianjin, China*, (2008) 48–50.
- [3] Christov C. Study of bromide salts solubility in the $(m_1\text{NaBr} + m_2\text{MgBr}_2)(\text{aq})$ system at $T = 323.15$ K. Thermodynamic model of solution behavior and (solid + liquid) equilibria in the $(\text{Na} + \text{K} + \text{Mg} + \text{Br} + \text{H}_2\text{O})$ system to high concentration and temperature, *J. Chem. Thermodyn.*, **47**, (2012) 335–340.

D: POSTER 11

PREDICTION OF VAPOR PRESSURE DATA FOR MULTI-COMPONENT SYSTEMS CONTAINING IMIDAZOLIUM-BASED PHOSPHATE IONIC LIQUID BASED ON THE GROUP CONTRIBUTION

Wang J.F. and Li Z.B.

Key Laboratory of Green Process and Engineering, National Engineering Laboratory for Hydrometallurgical Cleaner Production Technology, Institute of Process Engineering, Chinese Academy of Sciences, Beijing 100190, PR China, e-mail: zhibao.li@home.ipe.ac.cn

Based on the new group segmentation method of ionic liquids, the vapor pressure data of water, 1-propanol and 2-propanol for the systems containing 1,3-dimethylimidazolium dimethylphosphate ([MMIM][DMP]) and 1-methyl-3-ethylimidazolium diethylphosphate ([EMIM][DEP]) ionic liquids (ILs) are calculated by the modified UNIFAC model embedded in Aspen Plus. Following our previous work, vapor pressure data for above solvents as well as their binary mixtures in the presence of ionic liquid (IL) 1-methyl-3-ethylimidazolium diethylphosphate ([EMIM][DEP]) at different temperatures and IL-content ranging from mass fraction 0.10 to 0.70 using a quasi-static ebulliometer method are presented. The correction of fugacity coefficient is equal to one at low pressure, and activity coefficients of these solvents in the [EMIM][DEP] have been determined from the vapor pressure data of binary systems. The activity coefficient of solvents in the [MMIM][DMP] are correlated by the modified UNIFAC model embedded in the Aspen Plus. The resulting temperature-dependent group interaction parameters of modified UNIFAC are used for the prediction of vapor pressure of other systems containing [EMIM][DEP] and [MMIM][DMP] with fair accuracy. Furthermore, the phase behavior of water + 1-propanol + [MMIM][DMP], water + 2-propanol + [MMIM][DMP], water + 1-propanol + [EMIM][DEP], and water + 2-propanol + [EMIM][DEP] with mass fraction of [EMIM][DEP] of 0.3 and 0.5 at 101.3kPa are investigated. It is shown that the relative volatility of 1-propanol and 2-propanol is enhanced, and the azeotrope of water + 1-propanol and water + 2-propanol mixtures eliminated completely. The separation ability of the two ILs is in the order [MMIM][DMP] > [EMIM][DEP].

**POSSIBILITY OF THE QUATERNARY SYSTEM $\text{KCl-NH}_4\text{Cl-CaCl}_2\text{-H}_2\text{O}$ AS
POTENTIAL PHASE MATERIAL — PREDICTION AND EXPERIMENTAL
VERIFICATION**

Dong¹ O.Y., Zeng^{1,2*} D., Han¹ H. J. and Yin² X.

¹Qinghai Institute of Salt Lakes, Chinese Academy of Sciences, Xining, 810008, P.R. China,
*e-mail: dewen_zeng@hotmail.com

²College of Chemistry and Chemical Engineering, Central South University, Changsha,
410083, P.R. China

Solubility isotherms of the quaternary system $\text{KCl-NH}_4\text{Cl-CaCl}_2\text{-H}_2\text{O}$ was elaborately determined at $T = 293.15$ K by using the isothermal method, as shown by symbols in Fig. 1. Phase diagrams of the binary and ternary systems in the quaternary system were simulated by a Pitzer-Simons-Clegg model [1,2] at different temperatures. The predicted solubility isotherm of the quaternary system was found in good agreement with the experimental data at 293.15 K, as shown in Fig. 1. The predicted invariant point (the symbol square in the Fig. 2) can be used as approximate phase change material with phase change temperature at 297.35 K.

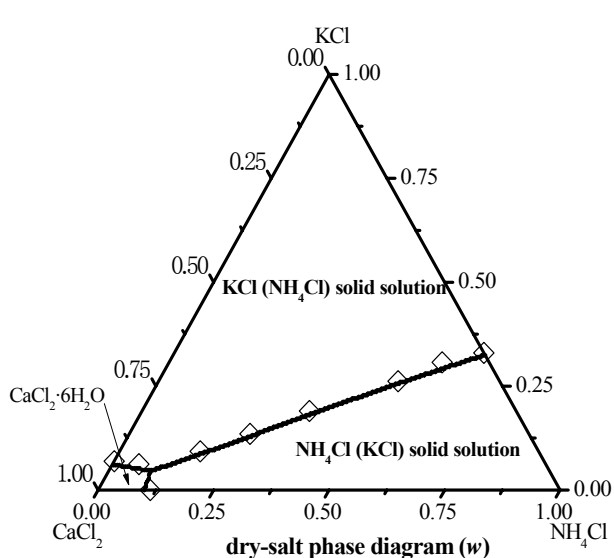


Fig. 1. Predicted solubility isotherms of the system $\text{KCl-NH}_4\text{Cl-CaCl}_2\text{-H}_2\text{O}$ comparing with exp. values. \diamond : exp. values at 293.15 K in this work; —: model value.

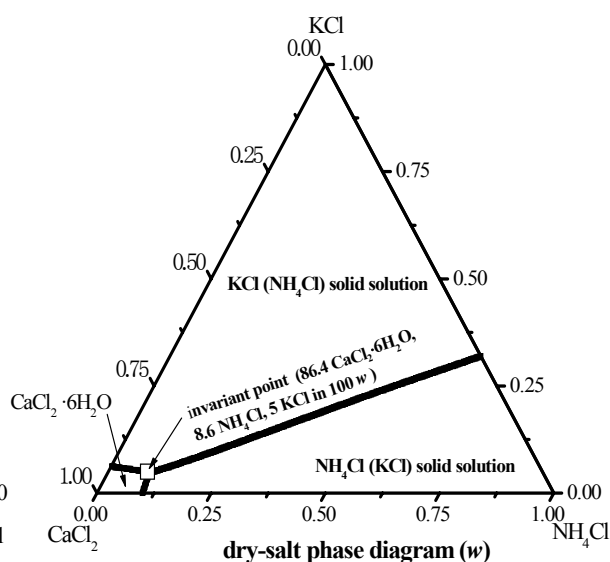


Fig. 2. Predicted solubility isotherm of the system $\text{KCl-NH}_4\text{Cl-CaCl}_2\text{-H}_2\text{O}$ at 297.35 K. \square : predicted invariant point.

References

- [1] Clegg S.L., Pitzer K.S., Thermodynamics of multicomponent, miscible, ionic solutions. generalized equations for symmetrical electrolytes, *J. Phys. Chem.*, **96**, (1992) 3513–3520.
- [2] Clegg S.L., Pitzer K.S., Brimblecombe P. Thermodynamics of multicomponent, miscible, ionic solutions. 2. mixture including unsymmetrical electrolytes, *J. Phys. Chem.*, **96**, (1992) 9470–9479.

THERMODYNAMIC UNDERSTANDING ON THE LIQUID-SOLID EQUILIBRIUM OF THE TERNARY SYSTEM $\text{CaCl}_2\text{-SrCl}_2\text{-H}_2\text{O}$

Guo¹ L., Zeng^{1,2} D. and Yao¹ Y.

¹Qinghai Institute of Salt Lakes, Chinese Academy of Sciences, 810008 Xining, P. R. China,

²College of Chemistry and Chemical Engineering, Central South University, 410083, Changsha, P. R. China, e-mail: dewen_zeng@hotmail.com

Because of the high similarity in properties of CaCl_2 and SrCl_2 , solubility isotherm of the ternary system $\text{CaCl}_2\text{-SrCl}_2\text{-H}_2\text{O}$, which is concerned in extracting resources from the Nanyishan oilfield brines in China, is very difficult to determine. It was reported [1] that there are two invariant points between the solid phase $\text{SrCl}_2\cdot 6\text{H}_2\text{O}$ and the solid solution ($x\text{SrCl}_2\cdot 6\text{H}_2\text{O}+(1-x)\text{CaCl}_2\cdot 6\text{H}_2\text{O}$) and between the solid solution and the pure solid phase $\text{CaCl}_2\cdot 6\text{H}_2\text{O}$ in the solubility isotherms at 298.15 K, which is thermodynamically impossible. To understand the solubility phenomena of the ternary system concerning solid solution, we elaborately determined water activities in the ternary system at 298.15 K by the isopiestic method, and selected a Pitzer-Simonson-Clegg (PSC) model [2] to justify the reliability of the reported solubility data [1] by correlating them with our measured water activities. It is found that the water activities of the ternary system can be represented with binary parameters only. We calculated the solubility isotherms for the $\text{SrCl}_2\cdot 6\text{H}_2\text{O}$, $\text{CaCl}_2\cdot 6\text{H}_2\text{O}$ and the solid solution which is assumed as ideal mixture, as shown in Fig. 1a, and equilibrium lines between aqueous phase and solid solution phase, as well as the liquid-solid corresponding composition lines for ideal solid solution ($x\text{SrCl}_2\cdot 6\text{H}_2\text{O}+(1-x)\text{CaCl}_2\cdot 6\text{H}_2\text{O}$), as shown in Fig. 1b. Conclusion can be drawn that the reported liquidus [1] were roughly reliable, corresponding the ideal solid phase in the whole concentration range for x from 0 to 1.

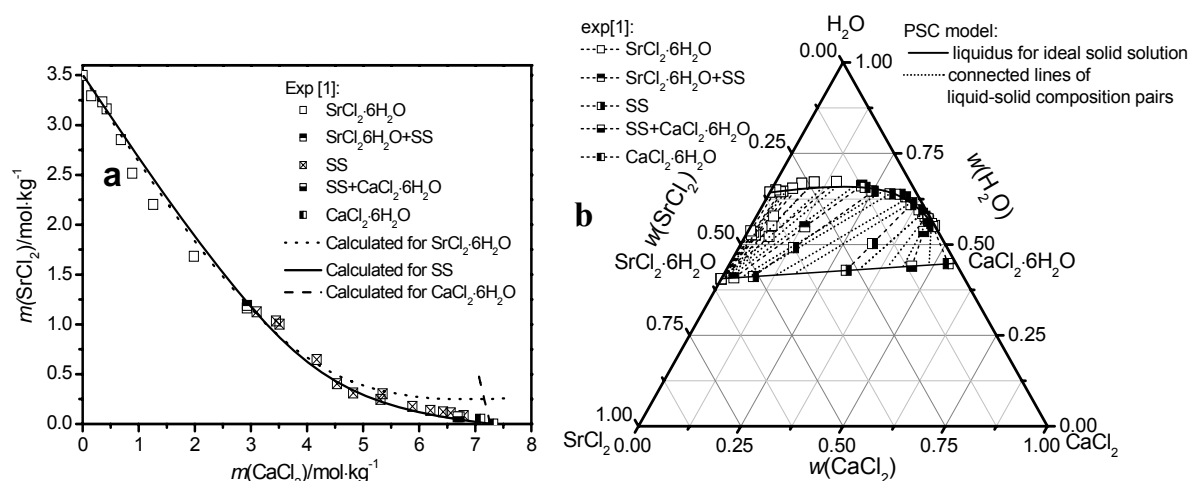


Fig. 1. Solubility isotherms of the ternary system $\text{CaCl}_2\text{-SrCl}_2\text{-H}_2\text{O}$ at 298.15 K. a: comparison of experimental [1] and calculated solubility isotherms; b: calculated liquid-solid equilibrium lines where solid phase is assumed as an ideal mixture ($x\text{SrCl}_2\cdot 6\text{H}_2\text{O}+(1-x)\text{CaCl}_2\cdot 6\text{H}_2\text{O}$).

References

- [1] Bi Y. J., Sun B., Zhao J., Song P. S., Li W., Phase equilibrium in ternary system $\text{CaCl}_2\text{-SrCl}_2\text{-H}_2\text{O}$ at 25 °C. *Chinese J. Inorg. Chem.*, **27**, (2011) 1765–1771.
- [2] Clegg S.L., Pitzer K.S., Brimblecombe P., Thermodynamics of multicomponent, miscible, ionic solutions. 2. mixture including unsymmetrical electrolytes. *J. Phys. Chem.*, **96**, (1992) 9470–9479.

PHASE DIAGRAM SIMULATION OF THE SYSTEMS $\text{ACl}+\text{MgCl}_2+\text{H}_2\text{O}$ ($\text{A} = \text{Na}, \text{K}$) AND THEIR APPLICATION IN PURIFICATION OF CHEMICAL REAGENTS

Li¹ D., Zeng^{1,2*} D., Zhou¹ H. and Dong¹ O.Y.

¹Qinghai Institute of Salt Lakes, Chinese Academy of Sciences, 810008 Xining, P.R. China,
e-mail: ddong_li@hotmail.com

²College of Chemistry and Chemical Engineering, Central South University, 410082
Changsha, P.R. China, *e-mail: dewen_zeng@hotmail.com

Recrystallization method is often used for purification of chemical reagents in laboratory. The theoretical basis of the method is solubility phase diagrams of concerned systems. When the recrystallization method is valid for purification for most reagents, a lot of exceptions exist, for example, the removal of trace amount of NaCl from MgCl_2 aqueous solution doesn't always work, and the purification effect depends on the initial amount of NaCl. For understanding the essence of these phenomena, we constructed the phase diagrams of the systems $\text{ACl}+\text{MgCl}_2+\text{H}_2\text{O}$ ($\text{A} = \text{Na}, \text{K}$) by simulating the experimental solubility isotherms [2] of these systems with a Pitzer-Simonson-Clegg model [1], and present the simulated results in Figure 1. Based on the constructed phase diagrams, how the initial amount of impurities (NaCl or KCl), the end crystallization temperature and the condensation extent influence the removal effect of impurities were discussed in detail.

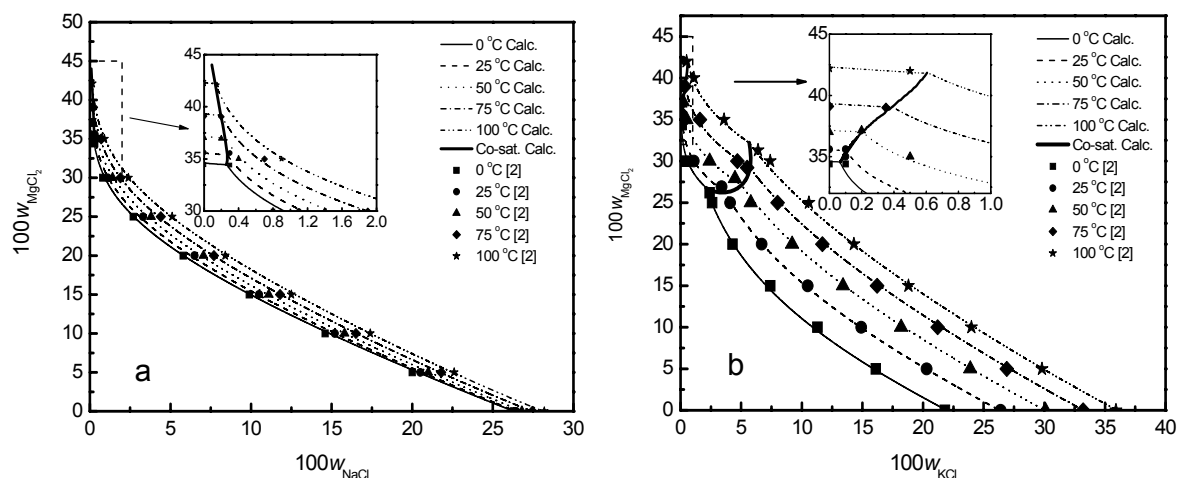


Fig. 1a and 1b. Solubility phase diagrams of system $\text{NaCl}-\text{MgCl}_2-\text{H}_2\text{O}$ and $\text{KCl}-\text{MgCl}_2-\text{H}_2\text{O}$ temperature range from 0 to 100 °C. All lines are simulated by using a Pitzer-Simonson-Clegg model, and all symbols at different temperatures are from [2].

References

- [1] Clegg S.L., Pitzer K.S., Brimblecombe P., Thermodynamics of multicomponent, miscible, ionic solutions. 2. mixtures including unsymmetrical electrolytes, *J. Phys. Chem.*, **96**, (1992) 9470–9479.
[2] Pelsha A. D., Handbook of experimental data for salt solubilities, ternary systems, vol. 1. and vol. 2., *Khimia*, Leningrad (1953).

PHASE DIAGRAM PREDICTION OF THE SYSTEM $\text{NaNO}_3\text{-LiNO}_3\text{-KNO}_3\text{-H}_2\text{O}$ AS ROOM TEMPERATURE PHASE CHANGE MATERIALS

Yin¹ X., Chen² Q. and Zeng^{2*} D.

¹College of Chemistry and Chemical Engineering, Hunan University, Changsha, 410082, China, e-mail: yinxia0405@yahoo.com.cn

²College of Chemistry and Chemical Engineering, Central South University, Changsha, 410083, China, *E-mail: dewen_zeng@hotmail.com

In our previous work [1-2], phase change materials (PCMs) with eutectic temperature at about 298-301 K were found in the systems of $\text{NaNO}_3(\text{KNO}_3)\text{-LiNO}_3\text{-H}_2\text{O}$. Theoretically, the eutectic material with melting temperature lower than 298 K could be obtained in the quaternary system $\text{NaNO}_3\text{-LiNO}_3\text{-KNO}_3\text{-H}_2\text{O}$. In this work, a Pitzer-Simonson-Clegg model [3] was selected for calculating the phase diagrams of the system $\text{NaNO}_3\text{-LiNO}_3\text{-KNO}_3\text{-H}_2\text{O}$ and its sub-systems (see Figures 1a, 1b, 1c and 1d). A eutectic point consisting of 5.9 % NaNO_3 , 76.2 % $\text{LiNO}_3\cdot 3\text{H}_2\text{O}$, and 17.9 % KNO_3 (point E in Figure 1d) with melting temperature 295.6 K was found. Melting and crystallization behavior and DSC of the PCM at the eutectic point were measured. The measured heat-storage temperature is about 295 K, lower than the predicted one by 0.6 K, and fusion heat of the PCM is $200.1 \text{ J}\cdot\text{g}^{-1}$.

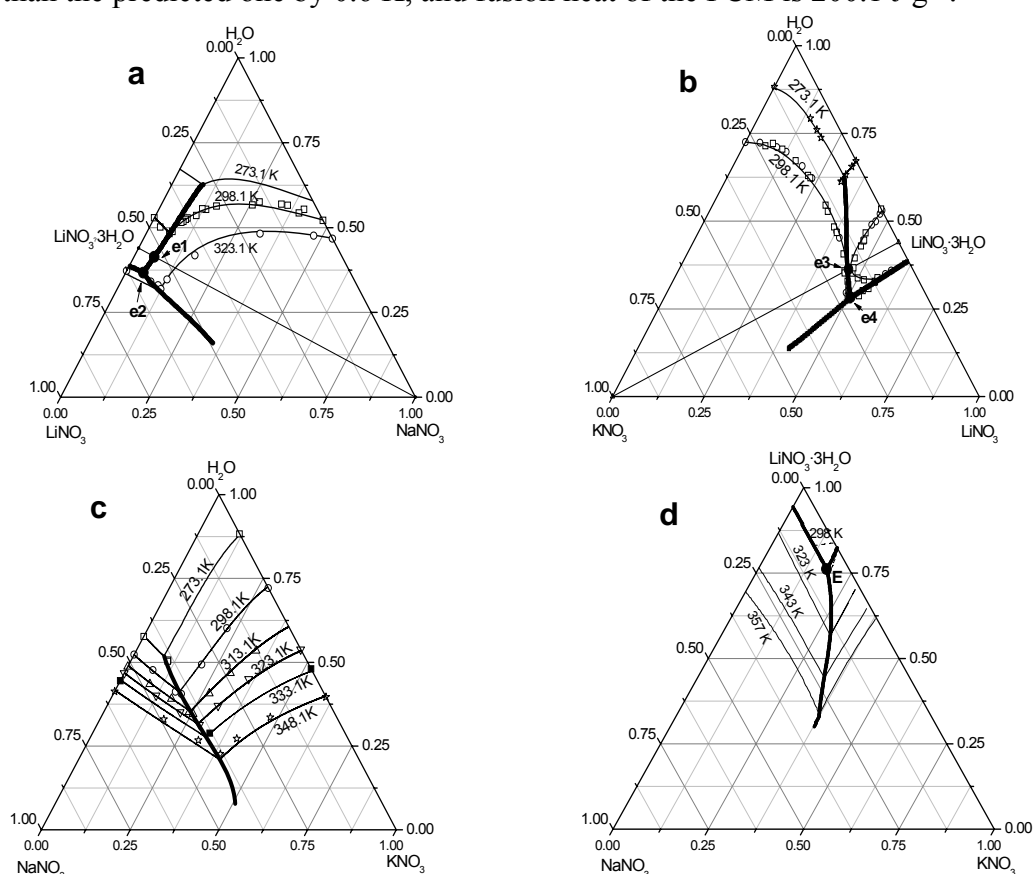


Fig.1. Phase diagrams of the system $\text{NaNO}_3\text{-LiNO}_3\text{-KNO}_3\text{-H}_2\text{O}$ and its sub-systems. symbols: exp. data; —: calculated isotherms; —: predicted polytherm; ●: predicted eutectic points.

References

- [1] Li B.H., Zeng D.W., Yin X., et al. *J. Thermal Analysis and Calorimetry*, **100**, (2010) 685–693.
- [2] Yin X., Chen Q.Y., Zeng D.W., et al. *CALPHAD*, **35**, (2011) 463–472.
- [3] Clegg S.L., Pitzer K.S., Brimblecombe P., *J. Phys. Chem.*, **96**, (1992) 9470–9479.

D: POSTER 16

SOLUBILITY PREDICTION OF THE QUATERNARY SYSTEM CaSO₄-MgSO₄-H₂SO₄-H₂O AT TEMPERATURES FROM 298.15 TO 363.15 K

Wang W. and Zeng* D.

College of chemistry and chemical engineering, Central south university, Changsha, 410083,
P. R. china, email: dewen_zeng@hotmail.com.

Hydrometallurgical processes of nickel often generate a plenty of waster liquid containing magnesium sulfate. On recovering magnesium sulfate by condensation at high temperatures, scale appears on the wall of evaporator. To understand the crystallization mechanism and to develop novel method to avoid the scale formation on the wall, solubility phase diagram of the quaternary systems CaSO₄-MgSO₄-H₂SO₄-H₂O are necessary. In this work, we simulated thermodynamic properties of the binary systems CaSO₄-H₂O, MgSO₄-H₂O, H₂SO₄-H₂O and the ternary systems CaSO₄-MgSO₄-H₂O, CaSO₄-H₂SO₄-H₂O, MgSO₄-H₂SO₄-H₂O by a Pitzer thermodynamic model, and predicted the solubility properties of the quaternary system over a wide temperature range from 298.15 K to 363.15 K. In order to verify the reliability of the predicted results, a series of solubility measurements of insoluble anhydrite in this quaternary system have been carried out at 348.15 K and 363.15 K and the measured results were compared with the predicted ones. It was shown that the Pitzer thermodynamic model can perfectly predict the solubilities of insoluble anhydrite in the quaternary systems. Furthermore, stable fields of gypsum and insoluble anhydrite as a function of temperature and concentration of H₂SO₄ and MgSO₄ were predicted.

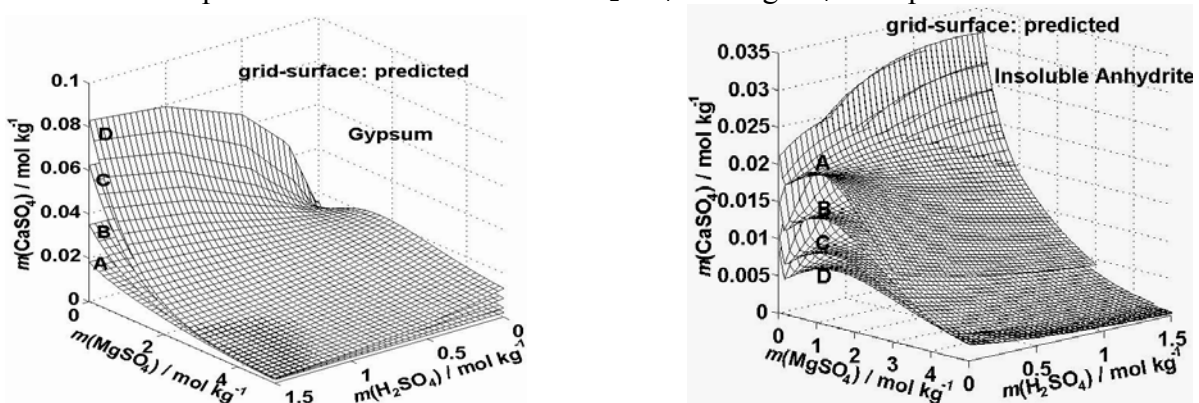


Fig. 1. Predicted solubility isotherms of gypsum and anhydrite in the system CaSO₄-MgSO₄-H₂SO₄-H₂O. grid-surface, predicted: A: 298.15 K; B: 323.15 K; C: 348.15 K; D: 363.15 K.

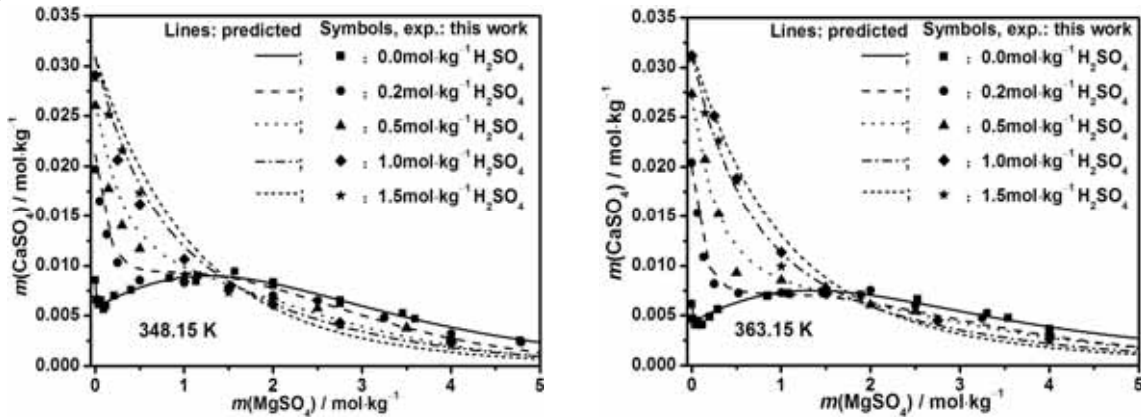


Fig. 2. Comparison of the predicted and experimental solubility data for insoluble anhydrite in the system CaSO₄-MgSO₄-H₂SO₄-H₂O at 348.15 K and 363.15 K. lines, predicted isotherms with both binary and ternary parameters; symbols, experimental values, this work.

D: POSTER 17

QUANTITATIVE ANALYSIS OF MULTI-COMPONENT ACID-BASE TITRATION AND SELECTIVE RECOVERY OF METALS FROM ACIDIC MINE DRAINAGE WATERS

Räsänen¹ L., Blomberg¹ P., Mäki² T. and Koukkari¹ P.

¹VTT Technical Research Centre of Finland, Process Chemistry, Espoo, Finland,
e-mail: firstname.surname@vtt.fi

²Pyhäsalmi Mine Oy, Pyhäsalmi, Finland, e-mail: timo.maki@pyhasalmi.fi

Recovery of metals from acidic mine drainage waters AMDW was modelled [1] using the software program ChemSheet [2]. A multicomponent multiphase thermochemical description of the system was constructed from thermodynamic data, atom balances, and select kinetic information. The aqueous solution was modelled by Pitzer equations and the thermodynamic parameters taken from the VTT Solution Database. Titration experiments were used to test and verify the model. A process for selective precipitation of metals from the waste water was developed. The presence of carbon dioxide plays an important role in selective precipitation. Iron, aluminium, copper, and zinc, were selectively precipitated from the AMDW.

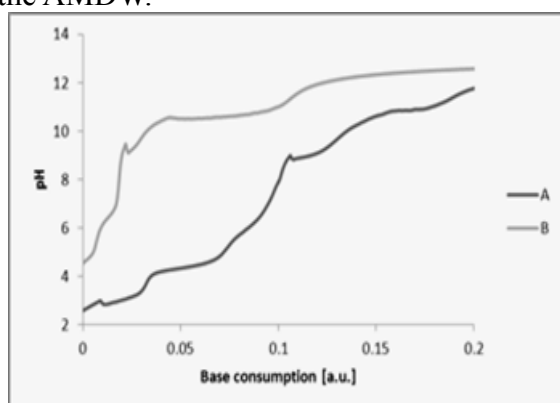


Fig. 1. Continuous titration curves for AMDW from Pyhäsalmi Mine. Curve A was measured in air using the entire mixture. Curve B is for a solution with most of the iron and aluminum removed by pH induced precipitation. The liquid volume and the strength of the base were different in the two experiments.

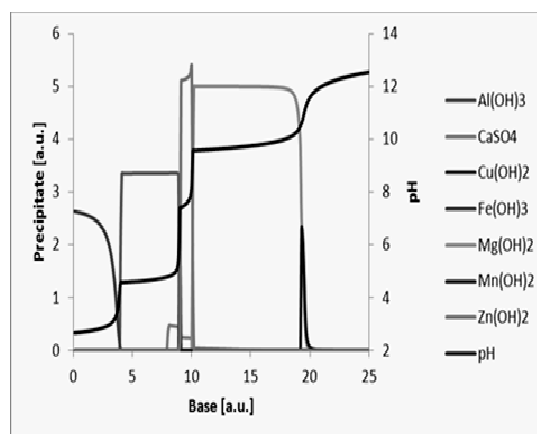
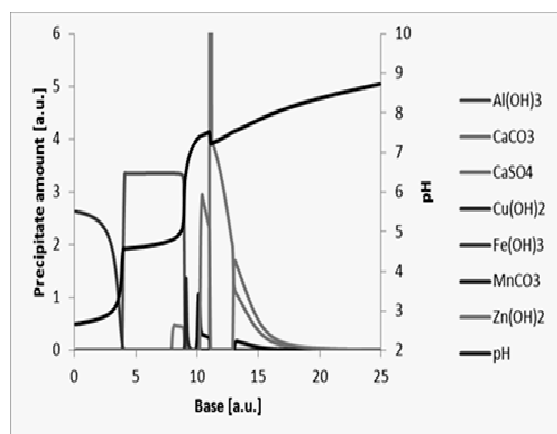


Fig. 2a and 2b. Order, identity, and magnitude of precipitates formed during titration with (left) and without (right) CO₂ in the system.

References

- [1] Part of the Project Promine 2009-2011; part of NMP – *Nanosciences, Nanotechnologies, Materials and New Production Technologies*, 7th Framework Programme.
- [2] Koukkari P., Advanced gibbs energy methods for functional materials and processes, *VTT Research Notes*, (2009) 2506.

D: POSTER 18

SOLUBILITY DIAGRAMS OF $\text{Na}_2\text{SO}_4\text{-Rb}_2\text{SO}_4\text{-MgSO}_4\text{-H}_2\text{O}$, $\text{Na}_2\text{SO}_4\text{-Cs}_2\text{SO}_4\text{-MgSO}_4\text{-H}_2\text{O}$ AND $\text{K}_2\text{SO}_4\text{-Cs}_2\text{SO}_4\text{-MgSO}_4\text{-H}_2\text{O}$ AT 298.15 K

Hu B.

Institute of Salt Lakes, Chinese Academy of Sciences, 810008 Xining, China,
e-mail: hubin@isl.ac.cn

High concentrations of rubidium and cesium have been found in the salt lake brines in Qinghai-Tibet plateau. These rare alkali metal ions coexist with Li^+ , Na^+ , K^+ , Mg^{2+} , Cl^- and SO_4^{2-} . There are relatively small number of solubility data on the systems containing rubidium and cesium. Calculation of phase diagrams in multicomponent electrolytes systems from subsystem information are of theoretical as well as of practical interest. The ion-interaction model advanced by Pitzer et al. [1] has been successfully applied to solubility calculations in nature water systems. On the basis of data concerning the binary and ternary subsystems, the phase-equilibrium diagrams of two quaternary systems $\text{Na}_2\text{SO}_4\text{-Rb}_2\text{SO}_4\text{-MgSO}_4\text{-H}_2\text{O}$ and $\text{Na}_2\text{SO}_4\text{-Cs}_2\text{SO}_4\text{-MgSO}_4\text{-H}_2\text{O}$ at 298.15 K have been calculated using Pitzer model. Figure 1a and 1b show calculated solubility isotherms of the systems investigated. The calculated results for the former system show good agreement with experimental results in the literature [2]. In the phase diagram of $\text{Na}_2\text{SO}_4\text{-Cs}_2\text{SO}_4\text{-MgSO}_4\text{-H}_2\text{O}$, the deviation between the theoretical and experimental data may be caused by the unreliable experimental eutonic point corresponding to the equilibrium with the solution of $\text{MgSO}_4\cdot 7\text{H}_2\text{O}$ and Bloedite. Phase equilibrium of $\text{K}_2\text{SO}_4\text{-Cs}_2\text{SO}_4\text{-MgSO}_4\text{-H}_2\text{O}$ has been predicted assuming that no new solid phases crystallize in them. The calculated phase diagram consists of five crystallization fields, three invariant points, and seven invariant curves. The five crystallization fields correspond to K_2SO_4 , Cs_2SO_4 , $\text{MgSO}_4\cdot 7\text{H}_2\text{O}$, $\text{Cs}_2\text{SO}_4\cdot \text{MgSO}_4\cdot 6\text{H}_2\text{O}$ and $\text{K}_2\text{SO}_4\cdot \text{MgSO}_4\cdot 6\text{H}_2\text{O}$.

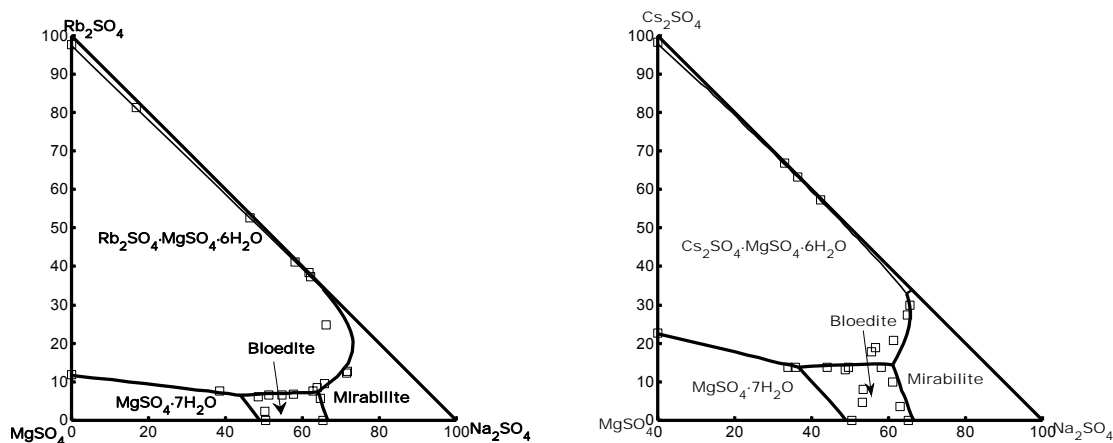


Fig. 1a and 1b. Solubility isotherms in the systems $\text{Na}_2\text{SO}_4\text{-Rb}_2\text{SO}_4\text{-MgSO}_4\text{-H}_2\text{O}$ and $\text{Na}_2\text{SO}_4\text{-Cs}_2\text{SO}_4\text{-MgSO}_4\text{-H}_2\text{O}$ at 298.15 K. Experimental data: squares. Calculated values: solid line.

Acknowledgments: This project was supported by National Natural Science Foundation of China (20903113).

References

- [1] Pitzer K.S., Activity coefficients in electrolyte solutions, 2nd edn., CRC, Boca Raton, (1991) 75.
- [2] Pel'sh A.D., A handbook on the solubility of salt systems, *Khimiya*, Leningrad, 2, (1973).

SOLUBILITY PHASE DIAGRAM OF THE SYSTEM Li^+ , $\text{Mg}^{2+} // \text{Cl}^-$, $\text{SO}_4^{2-} - \text{H}_2\text{O}$ AT 298.15 K ---- EXPERIMENTAL REDETERMINATION AND MODEL SIMULATION

Li¹ H., Zeng^{1,2,*} D., Yao¹ Y., Yin² X. and Li¹ D.

¹Qinghai Institute of Salt lakes, Chinese Academy of Sciences, Xining, Qinghai 810008, P.R.China, e-mail: hongxia_1li@126.com

²College of Chemistry and Chemical Engineering, Central South University, Changsha, Hunan 410083, P.R.China, *e-mail: dewen_zeng@hotmail.com

The quaternary reciprocal system Li^+ , $\text{Mg}^{2+} // \text{Cl}^-$, $\text{SO}_4^{2-} - \text{H}_2\text{O}$ is a most important subsystem concerning resource extraction from salt lake brine, which has been widely investigated [1-4]. However, the reported solubility data concerning this system are contradictory with each other. In this work, we elaborately measured solubility diagram of this quaternary system which is shown in Figures 1. A new phase $\text{MgSO}_4 \cdot 4\text{H}_2\text{O}$ was found to exist in the quaternary system for the first time. Then, a Pitzer-Simonson-Clegg model [5] was selected to simulate properties of the binary and ternary systems, and predict the solubility phase diagram of the quaternary system, as shown by curves in Figure 1. The predicted results are in good agreement with the experimental ones.

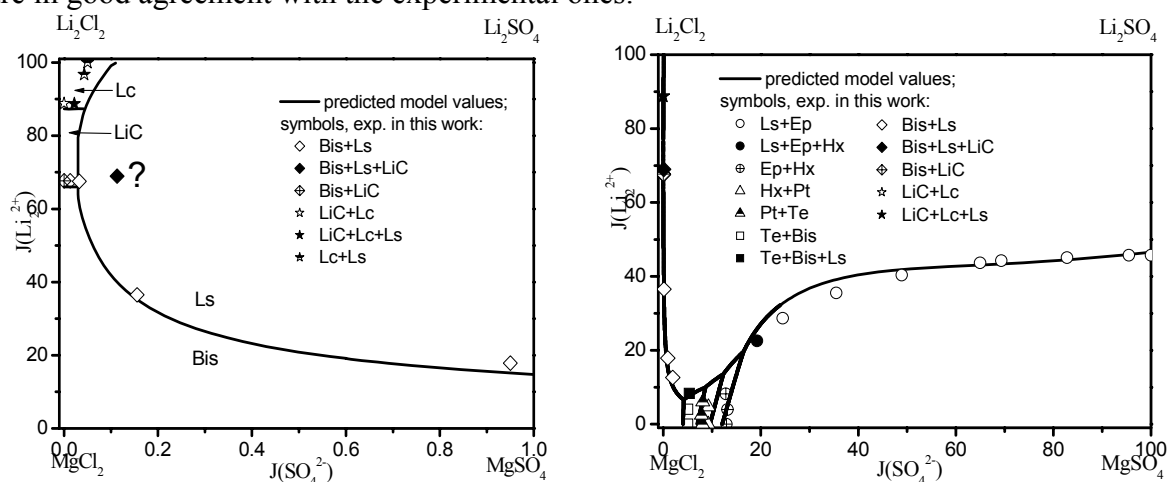


Fig.1. Experimental solubilities of the quaternary reciprocal system Li^+ , $\text{Mg}^{2+} // \text{Cl}^-$, $\text{SO}_4^{2-} - \text{H}_2\text{O}$ at 298.15 K compared with predicted results. Ep: $\text{MgSO}_4 \cdot 7\text{H}_2\text{O}$; Hx: $\text{MgSO}_4 \cdot 6\text{H}_2\text{O}$; Pt: $\text{MgSO}_4 \cdot 5\text{H}_2\text{O}$; Te: $\text{MgSO}_4 \cdot 4\text{H}_2\text{O}$; Bis: $\text{MgCl}_2 \cdot 6\text{H}_2\text{O}$; Ls: $\text{Li}_2\text{SO}_4 \cdot \text{H}_2\text{O}$; LiC: $\text{LiCl} \cdot \text{MgCl}_2 \cdot 7\text{H}_2\text{O}$; Lc: $\text{LiCl} \cdot \text{H}_2\text{O}$.

References

- [1] Kydynov M., Musuraliev K., Imanakunov B., Quaternary system of lithium and magnesium sulfates and chlorides in water at 25 °C, *Zh. Prikl. Khim.*, **39**, (1966) 2114–2117.
- [2] Guo Z., Liu Z., Chen J., The metastable equilibrium of quaternary system Li^+ , $\text{Mg}^{2+} // \text{Cl}^-$, $\text{SO}_4^{2-} - \text{H}_2\text{O}$ at 298.15 K, *Acta Chimica. Sinica*, **49**, (1991) 937-943.
- [3] Ren K., Song P., The study of phase equilibrium and physical and chemical properties of the quaternary reciprocal system Li^+ , $\text{Mg}^{2+} // \text{Cl}^-$, $\text{SO}_4^{2-} - \text{H}_2\text{O}$ at 25 °C, *Chin. J. Inorg. Chem.*, **10**, (1994) 69–74.
- [4] Kwok K.S., Ng K.M., Taboada M.E., Cisternas L.A., Thermodynamics of salt lake system: representation, experiments, and visualization, *AIChE J.*, **54**, (2008) 706–727.
- [5] Clegg S.L., Pitzer K.S., Brimblecombe P., Thermodynamics of multicomponent, miscible, ionic solutions. 2. Mixture including unsymmetrical electrolytes, *J. Phys. Chem.*, **96**, (1992) 9470–9479.

SOLUBILITY OF GYPSUM AND INSOLUBLE ANHYDRITE IN THE TERNARY SYSTEM $\text{CaSO}_4\text{-H}_2\text{SO}_4\text{-H}_2\text{O}$

Wang W. and Zeng* D.

College of chemistry and chemical engineering, Central south university, Changsha, 410083, People's Republic of China, email: dewen_zeng@hotmail.com.

Solubility properties of the ternary system $\text{CaSO}_4\text{-H}_2\text{SO}_4\text{-H}_2\text{O}$ are of essential importance in phosphoric acid production and hydrometallurgical process of heavy metal sulfates. However, solubility isotherms measured for this system [1-3] may be unreliable. For instance, Zdanovskii [1,3] measured solubilities of gypsum and anhydrite in this system with equilibrium time 5-8 h, which was not enough for reaching equilibrium, according to the experience of Azimi and Papangelakis [4]. In this work, the solubility isotherms of gypsum and insoluble anhydrite in the system $\text{CaSO}_4\text{-H}_2\text{SO}_4\text{-H}_2\text{O}$ have been elaborately determined at $T = (273.15, 323.15, 348.15 \text{ and } 363.15) \text{ K}$ and presented in Figures 1a and 1b. Generally, our measured solubility isotherms for gypsum are in good agreement with the literature [3]; however, those for anhydrite are lower than that reported by Zdanovskii and Vlasov [1]. A Pitzer thermodynamic model was selected to simulate and predict the solubility isotherms of this system with binary and ternary parameters. The lines in Figures 1a and 1b are the calculated results, agreeing well with the newly obtained experimental data in this work. At last, the stable fields for gypsum and anhydrite as a function of temperature and H_2SO_4 concentration are outlined by the thermodynamic model.

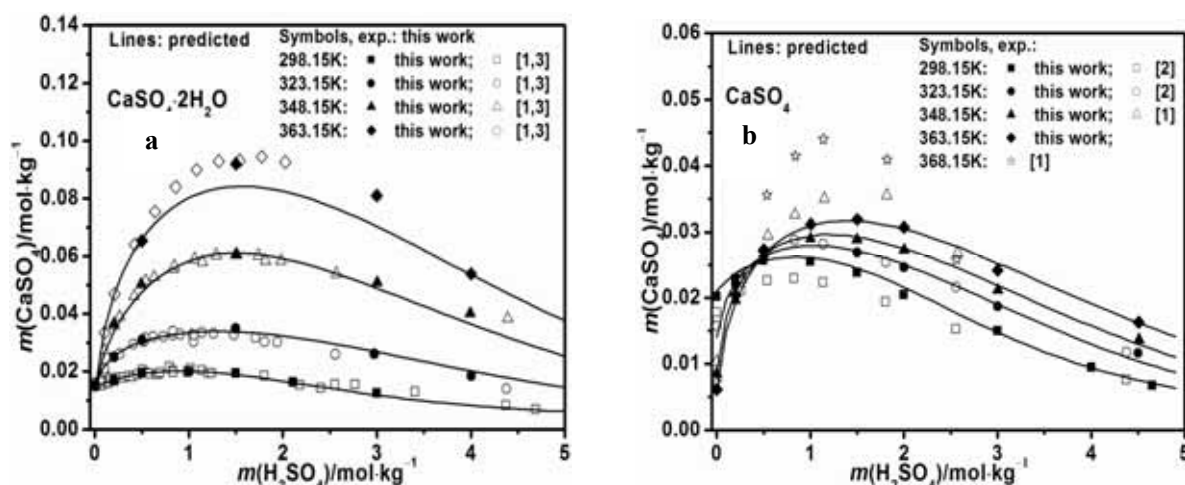


Fig.1a and 1b. Comparison of the newly obtained solubility data of gypsum and insoluble anhydrite with the literature [1-3] and calculated results in the $\text{CaSO}_4\text{+H}_2\text{SO}_4\text{+H}_2\text{O}$ system.

References

- [1] Zdanovskii A.B., Vlasov G.A., Dehydration of gypsum in sulfuric acid solutions, *Russ. J. Inorg. Chem.*, **13**, (1968) 1418–1420.
- [2] Dutrizac J.E., Calcium sulphate solubilities in simulated zinc processing solutions, *Hydrometallurgy*, **65**, (2002) 109–135.
- [3] Zdanovskii A.B., Vlasov G.A., Determination of the boundaries of the reciprocal transformation of $\text{CaSO}_4\cdot 2\text{H}_2\text{O}$ and $\gamma\text{-CaSO}_4$ in H_2SO_4 solutions, *Russ. J. Inorg. Chem.*, **13**, (1968) 1318–1319.
- [4] Azimi G., Papangelakis V.G., Mechanism and kinetics of gypsum-anhydrite transformation in aqueous electrolyte solutions, *Hydrometallurgy*, **108**, (2011) 122–129.

PHASE DIAGRAM OF THE SYSTEM $\text{MgCl}_2\text{-LiCl-NH}_4\text{Cl-H}_2\text{O}$ AT 298.15 K

Yang H.T., Zeng* D., Yin X. and Liang T. Y.

College of Chemistry and Chemical Engineering, Central South University, Changsha, 410083, China, *e-mail: dewen_zeng@hotmail.com

Phase diagram of the quaternary system $\text{MgCl}_2\text{-LiCl-NH}_4\text{Cl-H}_2\text{O}$ is needed for understanding the change in solution composition and solid phase when NH_3 gas is added to a saturated brine containing MgCl_2 and LiCl to precipitate magnesium. In this work, we measured the solubility data as well as the corresponding solid phases of the quaternary system at 298.15 K by equilibrium isothermal method and the results are shown in Fig. 1a. A Pitzer-Simons-Clegg thermodynamic model [1] was used to simulate and predict the phase diagrams of the quaternary and its subternary systems at 298.15 K. The model parameters were obtained by simulating experimental solubility and water activity of the binary systems $\text{LiCl-H}_2\text{O}$, $\text{NH}_4\text{Cl-H}_2\text{O}$, $\text{MgCl}_2\text{-H}_2\text{O}$ and the ternary systems $\text{NH}_4\text{Cl-LiCl-H}_2\text{O}$, $\text{MgCl}_2\text{-LiCl-H}_2\text{O}$, $\text{MgCl}_2\text{-NH}_4\text{Cl-H}_2\text{O}$. Four crystallization fields including two double salt ($\text{LiCl}\cdot\text{MgCl}_2\cdot 7\text{H}_2\text{O}$, $\text{NH}_4\text{Cl}\cdot\text{MgCl}_2\cdot 6\text{H}_2\text{O}$), one hydrate salt ($\text{MgCl}_2\cdot 6\text{H}_2\text{O}$) and one solid-solution phase ($\text{LiCl}\cdot\text{H}_2\text{O}+\text{NH}_4\text{Cl}$) were found in this system. The predicted stable fields of the phases (lines in Fig. 1b) are in good agreeing with the experimental results (solid circles in Fig. 1b), while the solid solution crystallization fields were predicted by assuming the solid solution as a regular solution. Based on the constructed phase diagram, profound understanding of the crystallization behaviors can be achieved in the separation process of Li(Mg) -containing brine using NH_3 gas.

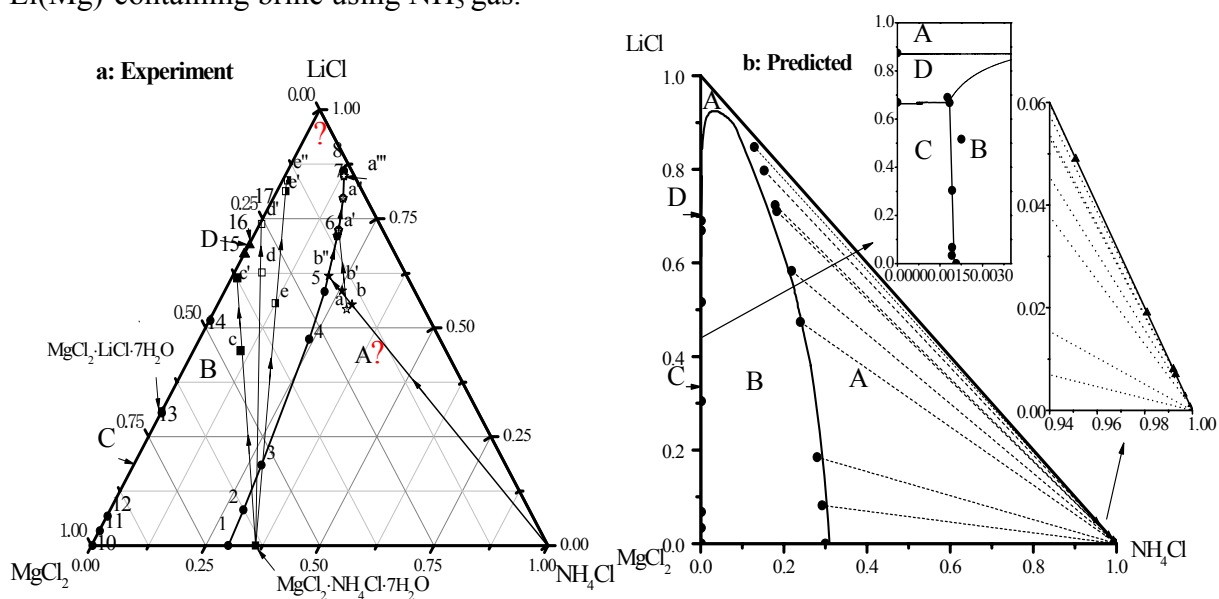


Fig. 1a and 1b. Isothermal solubility phase diagram as a function of dry-solid of the quaternary system $\text{MgCl}_2\text{-LiCl-NH}_4\text{Cl-H}_2\text{O}$ at 298.15 K; ●, experimental data located on two phases isotherm curve; ☆, ★, □, ■: experimental data located on one solid phase isotherm surface; ?: the isotherm curve not completely defined; Crystallization fields: A=solid-solution ($\text{LiCl}\cdot\text{H}_2\text{O}$ and NH_4Cl), B= $\text{NH}_4\text{Cl}\cdot\text{MgCl}_2\cdot 6\text{H}_2\text{O}$, C= $\text{MgCl}_2\cdot 6\text{H}_2\text{O}$, D= $\text{LiCl}\cdot\text{MgCl}_2\cdot 7\text{H}_2\text{O}$; —(1b): predicted results using PSC model; ▲: the mass fraction of NH_4Cl and $\text{LiCl}\cdot\text{H}_2\text{O}$ in solid-solution solid phase.

Reference

[1] Clegg S.L., Pitzer K.S., Brimblecombe P. *J. Phys. Chem.*, **96**, (1992) 3513–3520.

SOLUBILITY OF BASIC ZINC SULFATE IN THE SYSTEM $\text{ZnSO}_4\text{-H}_2\text{O}$

Yin¹ X., Zeng^{2*} D. and Wu¹ Y.

¹College of Chemistry and Chemical Engineering, Hunan University, Changsha, 410082, China, e-mail: yinxia0405@yahoo.com.cn

²College of Chemistry and Chemical Engineering, Central South University, Changsha, 410083, China, *E-mail: dewen_zeng@hotmail.com

Crystals of basic zinc sulfate formed in the process of zinc hydrometallurgy blocks the pipe and filter cloth, however, its generation conditions, such as temperature, pH and Zn^{2+} concentration, are unclear yet. In this work, solubility of basic zinc sulfate as a function of pH, Zn^{2+} concentration and temperature was detected (symbols of Fig. 1), the detected results at 298.15 K agree with literature values [1]. To avoid the formation of basic zinc sulfate, solution compositions should be controlled below the lines in Figure 1 at different temperatures. The solid phases were determined by XRD to be $\text{ZnSO}_4 \cdot 3\text{Zn}(\text{OH})_2 \cdot 5\text{H}_2\text{O}$. A Pitzer model [2] was applied to simulate the solubility isotherms at different temperatures. On simulation, different expressions for solubility product of $\text{ZnSO}_4 \cdot 3\text{Zn}(\text{OH})_2 \cdot 5\text{H}_2\text{O}$ have been tried, two of them were showed as follows:

$$\text{Assumpt. 1: } \text{ZnSO}_4 \cdot 3\text{Zn}(\text{OH})_2 \cdot 5\text{H}_2\text{O}_{(s)} = 4\text{Zn}^{2+}_{(aq)} + \text{SO}_4^{2-}_{(aq)} + 6\text{OH}^{-}_{(aq)} + 5\text{H}_2\text{O}_{(aq)}$$

$$\ln k_{\text{ZnSO}_4 \cdot 3\text{Zn}(\text{OH})_2 \cdot 5\text{H}_2\text{O}} = 4 \ln(a_{\text{Zn}^{2+}}) + \ln(a_{\text{SO}_4^{2-}}) + 6 \ln(a_{\text{OH}^{-}}) + 5 \ln(a_w) \quad (1)$$

$$\text{Assumpt. 2: } \text{ZnSO}_4 \cdot 3\text{Zn}(\text{OH})_2 \cdot 5\text{H}_2\text{O}_{(s)} = \text{Zn}^{2+}_{(aq)} + \text{SO}_4^{2-}_{(aq)} + 3\text{ZnOH}^{+}_{(aq)} + 3\text{OH}^{-}_{(aq)} + 5\text{H}_2\text{O}_{(aq)}$$

$$\text{Subjected to } \text{Zn}^{2+}_{(aq)} + \text{OH}^{-}_{(aq)} = \text{ZnOH}^{+}_{(aq)}, \quad \log(m_{\text{ZnOH}^{+}} / (m_{\text{Zn}^{2+}} m_{\text{OH}^{-}})) = 6.5 \pm 0.4 [3],$$

$$\ln k_{\text{ZnSO}_4 \cdot 3\text{Zn}(\text{OH})_2 \cdot 5\text{H}_2\text{O}} = \ln(a_{\text{Zn}^{2+}}) + \ln(a_{\text{SO}_4^{2-}}) + 3 \ln(m_{\text{ZnOH}^{+}}) + 3 \ln(m_{\text{OH}^{-}}) + 5 \ln(a_w) \quad (2)$$

Simulated curves under the assumption 2 and the equation (2) are agreed well with experimental data (see Fig. 1b), however, those under the assumption 1 and the equation (1) deviate from the experimental ones (see Fig. 1a).

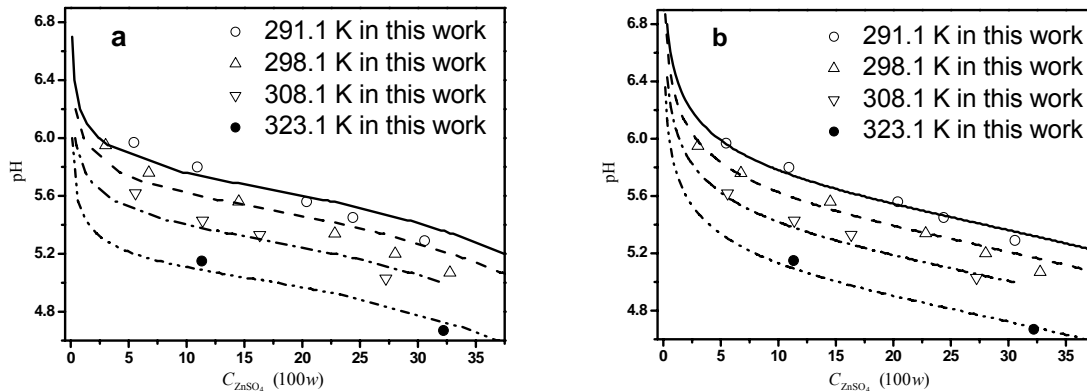


Fig.1. Solubility of $\text{ZnSO}_4 \cdot 3\text{Zn}(\text{OH})_2 \cdot 5\text{H}_2\text{O}$ as function of temperature, pH and Zn^{2+} concentration. Symbols: experimental data in this work; lines: calculated values in this work.

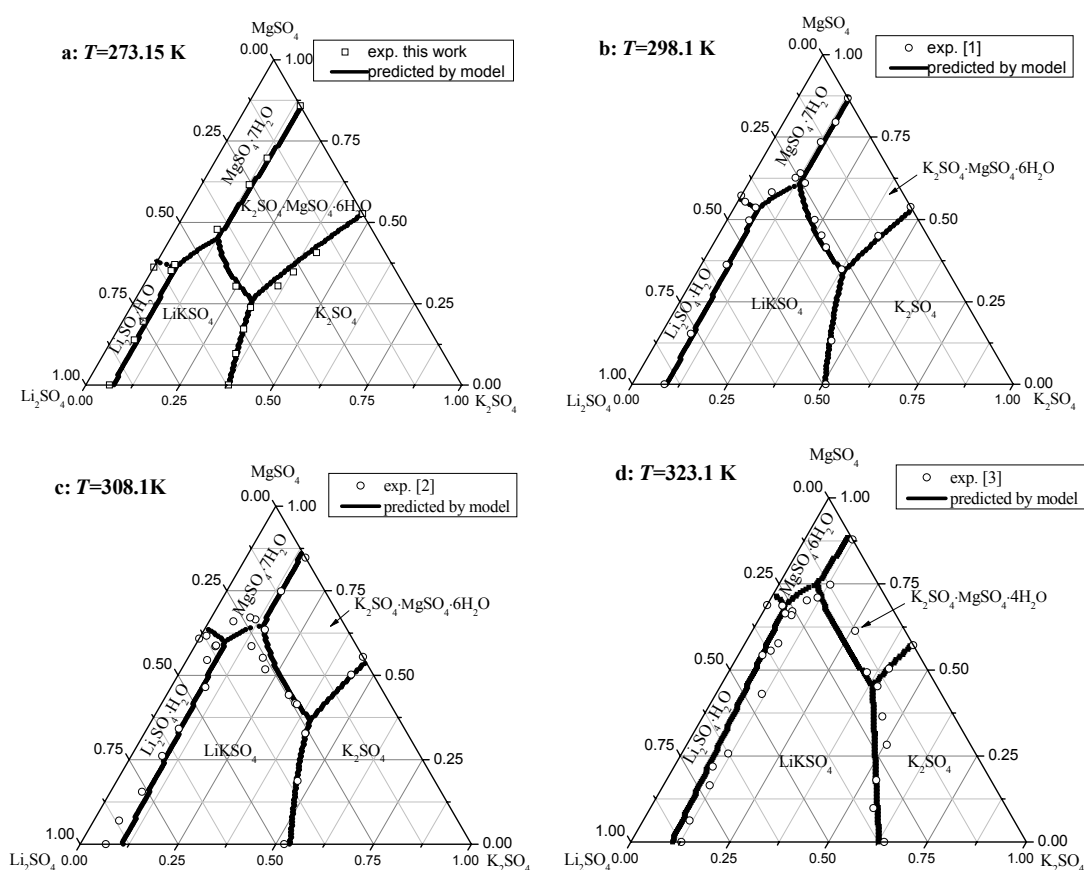
References

- [1] Gromov B.V., Values of pH in systems $\text{MSO}_4 + \text{MO} + \text{H}_2\text{O}$, *Zh. Prikl. Khim.*, **21**, (1948) 260–272.
- [2] Pabalan R.T., Pitzer K.S., Thermodynamics of concentrated electrolyte mixtures and the prediction of mineral solubilities to high temperatures for mixtures in the system $\text{Na-K-Mg-Cl-SO}_4\text{-OH-H}_2\text{O}$, *Geochim. Cosmochim. Acta*, **51**, (1987) 2429–2443.
- [3] Zhang Y., Muhammed M., Critical evaluation of thermodynamics of complex formation of metal ions in aqueous solutions VI. Hydrolysis and hydroxo-complexes of Zn^{2+} at 298.15 K, *Hydrometallurgy*, **60**, (2001) 215–236.

SOLUBILITY PHASE DIAGRAM OF THE SYSTEM $\text{Li}_2\text{SO}_4\text{-K}_2\text{SO}_4\text{-MgSO}_4\text{-H}_2\text{O}$ Zhou¹ H., Zeng^{1,2*} D., Han¹ H., Dong¹ O., Li¹ D. and Yao¹ Y.¹Qinghai Institute of Salt Lakes, Chinese Academy of Sciences, Xining, 810008, P.R. China²College of Chemistry and Chemical Engineering, Central South University, Changsha, 410083, P. R. China

*e-mail: dewen_zeng@hotmail.com

Extraction of lithium from salt lake brines concerns solubility phase diagrams of hundreds of systems in a wide temperature range, among which is the system $\text{Li}_2\text{SO}_4\text{-KSO}_4\text{-MgSO}_4\text{-H}_2\text{O}$. In this work, we measured the solubility isotherms of the quaternary system at 273.15 K which has never been reported, and the measured results are presented by the symbols in Figure 1a. Then, a Pitzer-Simonson-clegg model was selected to simulate the properties of the subbinary and subternary systems, and to predict the solubility of the quaternary system in a temperature range from 273 K to 373 K. The predicted results are presented by the curves in Figure 1. Both the predicted and experimental results from literatures [1-3] and in this work are in good agreement.

Fig. 1. Solubility phase diagram of the system $\text{Li}_2\text{SO}_4\text{-K}_2\text{SO}_4\text{-MgSO}_4\text{-H}_2\text{O}$

References

- [1] Fang C.H., Li B., Li J., Wang Q.Z., Song P.S., Studies on the phase diagram and solution properties for the quaternary system $\text{Li}^+, \text{K}^+, \text{Mg}^{2+}/\text{SO}_4^{2-}\text{-H}_2\text{O}$ at 25 °C, *Huaxue Xuebao*, **52**, (1994) 954–959.
- [2] Shevchuk V.G., Kost L.L., The lithium sulfate-potassium sulfate-magnesium sulfate system at 35 °C, *Zh. Neorg. Khim.*, **9**, (1964) 1242–1245.
- [3] Kost L.L., Shevchuk V.G., Lithium sulfate-potassium sulfate-magnesium sulfate-water system at 50 °C *Zh. Neorg. Khim.*, **13**, (1968) 271–276.

D: POSTER 24

MEASUREMENT AND CORRELATION OF LIQUID-LIQUID EQUILIBRIUM DATA FOR IONIC LIQUID-BASED AQUEOUS TWO-PHASE SYSTEM OF [C₈mim]Br-Cs₂CO₃-H₂O

Yin G.W., Li S.N., Zhai Q.G., Jiang Y.C. and Hu* M.C.

Key Laboratory of Macromolecular Science of Shaanxi Province, School of Chemistry & Chemical Engineering, Shaanxi Normal University, Xi'an, Shaanxi, 710062, P. R. China.

Email: hmch@snnu.edu.cn

In recent years, room-temperature ionic liquids, as a class of potential green solvents, have found wide application in chemistry and biochemistry including chemical synthesis, biocatalytic transformation, electrochemical device designs, and analytical and separation processes. Liquid-liquid equilibrium data have been determined for imidazolium ionic liquid ([C₈mim]Br + Cs₂CO₃ + H₂O) aqueous biphasic systems at $T = (288.15, 298.15, \text{ and } 308.15)$ K. The experimental binodal curves data are correlated by Merchuk's an empirical nonlinear expression. And the tie-line data are satisfactorily corrected by the Othmer-Tobias and Bancroft equations. It is found that an increase in temperature caused no significant expansion of the two-phase area. These data are expected to be useful for the development and design of the extraction process using ILs based on aqueous biphasic systems.

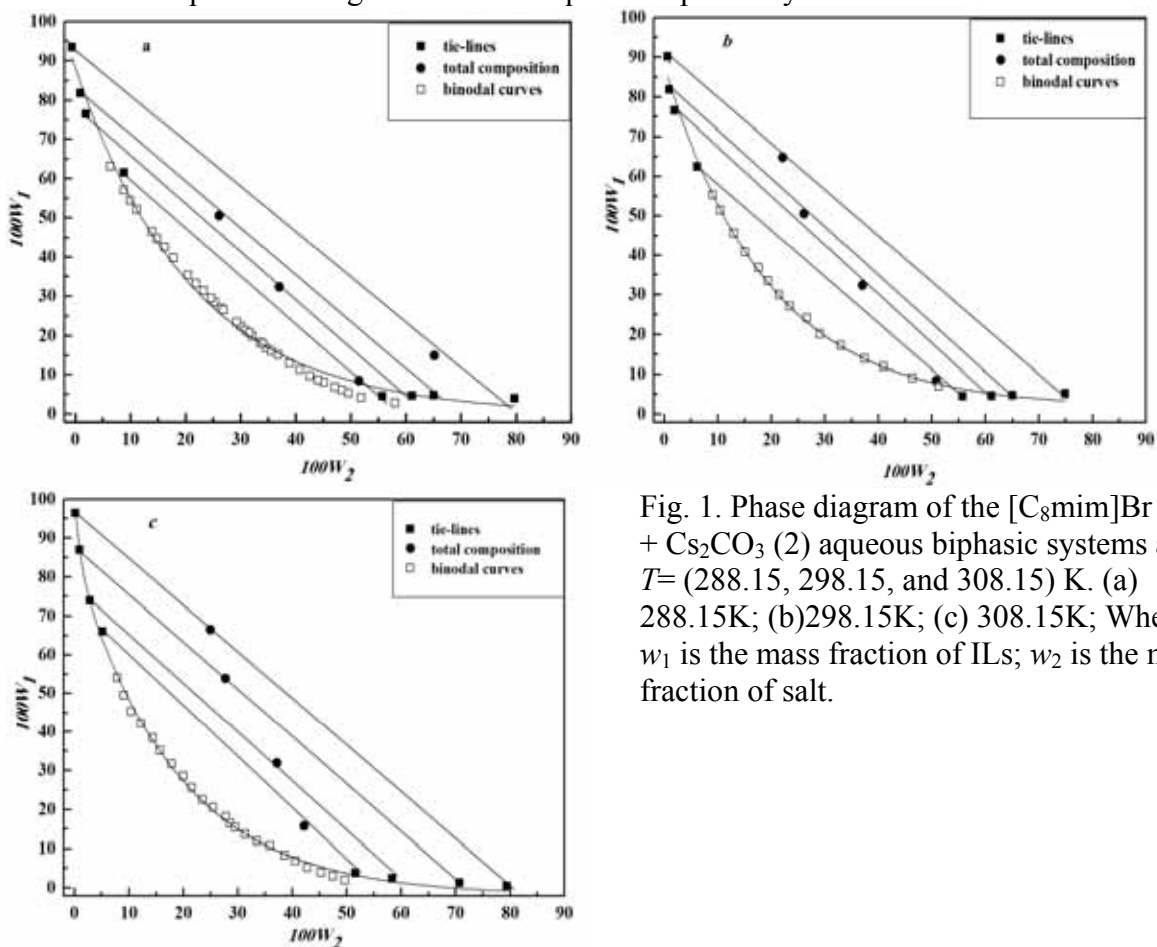


Fig. 1. Phase diagram of the [C₈mim]Br (1) + Cs₂CO₃ (2) aqueous biphasic systems at $T = (288.15, 298.15, \text{ and } 308.15)$ K. (a) 288.15K; (b) 298.15K; (c) 308.15K; Where w_1 is the mass fraction of ILs; w_2 is the mass fraction of salt.

Acknowledgements: Project supported by the National Natural Science Foundation of China (No.21171111) and the Fundamental Research Funds for the Central Universities (Program No. GK201001006).

SOLUBILITY DATA OF LITHIUM SULFATE IN BINARY AND HIGHER SYSTEMS: COMPILATION AND CRITICAL EVALUATION

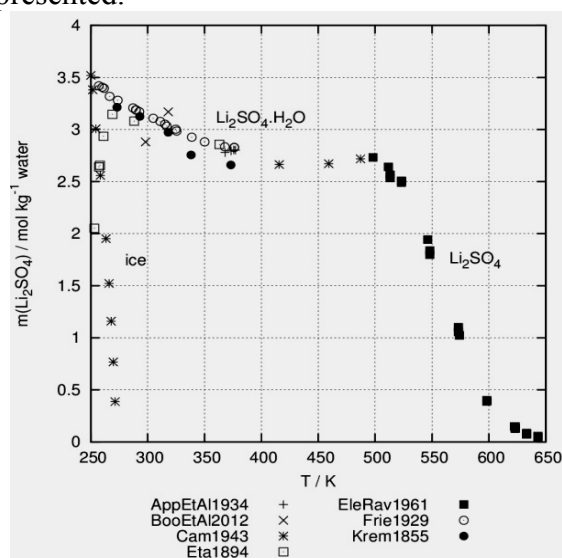
Schmitt J.¹ and Voigt W.²

¹Institute of Inorganic Chemistry, TU Bergakademie Freiberg, 09596 Freiberg, Germany
e-mail: julia.schmitt@chemie.tu-freiberg.de

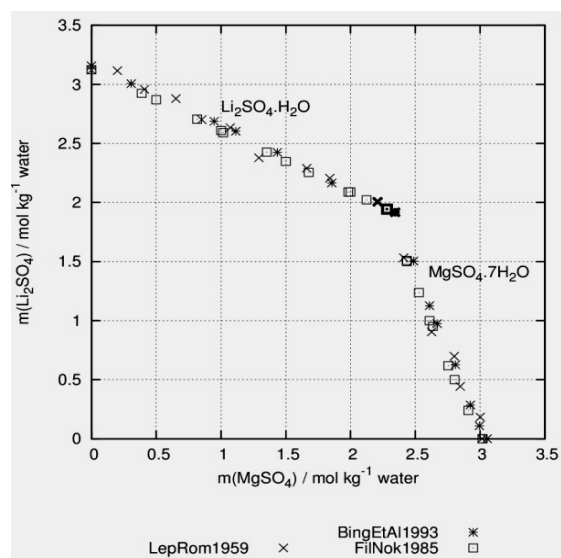
²Institute of Inorganic Chemistry, TU Bergakademie Freiberg, 09596 Freiberg, Germany
e-mail: wolfgang.voigt@chemie.tu-freiberg.de

As a contribution to the IUPAC-NIST Solubility Data Series (SDS) data on the solubility of lithium sulfate in aqueous solutions have been collected and evaluated.

The compilation consists of 7 data sets in the pure binary system lithium sulfate - water. Moreover, 33 ternary, 26 quaternary, 7 reciprocal and 6 higher systems containing lithium sulfate have been compiled. A review of the state of data and first evaluation results are presented.



(a) Binary system $\text{Li}_2\text{SO}_4\text{-H}_2\text{O}$



(b) System $\text{Li}_2\text{SO}_4\text{-MgSO}_4\text{-H}_2\text{O}$ at 298 K
(bold symbols: invariant point)

Figure (a) shows the binary diagram lithium sulfate - water. In the temperature range from 250 to 650 K, three solid phases are present: ice, $\text{Li}_2\text{SO}_4\cdot\text{H}_2\text{O}$ and anhydrous Li_2SO_4 .

In figure (b) the system magnesium sulfate - lithium sulfate - water is given as an example of a ternary diagram. Four independent data sets at 298 K show identical trend in solubility and report $\text{Li}_2\text{SO}_4\cdot\text{H}_2\text{O}$ and $\text{MgSO}_4\cdot 7\text{H}_2\text{O}$ as solids; no double salts are formed.

References

- [AppEtAl1934] M. P. APPLEBEY, F. H. CRAWFORD and K. GORDON, *Journal of the Chemical Society* -, pp. 1665–1671 (1934)
 [BingEtAl1993] L. BING, F. CHUNHUI, W. QINGZHONG, L. JUN and S. PENGSHENG, *Yanhu Yanjiu* 1(3), pp. 1–5 (1993)
 [BingEtAl1994] L. BING, W. QINGZHONG, L. JUN, F. CHUNHUI and S. PENGSHENG, *Wuli Huaxue Xuebao* 10(6), pp. 536–542 (1994) [BooEtAl2012] K. BOOPATHI, P. RAJESH and P. RAMASAMY, *Journal of Crystal Growth* 345, pp. 1–6 (2012)
 [Cam1943] A. N. CAMPBELL, *Journal of the American Chemical Society* 65, pp. 2268–2271 (1943) [EleRav1961] V. M. ELENEVSKAYA and M. I. RAVICH, *Zhurnal Neorganicheskoi Khimii* 6, pp. 2380–2386 (1961) [Eta1894] A. L. ETARD, *Annales de Chimie et de Physique* 2(7), pp. 503–574 (1894) [FilNok1985] V. K. FILIPPOV and V. I. NOKHRIN, *Zhurnal Neorganicheskoi Khimii* 30(2), pp. 501–505 (1985) [Frie1929] J. A. N. FRIEND, *Journal of the Chemical Society* -, pp. 2330–2333 (1929) [Krem1855] P. KREMERS, *Annalen der Physik und Chemie (Poggendorffs Annalen)* 95, pp. 468–472 (1855) [LepRom1959] I. N. LEPESHKOV and N. N. ROMASHOVA, *Zhurnal Neorganicheskoi Khimii* 4(2), pp. 2812–2815 (1959).

TOPOLOGICAL RULES TO CHECK THE POLYHEDRATION OF RECIPROCAL SALT SYSTEMS A, B, C||X, Y (A, B||X, Y, Z)

Lutsyk^{1,2} V.I. and Vorobjeva¹ V.P.

¹Institute of Physical Materials Science (Siberian Branch of RAS), Ulan-Ude, 670047, Russia

²Buryat State University, Ulan-Ude, 670000, Russia, e-mail: vluts@pres.bsnet.ru

Special formulas have been derived to verify the initial data completeness and correctness of quaternary reciprocal system polyhedration [1]. They connect numbers of compounds and simplest binary systems (or, the same – numbers of the graph tops P and connections between them J in the adjacency matrix). It is expressed as:

$$P = P_0 + P_e + P_f + P_i \text{ and } J = J_e + J_f + J_i, \quad (1)$$

with designation: P_0 - prism tops, P_e – points (compounds) on its edges, P_f – on faces, P_i – inside the prism; J_e – prism edges (or their fragments), i.e. binary systems without compounds, J_f – diagonals on faces, J_i – inner diagonals. Value J is equal to total number of simplest binary subsystems or number of adjacency matrix elements, equal to 1. As $P \cdot P$ is the number of all elements of the square adjacency matrix and $(P^2 - P)/2$ – all elements above (or below) of its main diagonal, then it is possible to calculate the J as $J = (P^2 - P)/2 - J_0$, where J_0 is equal to number of zero elements in the adjacency matrix.

As, a trigonal prism of reciprocal system A,B||X,Y,Z (A,B,C||X,Y) has $P_0=6$ tops, $J_e=9$ edges, $S_0=5$ faces (2 triangles and 3 squares), then edges are divided by P_e points to $J_e=9+P_e$ segments. Number of diagonals (J_f) and 2D simplexes (S_f) on faces, inner 2D simplexes (S_i) and 3D simplexes-tetrahedrons (T) are expressed as:

$$J_f = 3 + 2P_e + 3P_f, \quad S_f = 8 + 2P_e + 2P_f, \quad S_i = 2 + P_e + P_f + 2J_i - 2P_i, \quad T = 3 + P_e + P_f + J_i - P_i. \quad (2)$$

So, to define numbers of 3D simplexes T and inner 2D simplexes S_i in advance, it is enough to know numbers of binary P_e , ternary P_f and quaternary P_i compounds and inner diagonals J_i . Formulas (1)-(2) help to correct the results of polyhedration, especially at competition of alternative inner diagonals. E.g., in system A,B,C||X,Y with compounds $D_1=x_7=NaKWO_4$, $D_2=x_8=K_2Ba(WO_4)_2$, $D_3=x_9=Na_3FWO_4$, $D_4=x_{10}=K_3FWO_4$ the lines x_7x_8 and x_4x_6 are parallel, and microcomplex $x_4x_6x_7x_8$ is the plane with alternative diagonals x_4x_8 and x_6x_7 . There are 2 variants of polyhedration to 3D simplexes $T = 3 + P_e + P_f + J_i - P_i = 3 + 4 + 0 + 1 - 0 = 8$: 4 constant tetrahedrons $x_1x_3x_7x_9 + x_3x_4x_7x_9 + x_2x_4x_6x_{10} + x_4x_5x_6x_{10}$ plus 2 quartets of variable tetrahedrons $x_2x_4x_6x_8 + x_2x_4x_7x_8 + x_3x_4x_6x_8 + x_3x_4x_7x_8$ - at x_4x_8 (Fig. a-b); $x_2x_4x_6x_7 + x_2x_6x_7x_8 + x_3x_4x_6x_7 + x_3x_6x_7x_8$ - at x_6x_7 (Fig. c).

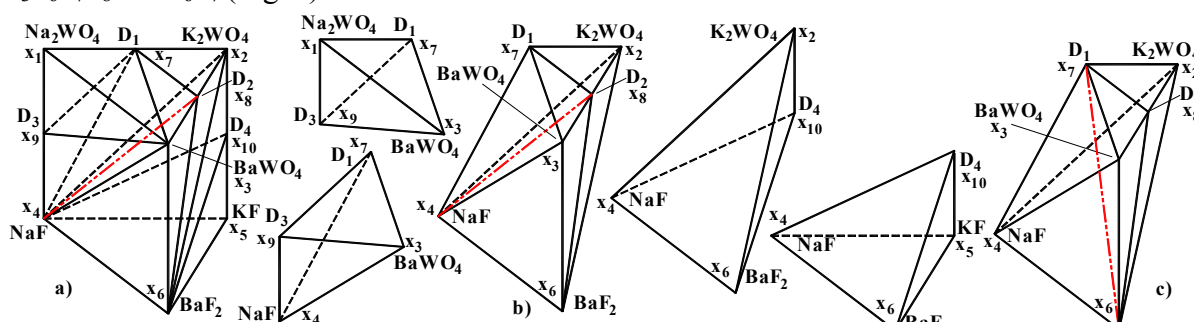


Fig. 1. System Na,K,Ba||WO₄,F tetrahedration with inner diagonal x_4x_8 (a), 4 simplexes and stable microcomplex (b), virtual microcomplex with diagonal x_6x_7 (c).

References

[1] Lutsyk V., Vorob'eva V., Sumkina O., Triangulation of salt systems with barium borate, *Crystallography Reports*, **57**, (2012) (to be published).

TIE-LINE METHODS TO SEARCH QUATERNARY EUTECTIC COMPOSITION

Lutsyk^{1,2} V.I. and Zyryanov² A.M.

¹Institute of Physical Materials Science (Siberian Branch of RAS), Ulan-Ude, 670047, Russia

²Buryat State University, Ulan-Ude, 670000, Russia, e-mail: vluts@pres.bsnet.ru

Problems with the graphics of some multidimensional phase diagrams without solid-phase solubility [1,5] were explained by means of their hypersurfaces detailed structuring [2]. When 4 liquidus hypersurfaces of Q_A -type (with a contour $A_e A_{eAB} A_{eAC} A_{eAD} E_{eABC} E_{eABD} E_{eACD} E_{e}$), 12 ruled ones of Q_{AB}^r -type with $e_{AB} A_{eAB}$ generated segment ($E_{eABD} E_{eAB} E_{eABC} A_{eAB} E_{eABC} A_{eABD} A_{eAB}$), 12 ruled ones of Q_{ABD}^r -type ($E_{eABD} E_{eAB} B_{eABD} A_{eABD}$) with $E_{eABD} B_{eABD} A_{eABD}$ generated plane and a horizontal hyperplane $H_e(A_e B_e C_e D_e E_e)$ composed of simplex $A_e B_e C_e D_e E_e$, and 4 simplexes of $A_e B_e C_e E_e$ -type, are cut by the vertical hyperplane, their lines are easy decoded. Traditional tie-line method for the invariant points determination was modified by means of the matrix transformation of concentration coordinates [3,4]. Composition of quaternary eutectic is taken from the cross-section of liquidus hypersurface with the eutectical horizontal hyperplane (Figs. 1d and 1e), or, exactly speaking – liquidus line 1-2 with the generated segment $A_e r_e$ (Fig. 1d).

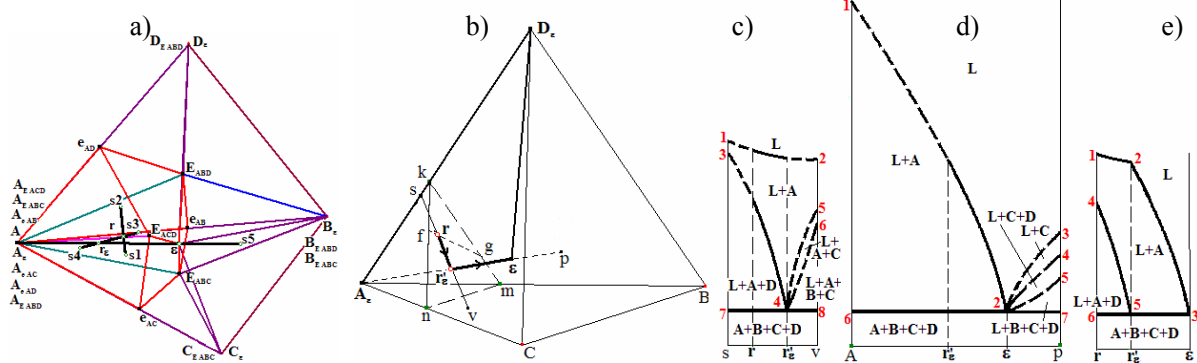


Fig. 1. Tie-line methods modernization: a) - non-planar tie-line matrix method [3-4] consists of 3 sections s_1s_2 , $s_3(r_e, \epsilon)s_4$, $A_e(r_e, \epsilon)s_5$ (first two lines s_1s_2 and s_3s_4 do not belong to the same plane); b) - non-planar tie-line “2-sections” method [5] with arbitrary chosen section fg and next 2 steps $s(r_e, \epsilon)v$ and $A_e(r_e, \epsilon)\epsilon$, usually shown as one section $r(r_e)\epsilon$; c) - cross-sections of hypersurfaces $Q_A(1-2)$, $Q_{AD}^r(3-4)$, $Q_{AC}^r(4-5)$, $Q_{ABC}^r(4-6)$ on section $s(r_e, \epsilon)v$; d) - cross-sections of hypersurfaces $Q_A(1-2)$, $Q_C(2-3)$, $Q_{CD}^r(2-4)$, $Q_{BCD}^r(4-6)$ on section $A_e(r_e, \epsilon)p$; e) - cross-sections of hypersurfaces $Q_A(1-2-3)$, $Q_{AD}^r(4-5)$ on complex section $A_e(r_e, \epsilon)\epsilon$ with the broken liquidus curve 1-2-3. In both cases the second section (s_3s_4 and sv) belongs to the plane $\epsilon I_e J_e$.

References

[1] Li G., Takagi R., Kawamura K., Eutectic composition and temperature of the $LiF-BaF_2-MgF_2$ system and liquidus temperature of the $(LiF-BaF_2-MgF_2)_{eutectic}-ZrF_4$ system, *Denki Kagaku*, **59**, (1991) 800–801.
 [2] Lutsyk V., Low-melting salt mixtures data: errors in concentration coordinates, *ECS Proceed.*, **PV2002-19**, (2002) 386–398.
 [3] Lutsyk V., Vorob’eva V., Relation between the mass-centric coordinates in the multicomponent salt systems, *Z. Naturforsch. A*, **63a**, (2008) 513–518.
 [4] Lutsyk V., Zelenaya A., Zyryanov A., Search of low-temperature solvents by the nonplanar tie-lines, *Crystallography Reports*, **57**, (2012) to be published.
 [5] Verdiev N., Trunin A., Gasanaliev A., Experimentally investigated pentatop $(NaF)_2-CaF_2-BaF_2-K_2Ba(MoO_4)_2-BaMoO_4$ of reciprocal system $Na, K, Ca, Ba || F, MoO_4$, *Russian J. Inorg. Chem.*, **33**, (1988) 1019-1023. In Russian.

D: POSTER 28

METASTABLE PHASE EQUILIBRIA OF THE QUINARY SYSTEM (Li^+ , Na^+ , Mg^{2+} // Cl^- , SO_4^{2-} - H_2O) AT 273.15 K

Wang¹ S.Q., Guo¹ Y.F., Gao¹ D.L. and Deng^{1,2} T.L.

¹Tianjin Key Laboratory of Marine Resources and Chemistry, College of Marine Science and Engineering, Tianjin University of Science and Technology Tianjin, 300457, P. R. China
e-mail: wangshiqiang@tust.edu.cn

²ACS Key Laboratory of Salt Lake Resources and Chemistry, Qinghai Institute of Salt Lakes, Chinese Academy of Sciences, Xining, 810008, P. R. China, e-mail: tldeng@isl.ac.cn

The metastable phase equilibria of the quinary system (Li^+ , Na^+ , Mg^{2+} // Cl^- , SO_4^{2-} - H_2O) were studied at 273.15 K by the isothermal evaporation method. The solubilities and the physicochemical properties (density, refractive index, conductivity, and pH value) of the equilibrium solution were determined. On the basis of the Jäneche index values, the dry-salt phase diagram saturated with salt NaCl, the water phase diagram, the sodium phase diagram, and the physicochemical properties versus composition were plotted. In the metastable phase diagram saturated with salt NaCl, there are five invariant points, eleven univariant metastable solubility isotherm curves, and seven crystallization fields corresponding to the single salts mirabilite, epsomite, bischofite, lithium sulfate monohydrate, lithium chloride dihydrate ($\text{LiCl}\cdot 2\text{H}_2\text{O}$) and lithium carnallite ($\text{LiCl}\cdot \text{MgCl}_2\cdot 7\text{H}_2\text{O}$), double salts lithium sodium sulphate dodecahydrate ($\text{Li}_2\text{SO}_4\cdot 3\text{Na}_2\text{SO}_4\cdot 12\text{H}_2\text{O}$). There were no solid solutions formed in this quinary system. The crystallizing region of mirabilite cosaturated with NaCl is the largest, while the region of $\text{LiCl}\cdot \text{MgCl}_2\cdot 7\text{H}_2\text{O}$ is the smallest with the highest concentration. The metastable phase diagram of the quinary system is shown in Figure 1.

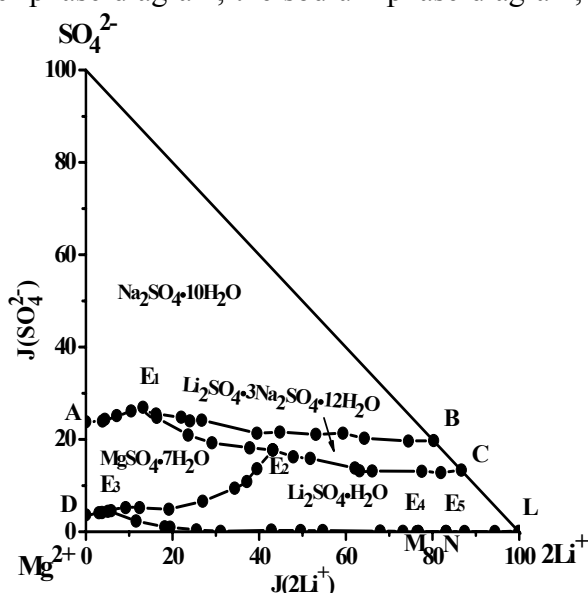


Fig. 1. Metastable phase diagram of the quinary system (Li^+ , Na^+ , Mg^{2+} // Cl^- , SO_4^{2-} - H_2O) at 273.15K; Lc, $\text{LiCl}\cdot \text{H}_2\text{O}$; Lic, $\text{LiCl}\cdot \text{MgCl}_2\cdot 6\text{H}_2\text{O}$; Bis, $\text{MgCl}_2\cdot 6\text{H}_2\text{O}$.

Acknowledgments: Financial support from the State Key Program of NNSFC (20836009), the NNSFC (21106103), and the Specialized Research Fund for the Doctoral Program of Chinese Higher Education (20101208110003 and 20111208120003), The Key Pillar Program in the Tianjin Municipal S&T (11ZCKFGX2800) and Senior Professor Program for TUST (20100405) is acknowledged.

References

- [1] Zheng X.Y., Tang Y. et al., Tibet saline lake, Beijing: Chin. Science Press, (1988).
- [2] Song P.S., Yao Y. *CALPHAD*, **25**, (2001), 329–341
- [3] Wang S.Q., Gao J., Yu X. et al., *J. Salt Lake Res.*, **15**, (2007), 44–48.
- [4] Deng T.L., Wang S.Q., *J. Chem. Eng. Data*, **53**, (2008), 2723–2727.

STABLE AND METASTABLE PHASE EQUILIBRIA OF THE TERNARY AQUEOUS SYSTEM OF SODIUM SULFATE AND LITHIUM SULFATE

Guo¹ Y.F., Han² H.J., Wang² Q., Wang¹ S.Q. and Deng^{1,2} T.L.

¹Tianjin Key Laboratory of Marine Resources and Chemistry, College of Marine Science and Engineering, Tianjin University of Science and Technology Tianjin, 300457, P. R. China
e-mail: tldeng@tust.edu.cn

²ACS Key Laboratory of Salt Lake Resources and Chemistry, Qinghai Institute of Salt Lakes, Chinese Academy of Sciences, Xining, 810008, P. R. China

Salt lakes in China are mainly located in the area of the Qinghai-Xizang (Tibet) Plateau, and the Autonomous Regions of Xinjiang and Inner Mongolia. The composition of salt lake brines can be summarized to the complex multi-component system (Li–Na–K–Ca–Mg–H–Cl–SO₄–B₄O₇–OH–HCO₃–CO₃–H₂O) [1]. However, the phenomena of super-saturation of brines are often found both in salt lakes and solar ponds around the world [2-5].

In this paper, the stable and metastable phase equilibria of the ternary system (Na₂SO₄–Li₂SO₄–H₂O) at 308.15 K were investigated using the methods of isothermal dissolution and isothermal evaporation, respectively. It was found that there are four crystallization regions corresponding to thenardite (Na₂SO₄, Th), double salt 1 (Li₂SO₄·3Na₂SO₄·12H₂O, Db1), double salt 2 (Li₂SO₄·Na₂SO₄, Db2), and lithium sulfate monohydrate (Li₂SO₄·H₂O, Ls), four univariant curves, and three invariant points of the ternary system both in the stable and metastable system at 308.15 K. A comparison of the stable and metastable phase diagram of the ternary system shows in Figure 1.

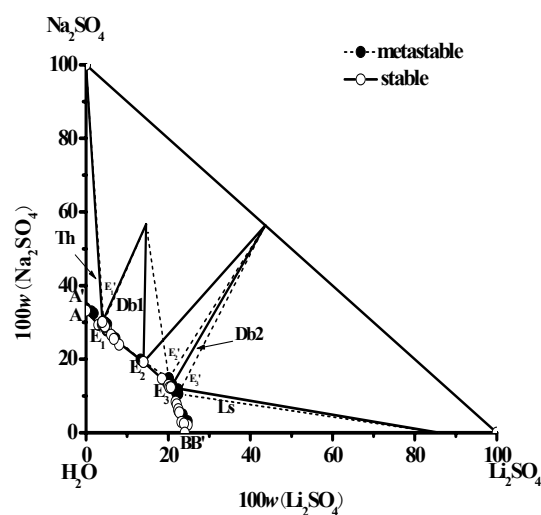


Fig. 1. Comparison of the stable and metastable phase diagram of the ternary system (Na₂SO₄ - Li₂SO₄ - H₂O) at 308.15 K; ●, metastable; ○, stable; ..., metastable isotherm curve; —, stable isotherm curve; Th, Na₂SO₄; Db1, Li₂SO₄·3Na₂SO₄·12H₂O; Db2,

Acknowledgments: Financial support from the State Key Program of NNSFC (20836009), the NNSFC (21106103), and the Specialized Research Fund for the Doctoral Program of Chinese Higher Education (20101208110003 and 20111208120003), The Key Pillar Program in the Tianjin Municipal S&T (11ZCKFGX2800) and Senior Professor Program for TUST (20100405) is acknowledged.

References

- [1] Zheng M.P., Xiang J., Wei X.J., Zheng Y., Saline lakes on the Qinghai-Xizang (Tibet) Plateau, *Beijing: Beijing Science and Technology Press*, (1989).
- [2] Deng T.L., Advance in crystallization processes: stable and metastable phase equilibria in the salt-water systems, In: *Yitzhak Mastai ed., Croatia: InTech Publisher*, (2012)
- [3] Guo Y.F., Yin H.J., Wu X.H., Deng T.L., *J. Chem. Eng. Data*, **55**, (2010) 4215–4220.
- [4] Wang S.Q., Deng T.L., *J. Chem. Thermodyn.*, **40**, (2008) 1007–1011.
- [5] Li Z.Y., Deng T.L., Liao M.X., *Fluid Phase Equilib.*, **293**, (2010) 42–46.

METASTABLE PHASE EQUILIBRIA FOR THE TERNARY AQUEOUS SYSTEM SODIUM CHLORIDE AND SODIUM SULFATE

Shen¹ D.L., Guo¹ Y.F., Wang S.Q. and Deng^{1,2} T.L.

¹ Tianjin Key Laboratory of Marine Resources and Chemistry, College of Marine Science and Engineering, Tianjin University of Science and Technology Tianjin, 300457, P. R. China
e-mail: tldeng@tust.edu.cn

² ACS Key Laboratory of Salt Lake Resources and Chemistry, Qinghai Institute of Salt Lakes, Chinese Academy of Sciences, Xining, 810008, P. R. China

Salt lakes in China are mainly distributed in the regions of the Qinghai-Xizang (Tibet) Plateau, Xinjiang and Inner Mongolia with abundant resources of lithium, magnesium, potassium, sodium, boron and so on. It belongs to the complex multi-component aqueous system (Li–Na–K–Ca–Mg–H–Cl–SO₄–B₄O₇–OH–HCO₃–CO₃–H₂O). Salt-field engineering and solar ponds have been adopted as the technical process of exploitation and utilization for salt lake brine in order to make full use of various inorganic salt recourses. Although numerous of stable or metastable phase equilibria and phase diagrams for the salt lake brines in Qaidam Basin were reported as the representative references in the literature [1-6], the metastable phase equilibrium of the aqueous ternary system (Na₂SO₄–NaCl–H₂O) at 348.15 K is not reported.

In this paper, the metastable solubility and physicochemical property including density and pH for the mentioned ternary system at 348.15 K were investigated using the methods of isothermal evaporation. A comparison of the stable and metastable phase diagram of the ternary system shows in Figure 1.

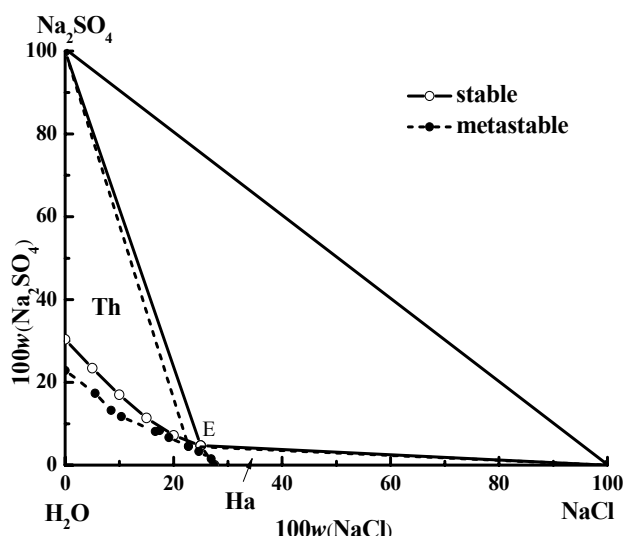


Fig. 1. Comparison of the stable and metastable phase diagram of the ternary system (Na₂SO₄–NaCl–H₂O) at 348.15 K; ●, metastable; ○, stable; ..., metastable isotherm curve; —, stable isotherm curve; Th, Na₂SO₄; Ha, NaCl.

Acknowledgments: Financial support from the State Key Program of NNSFC (20836009) and the Specialized Research Fund for the Doctoral Program of Chinese Higher Education (20101208110003), The Key Pillar Program in the Tianjin Municipal S&T (11ZCKFGX2800) and Senior Professor Program for TUST (20100405) is acknowledged.

References

- [1] Song P.S., Du X.H., *Chin. Sci. Bull.*, **31**, (1986) 209–213.
- [2] Song P.S., Du X.H., Sun B., *Chin. Sci. Bull.*, **32**, (1987) 1492–1495.
- [3] Su B., Du X.H., Song P.S., *J. Salt Lakes Res.*, **2**, (1994) 26–29.
- [4] Wang S.Q., Deng T.L., *J. Chem. Thermodyn.*, **40**, (2008) 1007–1011.
- [5] Guo Y.F., Yin H.J., Wu X.H., Deng T.L., *J. Chem. Eng. Data*, **55**, (2010) 4215–4220.
- [6] Li Z.Y., Deng T.L., Liao M.X., *Fluid Phase Equilib.*, **293**, (2010) 42–46.

**METASTABLE PHASE EQUILIBRIA OF THE QUATERNARY AQUEOUS SYSTEM
(Li⁺, Mg²⁺//Cl⁻, SO₄²⁻-H₂O) AT 348.15 K**

Wang¹ Q., Guo Y.F., Wang¹ S.Q., Yu² X.P. and Deng^{1,2} T.L.

¹Tianjin Key Laboratory of Marine Resources and Chemistry, College of Marine Science and Engineering, Tianjin University of Science and Technology Tianjin, 300457, P. R. China
e-mail: tldeng@tust.edu.cn

²ACS Key Laboratory of Salt Lake Resources and Chemistry, Qinghai Institute of Salt Lakes, Chinese Academy of Sciences, Xining, 810008, P. R. China, e-mail: tldeng@isl.ac.cn

Salt lakes of the Qaidam Basin consist of a series of lakes including Caerhan Lake, Dongtai Lake, Xitai Lake, and Yiliping Lake and are famous for their abundance of lithium, potassium, magnesium, and boron resources and also for having the highest concentration ratio of magnesium to lithium in brine around the world with ratios of 500–800 [1-4].

In this paper, the metastable phase equilibria of the quaternary system (Li⁺, Mg²⁺//Cl⁻, SO₄²⁻-H₂O) at 348.15 K were investigated using the method of isothermal evaporation. Solubilities and physico-chemical properties including density and pH in this system were determined experimentally. In the metastable diagram of the quaternary system at 348.15 K, there are five invariant points, eleven univariant curves, and seven crystallization zones corresponding to Hexahydrite (MgSO₄·6H₂O), Kieserite, Tetrahydrite (MgSO₄·4H₂O), lithium sulfate monohydrate (Li₂SO₄·H₂O), Bischofite (MgCl₂·6H₂O), lithium chloride monohydrate (LiCl·H₂O) and lithium carnallite (LiCl·MgCl₂·7H₂O). It was found that there is no solid solution except one double salt of lithium carnallite existed in the reciprocal quaternary system. The metastable phase diagram of the quaternary system is shown in Figure 1.

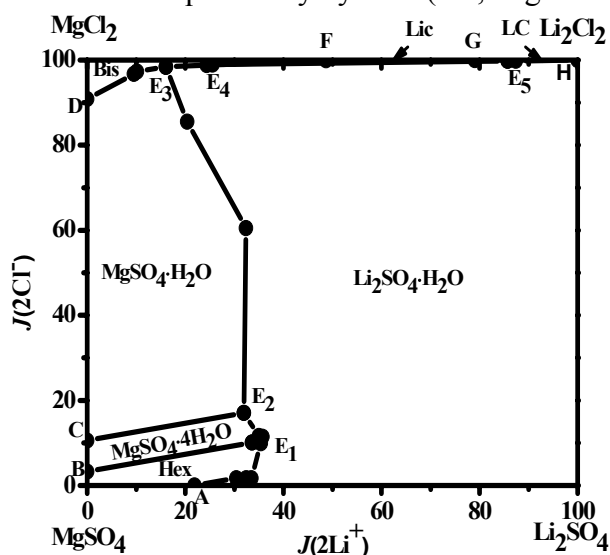


Fig. 1. Metastable phase diagram of the quaternary system (Li⁺, Mg²⁺//Cl⁻, SO₄²⁻-H₂O) at 348.15 K; Hex, MgSO₄·6H₂O; Lic, LiCl·MgCl₂·7H₂O; Lc, LiCl·H₂O; Bis, MgCl₂·6H₂O.

Acknowledgments: Financial support from the State Key Program of NNSFC (20836009), the NNSFC (21106103), and the Specialized Research Fund for the Doctoral Program of Chinese Higher Education (20101208110003 and 20111208120003), The Key Pillar Program in the Tianjin Municipal S&T (11ZCKFGX2800) and Senior Professor Program for TUST (20100405) is acknowledged.

References

- [1] Zheng X.Y., Tang Y. et al., Tibet saline lake, *Beijing: Chin. Science Press*, (1988).
- [2] Gao J., Deng T.L., *J. Chem. Eng. Data*, **56**, (2011) 1452–1458
- [3] Wang S.Q., Deng T.L., *J. Chem. Eng. Data*, **55**, (2010) 4211–4215
- [4] Deng T.L., Wang S.Q., *J. Chem. Eng. Data*, **53**, (2008) 2723–2727.

STUDY OF THE SOLUBILITY AND METASTABLE ZONE WIDTH OF BORAX DECAHYDRATE IN LITHIUM SULFATE SOLUTION

Peng^{1,2} J.Y., Dong^{2*} Y.P., Li^{1,2} L.L., Meng² Q.F. and Li² W.

¹Qinghai Institute of Salt Lakes, Chinese Academy of Sciences, 810008, Xining, China,

²Graduate University of Chinese Academy of Sciences, 100039, Beijing, China,

e-mail: pengjiaoyu84@126.com; e-mail: yapingdongqh@yahoo.com.cn

The metastable zone width determination is to obtain a more precise value of the $\Delta T_{\max}/\Delta c_{\max}$ as a crystallizer design choice. However, the metastable zone width is usually influenced by temperature, cooling rate, stirring, impurities, etc. In this study, the solubility and ultra solubility of $\text{Na}_2\text{B}_4\text{O}_7 \cdot 10\text{H}_2\text{O}$ in lithium sulfate solution at various temperatures was determined by means of the conventional polythermal method using the laser technique. The obtained experimental solubility data were demonstrated graphically in Fig. 1. It is found that the solubility of $\text{Na}_2\text{B}_4\text{O}_7 \cdot 10\text{H}_2\text{O}$ increases with increasing concentration of Li_2SO_4 . The higher concentration of Li_2SO_4 , the greater is the solubility of borax. This phenomenon can be mainly attributed to the salt effect of Li_2SO_4 . Fig. 2 shows the effect of Li_2SO_4 on the metastable zone width (ΔT_{\max}) of borax decahydrate at saturated solution of 31 °C. As seen from Fig. 2, the metastable zone of borax decahydrate tends to broaden both with the increase of Li_2SO_4 and the increasing cooling rate (β). A possible mechanism for the action of Li_2SO_4 on the metastable zone can be explained in terms of adsorption equilibrium of impurities on the crystal surface, which affects the nucleation and crystal growth [1,2].

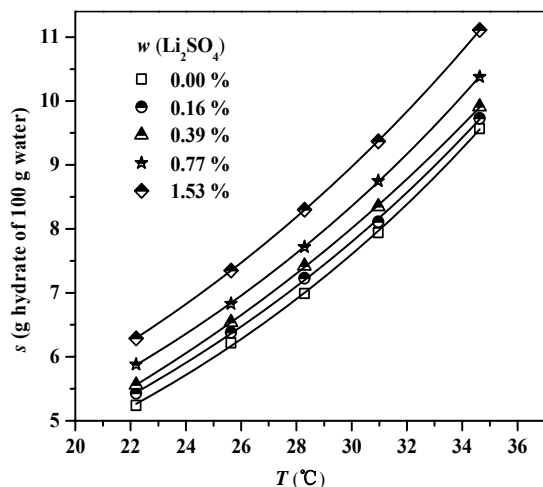


Fig. 1. Solubility of $\text{Na}_2\text{B}_4\text{O}_7 \cdot 10\text{H}_2\text{O}$ in lithium sulfate solution

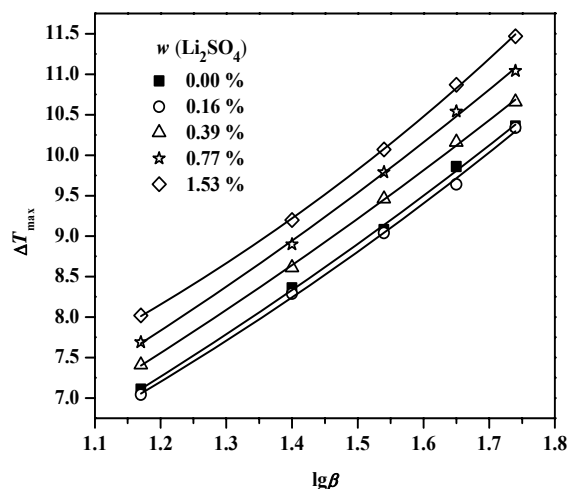


Fig. 2. Changes of metastable zone width of borax with concentrations of Li_2SO_4 at saturated solution of 31 °C

References

- [1] Poornachary S.K., Chow P.S., Reginald B.H.T., Influence of solution speciation of impurities on polymorphic nucleation in glycine, *Cryst. Growth Des.*, **8**, (2008) 179–185.
- [2] Rauls M., Bartosch K., Kind M., Kuch St., Lacmann R., Mersmann A., The influence of impurities on crystallization kinetics—a case study on ammonium sulfate, *J. Cryst. Growth*, **213**, (2000) 116–128.

D: POSTER 33

PREMARY STUDY ON CONCENTRATED OIL FIELD BRINE UNDER FRIGID CONDITIONS

Yang¹ H.J., Chai¹ X.L., Xiao^{1,2} S.Y., Li¹ W. and Li¹ B.

¹Qinghai Institute of Salt Lakes, Chinese Academy of Sciences, Xining, 810008, China,
e-mail: libing@isl.ac.cn

²Graduate University of Chinese Academy of Sciences, Beijing, 100049, China

The experiments of concentrated oil field brine under frigid condition were performed. According to the natural conditions of resource area, a series of temperatures were set as 0 °C, -5 °C, -10 °C, -15 °C, -20 °C, respectively. In each group of experiments, influence of stirred and unstirred condition on concentration of the brine and crystallization was obtained. Through the analysis of samples, enriched degree of trace elements including lithium, rubidium, cesium in the brine were obtained. On the other hand, crystallization ratios of trace elements including lithium, rubidium, cesium, strontium in solid phase were calculated. Meanwhile, crystallization ratios and content of calcium ion, magnesium ion etc existing in the brine were gained.

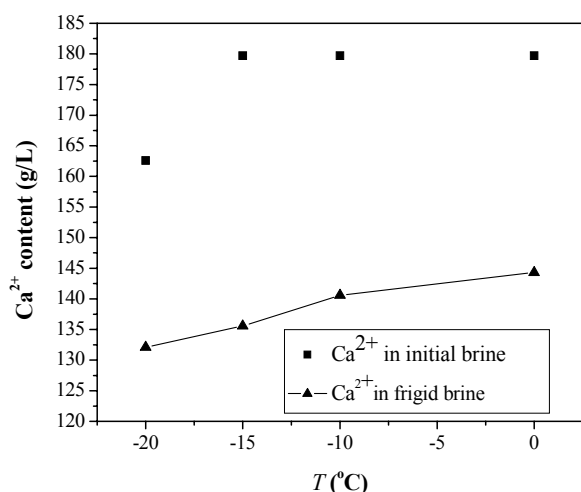


Fig. 1. Trend of Ca²⁺ in the solutions in the course of the experiments.

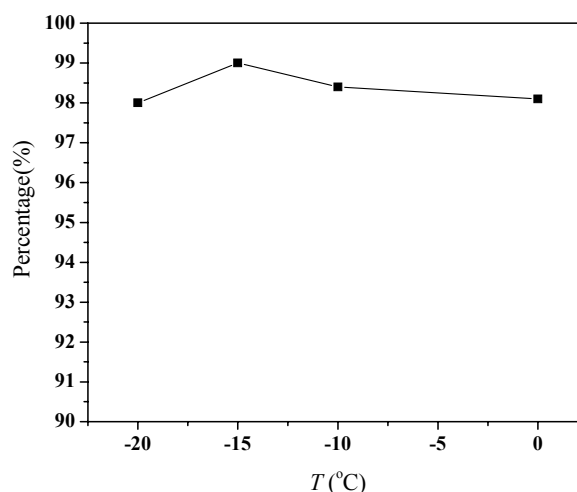


Fig. 2. Crystallization ratio of Sr²⁺ from the brine in the course of the experiments.

Acknowledgments: The project is financially supported by the National Nature Science Foundation of China (No.41073023) and the Ministry of Science and Technology of People's Republic of China (No.2006BAB09B07).

References

- [1] Nelson K.H., Thompson T.G., Deposition of salts from sea water by frigid concentration, Seattle: Office of Naval Research, *University of washington department of oceanography*, 1977: 1–30.
- [2] Thompson T.G, Nelson K.H., Concentration of brines and deposition of salts from sea water under frigid conditions, *Amer. J. Sci.*, **254**, (1956) 227–238.
- [3] Richardson B.G, Phase relationships in sea ice as a function of temperature, *J. Glaciol.*, **17**, (1976) 507–519.

LIQUID-SOLID METASTABLE EQUILIBRIA IN SYSTEM Na^+ , $\text{K}^+//\text{Cl}^-$, SO_4^{2-} , NO_3^- - H_2O AT 298K

Huang X.L., Zhou T., Li H., Liu N. and Feng T.

College of Chemistry and Chemical Engineering, Xinjiang University, Urumqi, Xinjiang
830046, China, e-mail: xuelih@163.com

In the region of Sinkiang Turpan, China, nitrate deposits have been found. By leaching this deposit with water, the brine that contains Na^+ , Cl^- , SO_4^{2-} , NO_3^- can be obtained and used to manufacture potassium nitrate by reacting with KCl [1], this process involves the quinary system Na^+ , $\text{K}^+//\text{Cl}^-$, SO_4^{2-} , NO_3^- - H_2O . In this work, the metastable equilibrium solubilities of this system under the condition saturated with NaCl and 298K have been investigated by isothermal evaporation method. The solvent-less projection of this system can be plotted in form of a trigonal prism as shown in Fig. 1 [2]. In this projection, three independent coordinates — $J(2\text{NO}_3^-)$, $J(2\text{Na}^+)$ and $J(\text{SO}_4^{2-})$ — are ion Jänecke index of NO_3^- , Na^+ and SO_4^{2-} , their units are $\text{mol/mol}(2\text{Cl}^-+2\text{NO}_3^-+\text{SO}_4^{2-})$. Fig. 2 is the Cl-less projection in which two independent coordinates — $J(2\text{NO}_3^-)$ and $J(\text{SO}_4^{2-})$ — are ion Jänecke index of NO_3^- and SO_4^{2-} with units of $\text{mol/mol}(2\text{K}^++2\text{NO}_3^-+\text{SO}_4^{2-})$.

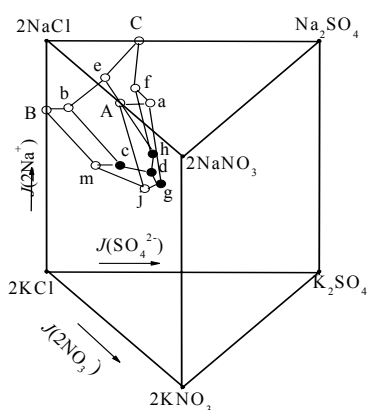


Fig. 1. The crystalization region of NaCl in the metastable equilibrium phase diagram of the quinary system at $T=298\text{ K}$.

- experimental data points

In the metastable phase diagram, there are six crystallization fields saturated with two salts, nine univariant curves saturated with three salts and four invariant points saturated with four salts. Six crystallization fields are $\text{Na}_2\text{SO}_4\cdot\text{NaNO}_3\cdot\text{H}_2\text{O}+\text{NaCl}$ (f-h-d-g-a), $\text{NaCl}+3\text{K}_2\text{SO}_4\cdot\text{Na}_2\text{SO}_4$ (e-h-d-c-b), $\text{Na}_2\text{SO}_4+\text{NaCl}$ (C-e-h-f), $\text{NaNO}_3+\text{NaCl}$ (A-a-g-j), KNO_3+NaCl (m-j-g-d-c), $\text{KCl}+\text{NaCl}$ (B-m-c-b). Four invariant points are c ($\text{NaCl}+\text{KCl}+3\text{K}_2\text{SO}_4\cdot\text{Na}_2\text{SO}_4+\text{KNO}_3$), d ($\text{NaCl}+\text{KNO}_3+\text{NaNO}_3\cdot\text{Na}_2\text{SO}_4\cdot\text{H}_2\text{O}+3\text{K}_2\text{SO}_4\cdot\text{Na}_2\text{SO}_4$), h ($\text{NaNO}_3\cdot\text{Na}_2\text{SO}_4\cdot\text{H}_2\text{O}+\text{NaCl}+3\text{K}_2\text{SO}_4\cdot\text{Na}_2\text{SO}_4+\text{Na}_2\text{SO}_4$), g ($\text{NaCl}+\text{NaNO}_3+\text{NaNO}_3\cdot\text{Na}_2\text{SO}_4\cdot\text{H}_2\text{O}+\text{KNO}_3$).

In the meastable phase diagram, the crystallization fields of KCl and Na_2SO_4 are larger than that in the stable one; the crystallization fields of $\text{Na}_2\text{SO}_4\cdot\text{NaNO}_3\cdot\text{H}_2\text{O}$ and $3\text{K}_2\text{SO}_4\cdot\text{Na}_2\text{SO}_4$ are obviously samller than that in the stable one.

References

- [1] Huang X.L., Advances of research and technology with nitrate in xinjiang Lop Nur, *Modern Chem. Ind.* (in Chinese), **26**(7), (2006) 10–12.
- [2] Huang X.L., Song P.S., Chen L.J., Lü B.L., Liquid-solid equilibria in quinary system Na^+ , $\text{Mg}^{2+}/\text{Cl}^-$, SO_4^{2-} , NO_3^- - H_2O at 298.15 K, *CALPHAD*, **32**(1), (2008) 188–194.

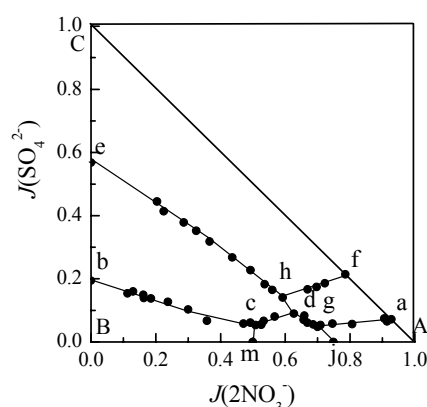


Fig. 2. The metastable equilibrium phase diagram of the quinary system at 298 K. (saturated with NaCl).

- experimental data points

THERMODYNAMICS OF MAGNESIUM CARBONATE PHASES IN DILUTE TO CONCENTRATED MAGNESIUM CHLORIDE SOLUTIONS AT 25 °C

Bube C., Altmaier M., Metz V., Schild D., Kienzler B. and Neck V.

Institute for Nuclear Waste Disposal (INE), Karlsruhe Institute of Technology,
P.O. Box 3640, 76021 Karlsruhe, Germany
e-mail: christiane.bube@kit.edu, marcus.altmaier@kit.edu, volker.metz@kit.edu,
dieter.schild@kit.edu, bernhard.kienzler@kit.edu

Magnesite, $\text{MgCO}_3(\text{s})$, is known to be the thermodynamically stable solid in the system $\text{Mg}-\text{Cl}-\text{HCO}_3-\text{CO}_3-\text{H}-\text{OH}-\text{H}_2\text{O}$ at 25 °C, but solution chemistry in experimental studies at room temperature is controlled by long-term metastable carbonates (hydromagnesite, $\text{Mg}_5(\text{CO}_3)_4(\text{OH})_2 \cdot 4\text{H}_2\text{O}$, and chlorartinite, $\text{Mg}_2\text{CO}_3\text{OHCl} \cdot 3\text{H}_2\text{O}$). For nuclear waste disposal it is of fundamental importance to assess geochemical conditions and a precise description of processes controlling aqueous carbonate chemistry is of highest importance. Therefore this study is aimed at determining stability fields and thermodynamic data for the two metastable magnesium hydroxo (chloro-) carbonates to account for the formation of these two solids from carbonate-containing MgCl_2 -rich solutions in a potential waste repository in rock salt.

Batch experiments were conducted in MgCl_2 solutions (0.25 to 4.5 M) and 0.05 M Na_2CO_3 in Ar glove boxes for >3 years. The pHm ($-\log(\text{mH}^+)$) were monitored with time and precipitates analyzed by different analytical methods (Raman, XRD, SEM-EDS, XPS).

Based on the equilibrium between hydromagnesite and chlorartinite at phase transition, the equilibrium constant for chlorartinite is calculated by solving the equilibrium equations for both coexisting solids at corresponding $a(\text{HCO}_3^-)$.

Using MgCl_2 concentration and pHm at this phase transition, activity coefficients calculated with the Pitzer database of Harvie et al. [1] and published solubility data for hydromagnesite [2,3], the equilibrium constant of chlorartinite under standard conditions is calculated as $\log K^{\circ}_{\text{CA}} = 13.15 \pm 0.36$ for the reaction $\text{Mg}_2\text{CO}_3\text{OHCl} \cdot 3\text{H}_2\text{O} + 2\text{H}^+ \leftrightarrow 2\text{Mg}^{2+} + \text{HCO}_3^- + \text{Cl}^- + 4\text{H}_2\text{O}$.

The extended dataset including the two long-term metastable solids allows for a comprehensive thermodynamic description of the system $\text{Mg}-\text{Cl}-\text{HCO}_3-\text{CO}_3-\text{H}-\text{OH}-\text{H}_2\text{O}$ at 25 °C and contributes to a significantly improved description of geochemical processes in MgCl_2 brines relevant for nuclear waste disposal in rock salt.

References

- [1] Harvie C.E., Møller N., Weare, J.H., *Geochim. Cosmochim. Acta*, **48**, (1984) 723–751.
[2] Königsberger E., Königsberger L.C., Gamsjäger H., *Geochim. Cosmochim. Acta*, **63**, (1999) 3105–3119.
[3] Robie R.A., Hemingway B.S., *Geological Survey Bulletin*, **2131**, (1995) 461.

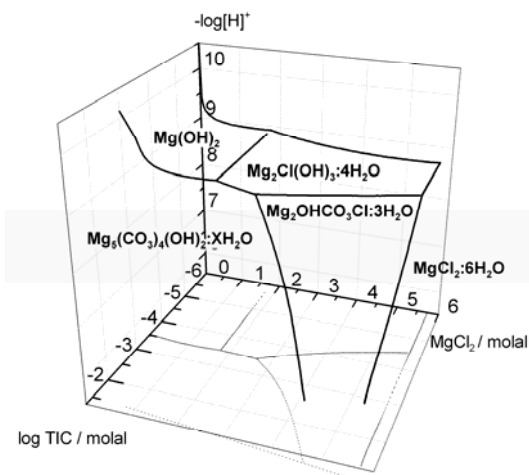


Fig. 1. Stability fields of solid phases in the system $\text{Mg}-\text{Cl}-\text{HCO}_3-\text{CO}_3-\text{H}-\text{OH}-\text{H}_2\text{O}$ at 25 °C ($\text{MgCO}_3(\text{s})$ formation suppressed)

D: POSTERS 36

DISSOLUTION OF ZINNWALDITE AND MOBILIZATION OF LITHIUM

Hertam¹ A. and Voigt² W.

¹Department of Inorganic Chemistry; TU Bergakademie Freiberg, 09596 Freiberg, Germany,
e-mail: anke.hertam@chemie.tu-freiberg.de

²Department of Inorganic Chemistry; TU Bergakademie Freiberg, 09596 Freiberg, Germany,
e-mail: wolfgang.voigt@chemie.tu-freiberg.de

Zinnwaldite $\text{KFe}^{\text{II}}_{0.5-1.5}\text{Li}_{1.5-0.5}(\text{AlFe}^{\text{III}})(\text{Al}_{0.5-1.5}\text{Si}_{3.5-2.5})\text{O}_{10}(\text{FOH})_2$ is a member of the mica group. Due to its amount of 1.5 wt% Li it is a possible lithium source. Known methods of extracting lithium are coupled with high temperature silicate decomposition [1-5] or the digestion with great amounts of a strong acid [6-7]. To reduce the costs of production a new process to recover lithium should be established. In order to decrease the necessary temperatures a hydrothermal procedure is intended. By this approach the natural weathering and the formation of minerals is implemented, respectively. Thus a high pressure apparatus was developed to investigate the dissolution of the mineral and to eventually observe secondary precipitations. A systematic research program is running, where particularly the lithium mobilization is investigated under hydrothermal conditions up to 200 °C and 40 MPa. The composition of the dissolution medium is varied by additions of different salts, acids and bases partly in presence of supercritical CO_2 . The first results are presented.

References

- [1] Jandová J., Dvorák P., Vu H.N., *Hydrometallurgy*, **103**, (2010) 12–18.
- [2] Jandová J., Vu H.N., Belková T.D.P., Kondás J., *Ceramics-Silikaty*, **53**, (2009) 108–112.
- [3] P. Alex A.K., Suri in *Light metals 1996, California, February 4–8, 1996* (Ed.: W. Hale), Minerals, Metals & Materials Society, Warrendale, Pa, **1996**.
- [4] Kondás J., Jandová J., *Acta Metallurgica Slovaca*, **12**, (2006) 197–202.
- [5] Schneider J., *Chem. Prum*, **5**, (1955) 320–323.
- [6] Distin P.A., Phillips C.V., *Hydrometallurgy*, **9**, (1982) 1–14.
- [7] Crocker L., Lien R.H., *Lithium and its recovery from low-grade Nevada clays*, United States Department of the Interior, Bureau of Mines, Pgh. [i.e. Pittsburgh] Pa, **1987**.

D: POSTERS 37

STUDIES OF PHASE BEHAVIORS AND THERMODYNAMICS FOR SYSTEMS $\text{MgB}_4\text{O}_7 + \text{H}_2\text{O}$ AND $\text{MgSO}_4 + \text{MgB}_4\text{O}_7 + \text{H}_2\text{O}$ AT 298.15 K

Ge H.W., Yao Y., Deng T.L., Guo L.J. and Li D.

Qinghai Institute of Salt Lakes, Chinese Academy of Sciences, 18 Road, Xining, Qinghai 810008, P. R. China, e-mail: yaoy@isl.ac.cn

The Solubility and behavior of phase transform for $\text{MgB}_4\text{O}_7 + \text{H}_2\text{O}$ at 298.15 K were studied by the method of isothermal dissolution equilibrium with a twin-walled glass cell in an air constant temperature box. The temperature of the solution in the cell was maintained by a constant temperature bath controlled to a precision of about ± 0.03 K, and was monitored by a digital probe calibrated against a standard platinum thermometer with an accuracy of ± 0.001 K. The solution and the solid phase were avoided to contact CO_2 in air during all experimental runs. The results indicated the equilibrium solid phase of $\text{MgB}_4\text{O}_7 \cdot 9\text{H}_2\text{O}$ kept in the solution for 9 days and then started to be transformed into inderite ($\text{Mg}_2\text{B}_6\text{O}_{11} \cdot 15\text{H}_2\text{O}$). The measured concentration of equilibrium liquid phase of the magnesium borate corresponding to the solid phase of $\text{MgB}_4\text{O}_7 \cdot 9\text{H}_2\text{O}$ is $0.03515 \text{ mol} \cdot \text{kg}^{-1}$ as metastable solubility.

The solubility, the osmotic coefficient and the water activity for the solution saturated with $\text{MgB}_4\text{O}_7 \cdot 9\text{H}_2\text{O}$ at 298.15 ± 0.005 K were measured by using isopiestic method with aqueous NaCl as the isopiestic reference standard and taking 9 days to equilibrate, the values of $0.03536 \text{ mol} \cdot \text{kg}^{-1}$, 1.8747 and 0.99762 were obtained respectively. A comparison of the solubility data by isopiestic method and the value by isothermal dissolved equilibrium method shows a good agreement with a deviation of 0.00021. The deviation from the literature value of $0.0358 \text{ mol} \cdot \text{kg}^{-1}$ [1] is 0.00044.

The Pitzer's ion-interaction parameters and the equilibrium constant $\ln K$ for the $\text{MgB}_4\text{O}_7 + \text{H}_2\text{O}$ system at 298.15 K were evaluated by fitting the experimental data of osmotic coefficients from the literature [2] and the present measurements of solubility and activity properties by isopiestic method using the modified Pitzer equation of osmotic coefficient with an adjusted α_2 value and the equilibrium constant equation simultaneously. The standard deviation is 0.00386 for the fit. The solubility of MgB_4O_7 was calculated using the parameterized equations and the $\ln K$. The calculated solubility is $0.03510 \text{ mol} \cdot \text{kg}^{-1}$, and the relative differences from those by isothermal method in this work, isopiestic method and the literature are 0.142%, 0.735%, and 1.955%, respectively. The thermodynamic representations of the solubilities for $\text{MgSO}_4 + \text{MgB}_4\text{O}_7 + \text{H}_2\text{O}$ were studied on the basis of the ion-interaction model [3] and the results were discussed in this work.

Acknowledgments: Project supported by the State Key Program of NNSFC (20836009).

References

- [1] Song P.S., Du X.H., Sun B., Study on the ternary system $\text{MgB}_4\text{O}_7 - \text{MgSO}_4 - \text{H}_2\text{O}$ at 25 °C, *Kexue Tongbao*, **33**, (1988) 1971–1973.
- [2] Yin S.T., Yao Y., Li B., Tian H.B., Isopiestic studies of aqueous MgB_4O_7 and $\text{MgSO}_4 + \text{MgB}_4\text{O}_7$ at 298.15 K and representation with Pitzer's ion-Interaction Model, *J Solution Chem.*, **36**, (2007) 1745-1761.
- [3] Pitzer K. S. (Ed), *Activity Coefficients in Electrolyte Solutions*, 2nd edition, Boca Raton, Florida: CRC Press, 1991, 75–153.

D: POSTERS 38

CHARACTERISTICS OF THE PHOSPHONIC ACID DTPMP AND THEIR SALTS

Winkler A. and Voigt W.

Institut für Anorganische Chemie, TU Bergakademie Freiberg, D-09596 Freiberg, Germany,
e-mail: Andrea.Winkler@chemie.tu-freiberg.de
e-mail: Wolfgang.Voigt@chemie.tu-freiberg.de

Diethylenetriaminpenta(methylenephosphonic acid) – DTPMP – is an important industrial product which has a wide field of application. It is an excellent scaling inhibitor and prevents the precipitation of alkaline earth metal salts even by use of understoichiometric amounts (Threshold-effect). This makes DTPMP useful for water- and oil treatment.

DTPMP has a solubility of about 64.5 g/L in water determined by stepwise addition of water till complete dissolution of the solid at room temperature. The solubility increases greatly with rise in temperature. With cooling highly super-saturated solutions are produced. However, DTPMP does not crystallize from such solution without adding seed crystals.

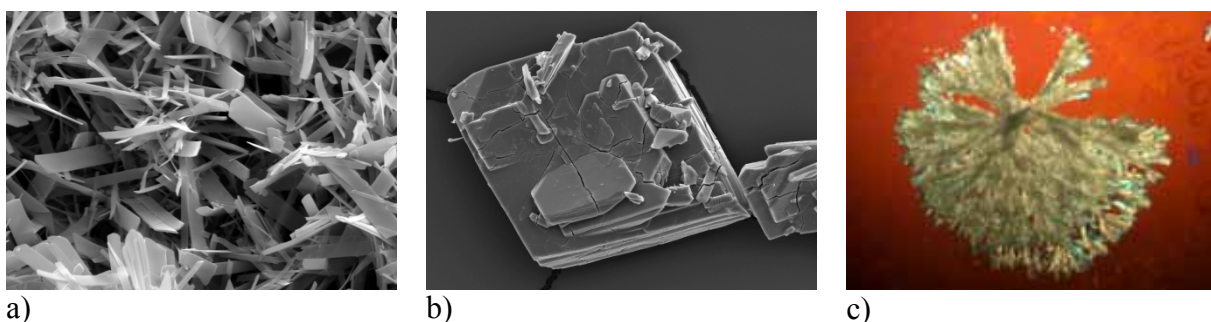


Fig. 1. REM images of DTPMP grown in a) water and b) aq. HCl, c) microscopic image of Na-DTPMP crystals grown by sitting-drop method.

The solubility of Na-DTPMP salts is much higher than that of the pure acid. Crystals of unknown stoichiometry were received over the “sitting-drop method” via ethanol diffusion and show a dendritic growth.

Alkaline earth metal-DTPMP salts have a very low solubility. As yet only amorphous solids precipitate from aqueous solutions.

Furthermore thermal analyses were made and the products of decomposition were detected. Both DTPMP and Ca-DTPMP form hydrates.

Due to the method of synthesis it is up to now not possible to produce pure DTPMP. Also after several purification steps three impurities (Hydroxymethylenephosphonic acid and other unknown compounds) remain in the product.

In this work the purification of DTPMP is in the foreground exploiting solubility properties of DTPMP and its impurities as well as kinetics of crystallization depending on degree of purity.

D: POSTERS 39

EQUILIBRIUM CALCULATIONS OF SO₂ ABSORPTION FOR THERMAL POWER PLANT STACK GASES

Mondal M.K.

Department of Chemical Engineering and Technology, Institute of Technology, Banaras Hindu University, Varanasi 221005, Uttar Pradesh, India
email: mkmondal.che@itbhu.ac.in; mkmondal13@yahoo.com

Sulphur dioxide emitted from thermal power plants is the main cause of global environmental problems such as air pollution and acid rain. Wet-scrubbing is the dominating process for removal of SO₂ from thermal power plant stack gases [1]. To study such processes the absorption of SO₂ in water must be known theoretically and experimentally. The aim of the present study is to develop a steady-state model for the design and simulation of packed column used for absorption of SO₂ into water. The model is based on the film theory of mass transfer alongwith chemical reaction. The effects of gas and liquid flow rates, and other parameters have been studied experimentally to predict absorption rate and mass transfer coefficient. The liquid flow rate was varied from 8.333×10^{-6} to 25.00×10^{-6} m³/s, and gas flow rate in the range of 32.839×10^{-6} to 249.672×10^{-6} m³/s. The partial pressure of SO₂ in the inlet gas stream was fixed at 0.436 kPa. Flooding was not observed for the range of liquid and gas flow rates used, which was also confirmed by theoretical calculations. The overall mass transfer coefficient based on liquid film on volume basis ($K_{L}a$) for SO₂ absorption shows all the characteristics of a system where both gas and liquid film exert an appreciable effect. The value of $K_{L}a$ increases linearly with gas flow rate for any fixed liquid flow rate. The mass transfer rate is linear in gas flow rate, and increases with gas flow rate. A model of a counter-current absorption process associated with chemical reaction has been developed for the absorption of SO₂ into water in a packed column. The model uses the concept of film theory, includes diffusion of reacting species, and assumes the thermodynamic equilibrium among the reacting species exists in the bulk liquid. Model predictions were compared to experimental data of the present work.

Validation of proposed model was established using the experimental absorption data of the present work (Fig. 1). There is an acceptable degree of agreement between the measured absorption rates and theoretical predictions from the model.

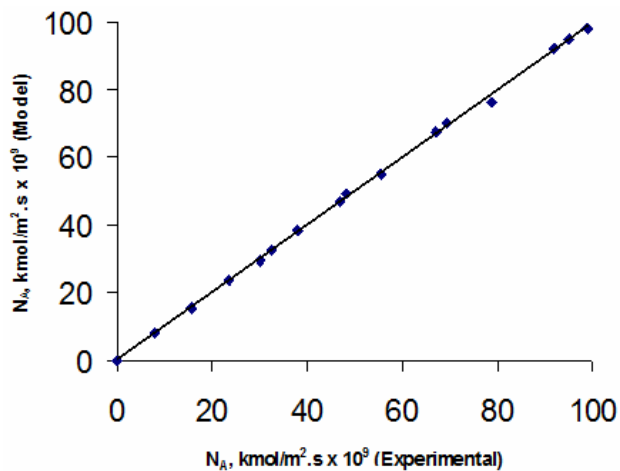


Fig. 1. Absorption rate (N_A) model versus experimental values.

References

[1] Mondal M.K., Experimental determination of dissociation constant, Henry's constant, heat of reactions, SO₂ absorbed and gas bubble-liquid interfacial area for dilute sulphur dioxide absorption into water, *Fluid Phase Equilib.*, **253**, (2007) 98-107.

D: POSTERS 40

HIGHLY WATER SOLUBLE COMPOUND METOPROLOL: STUDY USING DRUG RELEASE RETARDANTS

Kulkarni¹ A., Toshniwal² S. and Naik³ J.

¹Department of Chemical Technology, Dr. Babasaheb Ambedkar Marathwada University, Aurangabad, (M.S.), India.
e-mail: anakulw@gmail.com

²Vidarbha Institute of Pharmacy, Washim, (M.S.), India. e-mail: toshniwal_ss@yahoo.com

³Department of Chemical Technology, North Maharashtra University, Jalgaon, (M.S.), India.
e-mail: jitunaik@gmail.com

Highly water soluble compounds with short half life are always challenging for pharmaceutical development as a sustained or controlled drug delivery system. The BCS Class I (Biopharmaceutical Classification System based on Solubility and Permeability) compounds are usually better candidates to evaluate the drug release retardation by including various polymers which can assist to modulate the drug release profile.

The presented study was focused using Metoprolol tartarate as a model drug which is commonly used as an anti-hypertensive drug to control elevated blood pressure. In the present study, various matrix systems were designed and tested for controlled delivery of Metoprolol. The objectives of the study were (i) to investigate the performance of hydrophilic and hydrophobic matrix systems in controlling the release of this freely soluble drug, and (ii) to investigate the effect of ethylcellulose (water insoluble polymer) as a release-retarding agent, either in the tablet matrix or when used as a coating material, on the release rate of Metoprolol. (iii) Metoprolol was sprayed on the sugar spheres followed by coating using Surelease (Ethylcellulose) in different percentage weight gain to control the drug release.

The drug release retardation rate was studied using tablet dosage form by conducting dissolution in pH 6.8 phosphate buffer. The results of different mechanism are presented in Fig. 1-2. The different mechanisms indicates that appropriate combination use of hydrophobic and hydrophilic polymer matrix or pore former in coated formulation can modulate the drug release for water soluble compounds.

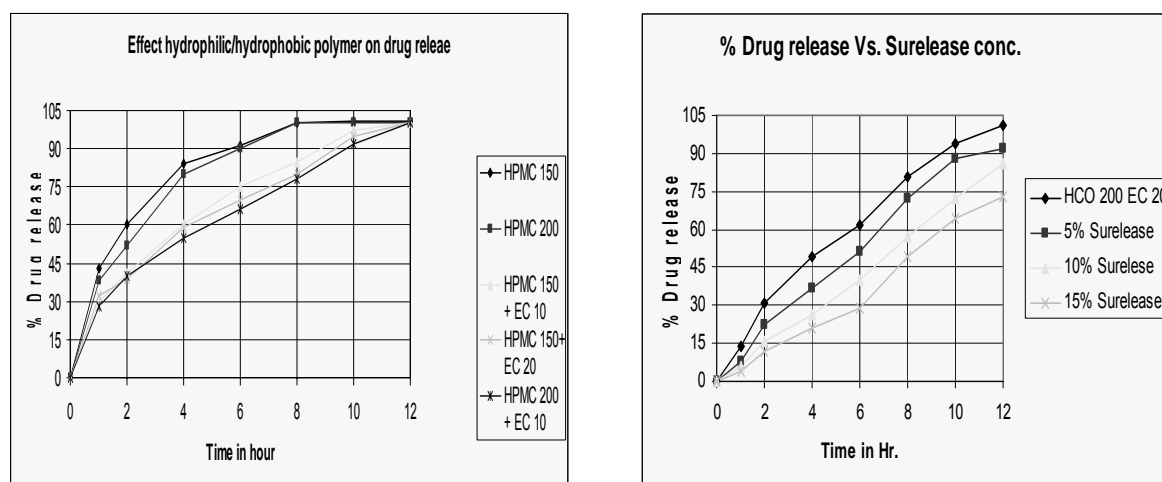


Fig. 1. Effect of hydrophilic/hydrophobic polymer on drug release of water soluble compound.

D: POSTERS 40

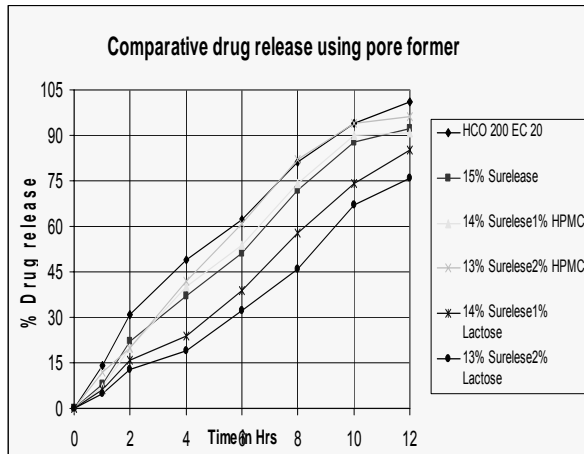


Fig. 2. Effect of water insoluble polymer coating on drug release and microscopic observation.

Acknowledgements: Author would like to acknowledge M/s Wockhardt Ltd. India, M/s Ipca Labs for drug sample. M/s Navketan Pharma, India for providing the opportunity for research. Author acknowledges Dr. Deepak Hegde, Vice President and Mrs. Sushma K. Scientist at WuXi AppTec, Shanghai, China for valuable suggestions and support for the research work.

References

- [1] Liberman H., Lachman L., Schwartz J., Sustained drug release from tablets and particles, *Pharmaceutical Dosage forms Tablet Vol. 3*, 2nd edition, *Marcel Dekker Inc.*, (1990) 199.
- [2] Fujisaki Y., Sugibayashi K., Motomu T., Okumura M., Ukigaya T., Development of sustained release tablets containing sodium valproate in vitro and in vivo correlation, *Drug Dev. Ind. Pharm.*, **32**, (2006) 207–217.
- [3] Hui H., Robinson J., Lee V., Design and fabrication of oral controlled release drug delivery systems. In: Robinson, J.R., (Ed.), *Controlled drug delivery fundamentals and applications*. *Marcel Dekker Inc.*, New York, (1987) 32.

D: POSTERS 41

SPECIES DISTRIBUTION AND PHYSICOCHEMICAL PROPERTIES IN AQUEOUS MAGNESIUM BORATE SOLUTIONS AT 298.15 K

Chen^{1,2} Q.L., Fang¹ C.H., Deng¹ T.L., Fang¹ Y., Zhou^{1,2} Y.Q., Zhu^{1,2} F.Y. and Ge¹ H.W.

¹Qinghai Institute of Salt Lakes, Chinese Academy of Sciences, Xining, 810008 China;

²Graduate School of the Chinese Academy of Science, Beijing 100049, China

e-mail: fangch@isl.ac.cn

Crystalline and amorphous inderite $2\text{MgO}\cdot 3\text{B}_2\text{O}_3\cdot 15\text{H}_2\text{O}$, mcallisterite $\text{MgO}\cdot 3\text{B}_2\text{O}_3\cdot 7.5\text{H}_2\text{O}$ and hungchaoite $\text{MgO}\cdot 2\text{B}_2\text{O}_3\cdot 9\text{H}_2\text{O}$ were synthesized [1] and identified by XRD and Raman spectra. Density, conductivity, viscosity, and *pH* of aqueous magnesium borate solutions during isothermal evaporation have been measured at 298.15 K. The chemical species distributions were calculated by Newton iteration method from *pH* and the chemical equilibrium constants of borates [1], as shown in Fig 1. The dominant species [2] in aqueous solutions of crystalline and amorphous inderite are $\text{B}_3\text{O}_3(\text{OH})_5^{2-}$ and $\text{B}(\text{OH})_4^-$, agreed with a congruent inderite in the system $\text{MgO}\text{-B}_2\text{O}_3\text{-H}_2\text{O}$. However, the predominant species in aqueous solutions of mcallisterite and hungchaoite are $\text{B}_3\text{O}_3(\text{OH})_5^{2-}$ and H_3BO_3 , identified with the incongruent mcallisterite and hungchaoite. The findings suggest that the hydrolysis reactions as follows



occurs in the solutions. Density, conductivity, viscosity were fitted and calculated further.

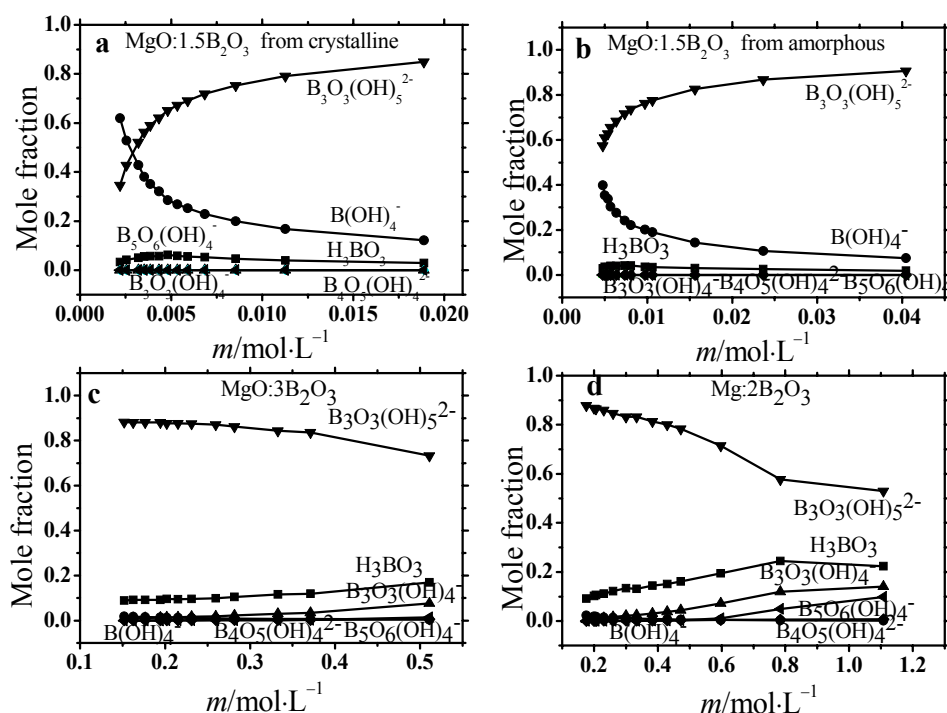


Fig.1. Polyborate distribution in aqueous magnesium borate solutions of crystalline(a) and amorphous(b) inderite, mcallisterite(c) and hungchaoite(d). ■, H_3BO_3 ; ●, $\text{B}(\text{OH})_4^-$; ▲, $\text{B}_3\text{O}_3(\text{OH})_4^-$; ►, $\text{B}_3\text{O}_3(\text{OH})_5^{2-}$; ◀, $\text{B}_4\text{O}_5(\text{OH})_4^{2-}$; ▶, $\text{B}_5\text{O}_6(\text{OH})_4^-$

References

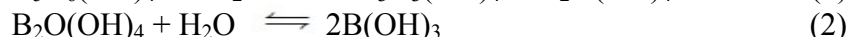
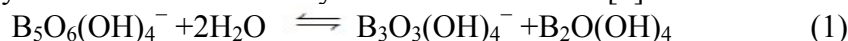
- [1] Spessard J.E., Investigations of borate equilibria in neutral salt solutions, *J. Inorg. Nucl. Chem.*, **32**, (1970) 2607–2613.
- [2] Schubert D.M., Knobler C.B., Recent studies of polyborate anions, *Phys. Chem. Glasses: Eur. J. Glass Sci. Technol. B.*, **50**, (2009) 71–78.

POLYBORATE SPECIATION IN AQUEOUS LITHIUM PENTABORATE SOLUTION AT 323.15K

Ge¹ H.W., Fang¹ C.H., Deng¹ T.L., Fang¹ Y., Zhou^{1,2} Y.Q. and Zhu^{1,2} F.Y.¹Qinghai Institute of Salt Lakes, Chinese Academy of Sciences, 18 Road, Xining, Qinghai 810008, P. R. China, e-mail: fangch@isl.ac.cn²Graduate School of the Chinese Academy of Science, Beijing 100049, China

The chemistry of borates in salt lake brines is surprisingly intricate. Polyborates exist predominantly within narrow temperature, pH, a limited time interval, and particularly instict and concentration of anion and its counterion in aqueous solution.

We present the measurement and calculation results of properties, such as density, conductivity, pH and viscosity, in aqueous solution of lithium pentaborate. Polyborate distribution was calculated from pH measurement and the equilibrium constants interpolated in literature [1] by Newton iteration method, as shown in Fig 1. As Fig.1 shows, the total boron concentration $B < 0.35 \text{ mol}\cdot\text{kg}^{-1}$, the main species is H_3BO_3 and $\text{B}_3\text{O}_3(\text{OH})_4^-$, for $\text{B}_5\text{O}_6(\text{OH})_4^-$ hydrolyzes or depolymerizes into $\text{B}_3\text{O}_3(\text{OH})_4^-$ and $\text{B}_2\text{O}(\text{OH})_4$ with cleavage of two epoxy bonds when attacked by two water molecules[2]



With the total boron concentration $B > 0.35 \text{ mol}\cdot\text{kg}^{-1}$, the dominant species in aqueous solutions is $\text{B}_5\text{O}_6(\text{OH})_4^-$, the secondary species are H_3BO_3 and $\text{B}_3\text{O}_3(\text{OH})_4^-$, and the others including $\text{B}(\text{OH})_4^-$, $\text{B}_3\text{O}_3(\text{OH})_5^{2-}$ and $\text{B}_4\text{O}_5(\text{OH})_4^{2-}$ are negligible. One of them, $\text{B}_5\text{O}_6(\text{OH})_4^-$ can be identified by Raman spectrum qualltatively.

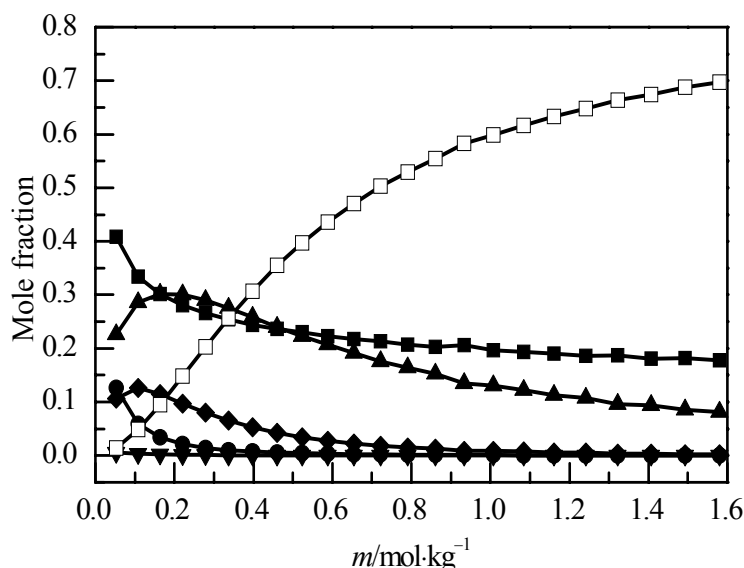


Fig. 1. Polyborate distribution in aqueous lithium pentaborate solutions.

■: H_3BO_3 ; ●: $\text{B}(\text{OH})_4^-$; ▲: $\text{B}_3\text{O}_3(\text{OH})_4^-$; ▼: $\text{B}_3\text{O}_3(\text{OH})_5^{2-}$; ◆: $\text{B}_4\text{O}_5(\text{OH})_4^{2-}$; □: $\text{B}_5\text{O}_6(\text{OH})_4^-$.

References

- [1] Schubert D.M., Knobler C.B., Recent studies of polyborate anions, *Phys. Chem. Glasses: Eur. J. Glass Sci. Technol. B.*, **50**, (2009) 71–78.
 [2] Zhou Y.Q., Fang C.H., Fang Y. et al., Polyborates in aqueous borate solution: A raman and DFT theory investigation, *J. Spectrochim. Acta. A*, **83**, (2011) 82–87.

**CHEMICAL SPECIES DISTRIBUTION AND PHYSICO-CHEMICAL PROPERTIES
IN AQUEOUS LITHIUM TETRABORATE SOLUTION AT THE METASTABLE
STATE**

Xu^{1,2} S., Deng¹ T.L., Fang¹ Y., Fang¹ C.H., Zhou^{1,2} Y.Q., Zhu^{1,2} F.Y. and Tao^{1,2} S.

¹Qinghai Institute of Salt Lakes, Chinese Academy of Sciences, Xining, 810008 China;

²Graduate School of the Chinese Academy of Science, Beijing 100049, China

The metastable phenomenon of aqueous $\text{Li}_2\text{B}_4\text{O}_7$ solution has been observed at 298 and 323 K by isothermal evaporation. The density, conductivity and pH of the supersaturated solutions at the different evaporation stage have been tracked and measured at 298.15 and 323.15 K, respectively. The chemical species distributions were calculated by Newton iteration method from pH and the chemical equilibrium constants of borates¹. Among them, the dominant species in the supersaturated solution at 298.15 K is cyclic chained anion $\text{B}_4\text{O}_6(\text{OH})_2^{2-}$, the minor species isolated anions $\text{B}_3\text{O}_3(\text{OH})_5^{2-}$, $\text{B}_3\text{O}_3(\text{OH})_4^-$ and $\text{B}(\text{OH})_3$, and the negligible species $\text{B}_5\text{O}_6(\text{OH})_4^-$ and $\text{B}(\text{OH})_4^-$; while the dominant species at 323.15 K is still $\text{B}_4\text{O}_6(\text{OH})_2^{2-}$, the minor species $\text{B}_3\text{O}_3(\text{OH})_4^-$ and $\text{B}(\text{OH})_3$, and the negligible species $\text{B}_3\text{O}_3(\text{OH})_5^{2-}$, $\text{B}_5\text{O}_6(\text{OH})_4^-$ and $\text{B}(\text{OH})_4^-$. The lithium tetraborate trihydrate $\text{Li}_2\text{B}_4\text{O}_7 \cdot 3\text{H}_2\text{O}$ is the most stable congruent compound in the ternary system $\text{Li}_2\text{O}-\text{B}_2\text{O}_3-\text{H}_2\text{O}$ phase diagrams² at 283-353K, having the structural formula $\text{Li}[\text{B}_2\text{O}_3(\text{OH})] \cdot \text{H}_2\text{O}$ or $\text{Li}_2[\text{B}_4\text{O}_6(\text{OH})_2] \cdot 2\text{H}_2\text{O}$. According to the chemical species distribution, the inter-conversion rules among all the borate anions and their variation rules with temperature in the metastable aqueous solutions have been summarized in the present paper, and the origin of the metastable phenomenon of $\text{Li}_2\text{B}_4\text{O}_7-\text{H}_2\text{O}$ system revealed also. Based on the concentrations of 6 lithium borates above-mentioned, the empirical coefficients in Ezrokhi's equation of density and Onsager's equation of molar conductivity were fitted and extended to the calculation of the highly concentrated solution.

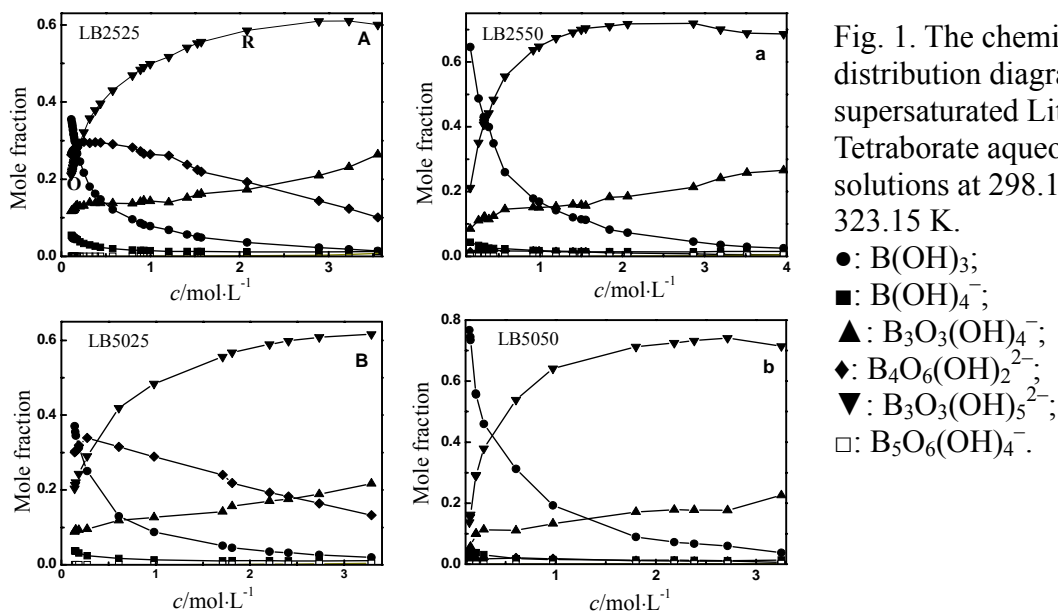


Fig. 1. The chemical species distribution diagram of supersaturated Lithium Tetraborate aqueous solutions at 298.15 and 323.15 K.

●: $\text{B}(\text{OH})_3$;
 ■: $\text{B}(\text{OH})_4^-$;
 ▲: $\text{B}_3\text{O}_3(\text{OH})_4^-$;
 ◆: $\text{B}_4\text{O}_6(\text{OH})_2^{2-}$;
 ▼: $\text{B}_3\text{O}_3(\text{OH})_5^{2-}$;
 □: $\text{B}_5\text{O}_6(\text{OH})_4^-$.

References

- [1] Spessard J.E., Investigations of borate equilibria in neutral salt solutions, *J. Inorg. Nucl. Chem.*, **32**, (1970) 2607–2613.
- [2] Reburn W.T., Gale W.A., The system lithium oxide- boric oxide- water, *J. Phys. Chem.*, **59**, (1955) 19–24.

D: POSTERS 44

STRUCTURE OF AQUEOUS ALKALINE SODIUM BOROHYDRIDE SOLUTIONS

Tao^{1,2} S., Fang¹ Y., Fang¹ C.H., Zhou^{1,2} Y.Q., Zhu^{1,2} F.Y., Xu^{1,2} S. and Chen^{1,2} Q.L.

¹Qinghai Institute of Salt Lakes, Chinese Academy of Sciences, Xining, 810008 China;

²Graduate School of the Chinese Academy of Science, Beijing 100049, China

e-mail: fangch@isl.ac.cn

The time-space-averaged structure of aqueous alkaline sodium borohydride solutions at the water/salt mole ratio of 4 and 8 has been measured by X-ray scattering [1], with a Huber five-circle diffractometer at Synchrotron Radiation Facility II of Beijing Electron Positron Collider II at 298 K. The radial distribution function (RDF) and structural function were obtained by data processing procedure developed by us. The calculation of geometrical models shows that the B-O distance and the coordination number(CN) of hydrated $\text{BH}_4(\text{H}_2\text{O})_n^-$ in highly concentrated solutions were determined to be 0.34 nm and 2~3. Compared with DFT calculation, the B-O distance and CN are agreement. Especially, DFT calculation [1] demonstrates that a dihydrogen bond $\text{BH}-\text{H}_2\text{O}$, which a H atom with positive charge in H_2O bonded to another H atom with negative charge in BH_4^- , occurs in the hydrated $\text{BH}_4(\text{H}_2\text{O})_n^-$. There are two kinds of associating structures of BH_4^- and Na^+ in highly concentrated solutions. One of them is a sharing octagonal edge of two water molecules in $(\text{H}_2\text{O})_4\text{Na}(\text{H}_2\text{O})_2\text{Na}(\text{H}_2\text{O})_4$ to form an O-bridged Na-Na dimer, the other H-bridged Na-Na dimer $(\text{H}_2\text{O})_4\text{Na}(\text{BH}_4)_2\text{Na}(\text{H}_2\text{O})_4$. The Na-Na distance of the former is 0.363 nm with $\text{CN}=0.8$, and the latter 0.421 nm with $\text{CN}=0.4$. These data are the latest results which have not reported in the literature we can find. The structure information as mentioned above has very important significance to explain the hydrolysis reaction progress and mechanism of sodium borohydride in solution at the molecular level.

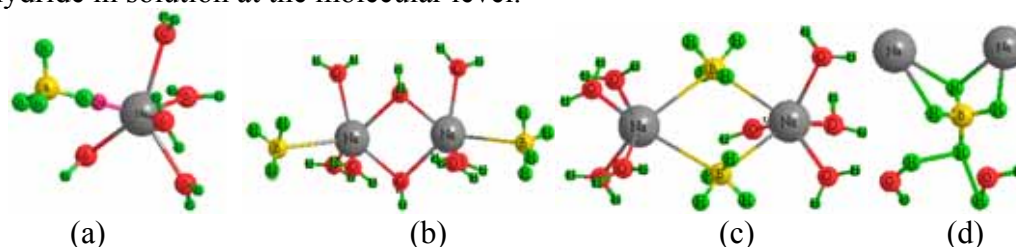


Fig. 1. Schematic diagrams of hydrated $[(\text{BH}_4)\text{Na}(\text{H}_2\text{O})_5]^+$ (a), dimer(I) $(\text{H}_2\text{O})_4\text{Na}(\text{H}_2\text{O})_2\text{Na}(\text{H}_2\text{O})_4$ (b), dimer(II) $(\text{H}_2\text{O})_4\text{Na}(\text{BH}_4)_2\text{Na}(\text{H}_2\text{O})_4$ (c) and BH_4^- coordination(d)

References

- [1] Zhou Y.Q., Fang. C.H., Fang Y., Structure of supersaturated aqueous sodium pentaborate solution. *Acta Phys. Chim. Sin.*, **26** (2010), 2323–2330.
- [2] Kim K.C., Sholl D.S., Crystal structures and thermodynamic investigations of $\text{LiK}(\text{BH}_4)_2$, KBH_4 , and NaBH_4 from first-principles calculations, *J. Phys. Chem. C*, **114**, (2010) 678–686.

D: POSTERS 45

AQUO-B(OH)₄⁻ CLUSTERS IN SOLUTION: A DFT AND VIBRATIONAL SPECTRUM STUDY

Zhou^{1,2} Y.Q., Fang¹ C.H., Fang¹ Y., Zhu^{1,2} F.Y., Ge¹ H.W. and Chen^{1,2} Q.L.

¹Qinghai Institute of Salt Lakes, Chinese Academy of Sciences, Xining, 810008 China;

²Graduate School of the Chinese Academy of Science, Beijing, 100049 China

e-mail: fangch@isl.ac.cn

Theoretical studies on small size clusters B(OH)₄⁻(H₂O)_n are reported by Oi *et al.* [1] who mainly focus on the ratios of reduced partition function of monoborate hydration. However, none report on Raman spectra of these clusters is available in the literature. In present paper, a systematic study on the structure, stability and Raman shifts of monoborate hydrated clusters, B(OH)₄⁻(H₂O)_n, (*n*=1-8) was carried out by DFT calculation in both gas and aqueous phase. Several possible initial configurations were considered for each size cluster to locate equilibrium geometry at the B3LYP/aug-cc-pVDZ level, all these stable configurations were described and the most stable hydrated clusters were chosen (Fig. 1). The hydrogen-bonds in those hydrated clusters were described in four different items: symmetrical double hydrogen bonding (DHB), single hydrogen bonding (SHB), inter-water hydrogen bonding (WHB) and weak interaction hydrogen bond (WIHB). A structure with double hydrogen bonding is more stable compared to other arrangements. The distance of SHB is shorter than that of DHB, and the former is more stable over the latter. The total symmetrical stretching vibration of B(OH)₄⁻ in hydrated B(OH)₄⁻(H₂O)_n is blue shift with the size of cluster increased. After consideration of hydration, the calculated characteristic frequencies are nearly the same as the experiment total stretching frequency of B(OH)₄⁻.

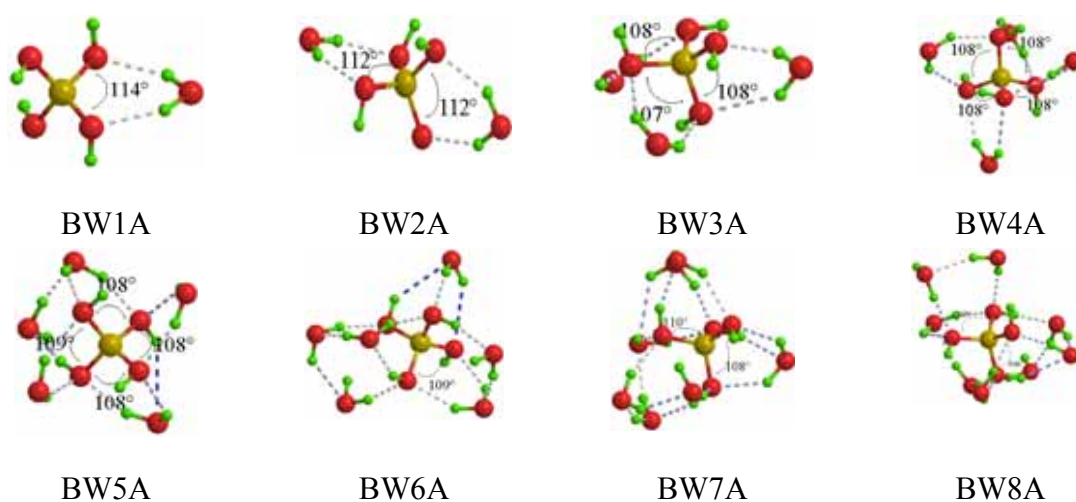


Fig. 1. Optimized lowest-energy structures of B(OH)₄⁻(H₂O)_n with *n* = 1-8 at the B3LYP/aug-cc-pVDZ level.

References

[1] Oi T., Yanase S., Calculations of reduced partition function ratios of hydrated monoborate anion by the ab initio molecular orbital theory. *J. Nucl. Sci. Technol.*, **38**, (2001) 429-432.

D: POSTERS 46

STRUCTURE OF AQUEOUS POTASSIUM TETRABORATE SOLUTIONS BY X-RAY SCATTERING

Zhu^{1,2} F.Y., Fang¹ C.H., Fang¹ Y., Zhou^{1,2} Y.Q., Xu^{1,2} S. and Tao^{1,2} S.

¹Qinghai Institute of Salt Lakes, Chinese Academy of Sciences, Xining, 810008 China; e-mail: fangch@isl.ac.cn

²Graduate School of the Chinese Academy of Science, Beijing, 100049 China;

The chemical species distribution diagram [1-2] and the Raman spectrum gave the chemical species in highly concentrated aqueous solutions. It shows that major chemical species $B_4O_5(OH)_4^{2-}$ and minor species $B_3O_3(OH)_4^-$, $B(OH)_4^-$ exist in solutions. X-ray scattering was used to studying the solutions with a salt-water molar ratio of 1:25, 1:20 and 1:15 at 298 and 323 K. Difference radial distribution functions (DRDFs) were obtained from accurate diffraction data. The model calculation and model refinement programs were used to calculating the structure parameters r_{i-j} , b_{i-j} and n_{i-j} . It manifests that the first hydration distance of K^+ is ~ 0.29 nm, with an average hydrated number of 8.0 (Figure 1 a). The hydration bond peak is around 0.278 nm, the coordination number (CN) is from 1.9 to 2.4. Borate anions coordinate with K^+ ions in the mono-dentate form, the average distance of K-B is 0.38 nm (Figure 1 b and c). The distance of B-H₂O in hydrated anion is from 0.37 to 0.38 nm with the hydrated number of 4~9, which depend on temperature and concentration. The other interactions such as water shared pairs $K^+ \cdots K^+$ interaction and the intra-anion interactions were also discussed.

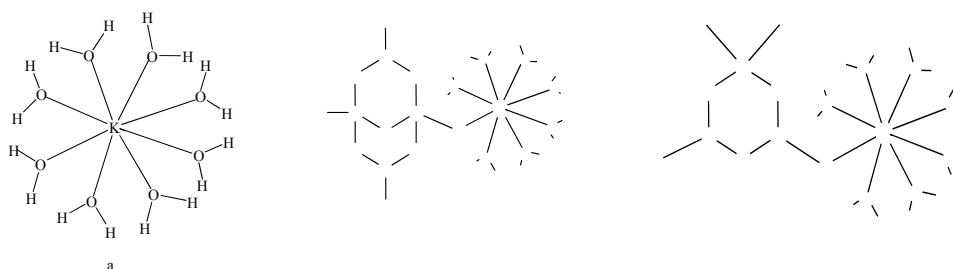


Fig. 1. The hydration structure of K^+ (a) and the configurations of the contact ion pairs $[KB_4O_5(OH)_4]^-$ (b) and $[KB_3O_3(OH)_4]^0$ (c) in aqueous solutions.

References

- [1] Spessard J.E., Investigations of borate equilibria in neutral salt solutions, *J. Inorg. Nucl. Chem.*, **32**, (1970) 2607–2613.
- [2] Zhu F.Y., Fang C.H., Fang Y., Zhou Y.Q., Cao L.D., Raman spectroscopic investigation and pH of aqueous $K_2B_4O_7$ and KBO_2 solutions, *J. Salt Lake Res.*, **24**, (2010) 497–501.

D: POSTERS 47

ACTIVITY COEFFICIENT OF CsCl IN AQUOUS MIXTURES WITH HIGH DIELECTRIC CONSTANT SYSTEM: N-METHYLFORMAMIDE + WATER BY POTENTIOMETRIC MEASUREMENTS AT 298.15 K

Lu J., Li S.N., Zhai Q.G., Jiang Y.C. and Hu* M.C.

Key Laboratory of Macromolecular Science of Shaanxi Province, School of Chemistry & Chemical Engineering, Shaanxi Normal University, Xi'an, Shaanxi, 710062, P. R. China.

*e-mail: hmch@snnu.edu.cn

Activity coefficients can be directly used to analyze the ion-ion and ion-solvent interactions occurring in the mixtures [1]. N-methylformamide is extensively used as a solvent and reagent in organic synthesis and chemical analysis [2].

To determine the thermodynamic properties of CsCl in the high relative permittivity co-solvent system: Water + N-methylformamide mixtures solvents at 298.15 K by using potentiometric measurements in the range 0.00-0.40 weight percent of N-methylformamide. The model of Pitzer and Debye-Hückel was chosen to depict the behavior of electrolyte. The potential of the cell can be expressed by the Nernst equation: $E = E^0 + 2k \ln(m\gamma_{\pm})$. The typical value of k obtained from the linear regression analysis of the experimental points is 25.65 ± 0.03 mV and a linear correlation coefficient of 0.9999. The experimental value got a good agreement with the theoretical value which is 25.69 mV at 298.15 K. It can be observed that $\ln\gamma_{\pm}$ decrease with increasing concentration of the electrolyte in molarity, and increase with increasing the N-methylformamide mass percentages in the mixed solvent.

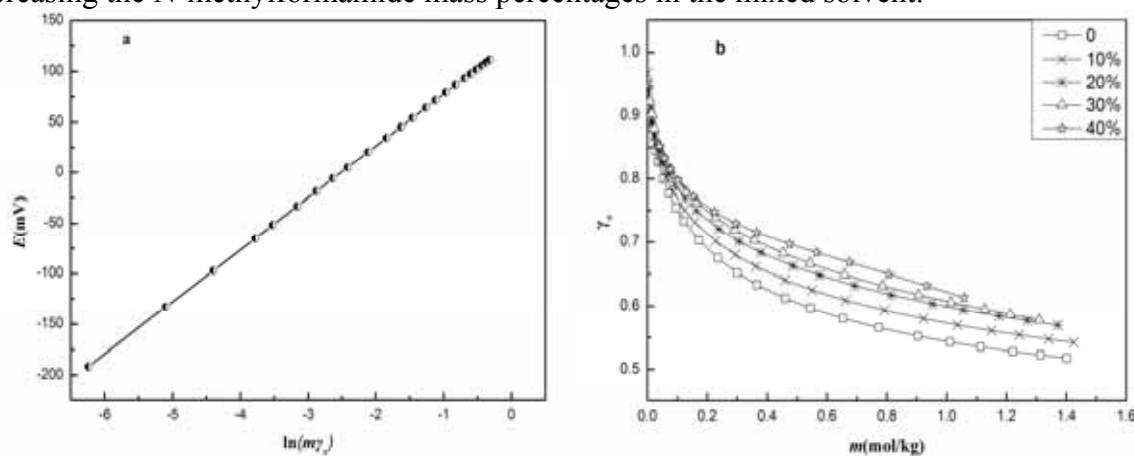


Fig. 1. a) Plot of the E of cell versus $\ln(m\gamma_{\pm})$ used for calibration of the Cs-ISE and Ag-AgCl electrode pair at 298.15 K; b) Plot of $\ln\gamma_{\pm}$ against molalities m of CsCl in CsCl + N-methylformamide + H₂O at 298.15 K.

Acknowledgements: Project supported by the National Natural Science Foundation of China (No:21171111) and the Fundamental Research Funds for the Central Universities (Program No: GK201001006).

References

- [1] Galleguillos H.R., Graber T.A., Taboada M.E., Activity coefficients of LiCl in ethanol water mixtures at 298.15 K, *Ind. Eng. Chem.*, **47**, (2008) 2056–2062.
- [2] Hernández-Luis F., Rodríguez-Raposo R., Ruiz-Cabrera G., Activity coefficients of NaCl in aqueous mixtures with ϵ -increasing co-solvent: N-methylformamide-water mixtures at 298.15 K, *Fluid Phase Equilib.*, **310**, (2011) 182–191.

D: POSTERS 48

ACTIVITY COEFFICIENTS OF CsNO₃ IN ALCOHOL-WATER MIXED SOLVENT FROM POTENTIOMETRIC METHOD

Tang J., Li S.N., Zhai Q.G., Jiang Y.C. and Hu* M.C.

Key Laboratory of Macromolecular Science of Shaanxi Province, School of Chemistry & Chemical Engineering, Shaanxi Normal University, Xi'an, Shaanxi, 710062, P. R. China.ia
*e-mail: hmch@snnu.edu.cn

Over the past century, the study of the thermodynamic properties of alkali metal chlorides in aqueous-organic mixed solvents has received considerable attention. Moreover, electrolyte systems are application in many chemical industries, geochemistry, biological, and environmental systems to solve environmental problems and optimize industrial processes. In previous work, the mean activity coefficients of CsNO₃ in ROH/water mixed solvents (where R = Me, and Et) were determined using potentiometric method at 298.15 K. The Pitzer equation[1] were applied to the experimental data. The figures illustrate that γ decreases with increase of alcohol content in the solvent mixture. One possible explanation for this phenomenon is ion-ion and ion-solvent interactions in the mixture. From the figures, it can be assumed that for the alcohol-water mixture, the relative permittivity of the mixed solvent decreases when the mass fraction of alcohol increases, while the ion-ion interaction was more significant than the ion-solvent interaction [2].

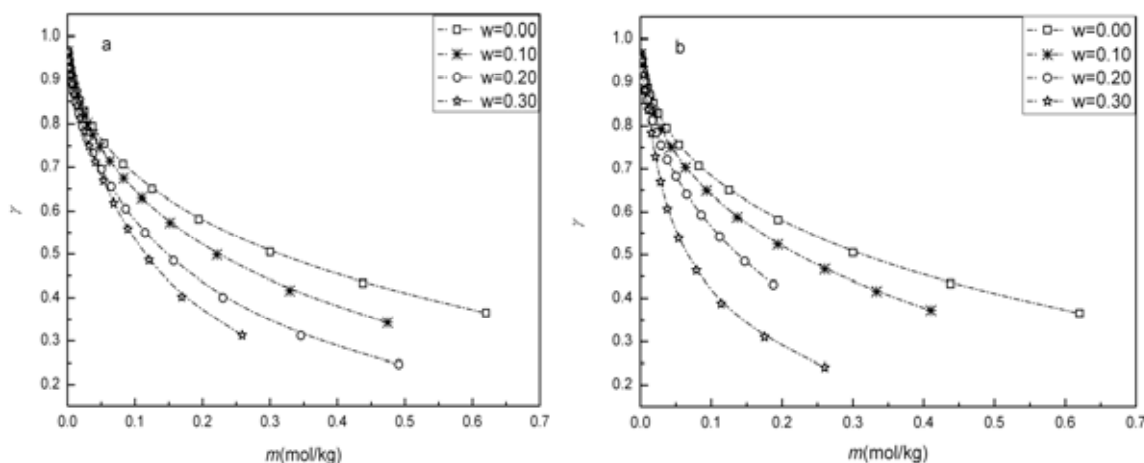


Fig. 1a and 1b. Variation of mean activity coefficient γ with molality of CsCl in methanol-water solvents and ethanol-water at 298.15 K, respectively.

Acknowledgements: Project supported by the National Natural Science Foundation of China (No:21171111) and the Fundamental Research Funds for the Central Universities (Program No: GK201001006 and 2010ZYGX027).

References

- [1] Pitzer K.S., Thermodynamics of electrolytes. I. theoretical basis and general equations, *J. Phys. Chem.*, **77**, (1973) 268–277.
- [2] Hernández-Luisa F., Galleguillosb H.R., Fernández-Méridaa L., González-Díazc O., Activity coefficients of NaCl in aqueous mixtures with ϵ -increasing co-solvent: formamide–water mixtures at 298.15K, *Fluid Phase Equilib.*, **275**, (2009) 116–126.

D: POSTERS 49

PARTIAL MOLAR VOLUMES OF AMINO ACIDS IN AQUEOUS SOLUTIONS CONTAINING AMMONIUM SULFATE

Martins¹ M.A., Mota¹ P.C., Ferreira¹ O., Hnědkovský² L., Pinho¹ S.P. and Cibulka² I.

¹LSRE/LCM-Laboratory of Separation and Reaction Engineering, Escola Superior de Tecnologia e de Gestão, Instituto Politécnico de Bragança, Campus de Santa Apolónia, 5301-857, Bragança, Portugal, e-mail: spinho@ipb.pt

²Department of Physical Chemistry, Institute of Chemical Technology, 16628 Prague, Czech Republic, e-mail: ivan.cibulka@vscht.cz

Because proteins are large complex molecules, direct study of protein-electrolyte interactions is difficult. It is therefore useful to investigate the interaction of model compounds such as amino acids, peptides, and their derivatives that constitute part of the protein structures. This feature of amino acids has been strongly attracting the attention of researchers to describe their physico-chemical properties.

Hydrophobic, charged atomic groups and ions are components of almost every biologically important system. It is generally acknowledged that the hydration of such atomic groups plays an important role in the conformational stability of biopolymers [1]. Consequently, characterization of the hydration properties of both hydrophobic and charged groups should provide insights into the role of solute-solvent interactions associated with fundamental biopolymers phenomena such as folding-unfolding transitions, solubility and denaturation [2].

In this work, density measurements were carried out in aqueous ammonium sulphate solutions containing the amino acids alanine, glycine, serine or threonine, in the temperature range between 278.15 and 318.15 K. From the measured data, the partial molar volumes of amino acids were calculated, allowing the interpretation of the physico-chemical properties of those solutions. The new experimental information was combined with the one collected from the open literature in order to have an insight on the forces that rule biologically important structures.

References

- [1] Chalikian T.V., Sarvazyan A.P., Breslauer K.J., Partial molar volumes, expansibilities, and compressibilities of aminocarboxylic acids in aqueous solutions between 18 and 55 °C, *J. Phys. Chem.*, **97**, (1993) 13017–13026.
- [2] Ferreira L.A., Macedo E.A., Pinho S.P., The Effect of ammonium sulfate on the solubility of amino acids in water at 298.15 and 323.15 K, *J. Chem. Thermodyn.*, **41**, (2009) 193–196.

D: POSTERS 50

SOLUBILITIES, DENSITIES AND REFRACTIVE INDICES FOR THE TERNARY SYSTEMS ETHYLENE GLYCOL + MBr (M = K, Rb, Cs) + H₂O AT 288.15 K

Li Y.J., Li S.N., Zhai Q.G., Jiang Y.C. and Hu* M.C.

Key Laboratory of Macromolecular Science of Shaanxi Province, School of Chemistry & chemical Engineering, Shaanxi Normal University, Xi'an, Shaanxi, 710062, China.

*e-mail:hmch@snnu.edu.cn

The study of phase equilibria in salt-containing systems is very important for many industrial applications [1,2]. Addition of an organic solvent to an aqueous salt solution normally reduces the solubility of the salt. This process has a number of potential advantages over alternative crystallization techniques because it creates the possibility of carrying out the operation at room temperature, producing crystals of high purity.

In this work, the solubility, density and refractive index of MBr (M = K, Rb, Cs) in ethylene glycol-H₂O mixed solvent were obtained. The solubilities and the densities for the three ternary systems significantly decreased with increasing mass fraction of ethylene glycol in the solvent. In our opinion, this phenomenon is mainly ascribed to one factor. The salt content should be the key factor that influenced the density for the three ternary systems. But the refractive indices for the three ternary systems increases with increasing mass fraction of ethylene glycol. It can be explained by the smaller refractive indice of water than that of ethylene glycol.

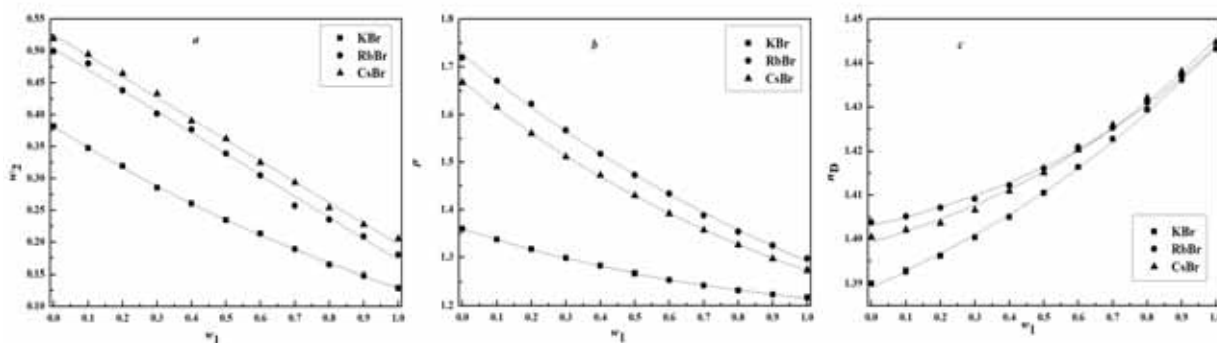


Fig. 1a, 1b and 1c. The solubility, density and refractive indices for the ternary systems of ethylene glycol (1) + MBr (M = K, Rb, Cs) (2) + H₂O (3) at 25 °C

Acknowledgements: Project supported by the National Natural Science Foundation of China (No:21171111) and the Fundamental Research Funds for the Central Universities (program No: GK201001006).

References

- [1] Pinho S.P., Macedo E.A., Solubility of NaCl, NaBr, and KCl in water, methanol, ethanol, and their mixed solvents, *J. Chem. Eng. Data*, **50**, (2005) 29–32.
- [2] Kim J.S., Lee H., Solubilities, vapor pressures, densities, and viscosities of the LiBr + LiI + HO(CH₂)₃OH + H₂O system, *J. Chem. Eng. Data*, **46**, (2001) 79–83.

D: POSTERS 51

THERMODYNAMIC PROPERTIES OF CsF IN WATER + L-ALANINE SYSTEM

Ma L., Li Sh.N., Zhai Q.G., Jiang Y.C. and Hu* M.C.

Key Laboratory of Macromolecular Science of Shaanxi Province, School of Chemistry and Chemical Engineering, Shaanxi Normal University, Xi'an, Shaanxi, 710062, P. R. China.

*e-mail: hmch@snnu.edu.cn

The ternary systems of amino acids in aqueous salt solutions are widely observed in some separation processes of biomolecules, such as reverse micellar extraction, salt-induced precipitation and aqueous two-phase extraction [1]. The thermodynamic properties give insight into the interactions of biomolecules and electrolytes [2]. The potentiometric measurements have been carried out for the ternary system (water + L-alanine + CsF) at 298.15 K in different molalities of L-alanine ($m=0.1, 0.15, 0.2, 0.25, 0.3, 0.35, 0.4$). The cells used in this work belong to the type of galvanic cell without a liquid junction with only one fluid, as follows: Cs-ISE| CsF(m), L-alanine (m), H₂O | F-ISE. The linear regression line in the figure has an equation of the form $y = a + bx$, a is 325.9 mV, and b is 50.44 for the Cs-ISE and F-ISE electrode. The Pitzer, the modified Pitzer and the extended Debye-Hückel equations were used to determine the mean activity coefficients, the osmotic coefficients and the excess Gibbs free energy. The variation of γ_{\pm} with the molalities of CsF and L-alanine are shown in Figure b. It can be observed that the values of the mean activity coefficients decrease with increasing the ionic strength of electrolyte. At the same time, when the ionic strength is fixed, the values of the mean activity coefficient increase with increasing the molalities of L-alanine in mixed solvent. Figure c shows that the excess Gibbs free energy is increased by increasing the molalities of L-alanine in mixed solvent. This can be interpreted in terms of the interaction model.

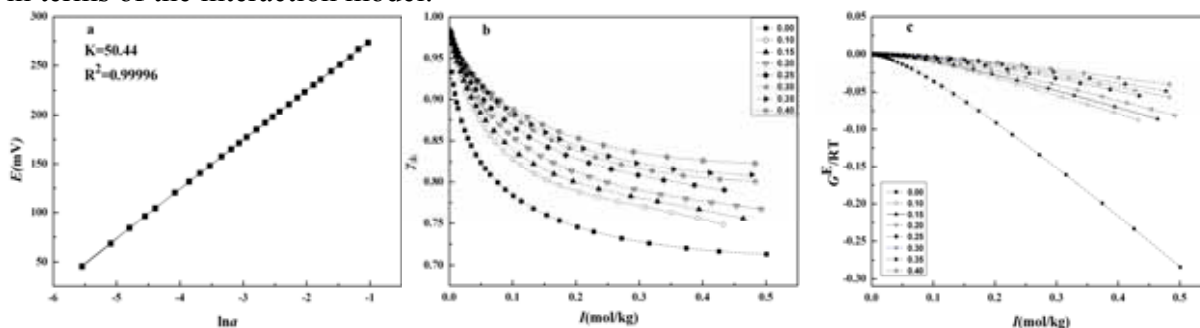


Fig. a. Plot of the emf versus $\ln a_{\text{CsF}}$ for calibration of Cs-ISE and F-ISE electrode pair at 298.15 K. Fig. b. Plot of the values of mean activity coefficients of CsF versus total ionic strength at different molalities of L-alanine. Fig. c. Plot of the excess Gibbs free energy for mixed electrolyte solution against total ionic strength at different molalities of L-alanine.

Acknowledgements: Project supported by the National Natural Science Foundation of China (No. 21171111) and the Fundamental Research Funds for the Central Universities (Program No. GK201001006).

References

- [1] Salabat A., Neshat S., Fazlali A., Activity coefficients of glycine, D-alanine and L-valine in aqueous solutions containing MgSO₄ at 298.15 K; experimental determination and correlation, *Fluid Phase Equilib.*, **314**, (2012) 198–202.
- [2] Sadeghi M., Ghotbi C., Jafar Abdekhodaie M., Activity coefficient prediction for binary and ternary aqueous electrolyte solutions at different temperatures and concentrations, *J. Solution. Chem.*, **41**, (2012) 75–88.

List of Participants (alphabetically by name)

Name	First name	Title	Institution	Country(region)/email
Ago	Ken-ichi	Dr.	Hosei University Institute for Sustainability Research and Education	Japan kenichi.ago.sk@hosei.ac.jp
Altmaier	Marcus	Dr.	Karlsruhe Institute of Technology Institute for Nuclear Waste Disposal	Germany marcus.altmaier@kit.edu
Bhattarai	Ajaya	Dr.	Tribhuvan University Department of Chemistry	Nepal bkajaya@yahoo.com
Bu	Lingzhong	Mr.	Chinese Academy of Geological sciences Institute of Mineral Resources	China Bulingzhong65@sohu.com
Bube	Christiane	Ms.	Karlsruhe Institute of Technology Institute for Nuclear Waste Disposal	Germany christiane.bube@kit.edu
Cao	Caifang	Dr.	Central South University School of Metallurgical Science and Engineering	China caocaifang@hotmail.com
Cao	Hongcui	Ms.	Qinghai University	China caohongcui_1975@sohu.com
Chen	Jianxin	Prof.	Hebei University of Technology School of Chemical Engineering	China chjx2000@gmail.com
Chen	Qiaoling	Ms.	Qinghai Institute of Salt Lakes CAS	China chenqiaoling@126.com
Deng	Tianlong	Prof.	Tianjin University of Science and Technology College of Marine Science and Engineering	China tldeng@tust.edu.cn
De Visscher	Alex	Prof.	University of Calgary Department of Chemical and Petroleum Engineering	Canada adevissc@ucalgary.ca
Dong	Hongxing	Prof.	Harbin Engineering University College of Materials Science and Chemical Engineering	China hongxingd6@yahoo.com.cn
Dong	Ouyang	Mr.	Qinghai Institute of Salt Lakes,CAS	China ouyang_dong@163.com
Du	Hao	Dr.	Institute of Process Engineering CAS	China duhao121@hotmail.com
Fang	Chunhui	Prof.	Qinghai Institute of Salt Lakes,CAS	China fangch@isl.ac.cn

Fang	Tao	Prof.	Xi'an Jiaotong University Dep.of Chem. Eng.	China taofang@mail.xjtu.edu.cn
Fang	Yan	Prof.	Qinghai Institute of Salt Lakes,CAS	China fangy8@isl.ac.cn
Freyer	Daniela	Dr.	TU Bergakademie Freiberg Institut für Anorganische Chemie	Germany daniela.freyer@chemie.tu-freiberg.de
Furia	Emilia	Dr.	University of Calabria Department of Chemistry	Italy e.furia@unical.it
Gao	Daolin	Dr.	Tianjin University of Science and Technology College of Marine Science and Engineering	China gaodaolin2000@163.com
Gumiński	Cezary	Dr.	University of Warsaw Department of Chemistry	Poland cegie@chem.uw.edu.pl
Ge	Haiwen	Mr.	Qinghai Institute of Salt Lakes CAS	China gehaiwen1207@126.com
Gong	Weiping	Prof.	Huizhou University Electronic Science Department	China gwp@hzu.edu.cn
Guo	Lijiang	Dr.	Qinghai Institute of Salt Lakes CAS	China l.j.guo@hotmail.com
Guo	Yafei	Dr.	Tianjin University of Science and Technology College of Marine Science and Engineering	China guoyafei@tust.edu.cn
Han	Haijun	Mr.	Qinghai Institute of Salt Lakes CAS	China haijunhan@126.com
Hefter	Glenn	Prof.	Murdoch University Chemistry Department	Australia g.hefter@murdoch.edu.au
Hertam	Anke	Ms.	TU Bergakademie Freiberg Institut für Anorganische Chemie	Germany anke.hertam@chemie.tu-freiberg.de
Hu	Bin	Dr.	Qinghai Institute of Salt Lakes CAS	China hubin@isl.ac.cn
Hu	Mancheng	Prof.	Shaanxi Normal University School of Chemistry & Chemical Engineering	China hmch@snnu.edu.cn
Huang	Xueli	Prof.	Xinjiang University College of Chemistry and Chemical Engineering	China xuelih@163.com
Huang	Ziping	Prof.	Qinghai University	China huangzpqd@163.com
Járvás	Gábor	Dr.	University of Pannonia	Hungary jarvasg@gmail.com

Jirsák	Jan	Dr.	J. E. Purkinje University in Ustin. L. Faculty of Science	Czech Republic jan.jirsak@ujep.cz
König	Axel	Prof.	University Erlangen Chair of Separation Science and Technology	Germany axel.koenig@cbi.uni-erlangen.de
Königsberger	Erich	Prof.	Murdoch University School of Chemical and Mathematical Sciences	Australia koenigsb@murdoch.edu.au
Königsberger	LanChi	Dr.	Murdoch University School of Chemical and Mathematical Sciences	Australia L.Koenigsberger@murdoch.edu.au
Kulkarni	Anand	Mr.	Dr. Babasaheb Ambedkar Marathwada University Dep. of Chem. Tech.	India anakulw@gmail.com
Lee	Ming-Jer	Prof.	National Taiwan University of Science & Technology Dep. of Chem. Eng.	Taiwan mjlee@mail.ntust.edu.tw
Li	Bing	Prof.	Qinghai Institute of Salt Lakes CAS	China libing@isl.ac.cn
Li	Chunli	Ms.	Qinghai University	China lxwlchl@163.com
Li	Dongdong	Mr.	Qinghai Institute of Salt Lakes CAS	China ddong_li@hotmail.com
Li	Hongru	Dr.	Nankai University College of Pharmacy	China lihongru@nankai.edu.cn
Li	Hongxia	Ms.	Qinghai Institute of Salt Lakes CAS	China hongxia_1li@126.com
Lutsyk	Vasily	Prof.	Institute of Physical Materials Science Russian Academy of Sciences	Russia vluts@pres.bscnet.ru
Ma	Haizhou	Prof.	Qinghai Institute of Salt Lakes CAS	China haizhou@isl.ac.cn
Ma	Lei	Ms.	Shaanxi Normal University, School of Chemistry and Chemical Engineering	China mlmwhwish@stu.snnu.edu.cn
Machanová	Karolina	Ms.	E.Hala Laboratory of Thermodynamics Acad Sci Prague	Czech Republic machanova@icpf.cas.cz
Magalhães	Maria Clara	Prof.	University of Aveiro Departamento de Química and CICECO	Portugal mclara@ua.pt
Manohar	Balaraman	Dr.	Central Food Technological Research Institute	India manoharmysore@yahoo.co.in

Matsuda	Hiroyuki	Dr.	Nihon University Dep. of Mater. and Appl. Chem.	Japan matsuda.hiroyuki@nihon-u.ac.jp
Meng	Lingzong	Dr.	Linyi University College of Chem. and Chem. Eng.	China menglingzong@lyu.edu.cn
Mondal	Monoj	Prof.	Banaras Hindu University Department of Chemical Engineering and Technology	India mkmondal13@yahoo.com
Naik	Jitendra	Prof.	North Maharashtra University Dep. of Chem. Tech.	India jitunaik@gmail.com
Nie	Zhen	Prof.	Chinese academy of geological sciences Institute of mineral resources	China nieezhen518@163.com
Nishiumi	Hideo	Prof.	Hosei University Chemical Engineering Laboratory	Japan nishi@hosei.ac.jp
Oestreich	Melanie	Ms.	TU Bergakademie Freiberg Institut für Anorganische Chemie	Germany melanie.oestreich@chemie.tu-freiberg.de
Papangelakis	Vladimiro	Prof.	University of Toronto	Canada vladimiro.papangelakis@utoronto.ca
Pinho	Simão	Prof.	Instituto Politécnico de Bragança	Portugal spinho@ipb.pt
Räsänen	Lea	Mrs.	VTT Technical Research Centre of Finland	Finland lea.rasanen@vtt.fi
Sang	Shihua	Prof.	Chengdu University of Technology Institute of materials and Chemistry & Chemical Engineering	China sangshihua@sina.com.cn
Schlosser	Stefan	Dr.	Slovak University of Technology Institute of Chemical and Environmental Engineering	Slovakia stefan.schlosser@stuba.sk
Schmitt	Julia	Ms.	TU Bergakademie Freiberg Institut für Anorganische Chemie	Germany julia.schmitt@chemie.tu-freiberg.de
Sedov	Igor	Dr.	Kazan Federal University Dep. of Phys. Chem.	Russia igor_sedov@inbox.ru
Shen	Dongliang	Dr.	Tianjin University of Science and Technology College of Marine Science and Engineering	China g491540954@qq.com
Song	Pengsheng	Prof.	Qinghai Institute of Salt Lakes CAS	China songpsh@isl.ac.cn

Steiger	Michael	Dr.	University of Hamburg Department of Chemistry	Germany steiger@chemie.uni-hamburg.de
Sun	Bai	Prof.	Qinghai Institute of Salt Lakes CAS	China sunb@isl.ac.cn
Sun	Hongwei	Prof.	National Natural Science Foundation of China	China sunhw@nsfc.gov.cn
Tamura	Kazuhiro	Prof.	Kanazawa University Division of Material Sciences and Material Engineering	Japan tamura@t.kanazawa-u.ac.jp
Tang	Jing	Ms.	Shaanxi Normal University, School of Chemistry and Chemical Engineering	China tangjing224@126.com
Tao	Song	Mr.	Qinghai Institute of Salt Lakes CAS	China taosong521@163.com
Thomsen	Kaj	Prof.	Technical University of Denmark Department of Chemical and Biochemical Engineering	Denmark kth@kt.dtu.dk
Toikka	Alexander	Prof.	Saint-Petersburg State University Department of Chemical Thermodynamics and Kinetics	Russia alexander.toikka@chem.spbu.ru
Tu	Lanying	Ms.	Qinghai University	China tulany1969@qq.com
Voigt	Wolfgang	Prof.	TU Bergakademie Freiberg Institut für Anorganische Chemie	Germany Wolfgang.Voigt@chemie.tu-freiberg.de
Waghorne	Earle	Prof.	University College Dublin Shool of Chemistry and Chemical Biology	Ireland earle.waghorne@ucd.ie
Wang	Gang	Prof.	Qinghai University	China wanggang5208@163.com
Wang	Junfeng	Dr.	Institute of Process Engineering, CAS	China junfwang@home.ipe.ac.cn
Wang	Peiming	Dr.	OLI Systems, Inc.	United States pwang@olisystems.com
Wang	Qin	Ms.	Tianjin University of Science and Technology College of Marine Science and Engineering	China 418707163@qq.com
Wang	Shaona	Dr.	Institue of Process Engineering CAS	China shnwang@home.ipe.ac.cn
Wang	Shiqiang	Dr.	Tianjin University of Science and Technology College of Marine Science and	China wangshiqiang@tust.edu.cn

Engineering

Wang	Tao	Mr.	Qinghai Institute of Salt Lakes CAS	China wd123987@126.com
Wang	Wenlei	Mr.	Central South University College of Chemistry and Chemical Engineering	China wenlei_wang@hotmail.com
Wang	Yunsheng	Dr.	Chinese Academy of Geological Sciences Institute of Mineral Resources	China wys0907@yahoo.com.cn
Wang	Zhonghua	Prof.	Kunming University of Science and Technology	China zhonghuakm@googlemail.com
Winkler	Andrea	Ms.	TU Bergakademie Freiberg Institut für Anorganische Chemie	Germany Andrea.Winkler@chemie.tu-freiberg.de
Winkler	Igor	Prof.	National University of Chernivtsi Department of Physical and Environmental Chemistry	Ukraine igorw@ukrpost.ua
Wu	Kezhong	Prof.	Hebei Normal University Department of Chemistry and Material Science	China wukzh688@163.com
Xu	Sha	Mr.	Qinghai Institute of Salt Lakes CAS	China xusha609@sohu.com
Yang	Haitang	Ms.	Central South University College of Chemistry and Chemical Engineering	China hai.tang.ouyang@hotmail.com
Yang	Hongjun	Dr.	Qinghai Institute of Salt Lakes CAS	China yanghongjun1973@163.com
Yang	Junlin	Prof.	National Natural Science Foundation of China	China yangjl@nsfc.gov.cn
Yang	Xiaoguang	Dr.	Harbin Engineering University College of Materials Science and Chemical Engineering	China yxg1122@163.com
Yao	Yan	Prof.	Qinghai Institute of Salt Lakes CAS	China yaoy@isl.ac.cn
Yin	Xia	Ms.	Hunan University College of Chemistry and Chemical Engineering	China yinxia0405@yahoo.com.cn
Yu	Xiaoping	Dr.	Tianjin University of Science and Technology College of Marine Science and Engineering	China yuxiaoping823@yahoo.cn
Yu	Xudong	Dr.	Chengdu University of Technology College of Materials and	China xwdlyxd@gmail.com

Chemistry & Chemical
Engineering

Zeng	Dewen	Prof.	Qinghai Institute of Salt Lakes CAS	China dewen_zeng@hotmail.com
Zhang	Hong	Prof.	Qinghai University	China 420856897@qq.com
Zhang	Jin	Mr.	Harbin Engineering University College of Materials Science and Chemical Engineering	China zhangjin8014484@163.com
Zhang	Li	Ms.	Huizhou University	China zhangli@hzu.edu.cn
Zhang	Ying	Dr.	Institute of Process Engineering CAS	China zhangying@home.ipe.ac.cn
Zhao	Xianyin	Dr.	Chengdu University of Technology College of Materials and Chemistry & Chemical Engineering	China zhaoxianyin09@cdut.cn
Zhao	Zhongwei	Prof.	Central South University School of Metallurgical Science and Engineering	China zhaozw@csu.edu.cn
Zheng	Shili	Prof.	Institute of Process Engineering CAS	China slzheng@home.ipe.ac.cn
Zhong	Yuan	Mr.	Qinghai Institute of Salt Lakes CAS	China zhongyuan231@163.com
Zhou	Hongyan	Ms.	Qinghai Institute of Salt Lakes CAS	China hy_zhou@yeah.net
Zhou	Huan	Prof.	Tianjin University of Science and Technology College of Marine Science and Engineering	China zhouhuan@tust.edu.cn
Zhou	Yongquan	Mr.	Qinghai Institute of Salt Lakes CAS	China yongqzhou@163.com
Zhu	Fayan	Mr.	Qinghai Institute of Salt Lakes CAS	China zhufayan@126.com
Zvereva	Irina	Prof.	Saint-Petersburg State University Department of Chemical Thermodynamics and Kinetics	Russia irina.zvereva@chem.spbu.ru

List of Participants (alphabetically by countries/regions)

Country/Region	Name	First Name	Title
Australia	Hefter	Glenn	Prof.
	Koenigsberger	Erich	Prof.
	Koenigsberger	LanChi	Dr.
Austria	Gamsjäger	Heinz	Prof.
Canada	De Visscher	Alex	Prof.
	Papangelakis	Vladimiros	Prof.
China	Bu	Lingzhong	Mr.
	Cao	Caifang	Dr.
	Cao	Hongcui	Ms.
	Chen	Jianxin	Prof.
	Chen	Qiaoling	Ms.
	Deng	Tianlong	Prof.
	Dong	Hongxing	Prof.
	Dong	Ouyang	Mr.
	Du	Hao	Dr.
	Fang	Chunhui	Prof.
	Fang	Tao	Prof.
	Fang	Yan	Prof.
	Gao	Daolin	Dr.
	Ge	Haiwen	Mr.
	Gong	Weiping	Prof.
	Guo	Lijiang	Dr.
	Guo	Yafei	Dr.
	Han	Haijun	Mr.
	Hu	Bin	Dr.
	Hu	Mancheng	Prof.
	Huang	Xueli	Prof.
	Huang	Ziping	Prof.
	Li	Bing	Prof.
	Li	Chunli	Ms.
	Li	Dongdong	Mr.
	Li	Hongru	Dr.
	Li	Hongxia	Dr.
	Ma	Haizhou	Prof.
	Ma	Lei	Ms.
	Meng	Lingzong	Dr.
	Nie	Zhen	Prof.
	Sang	Shihua	Prof.
Shen	Dongliang	Dr.	
Song	Pengsheng	Prof.	
Sun	Bai	Prof.	
Sun	Hongwei	Prof.	
Tao	Song	Mr.	

	Tang	Jing	Ms.
	Tu	Lanying	Ms.
	Wang	Gang	Prof.
	Wang	Junfeng	Dr.
	Wang	Qin	Ms.
	Wang	Shaona	Dr.
	Wang	Shiqiang	Dr.
	Wang	Tao	Mr.
	Wang	Wenlei	Dr.
	Wang	Yunsheng	Dr.
	Wang	Zhonghua	Prof.
	Wu	Kezhong	Prof.
	Xu	Sha	Ms.
	Yang	Haitang	Ms.
	Yang	Hongjun	Dr.
	Yang	Junlin	Prof.
	Yang	Xiaoguang	Dr.
	Yao	Yan	Prof.
	Yin	Xia	Mrs.
	Yu	Xiaoping	Dr.
	Yu	Xudong	Dr.
	Zeng	Dewen	Prof.
	Zhang	Hong	Prof.
	Zhang	Jin	Mr.
	Zhang	Li	Ms.
	Zhang	Ying	Dr.
	Zhao	Xianyin	Dr.
	Zhao	Zhongwei	Prof.
	Zheng	Shili	Prof.
	Zhong	Yuan	Mr.
	Zhou	Hongyan	Ms.
	Zhou	Huan	Prof.
	Zhou	Yongquan	Mr.
	Zhu	Fayan	Mr.
Czech Republic	Jirsák	Jan	Dr.
	Machanová	Karolina	Ms.
Denmark	Thomsen	Kaj	Prof.
Finland	Räsänen	Lea	Mrs.
Germany	Altmaier	Marcus	Dr.
	Bube	Christiane	Ms.
	Freyer	Daniela	Dr.
	Hertam	Anke	Ms.
	König	Axel	Prof.
	Oestreich	Melanie	Ms.
	Schmitt	Julia	Ms.

	Steiger Voigt Winkler	Michael Wolfgang Andrea	Dr. Prof. Mrs.
Hungary	Járvás	Gábor	Dr.
India	Manohar Kulkarni Mondal Naik	Balaraman Anand Monoj Jitendra	Dr. Mr. Prof. Prof.
Ireland	Waghorne	Earle	Prof.
Italy	Furia	Emilia	Dr.
Japan	Ago Matsuda Nishiumi Tamura	Ken-ichi Hiroyuki Hideo Kazuhiro	Dr. Dr. Prof. Prof.
Nepal	Bhattarai	Ajaya	Dr.
Poland	Gumiński	Cezary	Dr.
Portugal	Magalhães Pinho	Maria Clara Simão	Prof. Prof.
Russia	Lutsyk Sedov Toikka Zvereva	Vasily Igor Alexander Irina	Prof. Dr. Prof. Prof.
Slovakia	Schlosser	Stefan	Dr.
Taiwan	Lee	Ming-Jer	Prof.
Ukraine	Winkler	Igor	Prof.
USA	Wang	Peiming	Dr.

